Analysis of the roles of the plastidic E3 ligases SP1 and SPL2 in tomato and wheat

Najiah Mohd Sadali

Wolfson College

DPhil in Plant Sciences

Trinity 2018

Abstract

Plastids are an important group of plant organelles, and depending on their morphology and functions, plastids exist in different forms and have the ability to convert between these forms. Development of plastids depends on the import of preproteins from the cytosol through outer and inner envelope chloroplast membranes, TOC and TIC complexes. The TOC complex incorporates different client-specific receptors and these contact preproteins with differing specificity, controlling the proteomic composition, development fate, and functions of the plastid. The first identified chloroplast-localized E3 ligase of the plastid outer membrane, SP1, is a regulator of the TOC translocon. In Arabidopsis, SP1 functions to attach ubiquitin to TOC proteins for ubiquitin-proteasome system (UPS)-mediated degradation, controlling the proteomic composition of plastids.

In this thesis, detail analyses of the role of SP1 were conducted in tomato and wheat plants with altered SP1 expression (both overexpression [OEX] and RNA interference-based knockdown, in each case), to further assess the extent to which its functions are conserved in different species, and to elucidate possible practical applications in crops.

In accordance with previous findings in Arabidopsis, SP1 OEX promoted abiotic stress tolerance and leaf senescence in both tomato and wheat. SP1 was found to influence the abiotic stress tolerance where its particular effect on the plants' responses to stress conditions was dependent on the developmental stage at which the exposure to stress occurred. SP1 RNAi delayed senescence under dark-induced and natural senescence conditions, and influenced yield in 'stay-green' SP1 RNAi wheat plants. SP1-mediated changes in tomato were found to alter the duration of fruit ripening, without affecting the size and firmness of the fully ripened fruit. Specifically, SP1 OEX fruit showed accelerated ripening, and SP1 RNAi fruit showed delayed ripening.

Finally, the role of SPL2, a homologue of SP1, in tomato was investigated. The RNAi-mediated knockdown of *SPL2* expression in tomato plants had similar effects on fruit ripening, leaf senescence, and abiotic stress tolerance to SP1 RNAi, even though the transcript abundance of tomato *SPL2* in various plant tissues was much less than that of tomato *SP1*.

Acknowledgements

Alhamdulillah! My DPhil journey has come to an end. Undertaking this DPhil has been a truly life-changing experience for me and it would not have been possible to do without the support and guidance that I received from many people. I would like to acknowledge and thank the following important people who have supported me endlessly throughout this amazing and special journey.

I would like to first thank my supervisor, Professor Paul Jarvis, for all his advice, support, productive conversation, and unequivocal guidance throughout this journey. Without his guidance and constant feedback this DPhil would not have been achievable. Thank you for opening the door for me to be part of this amazing research group. I could not have hoped for more inspiring mentorships.

Thanks are also due to the Post-docs, DPhil students and technicians in the Jarvis group, and all members of the Department of Plant Sciences, for all of their assistance, advice, and motivational sessions. In particular, I would like to thank Dr Qihua Ling, for your mentorship to conduct my research. He never ceases to amaze me, with his breadth of scientific knowledge and experimental expertise.

I gratefully acknowledge my sponsors The Khazanah-Oxford Centre for Islamic Studies Merdeka Scholarships, and their continuous support for my doctoral work at Oxford University. I am also grateful to the four years' study leave granted by my employer, University of Malaya, Kuala Lumpur, to undertake my DPhil.

I must express my gratitude to Khairul Asrar, my husband, for his support and encouragement in every step of my DPhil journey. I could not have done this without him. Thank you for your love, positivity and patience. I love you very much.

Last but certainly not least, I would like to thank my friends and family. To my friends: Ardiyana, Asyura, Ayna, Aida, Hasila, and all, you are the best! You have all encouraged and believe in me. You have all helped me to focus on what has been a hugely rewarding and enriching process. To my parents and in laws, thanks for understanding my academic endeavour which causes years of absence by your sides.

Without their continuing support, cooperation, and encouragement this DPhil would not have become a reality. *Terima kasih!*

Statement of Authorship

The following people made contributions to the work presented in this thesis:

Dr Qihua Ling:	Produced the construct pK7WG2D-SlSP1 and pK7WG2D-amiRSlSP1, and generated the transgenic tomato lines with modified SlSP1 expression (over-expression, OEX; and silencing, RNAi); produced p2GWY7-SlSP1 construct and performed the confocal microscopy of protoplasts transiently expressing SlSP1-YFP (Fig. 3.1). He also prepared the entry vector, pEW271 (RNAi construct) and pEW272 (OEX construct) for wheat transformation.
Yunliu Zeng:	Produced the construct pK7WG2D-amiRSlSPL2 and generated the SlSPL2 RNAi transgenic tomato lines. He also produced p2GWY7-SlSPL2 construct and performed confocal microscopy of protoplasts transiently expressing SlSPL2-YFP (Fig. 6.1).
Dr Emma Wallington:	Finalized the construction of two binary vectors, pSc4Act-R1R2-SCV-TaSP1 and pAct-IR-2-amiRTaSP1 by transferred the entry clones [prepared by Dr Qihua Ling, pEW271 (RNAi construct) and pEW272 (OEX construct)] to their destination vectors. Performed the wheat transformation producing transgenic wheat lines with modified TaSP1 expression.

Abbreviations

3-PGA	D-glycerate 3-phosphate
AGPase	ADP-glucose pyrophosphorylase
AKR2	Ankyrin repeat protein 2
AP	Ammonium persulfate
ATP	Adenosine triphosphate
BE	Branching enzyme
BLAST	Basic Local Alignment Search Tool
BSA	Bovine serum albumin
cDNA	Complementary DNA
CDS	Coding DNA sequence
Da	Daltons
DAB	3, 3′-Diaminobenzidine
DBE	Debranching enzyme
DNA	Deoxyribonucleic acid
dNTP	Deoxyribonucleotide phosphates
DTT	Dithiothreitol
E3	E3 ubiquitin ligase
ECL	Enhanced chemiluminescence
EDTA	Ethylenediaminetetraacetic acid
GOI	Gene of interest
GTP	Guanosine triphosphate
H_2O_2	Hydrogen peroxide
HRP	Horse-radish peroxidase

Hsp_n	Heat-shock protein of n kDa
IEM	Inner envelope membrane
IMS	Intermembrane space
LHCP	Light-harvesting chlorophyll a/b protein
mRNA	Messenger RNA
MS	Murashige and Skoog
MG	Mature green
NaCl	Sodium chloride
NPQ	Non-photochemical quenching
OEM/OM	Outer envelope membrane
OEP	Outer envelope protein
PCR	Polymerase chain-reaction
PSI	Photosystem I
PSII	Photosystem II
ppi	Plastid protein import
qPCR	Quantitative real-time PCR
RING	Really interesting new gene domain
RNA	Ribonucleic acid
ROS	Reactive oxygen species
RT-PCR	Reverse-transcript PCR
Rubisco	Ribulose-1, 5-bisphosphate carboxylase/oxygenase
SDS	Sodium dodecyl sulfate
SDS-PAGE	SDS-Polyacrylamide gel electrophoresis
SEM	Standard error of the mean
SP1	Suppressor of ppi1 locus 1
SPL	SP1-Like

SPP	Stromal processing peptidase
SS	Starch synthase
T_n	Transformed plant generation
TBE	Tris-buffered EDTA
TBS-T	Tris-buffered saline with Tween20
T-DNA	Transfer-DNA
TEMED	Tetramethylethylenediamine
TGS	Tris glycine SDS buffer
TIC	Translocon at the IEM of the chloroplast
Tic_n	TIC protein of n kDa
TMD	Transmembrane domain
TOC	Translocon at the OEM of the chloroplast
Toc_n	TOC protein of n kDa
Tris	Tris(hydroxymethyl)aminomethane
USDA	United States Department of Agriculture
UPS	Ubiquitin-proteasome system
UTR	Untranslated region
YFP	Yellow fluorescent protein
v	$Volume\ (ml)$
w/v	$\frac{Weight\ (g)}{Volume\ (ml)}$
WT	Wild type

Table of Content

Chapter 1: General Introduction

1.1 Introduction to plastids

Approximately 1.5 billion years ago, ancient plastids developed from an endosymbiotic relationship between a cyanobacterium-like organism and an early eukaryotic cell (Yoon et al., 2004). Plastids began their existence as a group of bacteria capable of oxygenic photosynthesis, and modern-day plastids appear to be related to the extant cyanobacteria. This evolution event gives rise to three separate lineages, the glaucophytes, chloroplastida and rhodophytes (Zimorski et al., 2014). It is the chloroplastida which gives rise to the Viridiplantae, which include all of the green algae and land plants. Throughout Viridiplantae, chloroplasts have the same general structure, which consists of the outer-envelope membrane (OEM), the inner envelope membrane (IEM), and the thylakoid membrane. These three membranes enclose three distinct compartments, the intermembrane space (IMS), between the OEM and IEM, the stroma between IEM and thylakoid, and the thylakoid lumen enclosed by the thylakoid membrane (Zimorski et al., 2014).

During the course of plant evolution from the endosymbiotic progenitor into the chloroplast organelle, plastid has lost the vast majority of their genes. Many genes were either lost from plastids or being transferred into the nucleus (Martin et al., 1998; Martin et al., 2002). The genetic information has vanished because it was no longer needed in the cellular environment. Nevertheless, this gene loss was never completed as fully functional higher plant chloroplasts retained about 60 to 80 proteins in the organelle (Martin and Herrmann, 1998), mainly the proteins that maintain redox balance and overcome the side effects of electron transport through the photosynthetic and respiratory membranes (Race et al., 1999). In Arabidopsis, a total of 87 genes, including 79 unique ones, are encoded by the plastid chromosome (Sato et al., 1999). As nuclear genes now encode many of the chloroplast proteins, they must be imported as precursor proteins from the cytoplasm and coordinated by the mechanism of

protein translocation into the plastid from the cytosol to reach the inside of the chloroplast. These proteins are generally synthesized as precursor proteins with cleavable, N-terminal called chloroplast transit peptides (cTPs) (Bruce, 2000). A combination of cTP predictors was employed to estimate that around 2000 different cTP-bearing proteins should exist in Arabidopsis (Leister and Pesaresi, 2018).

Nowadays, modern-day plastids are an important group of plant cellular organelles and a defining feature of the plant cell. They are essential components for normal plant cell functions and exist in different forms. Chloroplasts accumulate the green pigment chlorophyll, and are the best known and founding members of the plastid family. Chloroplast is the only plastid type that is able to produce energy, and is responsible for photosynthesis. Mature chloroplasts consist of the thylakoids, which comprise two major domains, known as grana, which contain photosystem II (PSII) complexes and stroma lamella, which contain photosystem I (PSI) (Figure 1.1). Other derivatives play essential roles in diverse and important functions including lipid and amino acid syntheses, pigment synthesis and accumulation, and starch metabolism and storage.

The functions of plastids in plants extend far beyond photosynthesis. Plastids are able to take on different forms and functions in different tissues in higher plants. Plastid differentiation is influenced by developmental and environmental cues. Chromoplasts are brightly coloured plastids that have the ability to synthesize and accumulate the carotenoid pigments responsible for the yellows, oranges and reds of many flowers and fruits. Amyloplasts are major constituents of plant organs storing starch granules, such as the seed endosperm. Other plastid types are chloroplast precursor organelles called etioplasts, found in dark-grown plants of most angiosperms, which exhibit light-dependent chlorophyll synthesis (Sperling et al., 1998); and gerontoplasts in senescing leaves, which derive from chloroplasts due to chlorophyll breakdown and other catabolic processes. Plastids have the ability to differentiate their morphology and functions, or re-differentiate them, in response to developmental and

environmental signals (Lopez-Juez and Pyke, 2005; Jarvis and López-Juez, 2013). A diagrammatic representation of the diversity of plastid types and their interconversions is shown in Figure 1.2.

The metabolically and biosynthetically diverse function of plant plastids include the synthesis of amino acids, fatty acids, starch, chlorophylls, carotenoids, signalling molecules, molecular precursors, and the assimilation of nitrogen and sulphur (Wise, 2007; Sakamoto et al., 2008). Such diversity of functions mediated by plastids indicates that particular importance in cellular homeostasis, and in the perception and response to signals during plant development and response to stress. The latter point is especially significant as photosynthesis is a major source of reactive oxygen species (ROS), which act in signalling, but can easily become damaging if not regulated (Asada, 2006; Shapiguzov et al., 2012).

The biochemical functions and differentiation state of plastids are defined by the organellar proteome, which is itself influenced by the combined effects of gene expression, protein targeting, import and signalling (Pogson et al., 2008; Kessler and Schnell, 2009). The mechanisms that serve to coordinate expression of chloroplast nuclear genes to control the metabolic and developmental status of the chloroplast include both anterograde (nucleus-to-plastid) and retrograde (plastid-to-nucleus) controls. The regulation of anterograde signaling depends upon nuclear protein that regulate the transcription and translation of plastid genes (Goldschmidt-Clermont, 1997), while the retrograde signalling occurs when plastid send signals to the nucleus to control in response to the metabolic and/or developmental state of the plastid (Nott et al., 2006). Plastid biogenesis requires the coordinated expression of genes distributed between the nuclear and plastid genomes, therefore the integration of retrograde and anterograde signalling systems is essential to ensure the effective functioning of the chloroplast (Gray, 2005).

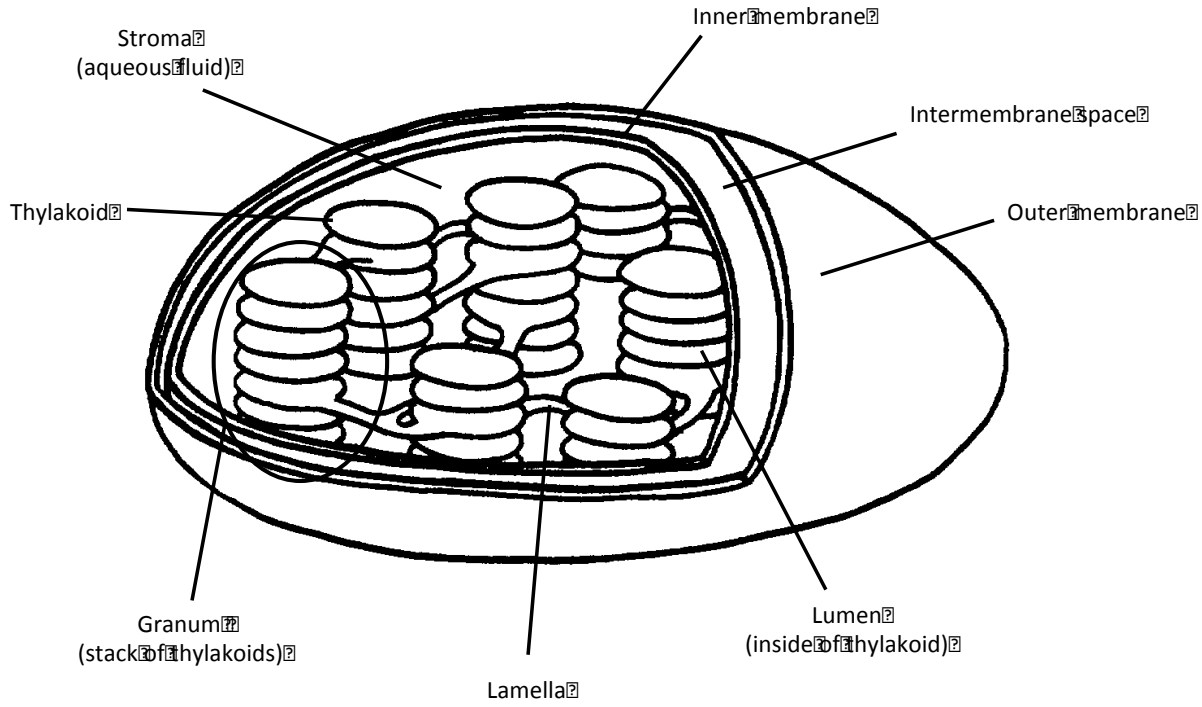

Figure 1.1 Structure illustrations of chloroplast. Chloroplasts can be found in the green tissue of plant. The chloroplast has an inner and outer membrane with an empty intermediate space in between. The outer and inner envelope chloroplast membranes are known as TOC and TIC, respectively. Stacks of thylakoids, called granum (plural grana), and the aqueous fluid, called stroma can be found inside of the chloroplast. The space inside the thylakoid discs is called the lumen. The thylakoids are the site of the light-dependent reactions of photosynthesis. All the thylakoids of a granum are connected with each other, and the grana are connected by intergranal lamellae.

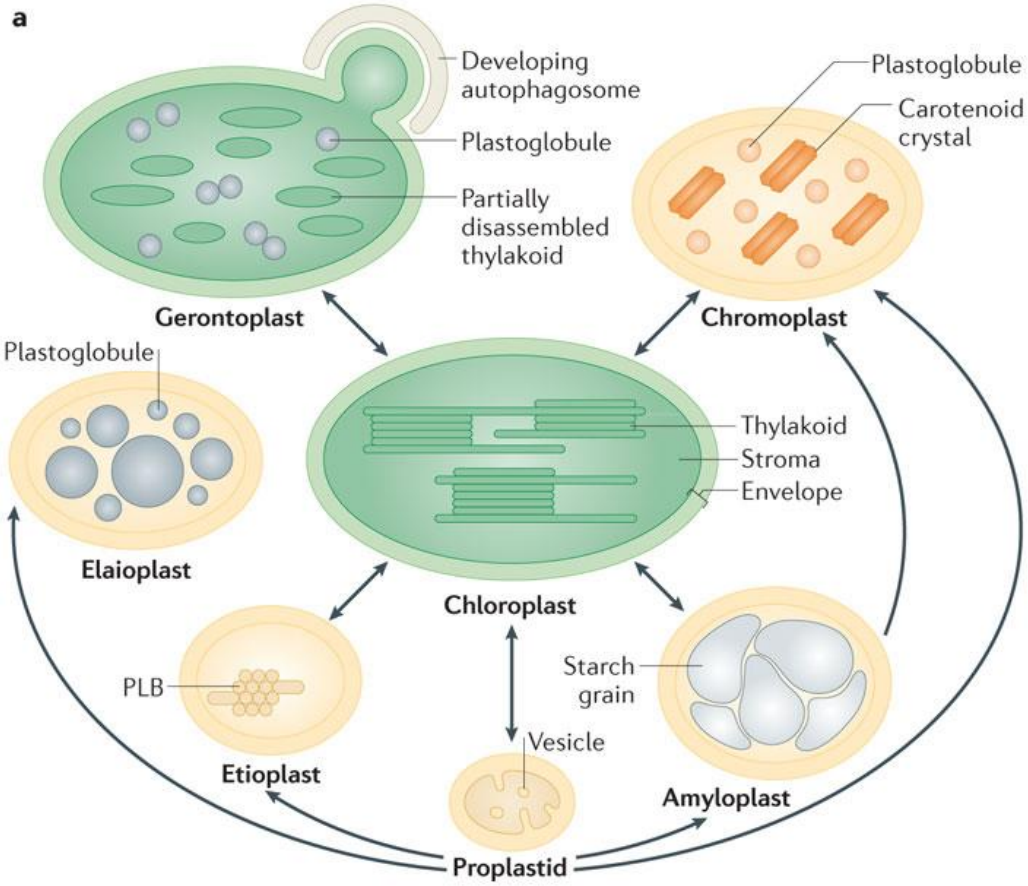

Figure 1.2. Diversity of plastid forms and their interconversions. Plastids exist in different forms that are functionally and morphologically distinct, and have the ability to re-differentiate between these forms in processes influenced by developmental and environmental signals. The interconversions, shown as the arrows, are controlled by the regulation of protein import from the cytosol into plastids. Well known plastid types include: chloroplasts, the photosynthetic plastids in leaves; chromoplasts, the coloured plastids for carotenoid pigment synthesis and accumulation in fruits and flowers; amyloplasts, the starch storage plastids in roots, tubers and seeds; etioplasts, the chloroplast precursor organelles in dark-grown plants; and gerontoplasts, the degraded plastids in senescent leaves. This diagram was taken from Jarvis and López-Juez (2013).

1.2 Plastid biogenesis and protein import

Plastid biogenesis is coordinated and integrated with environmental cues and endogenous signals, and an important component of the process is protein translocation into the plastid from the cytosol. Most plastid proteins are nuclear-encoded and synthesized in the cytosol as precursor proteins with N-terminal targeting signals, called transit peptides. These precursor proteins are targeted to plastids through the translocons at the outer/inner envelope of chloroplasts, TOC and TIC complexes (Jarvis, 2008). The identification of the components of the TOC and TIC complexes was initially achieved through the biochemical analysis of isolated pea chloroplasts (Hirsch et al., 1994; Kessler et al., 1994; Schnell et al., 1994; Wu et al., 1994; Seedorf et al., 1995; Tranel et al., 1995; Bédard and Jarvis, 2005).

All known chloroplast OEM proteins are encoded by nuclear genes (Lee et al., 2014). Like the plastid preproteins, these are translated in the cytosol, and then targeted to the chloroplast OEM for assembly. Chloroplast OEM proteins fall into two broad categories, those with α-helical transmembrane domains (TMD), and those which form a β-barrel structure from multiple β-strands. How TMD proteins are assembled into the membrane is not yet known. However, there is evidence that the TOC may be required for targeting and insertion of some of these proteins (Wallas et al., 2003; Tu et al., 2004; Huang et al., 2011). The well-established β-barrel OEM proteins, Toc75, and the close relative of Toc75, outer envelope protein of 80 kDa (OEP80), are first imported and then assembled (Oh and Hwang, 2015).

The TOC machinery plays critical roles in precursor protein recognition and outer membrane translocation (Jarvis, 2008). The major components of the TOC apparatus are Toc159, Toc34 and Toc75 (numbers indicate molecular weight in kDa). Toc159 and Toc34 are receptor proteins with GTPase domains that regulate recognition of precursor proteins, while Toc75 is a β-barrel protein that forms the channel for preprotein translocation (Schnell et al., 1994; Kessler and Schnell, 2002; Smith et al., 2002; Sun et al., 2002; Wallas et al., 2003). The complex exists in multiple forms with different protein import receptor isoforms. Another

putative component of the TOC apparatus is Toc64, but it does not play a major role in the import mechanism and its functions remain to be elucidated (Sohrt and Soll, 2000; Hofmann and Theg, 2005; Aronsson et al., 2007).

Genetic analysis in the model plant *Arabidopsis thaliana* identified mutants with defects in the protein import machinery, such as the *ppi1* mutant that lacks a Toc34 receptor isoform called atToc33 (Jarvis et al., 1998). Further analysis of the *ppi1* mutant led to the hypothesis that atToc33 is specifically involved in the import of photosynthesis-related preproteins (Kubis et al., 2003). It is now generally accepted that in Arabidopsis (and other plants), the main isoforms of the TOC receptors (i.e., atToc33 and atToc159) have specificity for highly-abundant photosynthetic precursor proteins, whereas other isoforms (i.e., atToc34 and atToc132/120, respectively) recognize non-photosynthetic, housekeeping precursor proteins (Bauer et al., 2000; Gutensohn et al., 2000; Kubis et al., 2003; Ivanova et al., 2004; Smith et al., 2004). The model for the operation of client-specific protein import pathways is shown in Figure 1.3. The regulated operation of these different import pathways influences the eventual composition of organellar proteome and may prevent highly abundant photosynthetic proteins from outcompeting the import of equally important but less abundant housekeeping proteins, and this in turn controls the developmental transitions by which plastids differentiate and interconvert from one type to another (Jarvis, 2008).

At the inner envelope membrane, the TIC complex mediates the translocation of the preprotein through the inner envelope membrane with the help of various molecular chaperones where the higher energy requirement is known to be required for import (Theg et al., 1989). Although several TIC components have been identified (Tic20, Tic21, Tic22, Tic32, Tic40, Tic55, Tic56, Tic62, Tic100, Tic110, and Tic214), some of the roles of the components remain unclear (Jarvis and López-Juez, 2013). Kouranov and Schnell (1997) identified Tic21, Tic22, and Tic14 as the major crosslinking targets during inner membrane translocation. Tic20 and Tic22 were later identified as proteins that associate with the transit peptide of preproteins under

conditions promoting full translocation (Kouranov et al., 1998). Tic110 has previously been identified as an integral inner membrane component in complexes containing proteins at the late stage in import (Schnell et al., 1994; Wu et al., 1994; Lübeck et al., 1996), and may function in association with the putative co-chaperone, Tic40 (Kessler and Schnell, 2009; Li and Chiu, 2010; Jarvis and López-Juez, 2013; Paila et al., 2015). Tic20, Tic110 and Tic40 had been proposed to be central to protein translocation across the inner envelope membrane. However, recent progress in identifying the TIC components has discovered a 1-megadalton (MDa) TIC complex, containing Tic20 (as a core), Tic56, Tic100, and Tic214 but excluding Tic110 and Tic40 (Kikuchi et al., 2013). One possible explanation is that the 1 MDa TIC complex acts upstream with a channel-forming role, with the putative Tic110-containing motor complex acting downstream of that (Nakai, 2015). Additional proteins, Tic32, Tic55 and Tic62 may be involved in the redox regulation of chloroplast protein import (Balsera et al., 2010). A schematic illustration of the components involved in the translocation of the preprotein across the chloroplast envelope membranes is shown in Figure 1.3.

In parallel with the action of chaperones during mitochondrial and endoplasmic reticulum protein transport, the chloroplast import system also hypothesize the use of chaperones to drive the protein translocation into the organelle interior to ensure the protein reaches its destination (Bruce, 2000). The cytosolic proteins (14-3-3, Hsp70 and Hsp90) are proposed to form ‘guidance complexes’ that deliver precursor proteins to the TOC complex. The TIC complex, with the aid of chaperones, mediates the translocation of preproteins through the inner envelope membrane. Upon arrival in the stroma, the transit peptide is cleaved by stromal processing peptidase (SPP). The TIC components, Tic110, Tic40, and the Hsp93 molecular chaperone have been proposed to function together at the inner envelope as part of a motor complex, which drives protein import at the expense of ATP hydrolysis. Further analysis of their involvement in chloroplast protein import, genetically, has suggested that these components are important for both photosynthetic and non-photosynthetic protein

translocation (Kovacheva et al., 2005). Many questions concerning the specific functions of chaperones during protein import into chloroplasts still remain to be addressed.

Schematic illustrations of chaperone involvement in the stroma, and in the cytosol and intermembrane space during protein transport to chloroplasts are shown in Figures 1.3 and 1.4, respectively.

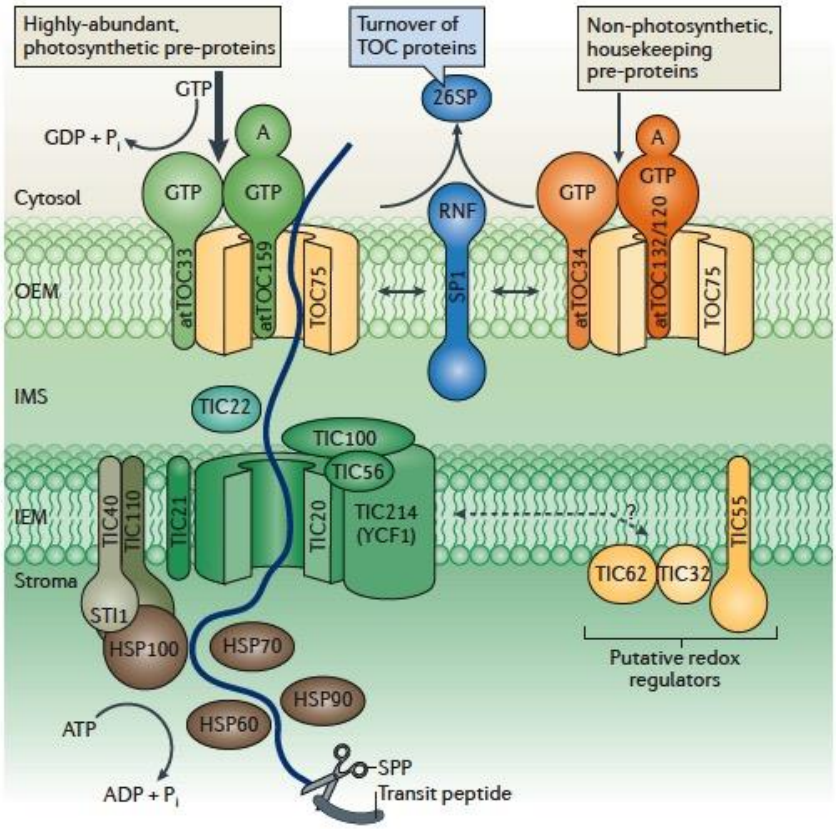

Figure 1.3. Model for the operation of TOC-TIC machinery mediates client-specific protein import pathways and is controlled by UPS system. A schematic illustration showing the TOC and TIC complexes (translocons at the outer/inner envelope of chloroplasts,) and other protein components as the chloroplast protein import apparatus including chaperone involvement in the stroma. The outer envelope membrane (OEM) components of TOC GTPases, accounting for the GTP requirement during the early stages of import that may participate in transit peptide recognition and to have different affinity to two different groups of preproteins. Toc33 and Toc159 associate in a TOC complex specific for photosynthesis-related preproteins, while Toc120 and Toc132 associate preferentially with Toc34 to form a TOC complex specific for non-photosynthetic or housekeeping preproteins. SP1 is a RING finger (RNF) E3 ligase in the OEM that targets TOC proteins for ubiquitination and turnover by the 26S proteasome (26SP), which results in the reorganization of the organellar proteome and balancing of client-specific pathways. While several TIC candidate proteins including Tic110, Tic40, Tic22, and Tic21

were identified, the core TIC complex remained unclear. Recently, the TIC complex consisting of Tic214 (formerly Ycf1), Tic100, Tic56, and Tic20 has been identified and characterized as a general TIC translocons of 1 MDa (Kikuchi et al., 2013). The latter complex drive protein import and/or assist in protein folding at the expense of ATP hydrolysis with the aid of various stromal chaperones. Components of a putative inner membrane regulatory system that controls protein import in response to redox signals (indicated by the question mark) names as Tic62, Tic32 and Tic55 are also shown. This model has not been widely accepted, and indeed one of the components (Tic55) was shown by Hauenstein et al. (2016) to be involved in chlorophyll catabolism, not import. HSP, heat shock protein; IMS, intermembrane space; SPP, stromal processing peptidase. This diagram was taken from Jarvis and López-Juez (2013).

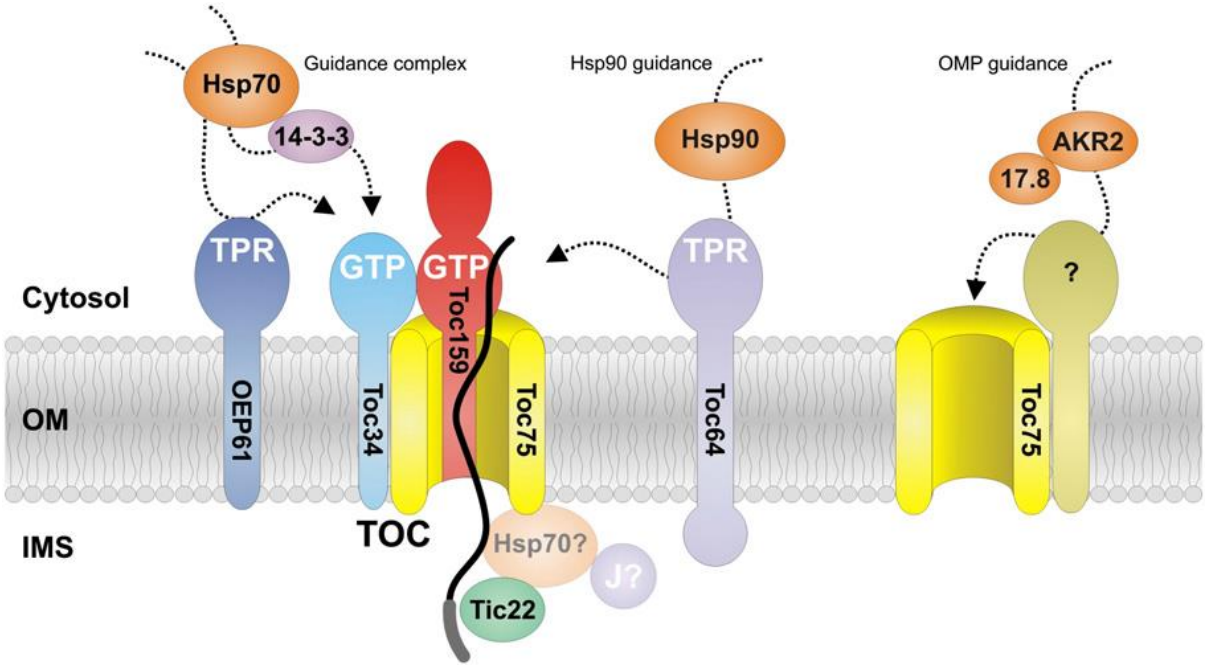

Figure 1.4. Chaperone involvement in the cytosol and intermembrane space during protein transport to chloroplasts. The cytosolic proteins (Hsp70, 14-3-3, Hsp90 and AKR2) recognized the nuclear-encoded proteins destined for the chloroplasts to the TOC complex. Each of these soluble factors mediates the delivery of different subset of preproteins (either phosphorylated or non-phosphorylated) to peripheral TOC component, before proceed to their onward passage to the core TOC machinery. The preproteins and its transit peptide are represented by a wavy black line and thick grey line, respectively. Functional domains of the proteins are indicated in white text. TOC, translocon at the outer envelope membrane of chloroplasts; OM, outer envelope membrane; IMS, intermembrane space. This diagram was taken from Flores-Pérez and Jarvis (2013).

1.3 Regulation of plastid biogenesis by the ubiquitin-proteasome system (UPS)

The discovery of the ubiquitin-proteasome system has developed new knowledge of major protein degradation pathway in the cell (Ciechanover, 1998). In recent years, increasing number of E3 ubiquitin ligases and their substrates further revealed the importance of the ubiquitination machinery in several eukaryotic cellular functions, including regulation of plant developmental processes and responses to abiotic and biotic stresses (Hellmann and Estelle, 2002). Proteolysis via the ubiquitin-proteasome system (UPS) involves the attachment of ubiquitin to a target protein. This attachment process is conducted by the sequential actions of three enzymes, termed E1 (activating enzyme), E2 (conjugating enzyme) and E3 (ligating enzyme, or ligase). Once modified, a ubiquitinated protein will typically then be degraded by the 26S proteasome (Vierstra, 2009).

Based on sequence homology to known ubiquitin-related proteins, it has been estimated that 5% of the predicted 25,000 proteins in Arabidopsis are function in the ubiquitin-proteasome pathway (Hellmann and Estelle, 2002). The E3 ubiquitin ligases have attracted the most attention, and the best-characterized plant nuclear RING protein is COP1 (constitutive photomorphogenesis). Studies have shown that COP1 functions as an E3 ubiquitin ligase responsible for the targeted degradation of HY5 through the 26S proteasome-mediated degradation in the nucleus (Osterlund et al., 2000). HY5 is a bZIP transcription factor that binds directly to the promoters of light-inducible genes, promoting their expression and photomorphogenic development (Oyama et al., 1997; Chattopadhyay et al., 1998), while COP1 is required to repress light-regulated development in the dark. Specificity of COP1–HY5 interaction is confirmed by direct correlation between the abundance of HY5 with the extent of photomorphogenic development (Osterlund et al., 2000). Genome-wide annotation of the human E3 superfamily identifies MULAN, another RING finger protein homologue, which function as the regulator of mitochondrial dynamics (Li et al., 2008a). MULAN has two transmembrane domains with an orientation in such that its C-terminal RING finger is exposed

to the cytosol, where it has access to other components of the ubiquitin system. Both an intact RING finger and the correct subcellular localization to the organelle's outer membrane were required for interfering with mitochondrial dynamics, which further suggest an ubiquitin-mediated mechanism responsible for mitochondrial trafficking and morphology (Li et al., 2008a).

As most UPS targets are identified by E3 ligases, the discovery of *SP1* (*SUPRESSOR OF PPI1 LOCUS1*), which encodes the RING-type ubiquitin E3 ligase in the plastid outer membrane, was of considerable interest in this regard. Moreover, it also revealed for the first time that the UPS directly regulates plastid biogenesis (Ling et al., 2012). SP1 was identified as a novel regulator of plastid protein import in a mutagenesis screen for second site suppressors of *plastid protein import1*, (*ppi1*) (Ling et al., 2012). The *sp1* mutation was found to partially recover the *ppi1* pale-yellow phenotype, and increased the ability to import photosynthetic proteins, resulting in better-developed chloroplasts and a greener plant. SP1 was shown to be an integral component of the plastid outer membrane, and was predicted to have two TMDs, a C-terminal cytosol-facing RING domain and an intermembrane space domain connecting the two TMDs (Figure 1.5). The orientation of its cytosolic RING domain gives SP1 access to other components of the UPS, and the intermembrane space domain of SP1 was shown to be important for interaction with target proteins. Substitution of a critical residue in the RING domain interfered with ubiquitination of SP1 *in vitro* and *in vivo*, which led to the conclusion that SP1 is regulated by auto-ubiquitination like other E3 ligases (De Bie and Ciechanover, 2011; Ling et al., 2012).

The levels of the TOC receptor isoforms vary developmentally depending on the biochemical requirements of the plastids. As noted earlier, the consequence of TOC complex reorganization controls the proteomic composition, developmental fate, and functions of the plastids. The mutants of TOC components differ in the extent to which they affect the import of different groups of preproteins, or the biogenesis of different plastid types. Mutants of

atToc33, have a pale-yellow phenotype, while mutants of atToc159 *plastid protein import2* (*ppi2*) have albino phenotypes. These phenotypes reflect reduced import of photosynthesis-related proteins and impaired chloroplast biogenesis (Jarvis et al., 1998; Bauer et al., 2000; Kubis et al., 2003). Although *ppi1* produced a distinctive pale-yellow phenotype and reduced the ability to import photosynthetic proteins, it is still able to complete its life cycle (Jarvis et al., 1998).

Ling et al. (2012) also revealed that the SP1 acts directly upon plastids to regulate their development by targeting components of the TOC machinery for proteasomal degradation. *In vivo* analysis of the *sp1* mutant and SP1 overexpressor in Arabidopsis showed an inverse correlation between SP1 expression levels and the abundance of TOC proteins. Co-immunoprecipitation and *in vitro* pulldown results showed that SP1 can interact with many Arabidopsis TOC proteins (atToc159, atToc132, atToc120, atToc34, atToc33 and atToc75), and the SP1 intermembrane space domain mediated such interaction. The ubiquitination of atToc159, atToc75 and atToc33 was shown to be mediated via an SP1-dependent manner in which the extent that these components were ubiquitinated was dependent on the expression level of SP1 (Ling et al., 2012). The stabilization of polyubiquitinated atToc33 upon addition of the proteasome inhibitor (MG132) was shown to be direct evidence that the ubiquitinated TOC components are directed to the proteasome for degradation. Further evidence supporting the link between protein import and the proteasome was described when phenotypes of *ppi1* and an atToc75-III hypomorphic mutant allele, *toc75-III-3*, were suppressed by the proteasome mutations *pbe1* or *rpn8a*, essentially phenocopying the suppression mediated by *sp1* (Ling et al., 2012).

Data described above suggest that SP1 acts to remodel TOC complexes in order to promote the interconversion of different plastid types. For example, SP1 has been shown to have important roles in leaf senescence and de-etiolation in Arabidopsis (Ling et al., 2012). Leaf senescence is considered a complex process that responds to various environmental and

internal factors and forms an integrated developmental age-dependent senescence pathways regulatory network. During leaf senescence, the process is accompanied by decreased expression of genes related to photosynthesis (e.g., *CAB2*) and protein synthesis (e.g., *RPS*, *RBC*) and an activation of the senescence-associated genes (*SAGs*) expression, which are responsible for executing the degeneration process and ultimately lead to cell death. The environmental factors that affect leaf senescence include both biotic and abiotic stresses, while the internal factors include various phytohormones and reproductive development as well as developmental age. During chloroplast-to-gerontoplast conversion in leaf senescence, with the assistance of SP1, TOC complexes might rearrange to contain different component isoforms, allowing different proteins to be imported as required. The level of chlorophyll contents and F_v/F_m was measured in dark-treated leaves of different genotypes with altered SP1 expression to analyse the extent of senescence. Elevated SP1 expression caused both parameters to decline more rapidly, indicating accelerated senescence, whereas reduced SP1 expression had the opposite effects (Ling et al., 2012).

Upon exposure to light, dark-grown (etiolated) plants undergo an extensive change in gene expression leading to accumulation of photosynthetic proteins that enables the greening of young plants, which is indicative of chloroplast biogenesis. During such de-etiolation, the import of high-abundant, photosynthesis-associated proteins leads to a major proteome changes in the chloroplast, and for this to occur efficiently, remodelling of the TOC complex is required, most notably, the ratio of atToc159 to atToc132/120 increased markedly in the WT, but hardly at all in the *sp1* mutant, possibly to enable the biogenesis of photosynthetic proteins, which rapidly accumulate during de-etiolation.

The remodelling of the import machinery therefore requires SP1 activity to target unwanted TOC components for degradation by the UPS (Kessler, 2012; Ling et al., 2012). An illustration of the involvement of SP1 and the UPS in remodelling the TOC complex during chloroplast biogenesis is shown in Figure 1.5.

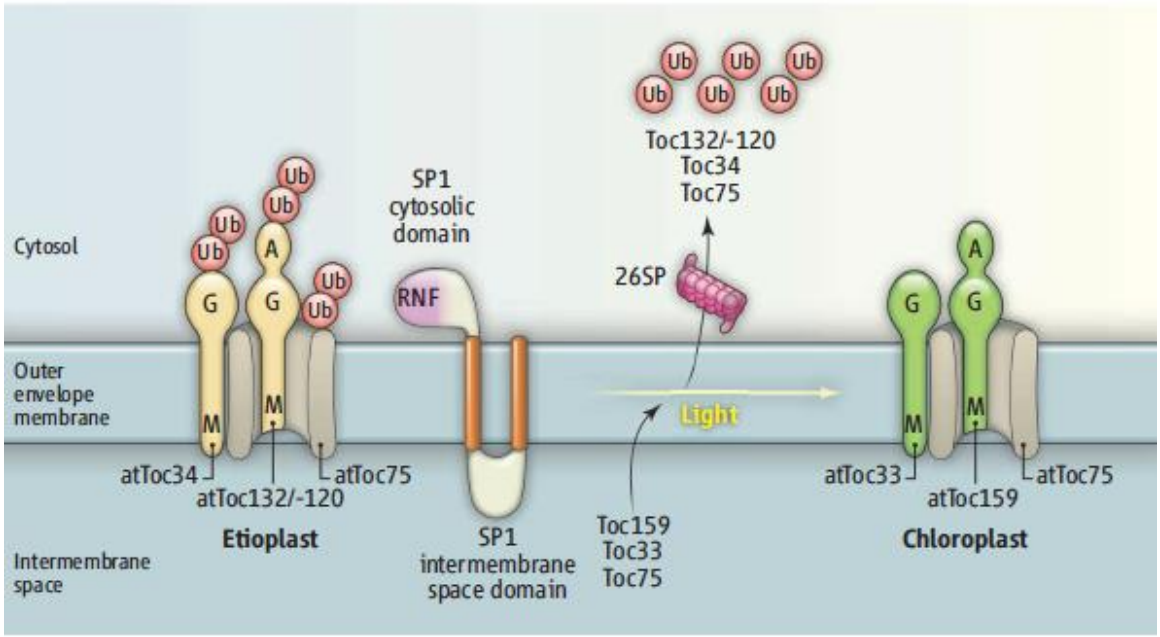

Figure 1.5. Model for the role of SP1 in chloroplast biogenesis. When a dark-grown plant containing etioplasts senses the presence of light, it undergoes an extensive change in gene expression leading to the accumulation of photosynthetic proteins. The necessary import of highly-abundant, photosynthetic proteins requires remodelling of the TOC machinery to allow efficient import of these proteins, using a TOC complex consisting of atToc159, atToc33 and atToc75. The model shows the reorganization of the TOC machinery and the role of SP1 and the UPS in this process. As part of this process, SP1 selectively targets unwanted TOC components (atToc132/120, atToc34 and atToc75) for degradation by the UPS. This diagram was taken from Kessler (2012) and is based on the results of Ling et al. (2012).

1.4 The potential role of SP1/SPL2 during plastid biogenesis in important crops

As already noted, the *SP1* gene encodes an E3 ligase of the plastid outer membrane that functions as a regulator of the TOC machinery (Ling et al., 2012). The dynamic regulation of the import machinery by SP1 can control the organellar proteome, promoting plastid interconversions (Jarvis and López-Juez, 2013). As already noted, studies have shown that mutant *sp1* plants of Arabidopsis undergo de-etiolation (etioplast-to-chloroplast conversions) and senescence (chloroplast-to-gerontoplast conversions) less efficiently than WT, whereas overexpression of SP1 accelerates these interconversions (Ling et al., 2012).

As plastids and their interconversions are important throughout plant development, the manipulation of SP1 activity may enable greater control over many aspects of plant development in crops. Thus, the discovery of SP1 suggested potential applications in agriculture. In fact, SP1 could conceivably find diverse applications, enabling modification of any developmental process in which plastids change type or otherwise undergo proteome reorganization.

In this thesis, I analysed the function of SP1 in two major crops, tomato and wheat, making use of transgenic plants with elevated or reduced levels of SP1 expression. Tomato was used to assess the consequences of SP1 manipulation in relation to chloroplast-to-chromoplast conversion during fruit ripening. In parallel, both crop species were used to assess for effects on leaf senescence, enabling direct comparison with the Arabidopsis senescence data of Ling et al. (2012).

1.4.1 Tomato

Tomato (*Solanum lycopersicum*) is one of the most important crops. Based on the world's tomato consumption as reported by the Food and Agriculture Organization (FAO) of the United Nations from the year 2002 to 2009, there was an increase in consumption pattern every year. In addition, the annual growth rate of tomato consumption worldwide for the same duration

was 3% over that period, while it was 2.4% for other vegetables (Valenciano and Battistuzzi, 2012). Numerous tomato cultivars are grown all over the world, differing in aspects related to yield, resistance, and fruit shape, taste and quality, to meet the differing demands and quality requirements of both the fresh and processing markets. Due to the plant's characteristics, such as self-pollination, diploid state, and ease of cross-pollination, tomato has also become a favourite model species for classical genetic studies (Rick and Yoder, 1988; Pavan et al., 2009). Moreover, with the advance of genome sequencing, its modestly sized genome (950 Mb/haploid genome) has been fully sequenced (Tomato Genome, 2012) and made publicly available (http://solgenomics.net/).

In recent years, with the aid of plant transformation using co-cultivation with the bacterium *Agrobacterium tumefaciens* (Sun et al., 2006; Garcia et al., 2015), the genetic basis of many important traits such as fruit quality, yield and stress resistance has been unravelled. Tomato has been an excellent model system to study both basic and applied aspects of plant biology, and has been subject to breeding to improve its qualities for both fresh market and processing purposes (Foolad, 2007). In the scope of my thesis, one particular advantage of tomato was that its use enabled me to investigate SP1 function in relation to chromoplast development in the fruits.

1.4.1.1 Chromoplast biogenesis and fruit ripening

Chromoplasts are carotenoid-accumulating plastids that give colour to many flowers and fruits, and, like all other plastids, chromoplasts are descendants of prokaryotes (Camara et al., 1995). Chromoplast differentiation proceeds from preexisting plastids, most often chloroplasts, the photosynthetic plastids. Transformation of chloroplasts to chromoplasts occurs in ripening fruits involve changes in morphology and plastid composition, including remodelling of the internal membrane system, an increase in the size and number of plastoglobulli, as well as changes in stromule morphology (Harris and Spurr, 1969; Bathgate et al., 1985; Simkin et al., 2007; Egea et al., 2010). However, the accumulation of pigments

during fruit ripening or flower development in chromoplasts is functionally different from senescence-derived plastids. The disappearance of chlorophyll and retention of carotenoids produces the yellow colour of senescent plastids without undergoing a *de novo* carotenoid biosynthesis, and in contrast to chromoplasts, they are subjected to an extensive loss of plastidic DNA and are called gerontoplasts (Matile, 2000).

During tomato fruit ripening, photosynthetic chloroplasts differentiate into chromoplasts. This transition process represents one of the most visible phenomena associated with fruit development. As chlorophyll autofluorescence and carotenoid autofluorescence emit light of wavelengths between 740 and 750 nm and between 500 and 510 nm, respectively, the transition from chloroplast to chromoplast can be visualized by exploiting the different autofluorescence properties of the chlorophyll and carotenoid pigments that characterize the different plastid types (Egea et al., 2010). Plastids containing mainly chlorophyll appear at the mature green stage, those containing only carotenoid appear at the fully ripe stage, and those containing both chlorophyll and carotenoid appear at the breaker stage (Egea et al., 2010). A representative image showing various fruit stages are shown in Figure 3.2B.

During the differentiation process, the plastid genome is essentially stable and transcriptional activity is restricted. The build-up of chromoplasts during fruit ripening is dependent heavily upon the import of nuclear-encoded non-photosynthetic proteins, which remodel the organellar proteome, and is needed to meet the metabolic shifts and energy demands of the cells (Chi et al., 2013). During chromoplast differentiation, many genes for plastid-localized proteins are known to display significant modifications in their expression, transcriptionally and translationally. For example, genes involved in carotenoid biosynthesis, such as the *Lycopene β-cyclase* (*CYC-B*) gene are up-regulated (Dalal et al., 2010), whereas other genes involved in photosynthetic activity, such as the major light harvesting chlorophyll *a/b*-binding protein (LHCP) and small subunit of ribulose-1,5-bisphosphate carboxylase/oxygenase (Rubisco) genes, are down-regulated during chromoplast formation (Pech et al., 2014).

The detection of TOC/TIC proteins, chaperonin-associated machinery and proteins translocated into the lumen, which represent the most abundant functional group in tomato fruit chromoplasts, has provided confirmation that the plastid protein import system and active protein metabolism are present within chromoplasts, indicating the translocation of proteins into plastids is of importance for chromoplast biogenesis. In addition, the presence of proteins involved in protein synthesis and degradation such as ribosomal proteins, GTP binding elongation factor Tu family proteins, peptidases, aspartic proteinases, Clp proteases, and FtsH proteases was also detected (Barsan et al., 2010; Egea et al., 2010; Wang et al., 2013; Suzuki et al., 2015). Moreover, a proteomic study of tomato chromoplasts also revealed extensive amounts of nuclear-encoded non-photosynthetic proteins, such as those involved in the biosynthesis of fatty acids, amino acids, carotenoids, vitamins, hormones and volatile compounds (Barsan et al., 2010; Barsan et al., 2012; Wang et al., 2013; Suzuki et al., 2015).

During the onset of tomato fruit ripening, the increased requirement for non-photosynthetic plastid proteins, particularly those involved in carotenoid biosynthesis and chromoplast differentiation, correlates with the increase in number and length of stromules at the inner mesocarp to provide a greater import area to meet the demand for novel proteins (Kwok and Hanson, 2004). Once the fruit reaches the mature red stage, a plastidic signal peptidase (PLSP1) involved in thylakoid development through its involvement in processing the Toc75 envelope protein and OE33 thylakoid luminal protein was absent (Shipman-Roston et al., 2010). This is consistent with the disruption of the machinery for thylakoids and photosystem biogenesis. The regulation of such a complex event involving morphological changes of plastids and the elements of protein import machinery would be expected to require the reorganization of the TOC machinery. In Arabidopsis, SP1 controls the plastid proteome and plastid developmental transitions by regulating protein import through the selective targeting of TOC complexes for degradation in order to promote the interconversion of different plastid types, such as during de-etiolation and leaf senescence (Ling et al., 2012). If SP1's roles in plastid transitions are conserved across plant species, SP1 action may also be important

during chromoplasts biogenesis, and could conceivably be manipulated to trigger a more rapid and/or delayed fruit ripening process, although the direct evidence of this is still unknown.

1.4.1.2 Fruit quality

In tomato, fruit quality is mainly determined by traits linked to the appearance, firmness, flavour, ripening behaviour, and shelf life. Yield, disease resistance, and ease of harvest are other important traits in tomato (Grierson and Kader, 1986). Among the main factors affecting the fruit appearance and consumer acceptance are colour and size. The external colour of tomatoes is the result of both flesh and skin pigmentation and varies dependent on the genotype. Since colour is one of the main indicators of tomato ripeness, several colour rating scales have been developed for classifying the ripeness stages of tomatoes. A subjective method with six classes of tomato ripeness from the US Department of Agriculture (USDA) (Anon, 1975) is shown in Table 1.1. An objective method based on precise, non-destructive colorimetric measurements made using a chroma meter (which measures *L**, *a** and *b** values) (López Camelo and Gómez, 2004) is also shown in Table 1.1. In this thesis, fruit ripening analysis was conducted by taking chroma meter readings (*a*/b** values) at the breaker stage all the way through to the mature red stage, and the readings were defined by reference to the USDA tomato colour stages (Anon, 1975) as determined by Batu (2004).

The range of fruit sizes varies among cultivars and the size preference differs among consumers and on the intended use of the fruits. Generally, when fruits are picked at the green stage, the smaller fruits are more likely to be immature and likely to be delayed in ripening. However, if the fruits are harvested at the breaker stage or more advanced stages of ripeness, no effect of size is noticeable on the ripening rate or composition and flavour at the table-ripe stage (Grierson and Kader, 1986). In this thesis, the size of fruit harvested at the breaker stage was analyzed by measuring the average equatorial diameter particularly to ensure that the fruits used in the analysis have the final size at harvest to avoid any interference with the ripening duration.

After visual appearance, the most important factor in tomato quality is firmness. Firmness is closely related to ripeness stage and can affect susceptibility of fruits to physical damage and consequently their shipping quality. Methods for measuring tomato firmness can be destructive or non-destructive. In this thesis, the fruit firmness at defined developmental stages was determined non-destructively by measuring resistance to compression force applied at multiple points on the fruit using a durometer following the method described by Arazuri et al. (2007).

Other important determinants of quality of tomatoes are flavour and nutritional value. As chromoplasts develop, carotenoid pigmentation increases. This developmental process participates in many other reactions including the synthesis of sugars, lipids, aromatic compounds, vitamins, and hormones, which impact on fruit quality directly (Egea et al., 2010). Thus, a better tomato variety may offer benefits such as fruit with a more sweet/acidic flavour, or healthier nutrient compositions.

Table 1.1. Ripeness classes of tomato fruit. Konica Minolta colour (*a**/*b**) values of tomatoes at the six USDA colour stages, defined as previously described (Batu, 2004). All percentages refer to both colour distribution and intensity following the USDA tomato ripening class descriptions (Anon, 1975).

Minolta colour (*a/*b**) values range**	**Class**	**Description**
-0.59 to -0.47	Green	Entirely light- to dark-green, but mature
-0.47 to -0.27	Breaker	First appearance of external pink, red or tannish-yellow colour; not more than 10%
-0.27 to 0.08	Turning	Over 10% but not more than 30% red, pink or tannish-yellow colour
0.08 to 0.60	Pink	Over 30% but not more than 60% pinkish or red colour
0.60 to 0.95	Light-red	Over 60% but not more than 90% red colour
0.95 to 1.21	Red	Over 90% red; desirable table ripeness

1.4.2 Wheat

Wheat (*Triticum aestivum*) is the leading cereal grain produced in the world today, in terms of total harvested weight and the amount used for human and animal nutrition (Bushuk and Rasper, 1994). Wheat is used for several purposes, depending on its varieties, each with different quality standards. For example, the common hard wheat for bread, and the common soft and durum wheat for biscuit and pasta, respectively (Bushuk and Rasper, 1994). Wheat is an important source of carbohydrate component in the diets of humans and livestock, and in numerous important industrial application (Shewry and Hey, 2015). When eaten as the whole grain, wheat is a source of fiber and multiple nutrients. Although wheat contains approximately 10-12% protein, wheat is mainly regarded as starch, which is an important source of metabolizable energy (Austin et al., 1986).

Wheat is one of the most important food crops as approximately 670 million tons are produced annually. The developing regions (including China and Central Asia) produced roughly 53% of the total harvested area and 50% of the production. Wheat production become even more significant as the global population increases as the food demand is growing by 1% annually (Shiferaw et al., 2013). Extensive wheat improvements through various conventional plant breeding approaches have significantly contributed to global wheat production. However, the future of wheat research requires integrated, multidisciplinary activity which includes novel technology to ensure an efficient crop production output (Mujeeb-Kazi, 2006).

1.4.2.1 Amyloplast development

Amyloplasts typically develop from proplastids (Neuhaus and Emes, 2000; Hurkman et al., 2008). In cereal crops such as wheat, amyloplast development is mainly linked to starch synthesis in the endosperm. Such organelles possess numerous enzymatic activities related to starch synthesis, including ADP-glucose pyrophosphorylase (AGPase), starch synthase (SS), starch branching enzyme (BE), and starch debranching enzyme (DBE) (James et al., 2003; Hannah and James, 2008). Interestingly, the endosperm proteome identified in

amyloplasts isolated from 10 days post-anthesis wheat endosperm varies considerably throughout its development (Balmer et al., 2006; Hurkman et al., 2008). At early developmental stages, protein synthesis and assembly are the principal endosperm functions. At later stages of development, the accumulation of stress/defence-related proteins and storage proteins is found. However, carbohydrate metabolism involving starch biosynthesis enzymes mentioned earlier remains a major function during both early and late phases of grain development (Balmer et al., 2006; Hurkman et al., 2008). Balmer et al. (2006) also detected the presence of TOC/TIC proteins (such as Toc75, Tic110 and Tic40) and chaperonin-associated machinery, which has provided confirmation that the plastid protein import system and active protein metabolism are present within amyloplasts, indicating the translocation of proteins into plastids is of importance for amyloplast biogenesis.

The proteome changes that occur during amyloplast development indicate a need for efficient protein import mechanisms. The import of starch-related and other preproteins presumably requires an import pathway with specific receptors to recognize them. For examples, the detection of TOC receptor isoforms Toc34 by Balmer et al. (2006) indicated a possibility that protein import during amyloplast biogenesis is mediated mainly by the TOC receptor isoforms, which have the specificity to non-photosynthetic precursor proteins, and that SP1 acts to enable an appropriate balance of the import pathways (Ling and Jarvis, 2013). Numerous biotechnological approaches for improving starch biosynthesis and its regulation have been explored (Bahaji et al., 2014), but the role of plastid protein import has not previously been examined.

1.4.2.2 Starch biosynthesis in different types of plastids

Starch is the major higher plant storage carbohydrate. It is composed of two types of essential glucose polymer, amylose and amylopectin, which associate to form the molecular architecture of starch granules. Amylose consists of linear helical α-D-glucose chains while amylopectin molecules are branched polymer of glucose. The proportion of amylose and

amylopectin is variable between plant species, the developmental age of plant organ, and growth conditions (Martin and Smith, 1995). Starch forms complex semi-crystalline structures, starch granules, which accumulate in both non-photosynthetic (amyloplasts) and photosynthetic (chloroplasts) plastids. In each case, starch biosynthesis requires different regulation and distinctive pathways between starch biosynthesis in leaves (chloroplasts) and heterotrophic starch-storing organs such as tubers, roots and seed endosperms (amyloplasts) (Martin and Smith, 1995; Bahaji et al., 2014). In both chloroplasts and amyloplasts, starch biosynthesis in the plastid is controlled by the activity of AGPase, but not during the exchange of metabolites and the flow of carbon between cytosol and each plastid type (Okita, 1992).

In actively photosynthesizing leaves, the CO_2 fixation in the chloroplasts is tightly integrated with the synthesis of the main end products of photosynthesis, which are starch and sucrose. Carbon enters the pathway of starch biosynthesis via the gluconeogenesis pathway where the D-glycerate 3-phosphate (3-PGA) formed from the CO_2 fixation is converted into hexose monophosphates (Preiss, 1991; Okita, 1992). The hexose sugars are metabolized via glycolysis in the cytosol and then transported via the inorganic phosphate (Pi) translocator into chloroplasts for starch biosynthesis (Heldt et al., 1991). The vast majority of the NADPH and ATP provided by photophosphorylation at the thylakoid membrane is used for ADP-glucose synthesis, where the 3-PGA serves as the substrate (Stitt et al., 2010; Geigenberger, 2011). In isolated chloroplasts, the rate of CO_2 incorporation into starch was found to be directly correlated with 3-PGA levels and inversely correlated with Pi levels, consistent with the evidence that ADP-glucose formation is controlled by the AGPase via these metabolites (Preiss, 1982; Okita, 1992).

The starch biosynthesis in the amyloplasts is dependent on the cytoplasm for both energy and carbon resources, indicating that the biochemistry of this organelle is distinct from the ATP-generation and CO_2 fixation of chloroplasts in leaf tissue. Studies by Heldt et al. (1991) have shown that non-photosynthetic plastids from pea roots contain a modified inorganic Pi

translocator to mediate a counter exchange between Pi, dihydroxyacetone phosphate, 3-phosphoglycerate and glucose 6-phosphate during hexose sugar metabolism via glycolysis into three-carbon intermediates to be metabolized further for starch synthesis. The flow of carbon and the exchange of metabolites into starch follow a pathway whereby hexose monophosphates formed from sucrose are transported into the amyloplast without involving any C_3 intermediates (ap Rees and Entwistle, 1989; Okita, 1992; Shannon et al., 2009).

The difference between metabolic pathways involved in starch biosynthesis of chloroplasts and amyloplasts has allowed a comprehensive analysis of the transcript levels of genes that encode starch-synthesis enzymes. Studies by Ohdan et al. (2005) had utilized the complete genome sequence of Arabidopsis and rice to predict the total number of rice genes involved in starch biosynthesis. Four patterns of gene expression were identified, i.e. genes expressed early in grain formation, throughout endosperm development, low at the onset, but rise steeply at the start of starch synthesis in the endosperm and at the onset of grain development. These expression patterns were based on the quantitative real-time RT-PCR expression analysis of 27 rice genes encoding six classes of enzyme, i.e. AGPAse, SS, BE, DBE, starch phosphorylase and disproportionating enzyme in the developing seeds and in comparison to their transcript levels in the leaves. This methodology also revealed the dramatic effects of the rice *shrunken* mutation defect in the cytosolic *AGPase small subunit2b* (*AGPS2b*) transcription of the *AGPS2* gene in endosperm on the expressions of endosperm and leaf plastidial *AGPS1*, the endosperm cytosolic *AGPase large subunit2* (*AGPL2*), and the leaf plastidial *AGPL1* (Ohdan et al., 2005).

1.4.2.3 Enhancement of plant productivity by manipulation of a ‘stay-green’ trait

Much of the current research has been focused toward improvements in agricultural productivity using an alternative approach using plant genetic manipulation to reduce the release of chemical fertilizers and pesticides in the environment. A less direct approach for future increases in crop yields will be a result of genetic improvements of plants in enhancing

photosynthesis by increasing the capacity of plants to store photosynthate in its nutrient reserves and their ability to protect themselves against pests and pathogens (Okita et al., 1993).

Extending the duration of photosynthesis can increase the total photosynthesis over the life of annual crops to further increase yield potential and biomass of cereal crops. Maintaining the supply of assimilated carbon to the grain during the grain-filling period ensures the mass per grain in crops is maximized. Attenuation of senescence is one of the ways in which this can be achieved (Spano et al., 2003). Studies by Spano et al. (2003) showed four mutant lines with delayed leaf senescence derived from seed of durum wheat mutagenized by ethylmethane sulphonate maintained photosynthetic competence for longer than the parental line, and had higher seed weights and grain yields per plant than the parental line under glasshouse conditions. However, further analysis is necessary to verify the effects of the 'stay-green' mutant under field conditions, particularly under drought stress, which has commonly affected grain-filling period and plant yield. Studies by Tian et al. (2012) investigated the effects of the drought resistance of a wheat 'stay-green' mutant, *tasg1* under field conditions for two years. In comparison to WT, *tasg1* delayed senescence under both normal and drought stress conditions and maintained chloroplasts and thylakoid ultrastructure. In both studies, extension of senescence was measured by the changes in the net photosynthetic rate, efficiency of PSII and chlorophyll concentration (Spano et al., 2003; Tian et al., 2012).

The characteristics of a 'stay-green' trait in wheat have potential for exploiting this trait to improve crop performance and yield. As noted earlier, Ling et al. (2012) showed that mutant *sp1* Arabidopsis plants displayed attenuated senescence, suggesting that manipulation of this component to alter senescence in field crops such as wheat might have beneficial effects on yield. I investigated this possibility using transgenic wheat plant analyses, and the results will be discussed in Chapter 4.

1.5 Overview of plant abiotic stress response: The introduction of molecular biological techniques into plant biology

Abiotic stresses are one of the major challenges facing agriculture, as under these conditions, plant growth and productivity is highly affected. Abiotic stress includes numerous stresses caused by complex environmental conditions, such as salinity, drought, extreme temperatures, strong light and heavy metals. According to reports from the Intergovernmental Panel of Climate Change (http://www.ipcc.ch), these stresses will increase in the near future because of global climate change. The climate trends in the future raise concern on food security and global agricultural productivity (Lobell and Gourdji, 2012). A recent study by Ciais et al. (2005) has reported that during the European heat wave of 2003, crop production was reduced by around 30%. Therefore, there is a need to continue to develop our understanding, and integrate our knowledge, concerning plant abiotic stress responses and tolerance. Because of this, numerous studies have explored ways in which the effects of stress can be mitigated.

Different types of abiotic stress such as drought, extreme temperature, light intensity, biotic stress and antioxidant defence are often interrelated (Murata et al., 2007; Shanker and Venkateswarlu, 2011), and so there is a possibility that plant stress tolerance is applicable in a variety of environmental stresses singularly or in combination. SP1 may act in extreme temperatures and light intensity (Murata et al., 2007), biotic stress (Basnayake et al., 2011) and antioxidant defence networks (Vickers et al., 2009; Caverzan et al., 2016). However, regulation of SP1 in plant stress tolerance under these conditions was not studied in the scope of this thesis.

Major progress in this research field has come from a great deal of effort in the application of physiological and molecular biology analyses to broaden and deepen our view of abiotic stress responses and tolerance in plants. After the introduction of molecular biological techniques into plant biology, many abiotic stress-inducible genes were identified and characterized using

differential screening or differential display techniques for various plant species, including Arabidopsis. The identification of stress-inducible genes, such as *RD29A* has succeeded in isolating genes that are responsible in plant stress responses. The overexpression of some of these stress-related genes confers some abiotic stress tolerance (Bartels and Sunkar, 2005; Umezawa et al., 2006). For example, a combination of the Arabidopsis *DREB1A* gene and stress-inducible *RD29A* promoter improved drought and low temperature stress tolerance in tobacco (Kasuga et al., 2004).

The availability of the complete genome sequence of Arabidopsis, rice, tomato and other plants (Initiative, 2000; Consortium, 2012), has provided access to essential information on gene products and their function, transcript levels, alternative splicing patterns, as well as the information on putative cis-regulatory elements involved in plant stress responses. Numerous other studies have also explored ways in which the effects of stress can be mitigated. These have involved the application of novel regulatory mechanisms involving the use of chromatin modulation, genomic DNA modification and marker-assisted breeding and small RNA molecules, such as micro RNA (miRNA) and small interference RNA (siRNA), which has facilitated elucidation of the complex regulatory network in response to abiotic stresses (Sunkar et al., 2007; Hirayama and Shinozaki, 2010; Khraiwesh et al., 2012).

For example, studies by Gao et al. (2015) in Arabidopsis have identified a natural *cis*-antisense transcript (NAT) of *NFYA5*, called the *NFYA5 Enhancing RING FINGER* (*NERF*), which encodes a RING E3 ligase. *NERF* formed a *cis*-NAT with NFYA5 in 3'-untranslated regions (3'-UTRs) and positively affected NFYA5 mRNA accumulation through the down regulation of microRNA, miR169, and this was reported as important for drought resistance. Several studies on microRNAs, including this miR169 family has indeed confirmed involvement of microRNA in plant stress responses. However, in contrast to findings in Arabidopsis, the accumulation of miR169 in both tomato (Zhang et al., 2011) and rice (Zhao et al., 2007) were induced by drought stress as plant can efficiently down-regulate the transcripts of the target genes. One

clear difference that may have caused the differences in miR169 regulations under drought stress condition in these three plant species is due to the presence of *NERF* in Arabidopsis but not in rice or tomato. This further suggests that *NERF* gene is not conserved across plant species.

In addition, comprehensive transcriptomic analyses also has enabled research on stress responses in various plant species other than Arabidopsis to increase our knowledge regarding the mechanisms of plant stress tolerance in nature. For example, Ren et al. (2005) discovered the *SKC1* locus encoding a high-affinity K^+ transporter (HKT)-type sodium transporter by analyzing a quantitative trait locus (QTL) for salinity tolerance using salt-tolerant and salt-susceptible rice varieties. Information on such genes or loci is useful to develop a strategy to improve the salinity tolerance of rice.

As plants require sophisticated regulation of stress tolerance systems to survive environmental challenges, so there is a need to continue to develop our understanding, and integrate our knowledge, concerning plant abiotic stress responses and tolerance. Other aspects concern the role of the chloroplast in targeting many stress tolerance processes including the regulation of phytohormones, which involve signals synthesized in the chloroplasts, and ROS management via avoidance and scavenging strategies (Suzuki et al., 2012; Baxter et al., 2013; Sowden et al., 2018).

1.5.1 The role of chloroplasts in plant response to abiotic stress

The plant relies on the chloroplast to produce photosynthetic products to survive. However, chloroplasts are also hubs of stress signalling and targets of many stress tolerance processes. While photosynthetic machinery is necessary for photoautotrophy, photosynthesis is sensitive to stress and therefore can be potentially very dangerous as it can generate toxic oxidation reactions with carbohydrates, lipid, nucleic acids and proteins, which happens due to overproduction of ROS (Asada, 2006; Gill and Tuteja, 2010; Demidchik, 2015). Although ROS play important signalling roles in plants (Shapiguzov et al., 2012; Wrzaczek et al., 2013; Bobik

and Burch-Smith, 2015), their production must be tightly regulated to protect from chloroplast dysfunction during abiotic stress.

ROS play a key role in the regulation of many plastid developmental processes (Muñoz and Munné-Bosch, 2018), and in plant responses to biotic (Torres, 2010; Baxter et al., 2013) and abiotic (Gill and Tuteja, 2010; Suzuki et al., 2012) stresses. The chloroplast is one of the major cellular sites responsible for ROS production (Foyer et al., 1994) and other redox signals through core processes such as photosynthesis and photorespiration. During photosynthesis, rapid transients of photon capture, electron fluxes and redox potentials cause ROS production, which includes the release of singlet oxygen ($^1O_2$), superoxide anion radical (O_2^-) and hydrogen peroxide (H_2O_2) at photosystem I and II (PSI, PSII) in the chloroplast thylakoidal membranes (Cruz de Carvalho, 2008; Dietz et al., 2016). Studies in Arabidopsis have described a chloroplast quality-control pathway that allows for selective elimination of damaged chloroplasts due to ROS accumulation during photosynthesis by the plant U-box 4 (PUB4) E3 ubiquitin ligase (Woodson et al., 2015). The findings reveal how cells balance inherently stressful energy production with organelle turnover via ubiquitination-dependent chloroplast degradation pathway. Another major source of photosynthesis-associated ROS is photorespiration. The photorespiratory pathway involves the recycling of by-products of the oxygenase activity of Rubisco, the formation of H_2O_2 in the peroxisomes and the conversion of glycine to serine in the mitochondria (Cruz de Carvalho, 2008).

Plants are natural producers of ROS. Most reactive oxygen species (ROS) are continuously produced in plants as by-products of aerobic metabolism and photosynthesis. However, under adverse environmental conditions, when the intercepted photon energy exceeds the chloroplast's ability to assimilate carbon, ROS is prone to overproduction, which will damage chloroplast components (Asada, 2006; Gill and Tuteja, 2010; Sowden et al., 2018). The degree of ROS toxicity depends on the type of ROS, and they can be detoxified by various cellular enzymatic and non-enzymatic mechanisms (Apel and Hirt, 2004). Several ROS

scavenging and avoidance mechanisms represent ROS management systems and help to cope with continuous ROS production during abiotic stress. ROS once generated may be scavenged in a number of different ways to minimize photoinhibition, depending on the type of ROS produced by each photosystem. For example, to avoid oxidative stress, $^1O_2$ produced at PSII is scavenged by membrane-bound α-tocopherol (Havaux et al., 2005) and carotenoids (Havaux and Niyogi, 1999; Peng et al., 2006; Dall'Osto et al., 2007), while O_2^- and H_2O_2 produced at PSI are scavenged enzymatically and non-enzymatically by ascorbate (Asada, 2006). The avoidance of ROS production during abiotic stress is another important strategy of plant stress tolerance. For example, when chlorophyll molecules are excited beyond the capacity of photosynthesis, the surplus energy may be released as heat through non-photochemical quenching (NPQ), which is responsible for the dissipation of intercepted light energy under field conditions (Endo et al., 2014).

Another way to reduce photon excess is by limiting the import of photosynthetic preproteins. Studies by Taylor et al. (2009) have indicated that under long-term stress conditions, nuclear-encoded photosynthetic genes become down-regulated. Recently, studies in Arabidopsis by Ling and Jarvis (2015) revealed that SP1 is an important mediator of a novel stress adaptive mechanism involving ROS avoidance as the import of photosynthetic preproteins into chloroplasts is reduced under stress conditions. In this work, plants with altered expression of SP1 were analysed under salinity, osmotic and oxidative stress conditions (Ling and Jarvis, 2015). Specifically, SP1 overexpressor plants showed enhanced tolerance and survival, whereas *sp1* mutants were more sensitive to stress than WT (Ling and Jarvis, 2015). The ROS regulatory mechanism involving SP1 helps survival of stressed plants by reducing photosynthetic activity to minimize ROS production, which it does by selectively controlling the level of TOC components of the protein transport machinery, through which new components of the photosynthetic apparatus must pass.

Under adverse environmental conditions, senescence can also be induced prematurely, and as a result reduces crop productivity (Gregersen et al., 2013). In Chapter 5, I investigated whether the modification of SP1 expression in tomato and wheat is similarly associated with ROS regulation and abiotic stress tolerance. In this work, the effect of stress on the activity of PSII was analysed using a CF imager to measure photochemical efficiency of photosystem II (F_v/F_m).

1.6 Conclusion

Plastids emerged as a result of an endosymbiotic relationship between a cyanobacterium-like organism and an early eukaryotic cell. Today, plastids are an integral and defining feature of the plant cell and their functions in plants extend far beyond photosynthesis. Its ability to differentiate into different type is dependent largely on the organellar proteome. Plastids import thousands types of protein from the cytosol through TOC/TIC machinery. Recently, SP1 E3 ligase was identified to regulate this import machinery by selectively targeting the TOC machinery for degradation by the UPS. The role of SP1 in protein import regulation is important for plastid biogenesis and homeostasis, as changes in SP1 activity have been shown to alter the organellar proteome and the developmental transitions of plastids. There has been tremendous progress in identifying the mechanisms underlying the import machinery. However, the plastid translocation machinery has not been satisfactorily investigated concerning fruit ripening and amyloplast development. Understanding these processes will require, amongst other things, the application of detailed molecular, cellular, genetic and biochemical approaches to describe the involvement of SP1 during plastid biogenesis. This understanding may enable new applications in crop improvement, such as increased tomato fruit quality and shelf life, enhancements in yield and maturation of cereals such as wheat, and promoting plant stress tolerance.

1.7 Aim of project

In this research, two important crops were used as model plants to study SP1 function: tomato and wheat. In each case, I analysed transgenic plant lines with either elevated (overexpressor) or reduced (RNA interference) levels of expression of the native *SP1* gene. I used tomato transgenics to study SP1's role during fruit ripening, where chloroplasts transform into carotenoid-rich chromoplasts, and the wheat transgenics to analyse the importance of SP1 function for grain development. Furthermore, I used both species to study the role of SP1 in leaf senescence. Although there are many factors and processes that influence and control fruit ripening (Pesaresi et al., 2014) and grain development (James et al., 2003; Hurkman et al., 2008), the role of the plastid protein translocation machinery during chromoplast and amyloplast development has not been satisfactorily explored.

SP1 homologues are widely distributed in plants and SP1 has been extensively studied in the model plant Arabidopsis, but its role during plastid development in other species is unknown. This research aimed to:

- Elucidate the role of SP1 (and its homologue SPL2) in different aspects of plastid development, and to explore the potential use of SP1 for modifying plastid biogenesis in two important crops.
- Elucidate the role of SP1 (and its homologue SPL2) in the responses of crop species to various stress conditions. In addition to its role during plastid development, studies in Arabidopsis have indicated that SP1 is also important during abiotic stress responses. Hence, further analysis of the transgenic tomato and wheat lines aimed to compare the regulation of SP1 under abiotic stress in different species.

Overall, the research has suggested approaches for improving crop performance.

Chapter 2: Materials and Methods

2.1 Plant growth conditions and physiological analyses

2.1.1 Tomato plant growth conditions

Solanum lycopersicum cv. Ailsa Craig was grown in Levington M2 modular compost mixed with a slow release fertilizer. Plants were watered to ensure a constant pool of water in the trays. The greenhouse received natural light during the day and was kept at 25/20°C day/night temperature, with an artificial light cycle of 16 hours of light followed by 8 hours of darkness.

2.1.2 Wheat plant growth conditions

Triticum aestivum cv. Fielder was sown to a depth of approximately 2 cm in Levington M2 compost mixed with a slow release fertilizer. The greenhouse received natural light during the day and the standard growth conditions for wheat were set at 20°C day and 15°C night temperature, with a light cycle of 16 hours of light length followed by 8 hours of darkness. Plants were kept well-watered and growing in the optimal growth conditions throughout the life cycle. The dormancy of the transgenic wheat seeds was broken by heat-treating the wheat seeds for 6 days with cycles of 32°C during the day and 4°C overnight.

2.1.3 Fruit ripening analysis

Tomato plants were grown under standard greenhouse conditions. Fruits at breaker stage were harvested and placed in a Percival, a growth chamber without lights at a constant temperature of 25°C with 60% humidity. The Minolta *a**/*b** value of tomato at breaker stage was -0.47. As characterized by Batu (2004), Minolta *a**/*b** value of the tomatoes corresponds to the United States Department of Agriculture (USDA) colour stages are as follows: Breaker: -0.47, Turning: -0.27, Pink: 0.08, Light red: 0.60, Red: 0.95. After harvesting, the fruit skin colour values were scored on a daily basis.

The fruit skin colour values were measured by reflectance using a Chroma Meter Model CR 400 (Konica Minolta, Warrington, UK). Average readings at four points on the blossom-end of the fruits were recorded. The instrument was calibrated against a standard white Calibration Plate CR-A4. This instrument function allows the input of several colour coordinate systems including Hunter *L a b* and the modified Commission Internationale de l'Eclairage's (CIE) *L* a* b**. The CIE *L* a* b** colour scales were commonly used in the food industry and provide more uniformity in relation to human perception of colour differences (Pathare et al., 2013).

The chroma meter measures the CIELAB coordinates (*L*, a*, b**). The *a** value represents colours from green to red (denotes greenness when negative, and redness when positive), whereas the *b** value represents measures blue and yellow colours (denotes blueness when negative and yellowness when positive). *L** is an approximate measurement of luminosity, which is the property according to which each colour can be considered as equivalent to a member of the greyscale, between black and white (Granato and Masson, 2010). The *a**/*b** ratio values were recorded as an indicator of colour development and maturation in tomato (Hobson et al., 1983). The subjective rating scales and colour charts were following the USDA colour classification (Anon, 1975). The corresponding *a**/*b** values to USDA tomato colour stages were determined by Batu (2004).

The ripening analysis was carried out on the transgenic fruits at the onset of breaker stage. Chroma meter measurements were done on a daily basis all the way through to the mature red stage. The fruits were then either detached from the plants or incubated at 25°C in the dark, or were kept to vine-ripe depending on the experimental requirement of the ripening analysis.

2.1.4 Fruit firmness

The firmness test was carried out using a Durofel XF basic durometer (Agrosta Sarl, Serqueux, France). An average value derived from four readings recorded at four points on the circumference of the fruit was calculated and employed. The firmness measurement scale

was 0–100 in durometer units. Values higher than 70 units indicated hard tomatoes, and those less than 60 units indicated soft tomatoes (Arazuri et al., 2007).

2.1.5 Fruit size

The diameter of tomato fruit was measured using a calliper when the fruit reached breaker stage. The fruit was then detached from the plant and incubated at 25°C in the dark for use in ripening analysis or fruit protein extraction.

2.1.6 Chlorophyll measurement

The estimated leaf chlorophyll concentration was measured using a SPAD-502 meter (Konica Minolta, Warrington, UK). The SPAD values were used to indicate the level of chlorophyll in leaves. (Cartelat et al., 2005; Parry et al., 2014).

2.1.7 DAB staining

DAB staining was performed to determine the H_2O_2 levels in leaf samples under abiotic stress conditions, following a protocol described by Thordal-Christensen et al. (1997). Comparable leaves from different plants were vacuum-infiltrated with DAB solution (1 mg/mL, pH 3.8; Sigma-Aldrich, Dorset, UK) and incubated at room temperature overnight before being fixed in a fixation solution (ethanol : acetic acid : glycerol = 3 : 1 : 1, v/v/v). When the chlorophyll in the leaves was completely depleted, the leaves were photographed to record the extent of DAB staining, to detect H_2O_2 accumulation (which is indicated in this assay by brown staining).

2.1.8 Quantification of photosynthesis-related parameters

Chlorophyll fluorescence imaging was performed on leaves using a CF Imager (Technologica Limited, Essex, UK). Plants were dark-adapted for 30 min before each measurement and were then illuminated with a pulse of saturating light before 1 min of constant light intensity (120 µmol m^{-2} s^{-1}). The following parameters were determined. F_v is the variable fluorescence from dark-adapted material. F_m is the maximum fluorescence signal of closed PSII. F_o is the minimal

fluorescence in the dark-adapted state. The F_v/F_m ratio was used to provide an estimate of the PSII maximum efficiency within dark-adapted plant material. The F_v/F_m value was calculated as $(F_m – F_o)/F_m$ (Genty et al., 1989).

2.2 Molecular biology methods

2.2.1 DNA extraction

DNA extraction from plant materials was done following the protocol of the DNeasy Plant Mini Kit (Qiagen, Manchester, UK). Approximately 100 mg of plant material was cut and ground in liquid nitrogen using a Tissue Lyser (Qiagen) into a fine powder in 2.0 mL microcentrifuge tubes for 1 min at 20 Hz. Mixture of 400 µL of Buffer AP1 and 4 µL of RNase A was added to the tissue powder. The samples were vortexed, then incubated for 10 min at 65°C with 2–3 times inversion during incubation, and then 130 µL of Buffer AP2 was added. The samples were mixed and incubated for 5 mins on ice, and then centrifuged at maximum speed and 4°C for 5 mins at 20,000 x*g* in a microfuge (Eppendorf 5417R, Stevenage, UK). The lysate was pipetted into a QIAshredder spin column placed in a 2 mL collection tube, and centrifuged at 20,000 x*g* for 2 mins at 20,000 x*g* in a microfuge (Eppendorf 5417R). The flow-through was transferred into a new tube without disturbing the pellet and 1.5 volumes of Buffer AP3/E was added and mixed by pipetting. A maximum volume of 650 µL of the mixture into a DNeasy Mini spin column placed in a 2 mL collection tube, and centrifuged at 6,000 x*g* for 1 min in a microfuge (Eppendorf 5417R). The flow-through was discarded and this step was repeated with the remaining sample.

The spin column was placed into a new 2 mL collection tube, and 500 µL of Buffer AW was added, and then centrifuged in a microfuge (Eppendorf 5417R) for 1 min at 6,000 x*g*. The flow-through was discarded. Another 500 µL of Buffer AW was added, and then centrifuged in a microfuge (Eppendorf 5417R) for 2 min at 20,000 x*g*.

The spin column was transferred to a new 1.5 mL microcentrifuge tube and 100 µL of Buffer AE was added for elution, and then incubated for 5 min at room temperature. The column was

centrifuged in a microfuge (Eppendorf 5417R) for 1 min at 6000 x*g*. The elution step was repeated one time. The extracted DNA was kept at -20°C for storage.

2.2.2 RNA extraction and quantification

RNA extraction from plant materials was done following the protocol of the Spectrum Plant Total RNA kit (Sigma-Aldrich). Approximately 100 mg of plant material was cut and ground in liquid nitrogen using a Tissue Lyser (Qiagen) into a fine powder in 2.0 mL microcentrifuge tubes for 1 min at 20 Hz. Mixture of lysis buffer containing 500 µl of Lysis Solution / 2-ME was added to the sample, and then it was vortexed to mix; 10 µl of 2-mercaptoethanol (2-ME) was added for every 1 mL of Lysis Solution before use. The samples were incubated at 56°C for 5 min. The mixture was then centrifuged at maximum speed (in an Eppendorf 5415D microcentrifuge) for 3 min to pellet cellular debris. The lysate supernatant was transferred to a filtration column and centrifuged at maximum speed for 1 min to remove residual debris. 500 µl of Binding Solution was added to the clarified lysate and mixed thoroughly.

For complete removal of traces of DNA during RNA purification, on-column DNase I digestion (Sigma-Aldrich) was performed according to the manufacturer's instructions after RNA had been bound to the binding column. For each digestion, 10 µl of DNase I was mixed with 70 µl of DNase digestion buffer and pipetted directly onto the centre of the filter inside the binding column. The samples were incubated at room temperature for 15 min. 500 µl of Wash Solution 1 was added onto the binding column and centrifuged at maximum speed in a microcentrifuge (Eppendorf 5415D) for 1 min to remove the digested DNA. 500 µl of Wash Solution 2 (an appropriate amount of 100% ethanol was added prior to use) was added to the column, which was then centrifuged at maximum speed for 30 s. An additional column wash was performed before centrifuging the column at maximum speed in a microcentrifuge (Eppendorf 5415D) for 1 min to dry. The dried column was transferred to a fresh tube. 50 µl of Elution Solution was pipetted directly onto the binding matrix inside the column and left to sit for 1 min at room

temperature. The sample was centrifuged at maximum speed in a microcentrifuge (Eppendorf 5415D) for 1 min to elute the RNA.

Purified RNA was quantified using a spectrophotometer (NanoPhotometer P330, Implen, Geneflow, Staffordshire, UK), and kept at -80°C for long-term storage.

2.2.3 cDNA synthesis

cDNA synthesis was carried out in 0.5 mL microcentrifuge tubes. 1 µL of oligo d(T) primer (50 µM), 1 µL of 10 mM dNTP mix, approximately 2 µg of purified RNA, and Nuclease-free Water (Sigma-Aldrich) were mixed to make a reaction volume of 11 µL. The reaction was incubated at 65°C for 5 min and then placed on ice for at least 1 min. 1 µL of SuperScript™ IV Reverse Transcriptase (Invitrogen) (200 U/µL), 4 µL of 5X first strand buffer, 1 µL of 0.1M DTT and 1 µL of RNasin Plus Ribonuclease Inhibitor (40 U/µL, Promega, Southampton, UK) were added. The reaction was then incubated at 55°C for 10 min. The reaction was stopped by inactivating the enzyme by incubation at 80°C for 10 min.

2.2.4 Quantitative real-time PCR

Quantitative real-time PCR was carried out using the PowerUp SYBR Green Master Mix (Applied Biosystems, Cheshire, UK) system to analyse the expression levels of genes using the $\Delta\Delta C_t$ method (Livak and Schmittgen, 2001). For quantitative real-time PCR (qPCR), cDNA was produced as described above (Section 2.2.3), and primers specific for the target that produce a 80-120 bp product, and anneal at 60°C, were designed (Table 2.1). The *ACTIN2* gene was chosen as a housekeeping reference gene. Reactions were prepared in a 20 µL volume, using 10 µL of PowerUp SYBR Green Master Mix (Applied Biosystems), 1 µL of cDNA template, 2 µL of each GOI primer (5 µM each) were mixed in each reaction. qPCR reactions were carried out in 96-well plates using an Applied Biosystems by Life Technologies StepOnePlus Real-Time PCR System. The relative expression of each gene was compared to the WT and normalized to *ACTIN2*.

Table 2.1. Primers used for qPCR experiments.

Primer Name	**Sequence: 5’ to 3’**	**Gene**
TaACT2-F TaACT2-R	CAAATCATGTTTGAGACCTTCAATG ACCAGAATCCAACACGATACCTG	*ACTIN2 (TaACTIN)* *AK457678*
TaSP1-F1 2B TaSP1-R1 2D	ATGTTGGTCCCGTGGG TCAGTGACGGAATGTTCTG	*TaSP1* *TRIAE_CS42_**2BS**_TGACv1_146843_AA0473840*
TaSP1-F2 2B TaSP1-R2 2B	GTTCTGCGGCAGGGTTAATTT ACTCCGAGCATCTTCAGTCCT	
SlACT-F SlACT-R	TTGCTGACCGTATGAGCAAG GGACAATGGATGGACCAGAC	*ACTIN2 (SlACTIN)* *Solyc11g005330.1*
SlSP1-F1 SlSP1-R1	ATGGTTCCATGGGCCGGACTCTC TCAATGGCGAAAAGTTTTCAC	*SlSP1* *Solyc06g084360.2*
SlSP1-F2 SlSP1-R2	TGCTGTCGGTGTATATCTACTTGT CTTCATCCTCATCTCCTGCTCTT	
SlSPL2-F1 SlSPL2-R1	ATGTCAATATACGATCAAGCGG GCTCGTCAAGAATCATATATCC	*SlSPL2* *Solyc12g049330.1*
SlSPL2-F2 SlSPL2-R2	TACGGAGTATTGTCAAGTTCA CTATCAGAGTTGTCGGAAGA	

2.2.5 Semiquantitative RT-PCR

Semiquantitative RT-PCR was performed using primers for the target gene (*SlNCED3* and *TaDi19a*), and the control gene primers (*ACTIN2*) using the primers listed in Table 2.2. An equal amount of cDNA was used for each sample, and a low number of PCR cycles (20- 25 cycles) were used to ensure PCR product would be doubling each cycle. The bands of the gel image were then quantified *in silico* using Aida Image Analyzer software by drawing boxes of equal size around each band, to quantify pixel values. The values for the target gene were normalized to the values for the control bands. To make all results relative to wild type, each sample value was then divided by the average wild type value.

Table 2.2. Primers used for semiquantitative RT-PCR experiments.

Primer Name	**Sequence: 5' to 3'**	**Gene**
TaACT2-F TaACT2-R	CAAATCATGTTTGAGACCTTCAATG ACCAGAATCCAACACGATACCTG	*ACTIN2 (TaACTIN)* *AK457678*
TaDi19a-F TaDi19a-R	TACGTGATGCTCATTTGCAG TCAGTCGTCTCCAAATAAAGTG	*TaDi19a* *FJ795369*
SlACT-F SlACT-R	TTGCTGACCGTATGAGCAAG GGACAATGGATGGACCAGAC	*ACTIN2 (SlACTIN)* *Solyc11g005330.1*
SlNCED3-F SlNCED3-F	TGAGAACTTCGTCGTCATTC ATCTTTCGCGTACTTATCCA	*SlNCED3* *Solyc07g056570*

2.2.6 Polymerase chain reaction

Polymerase chain reaction (PCR) was performed using Biometra Thermocycler T1 or T3 devices and standard reaction mixtures (10 mM Tris-HCl [pH 8.3], 50 mM KCl, 50 mM MgCl, 0.05% Tween20, 200 µM of each dNTP, 125 nM of each primer) with differences based on protocols for different DNA polymerases. DNA polymerases were mostly used at 0.5 units per

20 µL reaction, or otherwise depending on the user guide. Primers were designed and ordered from Sigma-Aldrich.

The thermocycler programme depended on the GOI but always contained an initial heating to 95°C for 2 min, and then 30 cycles of 95°C for 40 s, an annealing temperature step of 55-60°C depending on the GOI for 20 s, and an extension step of 72°C for at least 30 s. The time of the extension step depended on the length of the gene to be amplified, and was generally 1 min/kb.

2.2.7 DNA gel electrophoresis

Gel electrophoresis of nucleic acid samples used a submerged horizontal agarose gel set-up (Bio-Rad, Hertfordshire, UK). Agarose gels were prepared with 1-2% agarose (Melford, Suffolk, UK) in 1X TBE (44.5 mM Tris, 44.5 mM boric acid, 1 mM EDTA) in a microwave oven, and 1X SYBR Safe DNA gel stain (Invitrogen, Fisher Scientific, Loughborough, UK) was added to the molten agarose before pouring into suitable gel trays, to enable visualization of the DNA samples. Once set and immersed in 1X TBE buffer in a suitable electrophoresis tank (Bio-Rad), gels were loaded with samples; for example, 5 µL of the sample was mixed with 3 µL of Orange G loading dye and 3µL 1kb Plus DNA Ladder (Invitrogen) and run in tanks (Bio-Rad) containing at ~10 V/cm.

2.2.8 DNA gel imaging and band quantification

Images of RT-PCR SYBR Safe-stained agarose gels were acquired with an ImageQuant LAS-4000 imaging system (GE Healthcare Life Sciences, Buckinghamshire, UK), and the bands of interest were quantified using Aida Image Analysis Software (Raytek, Sheffield, UK). If the PCR product was to be purified, the gel band was cut on a UV dual intensity transilluminator (UVP) at low intensity and processed using the GenElute Gel Extraction kit (Sigma-Aldrich) following exactly the manufacturer's instructions.

2.3 Generation of transgenic plant lines

2.3.1 Wheat transformation

2.3.1.1 Wheat constructs preparation

Dr Qihua Ling prepared the entry vectors for TaSP1 OEX and TaSP1 RNAi, and Dr Emma Wellington at NIAB, Cambridge, prepared the final vectors and performed the transformation steps for the constructs.

To produce TaSP1 OEX in the entry vector, the coding sequence (CDS) of TaSP1 B homeologue (TRIAE_CS42_**2BS**_TGACv1_146843_AA0473840) was amplified from cDNA using the following primers containing the added sequences necessary for Gateway cloning (underlined), producing the orientation of the TaSP1 B insert in entry vector, pEW272 for TaSP1 OEX as attL1-5'-CDS-3'-attL2;

TaSP1-F; 5'-AAAAAGCAGGCTCCCCACCATGTTGGTCCCGTGGG-3', and TaSP1-R; 5'-AGAAAGCTGGGTTTCAGTGACGGAATGTTCTG-3'.

To produce TaSP1 RNAi in the entry vector, the RNAi construct was designed based on sequence of the TaSP1 D homeologue (TRIAE_CS42_**2DS**_TGACv1_178131_AA0591470), that targets different regions of the gene (Travella et al., 2006; Fu et al., 2007). The RNAi target sequences at coding regions 356-733 was amplified from cDNA using the following primers containing the added sequences necessary for Gateway cloning (underlined), producing the orientation of the TaSP1 B insert in entry vector, pEW271 for TaSP1 RNAi as attL1-5'-sense orientation-3'-attL2;

TaSP1-RNAi-F; 5'-AAAAAGCAGGCTCCATGGCACTGGGCGTGTCTATG-3' and TaSP1-RNAi-R; 5'-AGAAAGCTGGGTTGTGCACGCTTAGCAAGAAGAA-3'.

The amplified DNA sequences cloned into the entry vector pEW272 (OEX construct) and pEW271 (RNAi construct) as described above, were transferred to Dr Emma Wallington at NIAB, Cambridge. Dr Emma Wallington performed all of the following work in this section. The

inserts were recombined using a Gateway Clonase II kit (Invitrogen) into binary vectors containing Gateway attR1 and attR2 sites, pSc4Act-R1R2-SCV for overexpression and pAct-IR-2 for knockdown via RNAi silencing of the gene of interest. Both vectors containing the *nptII* (neomycin phosphotransferase II) gene under the control of the subterranean clover stunt virus Sc4 promoter (Schunmann et al., 2003) and *Arabidopsis thaliana* FAD2 intron (Okuley et al., 1994), for selection on Geneticin G418 (Sigma-Aldrich) in tissue culture. After transfer into wheat, the SP1 sequences would be expressed under the control of a rice ACTIN promoter (Mcelroy et al., 1990). The resultant plasmids were electrotransformed into the *Agrobacterium tumefaciens* strain *AglI* (Amoah et al., 2001). Plasmids were isolated from *Agrobacterium* and verified by restriction digestion prior to use in wheat transformation experiments.

2.3.1.2 Genetic transformation and transgenic wheat verification

The wheat transformation experiments and copy number determination were done at NIAB. Immature donor wheat seeds were collected 14-16 days after anthesis and surface sterilized. Before *Agrobacterium* infection, isolated embryos were pre-treated with a centrifugation step as described by Hiei et al. (2006). Treated embryos were co-cultivated with the *Agrobacterium* strains described above at 23°C in the dark for 2 days. Following removal of the embryonic axis, subsequent tissue culture of the plant material was performed essentially as described by Risacher et al. (2009). Wheat plantlets were analysed by quantitative genomic PCR for the copy number of the *nptII* selectable marker gene. Plants were grown to maturity at NIAB, and T1 seeds were transferred to the University of Oxford for analysis. WT plants were transformed with the TaSP1 OEX and TaSP1 RNAi constructs. The plant lines overexpressing or knockdown of the TaSP1 genes were identified by qPCR and numbered as #1, #2 and #3 as described in Table 2.3 and Figure 4.2 in Chapter 4.

2.3.1.3 Copy number analysis of transgenic wheat

The copy number data for each transgenic line was provided by NIAB based by quantitative genomic PCR analysis (of the kanamycin resistance marker) using the Applied Biosystems by Life Technologies 7500 Fast instrument (95°C for 2 min, then 40 cycles of 95°C for 40 s, annealing temperature of 60°C for 20 s and an extension condition of 72°C for 30 s). The copy number of the line was estimated based on the *nptII* gene marker using the comparative C_t method (Schmittgen and Livak, 2008). A total of 84 transformed plants and 12 non-transformed (control) were tested and the full copy number dataset provided by NIAB was described in Table 2.3.

Table 2.3. Copy number dataset of transgenic wheat lines. The copy number data on each transgenic line was provided by NIAB based by quantitative genomic PCR analysis (of the kanamycin resistance marker). The most interesting plant lines, overexpressing (TaSP1 OEX) or silencing (TaSP1 RNAi) of the transgenes used in the analysis, were identified by qPCR in T1 generation and numbered as #1, #2 and #3.

pEW271-taSP1 RNAi															
No.	**Transgenic plant lines**	**qPCR copy number**	**Plant number**	**No.**	**Transgenic plant lines**	**qPCR copy number**	**Plant number**	**No.**	**Transgenic plant lines**	**qPCR copy number**	**Plant number**	**No.**	**Transgenic plant lines**	**qPCR copy number**	**Plant number**
1	CW22.1	4 or 4+		13	CW22.13	4+		25	CW23.11	4+		37	CW42.13	2	
2	CW22.2	1		14	CW22.14	1		26	CW23.12	4+	taSP1 RNAi #2	38	CW42.14	3	
3	CW22.3	4+		15	CW23.1	1		27	CW42.1	4+		39	CW43.1	1	
4	CW22.4	1		16	CW23.2A	4+		28	CW42.3	2		40	CW43.2	2	
5	CW22.5	1		17	CW23.3	1		29	CW42.4	3		41	CW43.3	4+	
6	CW22.6	2		18	CW23.4	1		30	CW42.5	2		42	CW43.4	1	taSP1 RNAi #3
7	CW22.7	1		19	CW23.5	4+		31	CW42.6	4+		43	CW43.5	1	
8	CW22.8	4		20	CW23.6	1		32	CW42.7	2		44	CW43.6	2	
9	CW22.9	1		21	CW23.7	2		33	CW42.8	3					
10	CW22.10	4+		22	CW23.8	1		34	CW42.10	1					
11	CW22.11	2		23	CW23.9	1	taSP1 RNAi #1	35	CW42.11	4					
12	CW22.12	2		24	CW23.10	1		36	CW42.12	2					

pEW272-taSP1 OEX															
No.	**Transgenic plant lines**	**qPCR copy number**	**Plant number**	**No.**	**Transgenic plant lines**	**qPCR copy number**	**Plant number**	**No.**	**Transgenic plant lines**	**qPCR copy number**	**Plant number**	**No.**	**Transgenic plant lines**	**qPCR copy number**	**Plant number**
1	CW24.1	4+		13	CW25.1	1		25	CW27.7	4+		37	CW28.10	1	
2	CW24.2	4 or 4+		14	CW25.2	4		26	CW27.8	2		38	CW28.13	4+	
3	CW24.3	4 or 4+		15	CW25.3	1		27	CW27.9	2		39	CW28.14	4+	taSP1 OEX #3
4	CW24.4	4+	taSP1 OEX #1	16	CW25.4	4+		28	CW27.10	1		40	CW28.15	1	
5	CW24.5	4+		17	CW25.5	4+		29	CW28.1	2					
6	CW24.6	4		18	CW25.6	2		30	CW28.2	2					
7	CW24.7	1		19	CW27.1	3		31	CW28.3	2					
8	CW24.8	4		20	CW27.2	1		32	CW28.5	2					
9	CW24.9	1		21	CW27.3	4		33	CW28.6	2					
10	CW24.10	4+		22	CW27.4	3		34	CW28.7	1					
11	CW24.11	1		23	CW27.5	2		35	CW28.8	2	taSP1 OEX #2				
12	CW24.12	4+		24	CW27.6	2		36	CW28.9	2 or 3					

Control (non-transformed)		
No.	**Non-transgenic plant**	**qPCR copy number**
1	CW22.con1	0
2	CW22.con2	0
3	CW22.con3	0
4	CW22.con4	0
5	CW22.con5	0
6	CW23.con1	0
7	CW23.con2	0
8	CW23.con3	0
9	CW23.con4	0
10	CW23.con5	0
11	CW43.Con1	0
12	CW43.Con2	0

2.3.2 Tomato transformation

2.3.2.1 Tomato construct preparation

Dr Qihua Ling and Yunliu Zeng performed the construct preparation and transformation steps for the SlSP1 OEX, SlSP1 RNAi, and SlSPL2 RNAi genotypes.

To produce SlSP1 OEX, the CDS of Solyc06g084360 was amplified from cDNA using the following primers, containing the added sequences necessary for Gateway cloning (underlined):

AttB1-SP1-F; 5'-AAAAAGCAGGCTCCACCGGAAATGGTTCCATG-3', and AttB2-SP1-R; 5'-AGAAAGCTGGGTTTCAATGGCGAAAAGTTTTCAC-3'; and

To produce SlSP1 RNAi and SlSPL2 RNAi, the artificial microRNA (amiRNA) constructs were produced to target different regions of the gene (Ossowski et al., 2008; Fernandez et al., 2009). The amiRNAs target sequences are as follows: coding regions of Solyc06g084360 at 917-937 (5′-TCATATGACCACACGCGACAA-3′) and 698-718 (5′-TAAGTAGATATACACTGACAG-3′) for SlSP1; coding region of Solyc12g049330 at 92-112 (5′-TTGGCGTACGGAGTATTGTCA-3′) and 562-582 (5′-GAGACAGTTTATCATCACTTA-3′) for SlSPL2. The coding sequences of amiRNA against the corresponding target gene were designed using WMD3 (http://wmd3.weigelworld.org/cgi-bin/webapp.cgi) (Schwab et al., 2006), producing a 20 nucleotide complementary overlap either at their 5' end, 3' end or at the middle of CDS were amplified from cDNA using the primers listed in Table 2.4. The corresponding sequences were cloned into pRS300 (Schwab et al., 2006) to make the precursor of amiRNA, and amplified by primers A-attB1 and B-attB2 for gateway cloning into the pDNOR201 entry vector.

Table 2.4. Primers used to amplify coding sequence of amiRNA against the *SlSP1* and *SlSPL2* gene.

Primer Name	**Sequence: 5' to 3'**	**Gene**
SlSP1-AmR-1-I	gaTCATATGACCACACGCGACAAtctctcttttgtattcc	*SlSP1*
SlSP1-AmR-1-II	gaTTGTCGCGTGTGGTCATATGAtcaaagagaatcaatga	*Solyc06g084360.2*
SlSP1-AmR-1-III	gaTTATCGCGTGTGGACATATGTtcacaggtcgtgatatg	
SlSP1-AmR-1-IV	gaACATATGTCCACACGCGATAAtctacatatatattcct	
SlSP1-AmR-2-I	gaTAAGTAGATATACACTGACAGtctctcttttgtattcc	
SlSP1-AmR-2-II	gaCTGTCAGTGTATATCTACTTAtcaaagagaatcaatga	
SlSP1-AmR-2-III	gaCTATCAGTGTATAACTACTTTtcacaggtcgtgatatg	
SlSP1-AmR-2-IV	gaAAAGTAGTTATACACTGATAGtctacatatatattcct	
SlSPL2-AmR-92-I	gaTGACAATACTCCGTACGCCAAtctctcttttgtattcc	*SlSPL2*
SlSPL2-AmR-92-II	gaTTGGCGTACGGAGTATTGTCAtcaaagagaatcaatga	*Solyc12g049330.1*
SlSPL2-AmR-92-III	gaTTAGCGTACGGAGAATTGTCTtcacaggtcgtgatatg	
SlSPL2-AmR-92-IV	gaAGACAATTCTCCGTACGCTAAtctacatatatattcct	
SlSPL2-AmR-562-I	gaTAAGTGATGATAAACTGTCTCtctctcttttgtattcc	
SlSPL2-AmR-562-II	gaGAGACAGTTTATCATCACTTAtcaaagagaatcaatga	
SlSPL2-AmR-562-III	gaGAAACAGTTTATCTTCACTTTtcacaggtcgtgatatg	
SlSPL2-AmR-562-IV	gaAAAGTGAAGATAAACTGTTTCtctacatatatattcct	

The SlSP1 CDS and amiRNA precursor (for both SP1 and SPL2) sequences were subsequently cloned into the binary vector pK7WG2D using a Gateway Clonase II kit (Invitrogen), to generate pK7WG2D-SlSP1, pK7WG2D-amiRSlSP1 and pK7WG2D-amiRSlSPL2 vectors. This vector contains the neomycin phosphotransferase II (*nptII*) gene under the control of the 35S promoter, which confers resistance to kanamycin, and green fluorescent marker (GFP) to facilitate early confirmation of transformants (Karimi et al., 2002). The resultant plasmids were freeze-thaw transformed into the *Agrobacterium tumefaciens* strain GV3101 (Chetty et al., 2013). Plasmids were isolated from *Agrobacterium* and verified by restriction digestion prior to use in tomato transformation experiments.

2.3.2.2 Genetic transformation and transgenic tomato verification

Dr Qihua Ling and Yunliu Zeng did the tomato transformation experiments. Tomato seeds were surface sterilized as described by Zelman (2015). Before *Agrobacterium* infection, the cotyledon leaf segments were cut at both extremities and were pre-treated following steps as described by Sun et al. (2006). Treated cotyledon leaf segments were co-cultivated with the *Agrobacterium* strains described above at 25°C in the dark for 2 days. Following formation of shoots, the subsequent tissue culture of the transformed plant material was performed essentially as described by Sun et al. (2006). Tomato plantlets were analysed by genomic PCR for positive transformants carrying the *nptII* selectable marker gene in the T0 generation. The overexpression and silencing of *SlSP1* and *SlSPL2* in the T0 generation of the transgenic plants was confirmed by RT-PCR, relative to the expression in the WT plants, normalized to *SlACTIN.* The ploidy number of T0 plants was checked by counting the number of chloroplasts in guard cells (Koornneef et al., 1989). Several most interesting lines were grown to maturity, and T1 seeds were harvested and the identified homozygous lines were kept for the analysis in the T2 generation.

2.3.2.3 Segregation analysis of transgenic tomato

WT plants were transformed with the SlSP1 OEX, SlSP1 RNAi and SlSPL2 RNAi constructs. The plant lines overexpressing or silencing of the transgenes were identified (Table 2.5). Dr Qihua Ling and Yunliu Zeng did the copy number analysis of tomato transgenic lines. The three chosen lines, numbered as #1, #2 and #3 (Figure 3.4 and Figure 6.2), were identified as segregating in a 3:1 ratio for kanamycin resistance/sensitivity in the T1 generation, indicating that each possessed a single T-DNA insertion locus. In the T2 generation, the identified homozygous lines with the highest or lowest levels of transgenes expression by qPCR (Figure 3.4 in Chapter 3 and Figure 6.2 in Chapter 6) were chosen for further study.

Table 2.5. Copy number dataset of transgenic tomato lines. The copy number data on the each transgenic line was provided based by quantitative genomic PCR analysis (of the kanamycin resistance marker). The most interesting plant lines, overexpressing (SlSP1 OEX) or silencing (SlSP1 RNAi and SlSPL2 RNAi) of the transgenes used in the analysis, were identified by qPCR in T1 generation and numbered as #1, #2 and #3. These plant lines were identified as segregating in a 3:1 ratio for kanamycin resistance/sensitivity in the T1 generation, indicating that each possessed a single T-DNA insertion locus.

Tomato construct	**Transgenic plant lines**	**Copy number**	**Plant number**
SlSP1 OEX	OX7-1	1	SP1 OEX#1
	OX7-2	1	SP1 OEX #2
	OX13-1	1	SP1 OEX #3
	OX1-1	1	
	OX19-1	1	
SlSP1 RNAi	KD2-2	1	SP1 RNAi#1
	KD2-6	1	SP1 RNAi #2
	KD2-9	1	SP1 RNAi #3
	KD2-1	1	
	KD19-1	1	
SlSPL2 RNAi	KD562-13	1	SPL2 RNAi #1
	KD562-10	1	SPL2 RNAi #2
	KD92-4	1	SPL2 RNAi #3
	KD92-1	1	

2.4 Protein biochemistry

2.4.1 Leaf protein extraction

20-30 mg of plant material was ground up in liquid N_2 into fine powder using a Tissue Lyser (Qiagen) for 1 min 20 Hz. 200 µl of protein extraction buffer (100 mM Tris-HCl pH 6.8, 10% (v/v) glycerol, 2% (w/v) SDS, 0.1% (v/v) Triton-X, 5 mM EDTA), freshly prepared by the addition of 10 µl 1M DTT and 10 µl protease inhibitor cocktail (Sigma-Aldrich), was added to the ground tissue and mixed vigorously. Samples were centrifuged at maximum speed for 20 min in a microcentrifuge (Eppendorf 5415D), and then the supernatants were transferred each to a fresh tube. Protein concentrations were estimated using Bradford Protein Assay (Bio-Rad) according to the manufacturer's instructions, using a dilution series of 1:10 as a standard.

2.4.2 Fruit protein extraction

The tomato fruit protein extraction method used was that described for use with recalcitrant plant tissues by Faurobert et al. (2007). Tomato fruit was ground up in liquid N_2 into fine powder using a Tissue Lyser (Qiagen) for 1 min 20 Hz. 1 g of ground tissue was suspended in 3 mL of extraction buffer (500 mM Tris-HCl, 50 mM EDTA, 700 mM sucrose, 100 mM KCl; pH was adjusted to 8.0; 2% (v/v) β-mercaptoethanol and 1 mM phenylmethylsulfonyl fluoride were freshly added just before extraction) in a 15 mL Falcon tube, vortexed, and incubated with shaking for 10 min on ice. An equal volume of Tris-buffered phenol (Sigma-Aldrich) was added, and the solution was incubated on a shaker at 180 rpm for 10 min at room temperature. The sample was centrifuged (Sorvall Legend RT System) for 10 min at 5500 x*g* and 4°C. The phenolic phase, which was on the top of the tube, was transferred carefully to a new tube, and then extracted with 3mL of extraction buffer, mixed thoroughly, and centrifuged (Sorvall Legend RT System) for 10 min at 4°C and 5500 x*g*. The phenol phase was recovered and transferred into a new microfuge tube, and then 4 volumes of precipitation solution (0.1 M ammonium acetate in cold methanol) was added and mixed by inverting the tube. The sample

was incubated for at least 4 h or overnight at -20°C. Proteins were pelleted by centrifugation (Eppendorf 5417R, 10 min, 5500 x*g* at 4°C). The pellet was washed three times with cooled precipitation solution and finally with pre-cooled (-20°C) acetone. After each washing step, the sample was centrifuged (Eppendorf 5417R) for 5 min at 5500 x*g* and 4°C. Finally, the pellet was dried under vacuum for 1 hour. Pellet was resuspended in 2X Laemmli buffer (4% of SDS, 20% of glycerol, 120 mM Tris-HCl [pH 6.8], 50 mM DTT and 0.02% of bromophenol blue; Laemmli (1970)). Protein concentrations were estimated using Bradford Protein Assay (Bio-Rad) according to the manufacturer's instructions, using a dilution series of 1:10 as a standard.

2.4.3 Protein quantification by Bradford assay

Bovine serum albumin (BSA [NEB]; 10 µg/µL) was diluted 1:10 in sterile water to 1 µg/µL. Standards were made by adding 0, 1, 2, 4, 6, 8 and 10 µL of 1 µg/µL BSA to 7 microfuge tubes containing sterile water, to reach a total volume of 799 µL each. Then, 1 µL of protein extraction buffer was added to compensate for its absorption. For the actual samples, 1 µL of protein (in extraction buffer) was added to 799 µL of sterile water. Afterwards 200 µL of Bio-Rad Protein Assay (Bio-Rad) was added to each tube, and the samples were vortexed and incubated for 5 mins at room temperature. The absorbance of the samples were then measured at a wavelength of 595 nm using NanoPhotometer P330 (Implen), and disposable cuvettes (Fisherbrand). The control absorbance values were plotted against the BSA concentrations automatically in the onboard software of the NanoPhotometer, and the equation of a linear approximation was used to calculate the concentrations of all other samples.

2.4.4 Preparation of SDS-PAGE gels

For SDS-PAGE, either precast 4–15% Mini-PROTEAN TGX gels (Bio-Rad), or gels were prepared by hand were used. Polyacrylamide resolving gels containing 375 mM Tris-HCl, (pH 8.8) and 0.1% of SDS were generally prepared with acrylamide concentrations between 10% (w/v; lower resolution, shorter running time) and 15% (higher resolution, longer running time).

A 30% (w/v) acrylamide stock containing 0.8% (w/v) bis-acrylamide (ProtoGel) was diluted in the Tris-SDS buffer to reach the required concentrations. The stacking gel always contained 125 mM Tris-HCl, (pH 6.8), 0.1% of SDS and 5% (w/v) acrylamide. Before pouring, 50 µL of 10% (w/v) ammonium persulfate (AP) and 5 µL tetramethylethylenediamine (TEMED) were added in order to polymerize the acrylamide. To pour and run the gels, the Mini-PROTEAN III Cell gel system (Bio-Rad) was used. To make the resolving gel 3.33 mL of the liquid preparation was added to the mould, and immediately isobutanol was added to the top to maintain a flat surface and aid polymerization by excluding air. These were left for 45 mins, and after polymerization of the resolving gel, the isopropanol was decanted and remaining droplets were removed with a filter paper. The stacking gel was then poured on top, and a comb was inserted to form the wells. These were left for 45-90 mins to set.

2.4.5 SDS-PAGE

Then the comb and any packaging was removed from the desired polyacrylamide gels, and then the wells were washed with distilled water to rinse away any debris. Polyacrylamide gels were fitted into the Mini-PROTEAN gel chamber which was then filled with enough 1X TGS buffer (25 mM Tris, 192 mM glycine, 0.1% of SDS) to cover both electrodes. Prior to sample loading, all protein samples were diluted in an equal volume of 2X Laemmli buffer (4% of SDS, 20% of glycerol, 120 mM Tris-HCl [pH 6.8], 50 mM DTT and 0.02% of bromophenol blue; Laemmli (1970)), and the samples were heated to 95°C for 5 min in order to denature the proteins. Denatured protein samples were loaded into the wells of the gel alongside 3 µL of a protein ladder (Precision Plus Protein™ Dual Color Standards [Bio-Rad]) as a standard. Gels were run at 180 V using a Power Pac 300 station (Bio-Rad) until the bromophenol blue dye front reached the bottom of the resolving gel. Then, gels were either directly used for western blotting or Coomassie staining.

2.4.6 Coomassie gel staining

SDS-polyacrylamide gels were stained in 25 mL of InstantBlue Protein Stain (Expedeon) according to the manufacturer's instructions. To remove the dye from the background, gels were de-stained with deionized water 3 times, up to overnight, until the background was clear.

2.4.7 Western blotting

Resolved proteins were transferred from acrylamide gels to membranes for detection purposes by electroblotting using a Bio-Rad Mini Protean III system. One litre of 1X Transfer buffer was prepared fresh (3 g Tris, 14.4 g glycine, 1 g SDS, 200 mL methanol per 1 L). Enough 1X Transfer buffer was added to a plastic container to wet two filter papers, the sponge rectangles, the SDS-polyacrylamide gel, and the Hybond ECL membrane Amersham (GE Healthcare Life Sciences). The Hybond ECL membrane was cut to fit the size of the SDS-polyacrylamide gel.

The materials in the container prepared for transfer were assembled and placed in the transfer tank. This was done by first wetting the Hybond ECL membrane with methanol, then pressing the gel and membrane together in a cassette, with all items submerged in transfer buffer (25 mM Tris, 192 mM glycine, 20% of methanol); this was made as a sandwich: sponge, blotting paper, gel, Hybond ECL membrane, blotting paper, sponge. The cassette was closed and then placed in the Mini Trans-Blot Cell system (Bio-Rad), with the gel-side facing the cathode, and Hybond ECL membrane-side facing the anode. Transfer buffer was pre-cooled before added to fill the tank, and an ice pack was placed inside the tank. The transfer was set to run at 100 V for 60 min. Once transfer was completed, the Hybond ECL membrane was taken out of its encasing and placed in 50 mL of blocking buffer comprising TBS-Tween buffer with milk (Blotto: 10 mM Tris-HCl pH 8, 150 mM sodium chloride, 0.05% (v/v) Tween-20, 8% of milk). Blocking was done in a cold room on a shaker (Stuart Orbital Shaker SSM1) at 30 rpm for 60 min.

Following the blocking step, the Blotto was discarded and the membrane was incubated with primary antibody on a shaker (Stuart Orbital Shaker SSM1) at 4°C for overnight. All antibodies used were diluted at appropriate concentration in Blotto. At the end of the incubation, the primary antibody was removed and retained for future re-use (stored at -20°C), and then the membrane was rinsed with TBS-Tween three times before incubation with the secondary antibody. Secondary antibodies were used according to the organism in which the primary antibody had been raised, and were conjugated to horseradish peroxidase (HRP) (Abcam). The membrane was kept on a shaker (Stuart Orbital Shaker SSM1) at 30 rpm in the cold room for 60 min. At the end of the incubation, the primary antibody was removed and retained for future re-use (stored at -20°C). A further four washing steps followed, each one for 15 min using fresh TBS-Tween. Once the washing steps were completed, the membrane was incubated in EZ-ECL Chemiluminescence Detection Kit (Geneflow), following the manufacturer's guidelines.

Equal amounts of ECL solutions II and I were mixed and added to the membrane. The membrane then was quickly covered with cling film. The fluorescent light produced by the ECL reaction was then visualized using the chemiluminescence option on the ImageQuant LAS-4000 imager (GE Healthcare Life Sciences).

2.4.8 Protein semiquantification

The bands of a western blot image were quantified in silico using Aida Image Analysis Software (Raytek, Sheffield, UK) by drawing boxes of equal size around each band, to quantify pixel values. The values for the protein of interest were normalized to the values for the control protein. The blot of the protein of interest and control protein always came from the same sample and membrane to which proteins had been transferred. To make all results relative to WT, each sample value was then divided by the average WT value.

2.5 Phylogenetic tree assembly

The software used for phylogenetic tree assembly was MEGA7 (Kumar et al., 2016). Predicted protein sequences homologous to Arabidopsis SP1 from a variety of plants were retrieved from the National Center for Biotechnology Information (NCBI), Ensembl Plants and Phytozome 12 database and BLASTP analysis using Arabidopsis SP1 as the query (Johnson et al., 2008; Goodstein et al., 2012; Bolser et al., 2014). The maximum likelihood method was chosen for tree assembly. The software was also used to run alignments using sequence in FASTA format and to create phylogenetic trees with 1000 boot-strap confidence testing. The boot-strap method was selected in the MEGA7 software as the statistical test to determine significance in branching in the phylogenetic tree.

Chapter 3: Analysis of SP1 in Tomato

3.1 Introduction

Solanum lycopersicum (tomato) is one of the most economically important vegetables. Due to its popular demand for food consumption, numerous tomato cultivars with different yield, shape, resistance, taste and quality are grown all over the world. Although easy to grow, tomatoes can suffer from various problems throughout their developmental stages, which then affect production. Nowadays, tomato has become a model species for genetic and genomic studies of crop improvement because of the possibility of self-pollination, ease of cross-pollination, its diploid state, and ease of transformation (Pavan et al., 2009; Klee and Giovannoni, 2011). Recently, the tomato genome (cv. Heinz 1706) has been fully sequenced (Tomato Genome, 2012) and made publicly available (http://solgenomics.net/).

During tomato fruit ripening, chloroplasts transform into the carotenoid-accumulating plastids termed chromoplasts that give the red, orange and yellow colours found in ripe and ripening tomato fruits. The transition process involves remodelling of the plastid's internal membrane system leading to the formation of carotenoid-rich membranous sacs, and concomitant chlorophyll degradation. This modification is associated with fruit softening, the conversion of starch into simple sugars, and the synthesis of compounds that are associated with taste and aroma (proteins potentially involved in the lipoxygenase pathway, leading to the generation of aroma volatiles includes phospholipase Dα1, lipoxygenase C and hydroperoxide lyase), and it involves strong regulation by the essential plant development hormone, ethylene (Barsan et al., 2010; Egea et al., 2010; Li and Yuan, 2013; Pesaresi et al., 2014).

Several genes for plastid-localized proteins have been observed to display significant changes in expression, transcriptionally and translationally, during chromoplast differentiation. For example, the genes involved in carotenoid biosynthesis, such as *Lycopene β-cyclase* (*CYC-B*) (Dalal et al., 2010), are up-regulated, while the genes encoding proteins involved in

photosynthetic activity, such as the major chlorophyll *a*/*b* binding proteins (LHCP) and the small subunit of ribulose-1,5-bisphosphate carboxylase/oxygenase (Rubisco) are down-regulated during chromoplast formation (Pech et al., 2014). Large amounts of nuclear-encoded non-photosynthetic plastid proteins, such as proteins related to the biosynthesis of fatty acids, amino acids, carotenoids, vitamins, hormones, and aroma volatiles, have been observed in the chromoplastic proteome of tomato (Barsan et al., 2010). More importantly, Barsan et al. (2010) detected Toc/Tic proteins together with chaperonin-associated proteins in tomato fruit chromoplasts, indicating the presence of the plastid protein translocation system. In contrast, proteins associated with internal trafficking through the thylakoid to the lumen are absent as a result of the loss of thylakoid structure in the chromoplasts (Pech et al., 2014). Such circumstances imply the need for an active plastid import adaptation to meet the changing metabolic demands of the organelle. Although generally the photosynthetic apparatus is strongly down-regulated during chromoplast differentiation, several plastid-encoded photosynthetic genes such as *rbcL*, the gene for large subunit of Rubisco (LSU), remain highly expressed in ripened tomato (Barsan et al., 2012). However, the function of the corresponding proteins in chromoplasts, at a stage where chlorophylls have totally disappeared, is unknown.

A large body of evidence from studies of chloroplasts has revealed the importance of protein translocation (including protein import) machinery for plastid biogenesis (Jarvis, 2008; Kessler and Schnell, 2009). One of the known mechanisms underlying the transformation of plastids from one type to another involves the direct action of the ubiquitin-proteasome system (UPS) mediated by SP1, a RING-type ubiquitin E3 ligase located in the plastid outer envelope membrane (Ling et al., 2012). Studies in Arabidopsis have revealed that SP1 is important for regulation of developmental transitions that require reorganization of the plastid proteome, such as during de-etiolation and leaf senescence.

The SP1 protein regulates chloroplast protein import from the cytosol by selectively targeting TOC components for ubiquitination and promoting their degradation by the proteasome, and

this ultimately controls the plastid proteome and plastid development (Ling et al., 2012). The TOC receptors exist in different isoforms which enables the formation of substrate-specific translocons and the operation of substrate-specific protein import pathways (Jarvis, 2008). In Arabidopsis, the Toc159 and Toc33 receptors mediate import of photosynthetic preproteins, while Toc132/120 and Toc34 mediate import of non-photosynthetic preproteins (Jarvis, 2008). The selective turnover of certain TOC receptor isoforms by the action of SP1 may optimize plastid protein import and enhance plastid differentiation. The reduction of photosynthesis-related protein accumulation during tomato fruit chromoplast development implies a need for reorganization of the TOC machinery to accommodate a different set of preproteins: as different TOC receptor isoforms possess different specificities towards distinct types of precursor proteins, it is anticipated that the level of TOC machinery that recognizes photosynthetic precursor proteins will decrease during the transition, concomitant with changes in organelle morphology and chlorophyll degradation. In this way, SP1 action may trigger a more rapid fruit ripening process. Furthermore, studies by Yan et al. (2014) revealed that tomato Toc159 and Toc34 homologues share high sequence similarity with the comparable import apparatus components from Arabidopsis and pea, indicating similar specificity might also exist in tomato.

Studies on the potential role of SP1 in tomato may identify practical applications in agriculture. In addition, from a fundamental perspective, there is a particular advantage in employing tomato as an alternative model to study SP1 function, as it enables chromoplast development to be studied. As nuclear genes encode most of the proteins associated with the build-up of chromoplast metabolism and chlorophyll degradation, this developmental process depends on the import of these nuclear-encoded proteins into plastids. Therefore, along with many other factors that are known to influence and control plastid differentiation in tomato, SP1's known role in the regulation of the plastid translocation machinery suggests that it too may play a critical role in the process. However, at the outset of this project, this hypothesis had not been addressed.

I hypothesized that SP1 is associated with the regulation and reorganization of the TOC machinery not only during de-etiolation and leaf senescence (as shown in Arabidopsis), but also during fruit ripening in tomato where chloroplasts transform to chromoplasts. I further hypothesized that the SP1's roles in plastid transitions are conserved across plant species. To address these hypotheses, I conducted detailed analysis of tomato plants with altered expression of the single tomato SP1 gene.

SP1 has two homologues in Arabidopsis, SPL1 (SP1-Like Locus1) and SPL2 (SP1-Like Locus2). However in tomato, only SPL2 is present. A similar analysis of SPL2, was conducted in tomato and will be discussed in Chapter 6. The association of SPL2 with chloroplasts was first reported by Ling et al. (2012), who presented a subcellular localization analysis showing that Arabidopsis SPL2 is localized around the chloroplast envelope. Phylogenetic analysis in Figure 3.1 shown that SPL2 was separated into a different sub-clade from SP1 and SPL1 in the phylogenetic analysis (Pan et al., 2016). However, the function of both SPL1 and SPL2 proteins in plastid biogenesis remains to be elucidated.

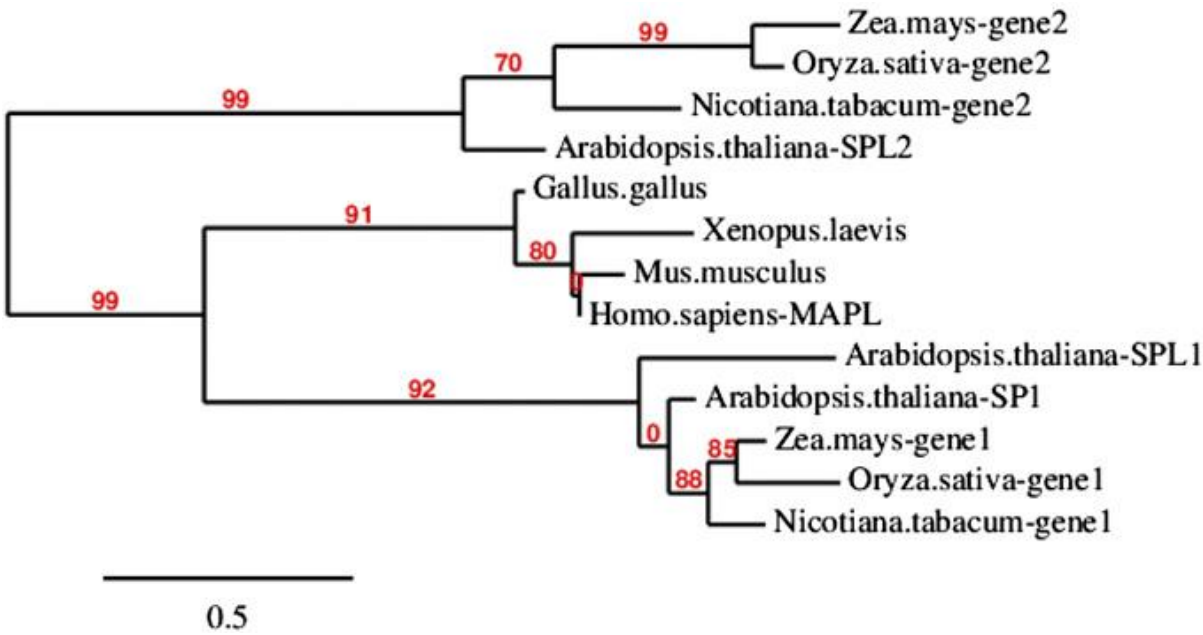

Figure 3.1 Phylogenetic analysis of SP1-related and human MAPL-related proteins. The analysis was done using Phylogeny.fr (www.phylogeny.fr/) using plant and non-plant protein sequences. The plant protein sequence include *Arabidopsis thaliana*, *Zea mays*, *Oryza sativa*, and *Nicotiana tabacum*, while non-plant species include *Homo sapiens*, *Mus musculus*, *Xenopus laevis*, and *Gallus gallus*. The analysis shows that the Arabidopsis SP1 protein family can be divided into two subclades, with SP1 and SPL1 in one subclade and SPL2 in the other. Scale bar represents 0.1 amino acid substitutions per site. The branch support values (%) are shown in red. This diagram was taken from Pan et al. (2016).

3.2 Results and discussion

3.2.1 Sequence analysis of SlSP1

The coding region of *SlSP1* (Solyc06g084360) was cloned from *Solanum lycopersicum*. *SlSP1* encodes 381 amino acids with two transmembrane domains (TMD) and a conserved C3HC4-type RING finger (RNF) domain (Figure 3.2A). The SlSP1 transmembrane domains were predicted using TMPred program (Hofmann, 1993). Alignment of SlSP1 with homologues from other species, namely AtSP1 (At1g63900) from *Arabidopsis thaliana* and mitochondrial protein MULAN (NM_024544) from humans, indicated a highly conserved RING motif (Figure 3.2B). The amino acid sequence identities shared between SlSP1 and AtSP1 or MULAN are, respectively: 73.3% and 26.1% over the full-length sequences, and 83.3% and 39.6% over just the RNF domains. The other tomato SP1 homologue, SlSPL2 (SP1-Like Locus2, Solyc12g049330), shares 47.1% identity to *Arabidopsis thaliana* (AtSPL2, At1g54150) at the protein level, and 62.3% over the RNF domains (Figure 6.1 in Chapter 6). In comparison to the SlSP1 protein sequence, SlSPL2 shares 18.5% and 39.6% identity over the full-length sequence and RNF domain, respectively (Figure 6.1 in Chapter 6).

Data on translational fusions to yellow fluorescent protein (YFP) in Figure 3.2C have supported SlSP1 protein localization to the chloroplast envelope. This localization is in-line with the subcellular localization of AtSP1 (Ling et al., 2012), and is likely dependent on the two predicted transmembrane spans shown in Figure 3.2A. Localization of SlSP1 to chloroplasts might also indicate a conserved function of SP1 in another species.

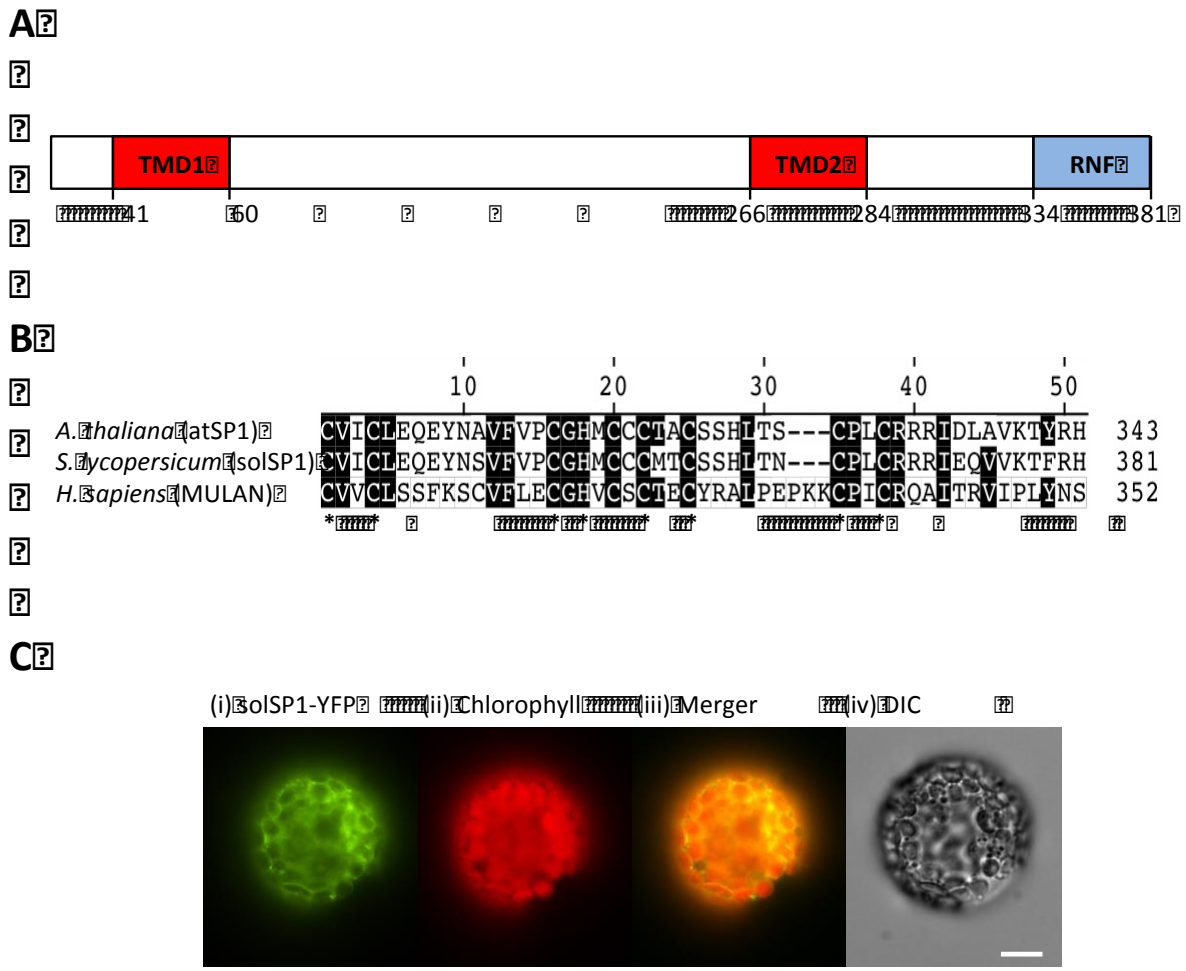

Figure 3.2. Sequence analysis of SlSP1. (A) Schematic drawing of the structure of SlSP1 protein showing two transmembrane domains (TMD) and a RING finger domain (RNF). (B) Amino acid sequence alignment of the C3HC4-type RNF domains of AtSP1 (*Arabidopsis thaliana*), SlSP1 (*Solanum lycopersicum*), and MULAN (*Homo sapiens*) performed using MegAlign by the Clustal W method (DNASTAR Lasergene). Identical residues to MULAN are marked in black. The critical conserved Cys and His residues are indicated with asterisks. (C) Confocal images of protoplasts transiently expressing SlSP1-YFP (i), chlorophyll fluorescent (ii), superimposition of YFP and chlorophyll fluorescent signal (iii) and image of differential interference contrast (DIC) microscopy (iv). Images were obtained from Dr Qihua Ling. Scale bar = 10 μm.

3.2.2 Gene expression analysis in different tomato plant tissues and fruit developmental stages

The transcript levels of *SlSP1* were analysed in different tissues of *Solanum lycopersicum* (cv. Ailsa Craig) during development using qPCR, relative to the expression of a housekeeping gene, *SlACTIN* (*ACTIN2*). The housekeeping gene *ACTIN2* was commonly used as a reference gene for expression analysis done in different tissue of tomato (Bemer et al., 2012). In addition, in a studies of selection of reference genes for qPCR in tomato fruit, González-Aguilera et al. (2016) evaluated the expression of the transcription factors FRUITFULL1 (*FUL1*) and APETALA2c (*AP2c*) across eight MT-*Rg1* fruit developmental stages using four commonly used tomato reference genes, namely *Clathrin Adaptor Complexes medium subunit family* (*CAC)*, *SAND family* (*SAND)*, *Expressed sequence (Expressed)*, and *ACTIN2*. Although *ACTIN2* was ranked as the third most stable reference gene, the trend of the *AP2c* and *FUL1* expression profile did not change substantively. In contrast, the evaluation of appropriate reference genes for gene expression studies in pepper revealed *ACTIN1*, the other gene-family of *ACTIN,* was more suitable reference gene for reliable qPCR data normalization for different pepper tissues (root, stem, leaf, and flower) (Bin et al., 2012).

Figure 3.3A shows that in vegetative plant organs, *SlSP1* is more highly expressed in leaf tissues than in root and stem. In reproductive organs, the expression of *SlSP1* was much higher in flowers (petal and sepal) and at later fruit developmental stages. Comparing the various fruit developmental stages, *SlSP1* transcript abundance was much higher in breaker and orange stages than in developing fruit (0.5 cm fruit size), pre-mature green (PreMG), and mature green (MG), but decreased when the fruits turned red. The higher levels of *SlSP1* transcript in coloured tissues and selected plant organs suggested a particularly important role for the SlSP1 protein at these developmental stages. As shown in Figure 3.3A, the expression analysis of *SlSPL2* revealed a very similar pattern, but with very much less abundance compared to *SlSP1*. The rigor and relevance of the results rely on the equal amount of total RNA used to synthesize cDNA as well as the efficiency between the primer pairs used in the

analysis, relative to *SlACTIN,* as an internal standard. However, this approach provides only comparative data between *SlSP1* and *SlSPL2*, as it has been difficult to quantitate the absolute amount of specific mRNA without an internal standard of known concentration.

The lower transcript abundance of *SlSPL2* suggested that this gene might play a less critical role in the regulation of chloroplast protein import via ubiquitin-proteasome system (UPS) under normal growth condition such as in controlling stomatal aperture and drought resistance (Gao et al., 2015). Whether SPL2 are involved in organelle biogenesis and/or dynamics has not been determined. Studies in Arabidopsis by Pan et al. (2016) showed that SPL2 was separated into a different sub-clade from SP1 in their phylogenetic analysis (Figure 3.1), further support the indication that SPL2 might be involved in other aspects of plant regulation distinct from SP1. The outcome of other work on SlSPL2 will be discussed in Chapter 6.

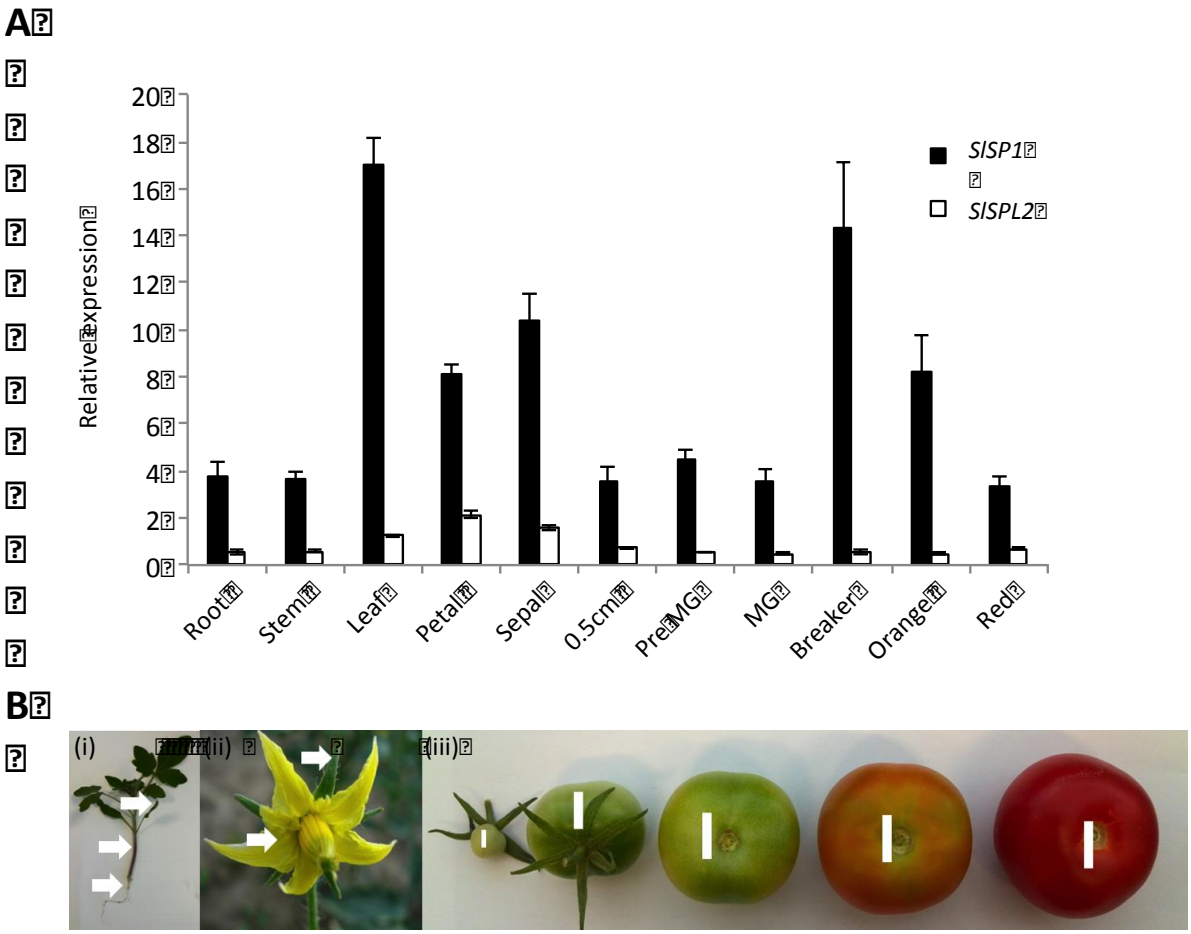

Figure 3.3. Expression analysis of *SlSP1* and *SlSPL2* in various tomato plant tissues and fruit developmental stages. (A) qPCR analysis of *SlSP1* and *SlSPL2* expression in different organs, normalized to the expression of a housekeeping gene, *SlACTIN*. (B) Images showing the samples used for the qPCR analysis of different tissues and fruit stages. (i) White arrows showing the root, stem and leaf tissues of 4-week-old tomato plants used in the analysis. (ii) White arrows showing the petal and sepal flower parts of 2-month-old tomato plants examined in the analysis. (iii) White bars representing the area of fruit flesh on fruits collected from developing (0.5 cm fruit size), pre-mature green (PreMG), breaker, orange and red fruit stages for the analysis. No image for mature green (MG) stage is shown here, but the fruit sample was collected from the equivalent area to other fruit samples. The data represent the mean +SEM for 3 biological replicates.

3.2.3 Gene expression analysis of SlSP1 transgenic lines

To investigate the function of SlSP1 in tomato, transgenic tomato lines with modified SlSP1 expression (overexpression, OEX; and silencing, RNAi) were generated in the lab by Dr Qihua Ling following the protocol by Sun et al. (2006). The overexpressing and silencing of *SlSP1*, young tomato leaf tissues from T1 and T2 generation of the transgenic plants were collected and assayed by qPCR, relative to the expression in the WT plants and normalized to *SlACTIN*, to confirm that the transgenes are stably expressed. Four to five independent T1 transgenic lines were screened for highest expression of the transgene. Two to three T1 transgenic plants that had overexpression and silencing were grown to generate T2 seeds. Twenty T2 seeds from each of the chosen T1 overexpressed and knockdown lines were tested kanamycin resistance indicating presence of the transgene. Three out of twenty seeds resistant to kanamycin for each were kept for expression analysis and subsequent experiments. To ensure continued stable overexpression or silencing of the transgene, subsequent confirmatory gene expression analysis as shown in Figure 3.4 was done prior to all the analyses involving T2 homozygous transgenic tomato plants (including abiotic stress experiments, discussed in Chapter 5).

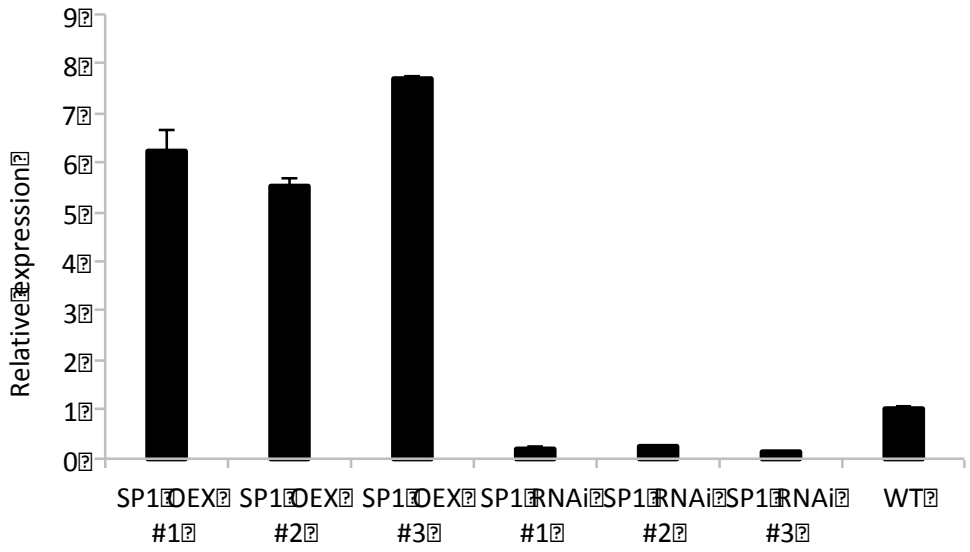

Figure 3.4. Expression analysis of *SlSP1*. The analysis was done using qPCR, relative to the expression in the WT plants, normalized to *SlACTIN* using the leaves of 2-week-old tomato plants in T2 generation. The numbers preceded by the # symbol identify independent transgenic lines. SP1 OEX represents transgenic tomato plants showing expression of more than 5.0-fold relative to WT, while SP1 RNAi represents transgenic tomato plants with expression less than 0.3-fold relative to WT. The data represent the mean +SEM for 3 biological replicates.

3.2.4 Fruit ripening analysis of SlSP1 transgenic plants: ripening of detached fruit

The high level of *SlSP1* transcript in breaker fruits (Figure 3.3A) suggested SP1 involvement during tomato fruit ripening. To investigate the potential role of SP1 during fruit ripening, transgenic fruits were harvested at the onset of breaker stage and incubated at 25°C in the dark. Then, a ripening analysis was carried out by taking chroma meter readings on a daily basis all the way through to the mature red stage. Chroma meter readings (*a**/*b** values) were used as a parameter to determine tomato ripeness based on colour. Colour is also a good indicator of consumer acceptance when tomatoes are fully ripened (López Camelo and Gómez, 2004). In this analysis, the *a**/*b** ratios were recorded and the tomato colour values used by reference to the United States Department of Agriculture (USDA), and following the estimation of the tomato colour *a**/*b** values as described by Batu (2004). Figure 3.5 shows that transgenic tomato lines with altered SP1 expression display changes in this developmental transition. The fruit ripening process in SP1 OEX lines was more rapid than that in WT, whereas the SP1 RNAi fruit showed an even longer ripening duration than WT. These points are further reinforced by Figure 3.6, which shows typical fruit with no differences and visible differences in colour on Day 1 at the breaker stage and Day 8 post breaker stage, respectively. Overall, the data indicate that tomato fruit ripening process is SP1-dependent.

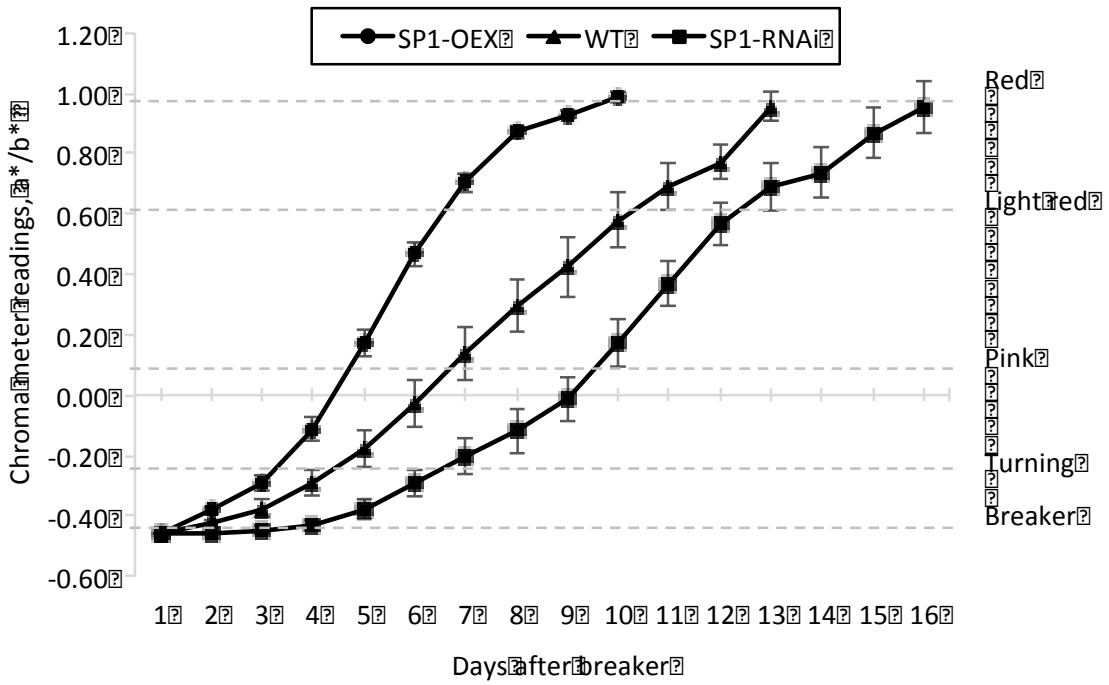

Figure 3.5. Ripening analysis of SlSP1 in detached tomato fruits. The fruit stages indicated to the right are defined following USDA standards (Anon, 1975). Fruits were collected at breaker stage (as determined by comparing the *a**/*b** ratios to the USDA standards), and then stored under darkness at 25°C. The analysis was carried out by determining chroma meter readings (*a** and *b** values) for the blossom-end of the fruits from T2 generation plants on a daily basis from breaker stage, and all the way through to the mature red stage. The colour (*a**/*b**) values of tomatoes at USDA colour stages were described by Batu (2004). The fruit populations used in the ripening analysis were collected from two individual T2 generation tomato plants of each of two independent transformants for both SP1 OEX and SP1 RNAi. WT fruits were collected from non-transformed plants. Data are mean +SEM for at least 30 fruits per genotype.

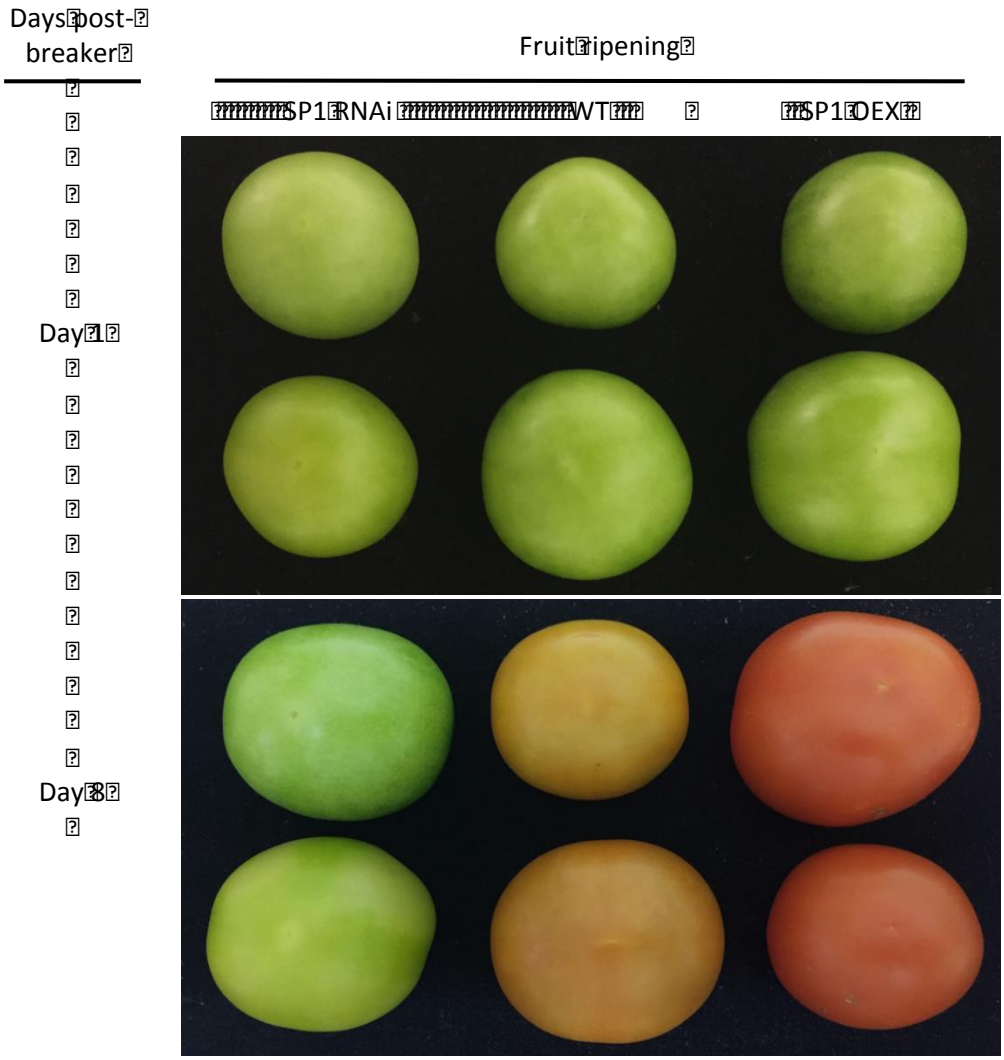

Figure 3.6. Evaluation of the effect of SlSP1 on ripening in detached tomato fruits. Representative images of tomato fruits of each genotype on the day after breaker stage is reached (Day 1) and Day 8 post breaker stage. The fruit populations used in the ripening analysis were collected from two individual T2 generation tomato plants of each of two independent transformants for both SP1 OEX and SP1 RNAi. WT fruits were collected from non-transformed plants. Two fruits shown for each genotype derived from different lines.

3.2.5 Analysis of quality of detached fruit in SlSP1 transgenic plants: fruit firmness and fruit size

Several ripening-related genes have been identified and characterized to understand their roles during fruit development (Gray et al., 1994). Since ripening involves various structural modifications (Rosso, 1968; Spurr and Harris, 1968; Harris and Spurr, 1969) and is tightly controlled by hormone homeostasis (Pandolfini, 2009), it was important to further assess the changes in ripening duration observed in the lines with altered SP1 expression by measuring another parameter linked to ripening.

I began by measuring the firmness of the ripening fruit using a durometer. Although the SP1 OEX and SP1 RNAi transgenes were both observed to alter ripening in detached tomato fruits (Figure 3.5), no obvious differences in fruit firmness were observed at breaker stage (Figure 3.7A). Thus, in spite of the changes in the rate of the ripening process seen in the transgenic lines, the modifications apparently caused no changes in the extent of softening of the fruits at defined stages.

Next, I measured fruit firmness at fixed time-points following the breaker stage. While there were no obvious differences in firmness shortly after the breaker stage (Day 1-2 and Day 5-6 post breaker stage), there was a clear difference in firmness on Day 9-10 post breaker stage between the SP1 OEX and WT fruits (Figure 3.7B). This observation is consistent with the colorimetric and visual indicators of ripeness (Figure 3.5 and 3.6), and establishes a clear pattern of accelerated ripening in SP1 OEX fruits. In contrast with SP1 OEX, the SP1 RNAi fruit did not display statistically significant changes in firmness at Day 9-10, relative to WT. This is most likely a reflection of the fact that even the WT fruit had not undergone much softening at this time point, indicating that fruit softening occurs rather late in the ripening process. I possibly would have seen a more clear difference if the analysis was continued to a later time point.

Proper ripening in detached tomato is dependent on the developmental stage the fruits were harvested. When a fruit enters the MG stage, it reaches its final size, becomes more susceptible to environmental influences, and is competent to ripen (Chevalier, 2007). During the onset of fruit ripening, which is referred to as breaker stage, chloroplasts begin their conversion to chromoplasts, as indicated by the change in colour to yellow-orange, owing to chlorophyll loss and accumulation of carotenoid pigments (Ho and Hewitt, 1986). Without having completed their normal growth up to the MG stage, however, the ripening process is inhibited by harvesting and is not inducible. To avoid mistakenly including immature fruit in the ripening analysis, which could cause delay in ripening due to their incomplete growth, fruit size was measured using a calliper at breaker stage, the point when the fruits were detached from the plants. Figure 3.8 shows that the fruit of the SP1 OEX and SP1 RNAi transgenic lines were not significantly different in size from those of the WT at breaker stage; the differences observed were relatively small and not statistically significant, and may possibly be a result of natural variation in fruit size (Grandillo et al., 1999) and not linked to the modifications in ripening duration. This result also indicated that the fruit used in the ripening analysis were not harvested too young, before reaching their full size, which is important because such interference could have affected the fruit ripening data.

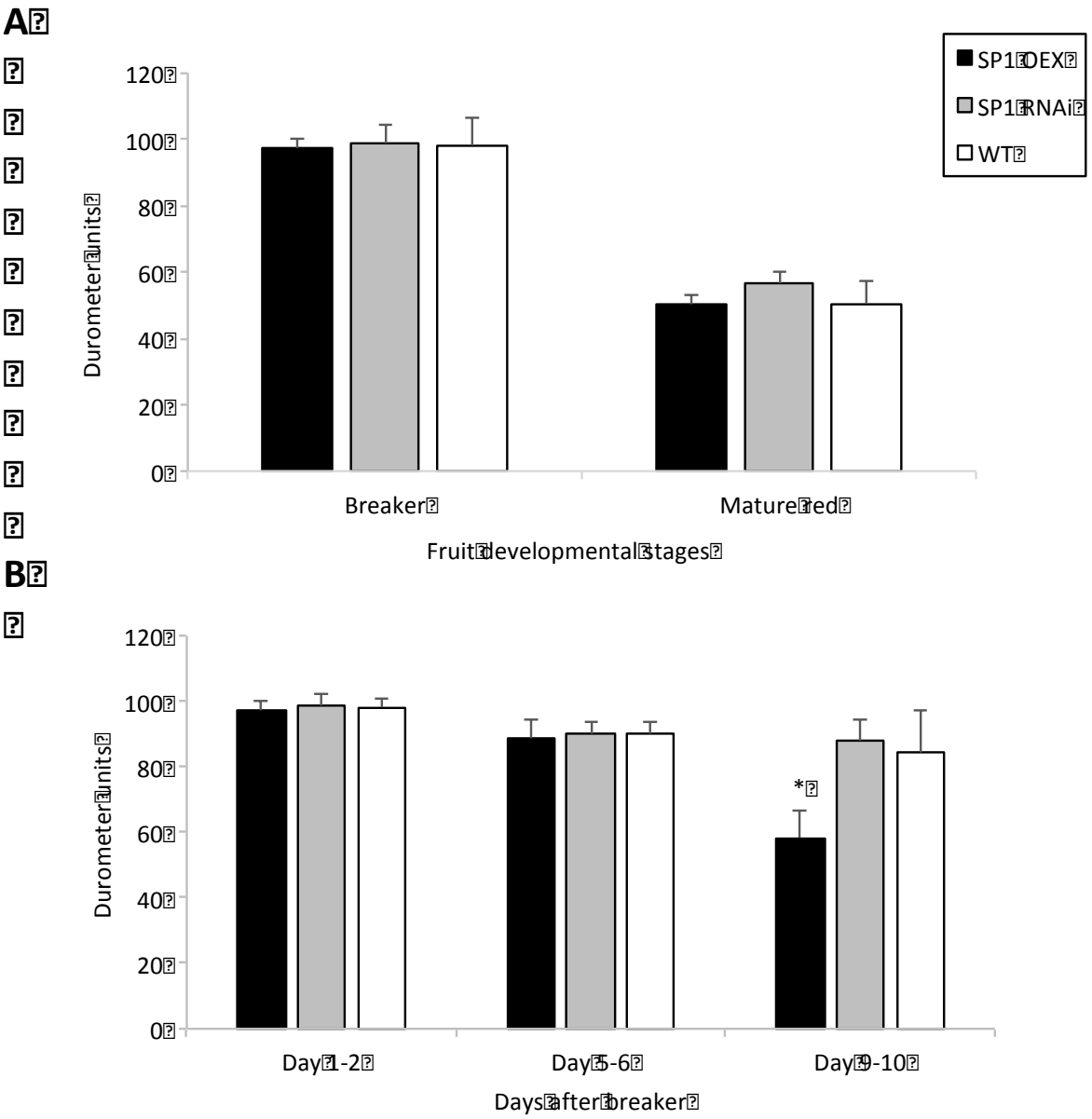

Figure 3.7. Measuring the effect of SlSP1 on firmness of detached tomato fruits using a durometer. (A, B) Fruit firmness measurements at breaker and mature red stages. Student's *t*-test revealed no significant differences between genotypes relative to WT at the defined stages (A) and on Day 1-2, Day 5-6 and Day 9-10 after the breaker stage (B). The fruit used in the analysis were randomly chosen from the fruit populations derived from T2 generation plants used in the ripening analysis in Figure 3.5. Shades representing genotype is shown at the top right. Data are mean +SEM for at least 5 fruits per genotype. Asterisks above the bars indicate a significant difference relative to WT (Student's *t*-test, **P*<0.05). Student's *t*-test also

revealed no significant differences in firmness of mature red fruits between genotypes and firmness of SP1 RNAi fruits on Day 9-10, relative to WT.

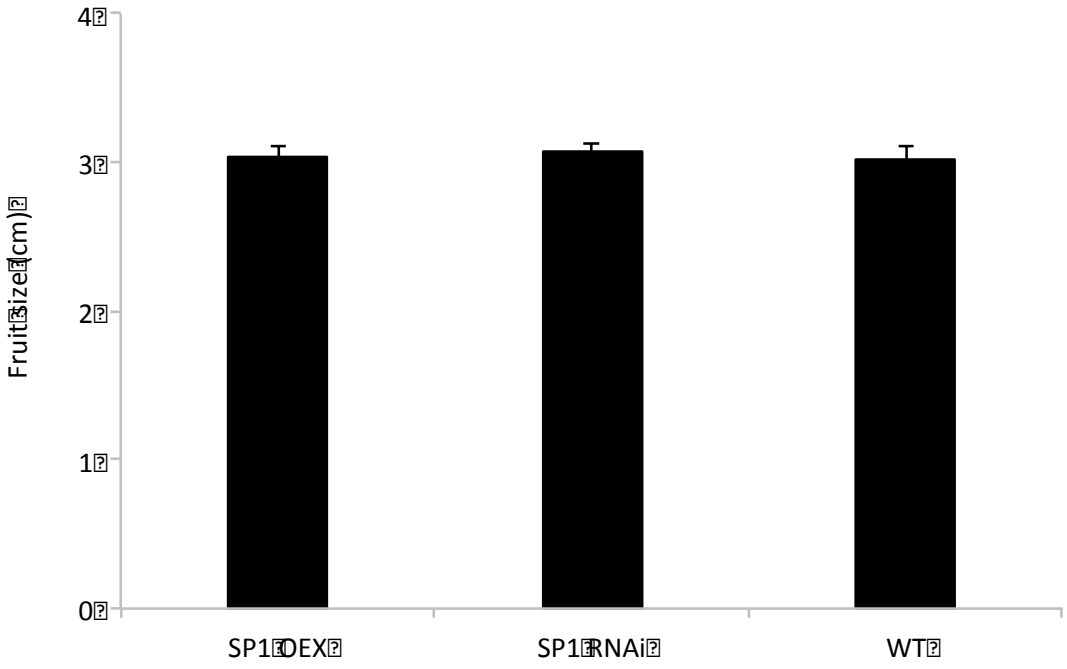

Figure 3.8. Measuring the effect of SlSP1 on size of the fruits used in the ripening analysis. The measurement of the average equatorial diameter of tomato from T2 generation plants was done using a calliper at breaker stage. The fruits were then detached from the plants and incubated at 25°C in the dark for the ripening analysis in Figure 3.5. Data are mean +SEM for 30 fruits per genotype. Student's *t*-test revealed no significant differences between genotypes relative to WT.

3.2.6 Fruit ripening analysis of SlSP1 transgenic plants: ripening of fruit on the vine

There is a general opinion that the quality of tomatoes ripened on the vine is better than tomatoes ripened off the vine, and this has influenced consumer perception of quality. However, ripening off the vine reduces time to harvest, increases turnover, allows longer time for transportation and distribution, and increases shelf life (Arias et al., 2000).

To compare the ripening trend between tomatoes ripened on the vine and detached tomatoes, a similar ripening analysis of tomato fruit on vine was conducted. A total of 10 fruits per genotype, from the same tomato plants used in the ripening of detached fruits experiment were randomly chosen and labelled at breaker stage. Ripening of the selected fruits was examined by recording the number of days to reach the mature red stage from breaker stage. However, no difference was observed between the genotypes (Figure 3.9). Although the transgenic lines with altered SP1 expression displayed no ripening alterations when the fruit were ripened on the vine (in term of the number of days to reach the mature red from breaker stage), the ripening duration of all genotypes was observed to be considerably longer (taking 20-22 days) (Figure 3.9) than detached fruits (taking 16 days for SP1 RNAi) (Figure 3.5).

In the case of ripening on the vine, assessing fruit ripening requires analysis of different types of ripening-related parameters to critically examine the SlSP1-mediated changes. The impact of SP1 on other factors related to tomato ripeness on the vine could be further analysed in the future by measuring fruit firmness and conducting suitable analytical methods to assess antioxidant components and chemical composition such as lycopene, β-carotene, ascorbic acid and total phenolic (Giovanelli et al., 1999). The characterization of tomatoes ripened on and off vine may further help to provide a better post-harvest procedure and improve the quality of ripening in detached tomato fruits (Arias et al., 2000).

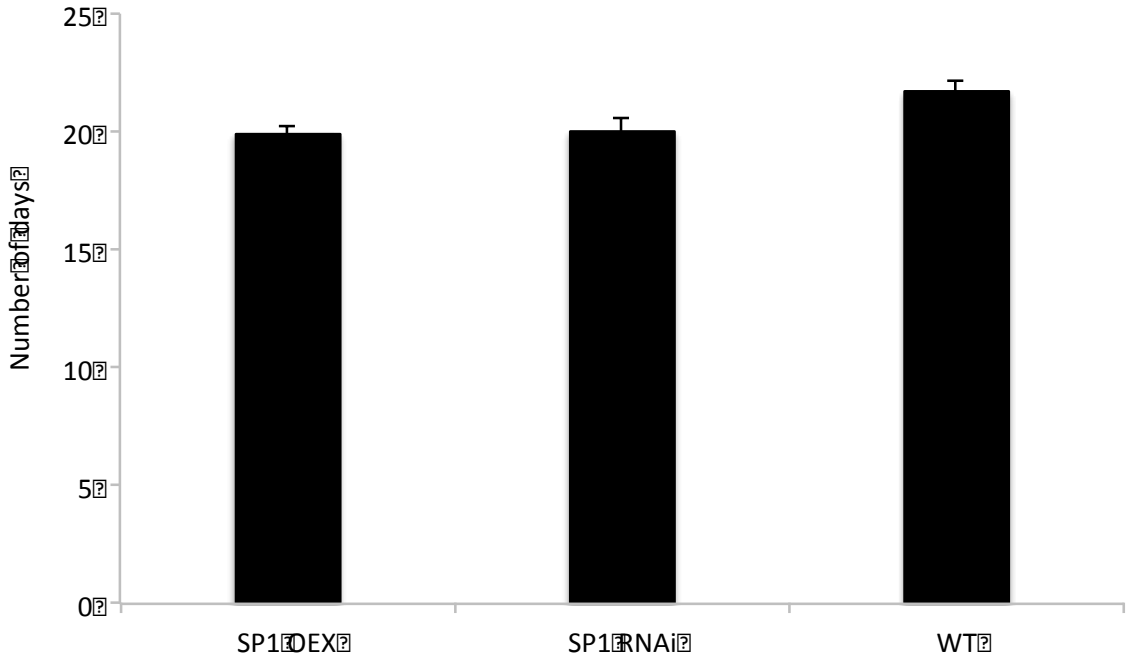

Figure 3.9. Evaluation of the effect of SlSP1 on ripening of tomato fruits on the vine. The analysis was carried out by recording the number of days to reach the mature red stage from breaker stage of the fruits from T2 generation plants. The fruit populations used in the analysis were collected from two individual T2 generation tomato plants of each of two independent transformants for both SP1 OEX and SP1 RNAi. WT fruits were collected from non-transformed plants. Data are mean +SEM for at least 10 fruits per genotype. Student's *t*-test revealed no significant differences between genotypes relative to WT.

3.2.7 Evaluation of the effect of SlSP1 on leaf senescence

To begin to assess whether the functions of SP1, as determined in Arabidopsis, are conserved in another plant species (tomato), the role of SlSP1 in the leaf senescence process was assessed by analysing the SP1 OEX and SP1 RNAi lines using analyses similar to those conducted in Arabidopsis (Ling et al., 2012). Here, the extent of senescence in leaves induced by dark treatment, or following the natural aging process, was characterized by measuring chlorophyll levels and the photochemical efficiency of photosystem II (F_v/F_m), which both decline during the process.

Leaf senescence can be induced prematurely by dark treatment (Schelbert et al., 2009). For senescence induction, at least three individual tomato leaves of 10-12 cm length from 2-month-old plants were covered with aluminium foil. To quantitatively measure the progression of symptoms of leaf senescence, chlorophyll levels were measured using a SPAD-502 meter in the same leaf on Day 1 (before covering with foil) and on Day 30 after the initiation of the dark treatment. Prior to conducting the final measurements, the leaves were also inspected visually. The SP1 OEX lines showed much more pronounced visible leaf yellowing than the WT, providing a clear indicator of accelerated leaf senescence, while the SP1 RNAi leaves appeared to be healthier and greener than WT, without showing visible signs of senescence (Figure 3.10A). These visible phenotypes were reflected in the chlorophyll content measurements, where greater and lower reductions were seen in the OEX and RNAi plants, respectively (Figure 3.10B). Accordingly, F_v/F_m values determined for the SP1 OEX leaves at Day 30 were lower than those for the equivalent WT leaves, whereas F_v/F_m values for SP1 RNAi leaves were higher than those for the WT (Figure 3.10C), although it should be noted that these ratio differences were not statistically significant.

To corroborate the results from the dark-induced senescence experiments, natural senescence in aging plants was similarly examined, and similar trends were observed. Although higher levels of chlorophyll were retained during natural senescence compared to

dark-induced senescence (over a similar 30 day period of analysis), chlorophyll contents nonetheless declined during the progression of senescence in all genotypes; as with the dark-induced experiment, the largest reduction occurred in the SP1 OEX leaves, and the smallest change occurred in SP1 RNAi leaves (Figure 3.11A). Natural leaf senescence progresses via a coordinated process across the leaf, which usually starts from the apex or margins and moves towards the base of the leaf (Lim et al., 2007). The chlorophyll fluorescence parameter images presented in Figure 3.11B are consistent with this, as they reveal that the reduction of F_v/F_m was greatest at the leaf edges towards the lower part of the leaf, most noticeably in SP1 OEX leaves but also in WT leaves to a lesser extent. On calculating average whole-leaf F_v/F_m values from the images, it was apparent that F_v/F_m values in senescent SP1 OEX leaves were lower than those in corresponding WT leaves, whereas those in SP1 RNAi leaves were slightly higher than those in WT (Figure 3.11C).

Overall, these results strongly support an important role for SP1 in promoting leaf senescence in tomato, under both natural and dark-induced senescence conditions.

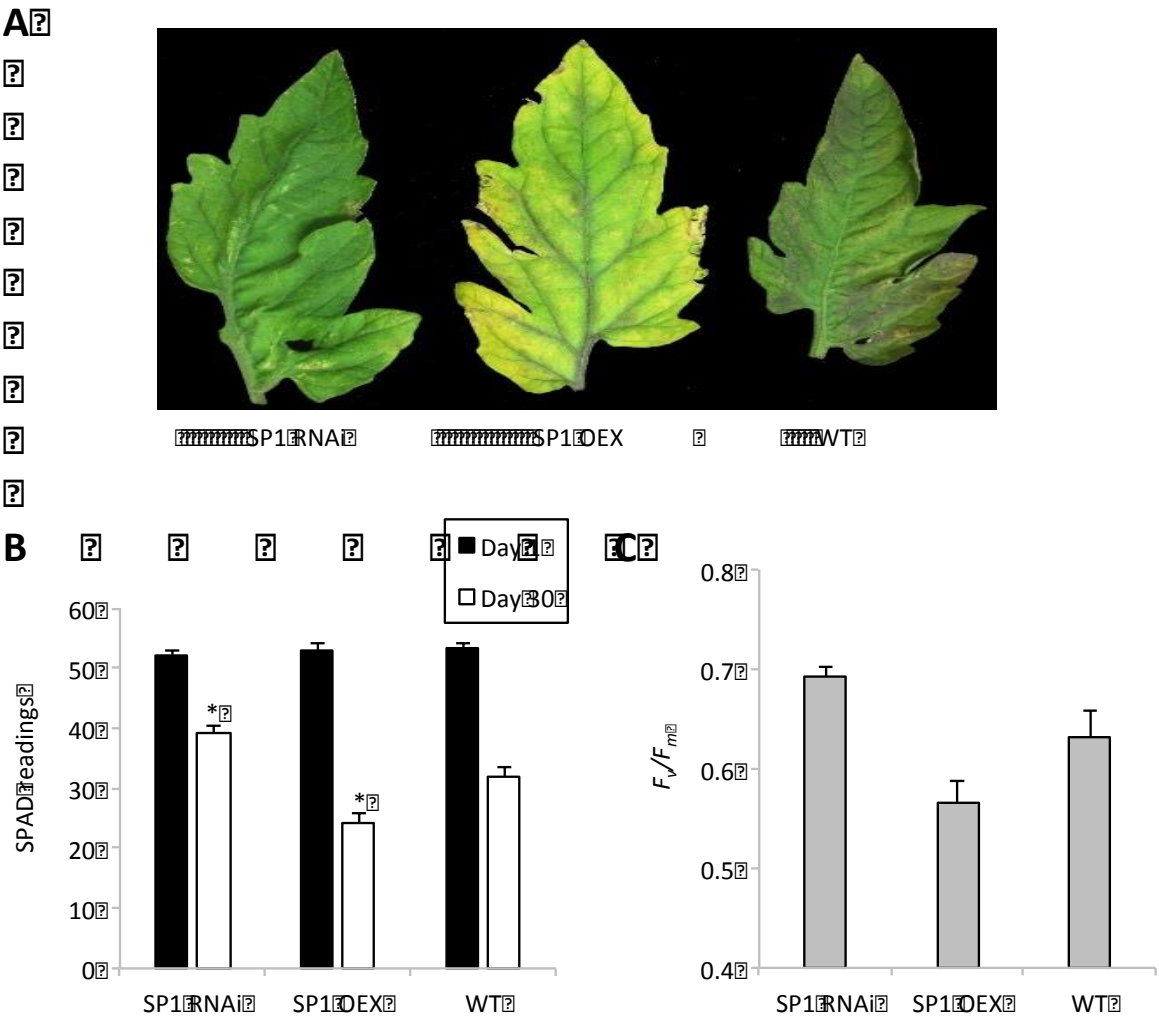

Figure 3.10. Evaluation of the effect of SlSP1 on dark-induced senescence in tomato leaves. (A) Leaves of 2-month-old plants of equal length (10-12 cm) were covered with aluminium foil for 30 days. At the end of the treatment, a representative leaf from each genotype was photographed and is shown. Pronounced yellowing was observed in SP1 OEX leaves, whereas SP1 RNAi leaves appeared greener than WT leaves. (B) Chlorophyll measurements were made using a SPAD-502 meter in the same leaf on Day 1 (before covering with aluminium foil) and on Day 30 after the initiation of the dark treatment. (C) Chlorophyll fluorescence parameters were recorded using CF Imager, and used to calculate F_v/F_m values for whole leaves on Day 30 after the completion of the dark treatment. Data are mean +SEM for at least 3 leaves per genotype. Asterisks above the columns indicate a significant

difference relative to WT (Student's *t*-test, **P*<0.05). Student's *t*-test also revealed no significant differences between genotypes relative to WT in (C).

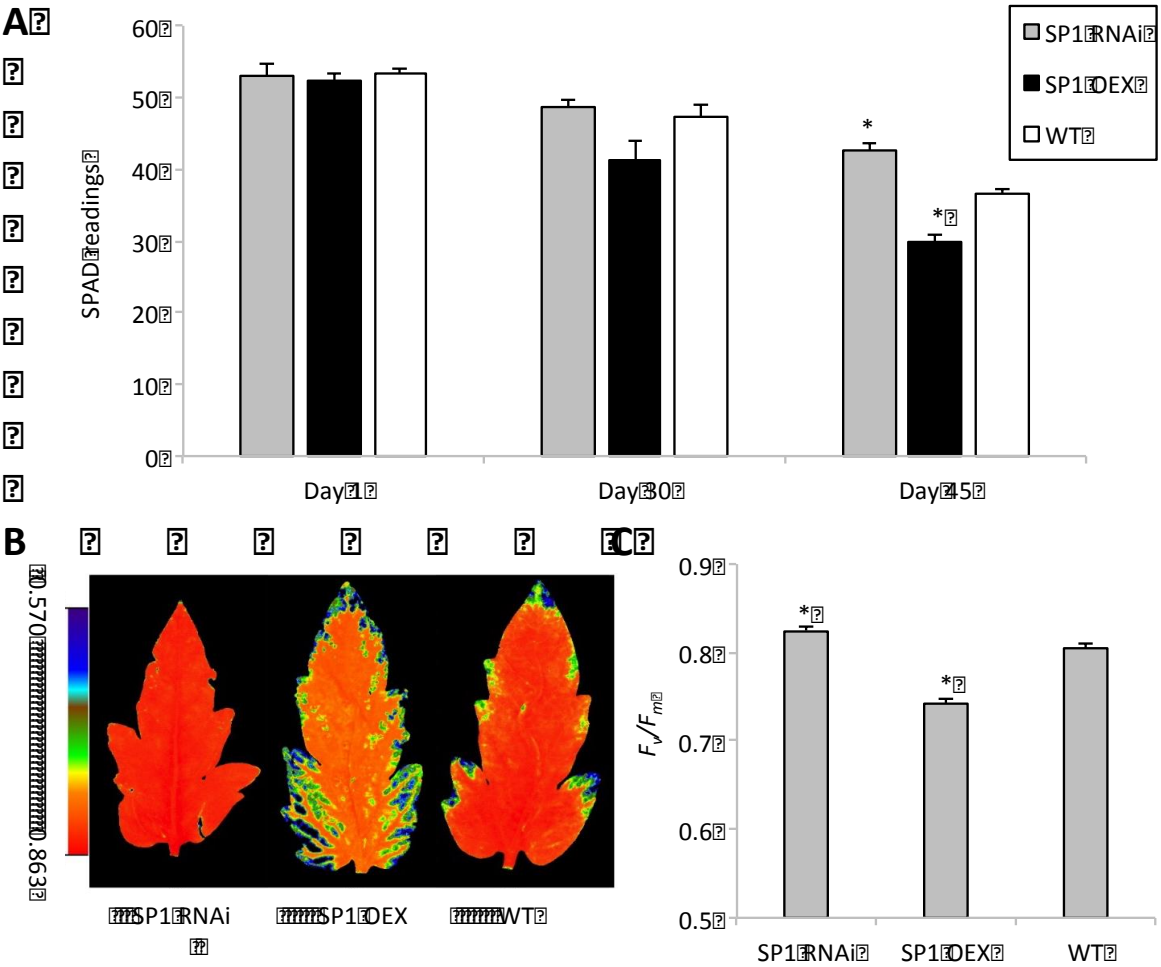

Figure 3.11. Measuring the effect of SlSP1 on the extent of senescence in tomato leaves following a natural aging process. Leaves of equal length (10-12 cm) were selected for analysis on Day 1. (A) Chlorophyll measurements were made using a SPAD-502 meter in the same leaf on Day 1, Day 30, and Day 45 of an experiment conducted on plants that were 2 months old at the outset. Data are mean +SEM for at least 3 measurements per two leaves per genotype per time-point. (B) Chlorophyll fluorescence analysis using a CF Imager revealed photosynthetic differences in naturally senescent leaves of SP1 OEX and SP1 RNAi plants, relative to corresponding WT leaves. The leaves analysed here are from Day 45. A colour spectrum representing the range of F_v/F_m values recorded is shown to the left of the panel. (C) Average F_v/F_m values for whole leaves were calculated using the images shown in

(B) and other similar images. Data are mean +SEM for at least 3 leaves per genotype. Asterisks above the columns indicate a significant difference relative to WT (Student's *t*-test, **P*<0.05).

3.2.8 Immunoblotting to assess for proteome changes in SlSP1 transgenic plants

The SP1 E3 ligase was shown to mediate ubiquitination of chloroplast TOC components and their degradation by the cytosolic ubiquitin-proteasome system (UPS) (Ling et al., 2012). In Arabidopsis, SP1 acts by selectively targeting TOC components to balance the client-specific preprotein import pathways and thereby influence the development fate and functions of the organelle. To further investigate whether SlSP1 functions in a similar way, total leaf protein extracts from mature tomato plants were analysed by immunoblotting. As shown in Figure 3.12, the abundance of Toc75 in SP1 OEX transgenic plants was significantly lower than in WT, and strongly elevated in SP1 RNAi transgenic plants. In contrast, the Tic40 protein level did not change significantly in response to altered expression of SlSP1. These results are in agreement with the data of Ling et al. (2012), which revealed specificity of SP1 for TOC components, with inner membrane components of the chloroplast import machinery being unaffected by SP1 expression in Arabidopsis. Specificity of SlSP1 action was further supported by analysis of 1-deoxy-d-xylulose 5-phosphate reductoisomerase (DXR), an important enzyme of plastid isoprenoid biosynthesis (Carretero-Paulet et al., 2002); like Tic40, the abundance of this protein was not affected by altered expression of SlSP1. Overall, these immunoblotting analyses supported a conserved function of SP1 in tomato and Arabidopsis.

To investigate if SP1 is similarly associated with the regulation of the TOC machinery during fruit ripening in tomato, plastid protein abundances in fruit were analysed by immunoblotting. For this analysis, total protein from detached tomato fruits at Day 7 post breaker stage were studied. As indicated in Figure 3.5 and 3.6, typically, at Day 7-8 post breaker stage, the SP1 OEX fruits were at light red stage (*a**/*b** values above 0.60), WT fruits were at pink stage (*a**/*b** values above 0.08), while SP1 RNAi fruits were at turning stage (*a**/*b** values above -0.27).

As shown in Figure 3.13, the abundance of Toc75 in SP1 RNAi transgenic plants was somewhat lower than in WT, and significantly elevated in SP1 OEX transgenic plants relative to WT. The pattern of expression differences between genotypes here is counterintuitive, and opposite to that seen in the leaves (Figure 3.12). The reason for this is most likely related to the fact that fruit ripening is a highly dynamic process, and that the different genotypes were here analysed at developmentally distinct time-points in the process (as the colour differences noted above indicate). The results suggest the light red stage (SP1 OEX) is associated with higher plastid protein import activity, and that the turning stage (SP1 RNAi) is associated with lower protein import activity.

Despite the obvious differences in carotenoid accumulation, reflected in the aforementioned colour differences between the genotypes, the amount of DXR protein was not affected by SP1 during ripening (Figure 3.13). This result is consistent with the observation that DXR expression is constitutive throughout tomato fruit development (Rodriguez-Concepcion et al., 2001), and lends further support to the specificity of SlSP1 action as determined in Figure 3.12. Finally, a representative photosynthetic protein, PsaD, one of the subunits that form the core complex of photosystem I (Amunts et al., 2008), was analysed and found to have a higher abundance in SP1 RNAi fruits, and reduced abundance in SP1 OEX fruits, relative to WT (Figure 3.13). The PsaD protein is the ferredoxin-binding site of photosystem I, and is encoded by the nuclear gene, *PsaD*. One of the main features of the chloroplast-to-chromoplast transition appears to be associated with major metabolic shifts, which include strong decrease in abundance of proteins of light reactions. The low abundance of PsaD protein in ripen, red fruit of SP1 OEX, which experienced accelerated ripening process, is in agreement with the observation of decreasing abundance of PsaD protein as fruits ripen (Barsan et al., 2012). This pattern of accumulation differences between the genotypes is consistent with the notion of accelerated ripening in SP1 OEX fruit, and retarded ripening in SP1 RNAi fruit. It is also reflective of the fruit colour differences: SP1 RNAi fruit skin is visibly green at this developmental stage, whereas that of WT and SP1 OEX fruits is not (Figure 3.5).

In order to investigate if SlSP1 is similarly involved in the plastid proteome changes that occur during leaf senescence in tomato, total leaf protein extracts from senescent leaves were analysed by immunoblotting. For this analysis, the leaves of 2-month-old plants were induced to senesce by dark treatment of individual leaves for 30 days prior to harvesting. The abundance of Toc75 was reduced in SP1 OEX leaves, relative to WT, and increased in SP1 RNAi leaves (Figure 3.14). These significant differences in Toc75 protein abundance between the genotypes are supportive of a role for SlSP1 in balancing client-specific preprotein import pathways and controlling chloroplast protein import during leaf aging in tomato, as proposed in Arabidopsis (Ling et al., 2012). As expected, the level of Tic40 protein did not change significantly in response to altered expression of SlSP1 (Figure 3.14), in line with the results from non-senescent leaves (Figure 3.12), and in agreement with the conclusions of Ling et al. (2012). In line with the results presented earlier showing differences in photosystem II (PSII) quantum efficiency between the genotypes under senescent conditions (Figure 3.10C), I observed that levels of the PSII component OE33 (Ettinger and Theg, 1991) are somewhat reduced in SP1 OEX leaves, compared to WT, and significantly elevated in SP1 RNAi leaves. These data are consistent with the evidently greener appearance of the dark-treated SP1 RNAi leaves (Figure 3.10A) under broadly similar dark treatment conditions, as well as with the corresponding chlorophyll content data (Figure 3.10B), and provide further support for the conclusion that SP1 OEX accelerates leaf senescence, while SP1 RNAi retards leaf senescence.

Overall, these immunoblotting results provided further confirmation that SP1's roles in plastid transitions are conserved in different plant species.

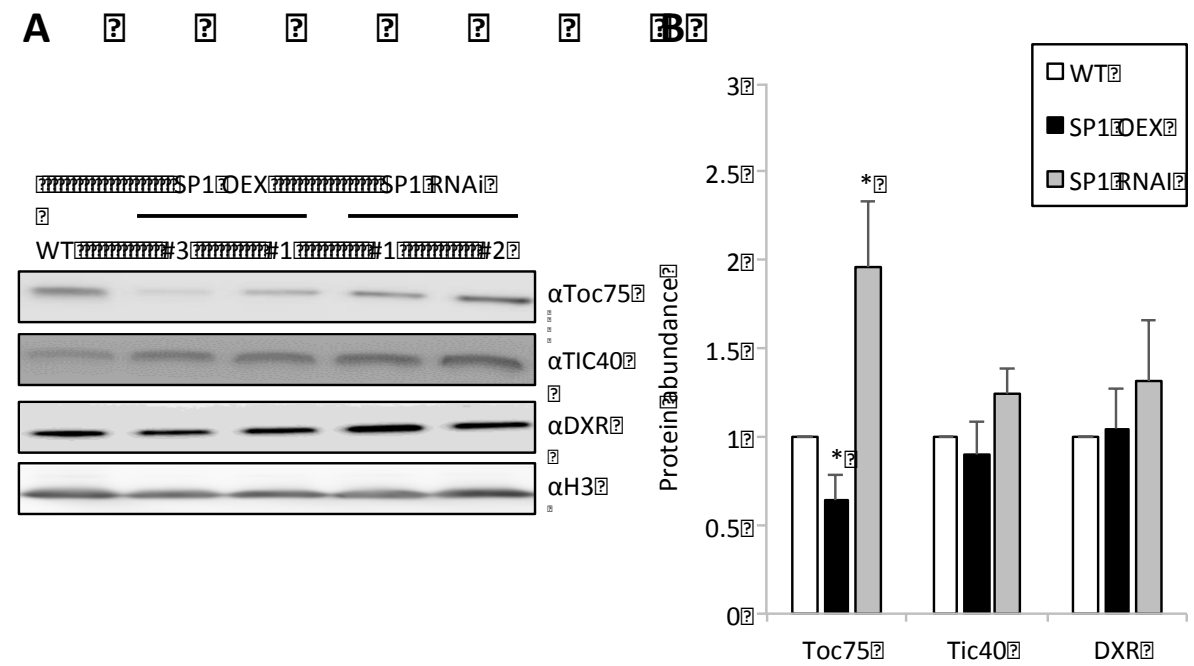

Figure 3.12. Evaluation of the effect of SlSP1 on plastid protein abundance in tomato plant leaves by immunoblotting. (A) Protein extracts were prepared from 2-week-old plant leaves of the indicated genotypes. The numbers preceded by the # symbol identify independent transgenic lines. The protein samples were analysed by immunoblotting using Toc75, Tic40, DXR and H3 antibodies (as loading control), and bands were visualized using chemiluminescence and an ImageQuant LAS-4000 imager. (B) The protein bands were quantified using Aida software. Data for the two independent lines were combined to give a single average. The values obtained were normalized relative to corresponding H3 data. All values were expressed relative to the corresponding WT value, which was set to 1. Data are mean +SEM for two biological replicates. Asterisks above the columns indicate a significant difference relative to WT (Student's *t*-test, **P*<0.05). Student's *t*-test also revealed no significant differences in Tic40 and DXR protein abundance between genotypes relative to WT in (B).

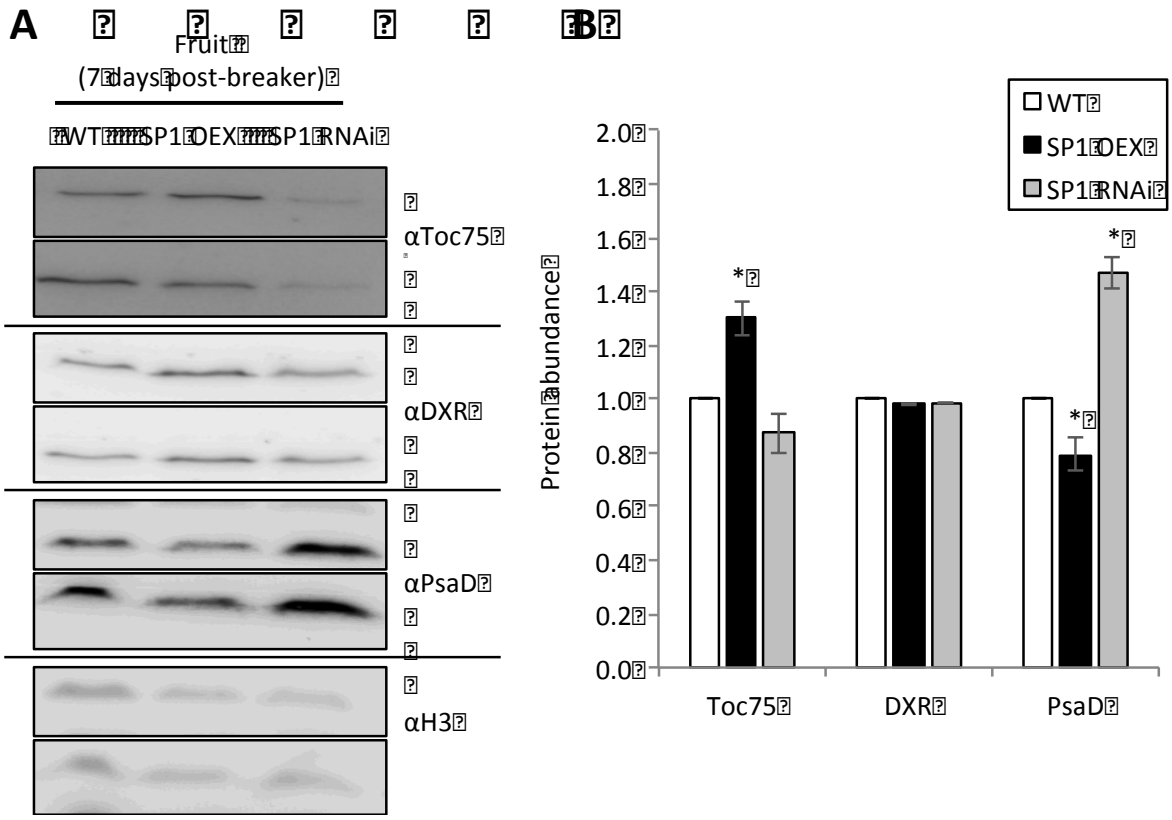

Figure 3.13. Evaluation of the effect of SlSP1 on plastid protein abundance changes during fruit ripening in tomato by immunoblotting. (A) Protein extracts were prepared from fruit of the indicated genotypes at 7 days post-breaker stage. The samples were analysed by immunoblotting using Toc75, DXR, PsaD and H3 antibodies, and bands were visualized using chemiluminescence and an ImageQuant LAS-4000 imager. (B) The protein bands were quantified using Aida software. Data from two technical replicates were combined to give a single average. The values obtained were normalized relative to corresponding H3 data. All the values were expressed relative to corresponding WT value, which was set to 1. Data are mean ± SEM for two technical replicates. Asterisks above the columns indicate a significant difference relative to WT (Student's *t*-test, *P<0.05). Student's *t*-test also revealed no significant differences in DXR protein abundance between genotypes and Toc75 protein abundance in SP1 RNAi, relative to WT in (B).

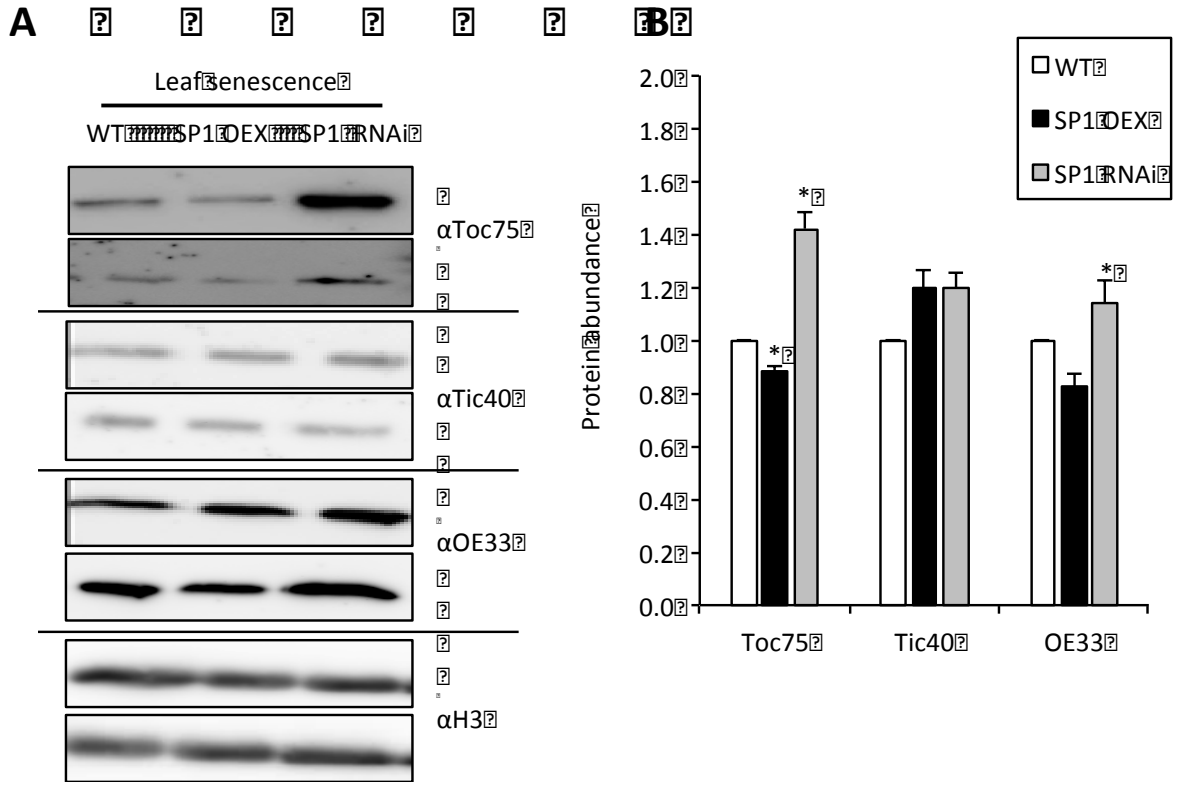

Figure 3.14. Evaluation of the effect of SlSP1 on plastid protein abundance changes during leaf senescence in tomato by immunoblotting. (A) The protein abundance analysis was done using protein extracts from leaves of 2-month-old induced-senescent plants. The samples were analysed by immunoblotting using Toc75, Tic40, OE33 and H3 antibodies, and bands were visualized using chemiluminescence and an ImageQuant LAS-4000 imager. (B) The protein bands were quantified using Aida software. Data for two technical replicates were combined to give a single average. The values obtained were normalized relative to corresponding H3 data. All the values were expressed relative to corresponding WT value, which was set to 1. Data are mean +SEM for two technical replicates. Asterisks above the columns indicate a significant difference relative to WT (Student's *t*-test, *P<0.05). Student's *t*-test also revealed no significant differences in Tic40 protein abundance between genotypes and OE33 protein abundance in SP1 OEX, relative to WT in (B).

3.3 Conclusion

This chapter shows that the SlSP1 protein has a significant impact on the fruit ripening and leaf senescence processes in tomato. The variation in *SlSP1* transcript levels across different tissues suggested an important role of the protein in certain developmental stages. Compared to other tissues, *SlSP1* is highly expressed in leaf, flower, and breaker and orange stage fruits, where plants perform developmental transitions that involve plastid proteome changes. In comparison with *SlSP1*, the expression of *SlSPL2* was much lower, suggesting that SlSPL2 may play rather distinctive or less critical roles than SlSP1. The analyses of SP1 function during fruit ripening showed that alterations in SP1 expression have a significant impact on the speed and duration of fruit ripening. Comparing the fruits at defined stages (breaker and mature red stages) revealed that the SlSP1-mediated changes in fruit ripening duration did not affect another important aspect of ripening, fruit softening. There was no variation in fruit size between the genotypes at breaker stage, and so this could be ruled out as a contributing factor to the modification in ripening duration. However, more experiments will be necessary to determine whether other quantitative aspects of fruit ripening such as fruit metabolism are affected. SP1 function in tomato is not limited to fruit ripening, where chloroplasts transform to chromoplasts. From my results, it is also evident that SlSP1 is also important during leaf senescence when chloroplasts convert to gerontoplasts. The overexpression of SlSP1 was seen to cause enhanced leaf senescence, both under dark-induced conditions and natural aging, whereas the reduction of SlSP1 expression attenuated these processes. A specific effect of SP1 expression levels on Toc75 protein abundance was observed, revealing a conserved function of SP1 in tomato, like that seen previously in Arabidopsis. The over-accumulation of photosynthetic proteins in the SP1 RNAi lines during fruit ripening and during leaf senescence further suggested that a lack of SP1 causes inefficiencies in developmental proteome transitions linked to these processes. It will be interesting to analyse further plastid proteins, such as ripening-related and senescence-related proteins, in the future to enhance our understanding of the underlying mechanisms.

Chapter 4: Analysis of SP1 in Wheat

4.1 Introduction

Wheat (*Triticum aestivum*) is the leading cereal grain produced in the world today, in terms of total harvested weight and amount used for human and animal nutrition (Bushuk and Rasper, 1994). Unlike rice and maize, wheat is best adapted in the temperate regions and occupies around 17% of all crop area to meet the demand for its several purposes for human, livestock and industrial needs.

Wheat is used for several purposes, depending on its varieties, each with different quality standards. For example, the common hard wheat for bread, and the common soft and durum wheat for biscuit and pasta, respectively (Bushuk and Rasper, 1994). Although wheat contains approximately 10-12% protein, nutritionist regard it mainly as a source of metabolizable energy, that is starch (Austin et al., 1986). Starch is the main storage carbohydrate in most vascular plants. It is an abundant, naturally occurring compound of living terrestrial biomass, and it serves as a primary carbohydrate component in the diets of humans and livestock, and in numerous important industrial applications. Because starch is the primary edible constituent of many agriculturally important plants, its synthesis and accumulation influences crop yields.

Starch is found in both non-photosynthetic (amyloplasts) and photosynthetic (chloroplasts) plastids, with different pathways of starch production in each case. Production of starch in long-term storage organs, such as tubers, roots and seed endosperms, takes place in amyloplasts, and depends upon an incoming supply of carbon precursors and energy from the cytosol. Starch may also be synthesized in other plastid types such as chromoplasts of fruits or leucoplasts of oilseeds, where it acts as a store of carbon precursors for intensive biosynthesis of carotenoids and fatty acids, respectively (Martin and Smith, 1995).

The amyloplast is one of several colourless plastid types, collectively called leucoplasts. Unlike proplastids and etioplasts, amyloplasts are not regarded as progenitors of other plastids. Amyloplasts typically differentiate from proplastid precursor organelles (Neuhaus and Emes, 2000; Hurkman et al., 2008). In cereal crops such as wheat (*Triticum aestivum*), amyloplast development is associated with starch synthesis in the endosperm. During such synthesis, two types of essential glucose polymers are developed to make up the molecular architecture of starch granules. Starch structure might be conceptually simple, but it is complex in synthesis involving numerous enzymatic activities including ADP-glucose pyrophosphorylase, starch synthase, starch branching enzyme and starch debranching enzyme (James et al., 2003; Hannah and James, 2008).

Considering the various regulated changes during different amyloplast developmental stages, it seems likely that the regulated import of starch-related and other preproteins from the cytosol into plastids is crucial during amyloplast biogenesis. Translocation of highly abundant starch preproteins may require an import pathway with specific receptors to recognize them. One possibility is that protein import during amyloplast development is mediated mainly by the TOC receptor isoforms Toc132/120 and Toc34, which have specificity for non-photosynthetic precursor proteins. The SP1 protein may act to enable an appropriate balance of the import pathways and this in turn may help to control the development of the amyloplasts (Ling and Jarvis, 2013).

Chloroplasts of leaf tissues retain a portion of the photosynthetically fixed carbon during the day as starch, which they remobilize during the night when CO_2 cannot be fixed by photosynthesis to support non-photosynthetic metabolism and plant growth. Maintaining the supply of assimilated carbon to grain during the grain-filling period ensures that mass per grain in determinate crops is maximized. Attenuation of senescence, the final stage of leaf development, is one of the ways in which this can be achieved (Spano et al., 2003). During senescence, leaf cells undergo important changes including relocation of their nutrients to developing seeds (Lim et al., 2007). Loss of chlorophyll is a characteristic symptom of leaf

senescence that occurs owing to chlorophyll catabolism (Hørtensteiner and Krautler, 2011; Thomas and Ougham, 2014). Delaying leaf senescence may increase crop yield by extending photosynthetic production or reducing susceptibility to pathogens (Thomas and Ougham, 2014). In contrast, if leaf senescence is induced prematurely then crop productivity may be reduced, as occurs under adverse environmental conditions (Gregersen et al., 2013). Thus, manipulating leaf senescence to optimize such processes has the potential to enhance productivity of crop plants. By increasing or decreasing SP1 levels in transgenic Arabidopsis plants, Ling et al. (2012) showed that leaf senescence can be accelerated or retarded, respectively. For example, mutant *sp1* plants perform senescence inefficiently under dark-induced conditions (Ling et al., 2012), indicating a requirement for SP1-mediated reorganization of the TOC machinery. In fact, SP1 may enable manipulation of any developmental process in which plastids type change, and so the protein has multiple potential applications in crops.

I hypothesized that the role of SP1 in modifying plastid biogenesis is conserved across plant species, including cereal crops. To address this hypothesis, and to begin to explore potential applications of SP1 as a technology for crop improvement, I analysed transgenic wheat plants with altered SP1 expression in relation leaf senescence and yield.

4.2 Results and discussion

4.2.1 Sequence analysis of TaSP1

SP1 is encoded by three homeologues in wheat, one representing each of the A, B and D genomes. The wheat SP1 homeologues share 99.4-99.7% amino acid sequence identity over the full-length sequences, or 100% identity over just the RNF domains. The relevant accession numbers for sequence retrieval from Ensembl Plants are listed in Table 4.1.

All three *TaSP1* homeologues encode 341 amino acid proteins with two transmembrane domains (TMD) and a conserved C3HC4-type RING finger (RNF) domains (Figure 4.1A). The transmembrane domains were predicted using the TMPred program (Hofmann, 1993), and showed identical positions in the three homeologues (Figure 4.1A). Alignment of the TaSP1 sequence with homologues from other species, namely AtSP1 (At1g63900) from *Arabidopsis thaliana*, SlSP1 (Solyc06g084360) from *Solanum lycopersicum*, and mitochondrial protein MULAN (NM_024544) from humans, indicated a highly conserved RING motif (Figure 4.1B). The amino acid sequence identities shared between TaSP1 and AtSP1, SlSP1 or MULAN over the RNF domains are 85.4%, 87.5% and 35.4%, respectively. In comparison to the full-length protein sequence, TaSP1 homeologues shares 69.1-69.4%, 72.1-72.4% and 26.1-26.7% identity with AtSP1, SlSP1 or MULAN, respectively.

Table 4.1. The accession numbers of wheat SP1 homeologues from Ensembl Plants.

SP1 homeologues	**Accession number**
TaSP1 A	TRIAE_CS42_**2AS**_TGACv1_114976_AA0370300
TaSP1 B	TRIAE_CS42_**2BS**_TGACv1_146843_AA0473840
TaSP1 D	TRIAE_CS42_**2DS**_TGACv1_178131_AA0591470

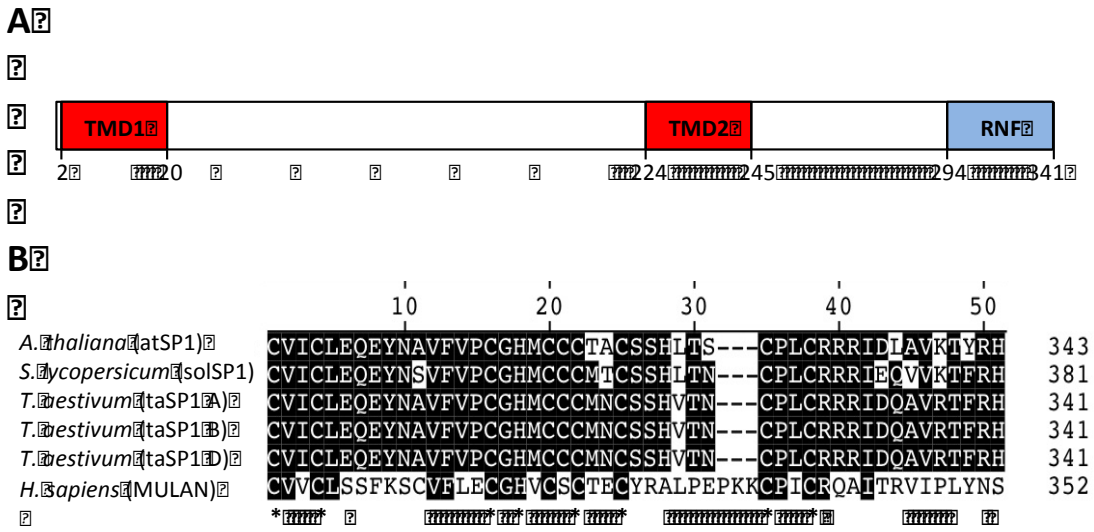

Figure 4.1. Sequence analysis of the three TaSP1 homeologues. (A) Schematic drawing of the structure of TaSP1 protein showing two transmembrane domains (TMD) and a RING finger domain (RNF). All three TaSP1 homeologues can be represented by the same schematic drawing. (B) Amino acid sequence alignment of the C3HC4-type RNF domains of AtSP1 (*Arabidopsis thaliana*), SlSP1 (*Solanum lycopersicum*), the three TaSP1 homeologues (*Triticum aestivum*), and MULAN (*Homo sapiens*) performed using MegAlign by the Clustal W method (DNASTAR Lasergene). Black marking shows residues that are identical in at least three of the six sequences. The critical conserved Cys and His residues are indicated with asterisks.

4.2.2 Gene expression analysis of TaSP1 transgenic wheat lines

To investigate the function of TaSP1 in wheat, Dr Qihua Ling generated transgenic wheat lines with modified TaSP1 expression in collaboration with Dr Emma Wallington at NIAB, Cambridge. The generation of an OEX construct were based on TaSP1 B homeologue. The reason for TaSP1 B being chosen reflected the detection of only TaSP1 B sequence from the amplified TaSP1 coding region from *Triticum aestivum* (cv. Fielder) leaf RNA by RT-PCR. As the publicly available EST data revealed that TaSP1 D is expressed at higher levels than TaSP1 B and TaSP1 A, the RNAi construct was designed based on TaSP1 D homeologue. Although the RNAi construct was designed based on one homeologue specifically, the sequence alignment revealed only a single and five polymorphisms between TaSP1 B and TaSP1 D and TaSP1 A, respectively, in the region that was selected for amplification for the RNAi construct, and thus the RNAi construct would still practically be targeting all three SP1 homeologues.

The overexpressing and silencing of *TaSP1* in the T1 generation of the transgenic plants was confirmed by qPCR, relative to the expression in the WT plants, normalized to *TaACTIN* (Figure 4.2). To ensure stable integration and transmission of the transgene, the gene expression analysis was done prior to all the analyses involving transgenic wheat plants (including abiotic stress experiments, discussed in Chapter 5). Figure 4.2 is the representative result among all *TaSP1* gene expression analyses that were carried out prior to each experiment.

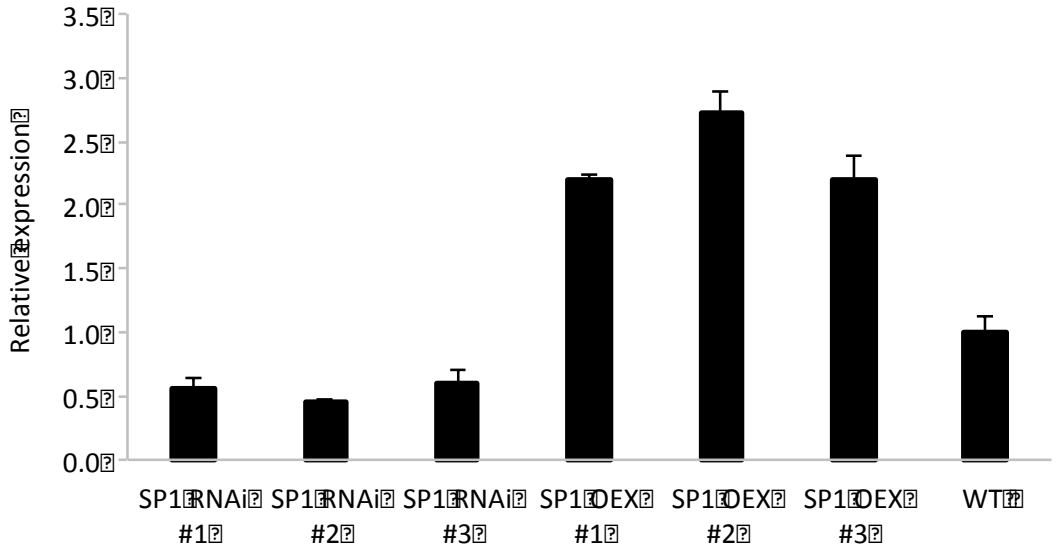

Figure 4.2 Expression analysis of *TaSP1*. The analysis was done using qPCR, relative to the expression in the WT plants, normalized to *TaACTIN* using the leaves of 1-week-old wheat plants. The number preceded by the # symbol identify independent transgenic lines. SP1 OEX represents transgenic wheat plants showing expression of more than 2.0-fold relative to WT, while SP1 RNAi represents transgenic wheat plants with expression less than 0.6-fold relative to WT. The data represent the mean +SEM for 3 biological replicates.

4.2.3 Evaluation of the effect of TaSP1 on leaf senescence

To begin to assess whether the functions of SP1 is conserved in another plant species (wheat), the role of TaSP1 in the leaf senescence process was assessed by analysing the TaSP1 OEX and TaSP1 RNAi lines following the similar analyses conducted in Arabidopsis (Ling et al., 2012). The extent of senescence in detached leaves induced by dark treatment following the natural aging process was characterized by measuring the decline in chlorophyll levels. Loss of photosynthetic competence depends on the function of the light-harvesting and electron transport systems within the chloroplasts, which is indicated by the photochemical efficiency of photosystem II, measured as the F_v/F_m ratio.

For evaluation of leaf senescence following the natural aging process, the primary wheat leaves of 10-day-old plants were marked around 10 cm from the leaf tip on Day 1 (the marked area is shown in Figure 4.3A) and were left growing under normal growth conditions. As wheat leaves senesce naturally, the marked areas on the leaves (Figure 4.3A) were examined for the extent of senescence by measuring chlorophyll content using a SPAD-502 meter on Day 1, Day 14, Day 30 and Day 40. On Day 40, the TaSP1 OEX lines showed much more pronounced visible leaf yellowing around the marked area than the WT, displaying an accelerated leaf senescence, while the TaSP1 RNAi leaves appeared to be greener than WT (Figure 4.3A). The clear difference in the representative image observed at Day 40 reflected the chlorophyll measurement shown in Figure 4.3B, with similar trends to the observation in plants growing under normal conditions in Section 5.2.3.3, Figure 5.7B. Although TaSP1 RNAi plants display only rather modest reductions (less than 60%) in expression of the wheat TaSP1 genes, relative to WT expression level (Figure 4.2), they show strong reductions in leaf senescence leading to a striking ‘stay-green’ phenotype on Day 40 (Figure 4.3C).

Although evaluation of leaf senescence is eminently better following the natural aging process, measuring natural senescence in wheat can be time consuming as it occurred over a relatively long time (40 days) and could limit the leaf suitability of the assay for photochemical efficiency

of photosystem II. Therefore the analysis of senescence in detached leaves induced by dark treatment were conducted, and similar trends with the natural senescence analysis was observed. For evaluation of leaf senescence on detached leaves, the extent of senescence was measured based on comparison between chlorophyll level at Day 1 and Day 7 after initiation of dark treatment and the photochemical efficiency of photosystem II (F_v/F_m), which both decline during the process.

The chlorophyll content of all genotypes on Day 1 and Day 7 is shown in Figure 4.4A. The greater percentage of chlorophyll content reduction was observed in TaSP1 OEX, the largest reduction occurred in the SP1 OEX leaves, and the smallest change occurred in SP1 RNAi leaves, relative to WT (Figure 4.4B). The chlorophyll fluorescence parameter images presented in Figure 4.5A are consistent with the detached leaf senescence evaluation, where the F_v/F_m values seen in the TaSP1 OEX leaves on Day 7 were significantly lower in comparison with the equivalent WT and TaSP1 RNAi leaves were significantly higher than WT (Figure 4.5B).

In contrast with the TaSP1 OEX leaves, the TaSP1 RNAi leaves showed attenuated senescence with significantly smaller reductions in chlorophyll content (Figure 4.4B) and higher F_v/F_m (Figure 4.5B) at Day 7, relative to WT. Overall, these results strongly support an important role for SP1 in promoting leaf senescence in wheat, under both dark-induced senescence on detached leaves and senescence following the natural plant aging process.

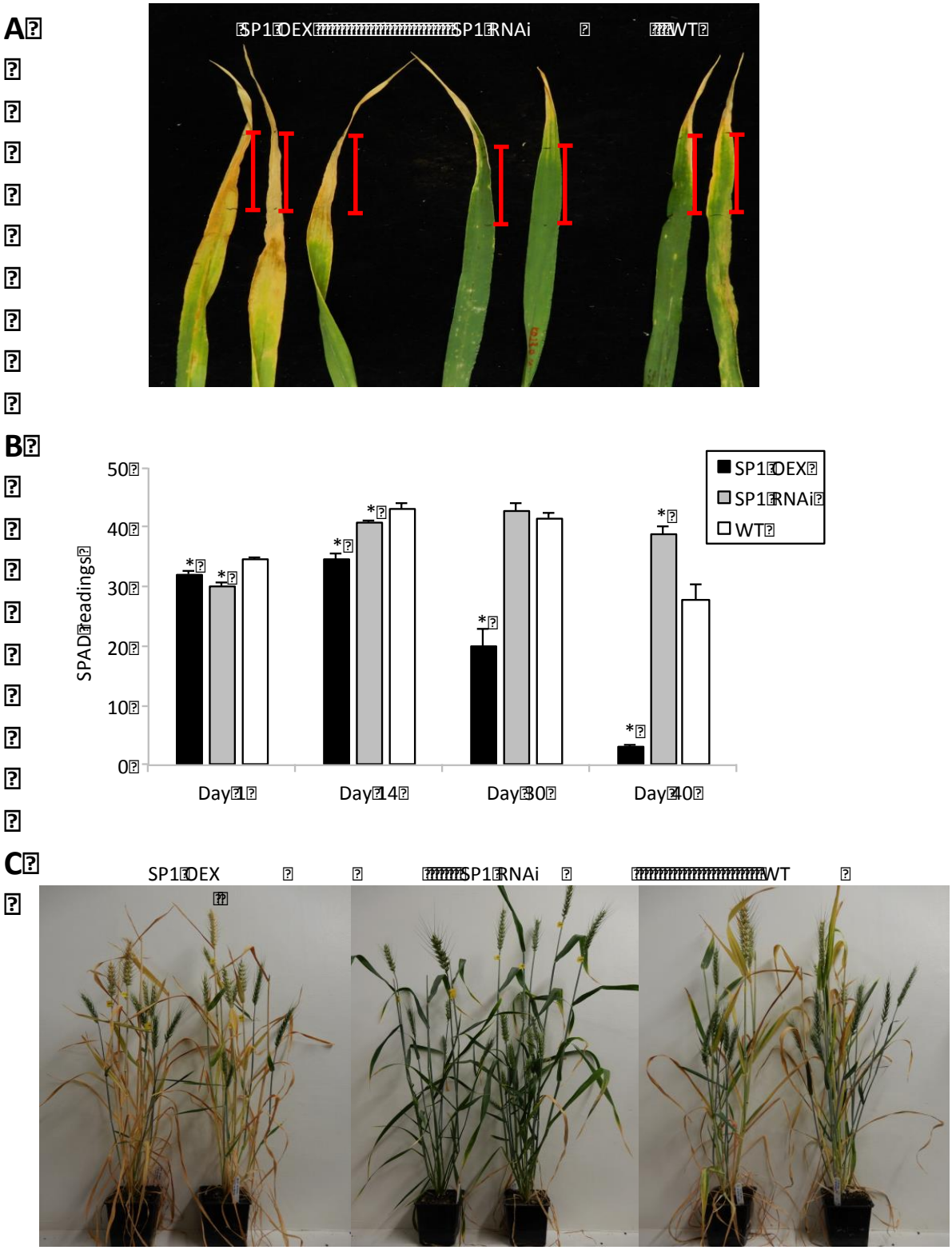

Figure 4.3. Measuring the effect of TaSP1 on the extent of senescence in wheat leaves following a natural aging process. The primary wheat leaves of 10-day-old plants were marked around 10 cm from the leaf tip (indicate by red bars) on Day 1 and were left growing under the

normal growth conditions. The chlorophyll measurements using the SPAD-502 meter were done at the marked area. (A) Representative images of each genotype of natural senescent leaves at Day 40 are shown. Pronounced yellowing was observed in SP1 OEX leaves, whereas SP1 RNAi leaves appeared greener than WT leaves. (B) Chlorophyll measurements were made in the marked area on Day 1, Day 14, Day 30 and Day 40. Data are mean +SEM for at least 3 measurements per two leaves per genotype per time-point. Asterisks above the columns indicate a significant difference relative to WT (Student's *t*-test, **P*<0.05). Student's *t*-test also revealed no significant differences in SP1 RNAi relative to WT on Day 30. (C) Representative images of plants from each genotype at Day 40 were photographed and are shown.

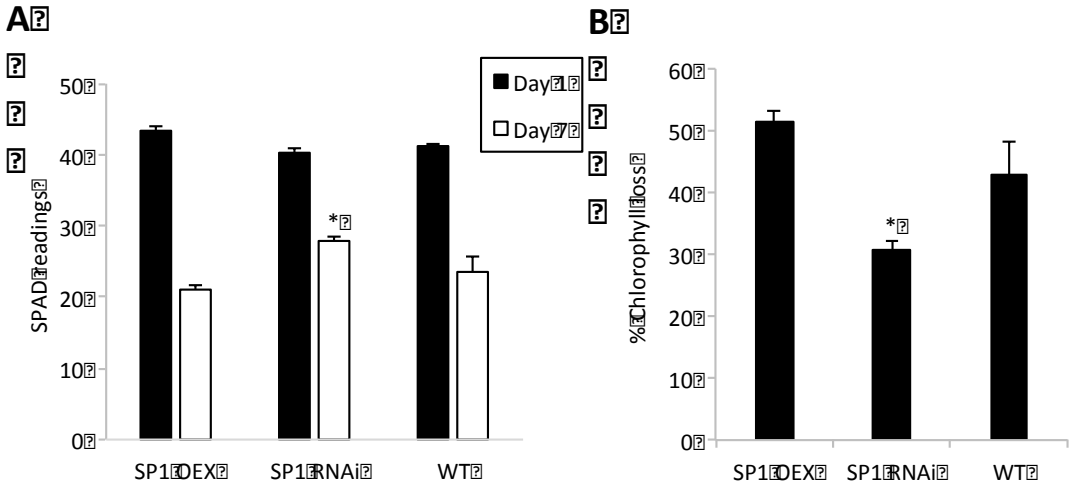

Figure 4.4. Evaluation of the effect of TaSP1 on leaf chlorophyll concentration during dark-induced senescence in detached wheat leaves. The primary wheat leaves of 10-day-old plants were detached at equal length (8 cm) and placed with the cut ends dipping into individual 2 mL tubes containing water. The leaves were placed in the light for 1 hour before being incubated in darkness at 21°C on Day 1. The solutions were changed each day. (A) Chlorophyll measurement using a SPAD-502 meter on Day 1 (before 1 hour light incubation) and on Day 7 after the initiation of the dark treatment. (B) The percentage of chlorophyll loss was calculated as the difference in chlorophyll level between Day 1 and Day 7. Data are mean +SEM for 4 measurements per leaf from 5 plants per genotype. Asterisks above the columns indicate a significant difference relative to WT (Student's *t*-test, *P<0.05). Student's *t*-test also revealed no significant differences in SP1 OEX relative to WT.

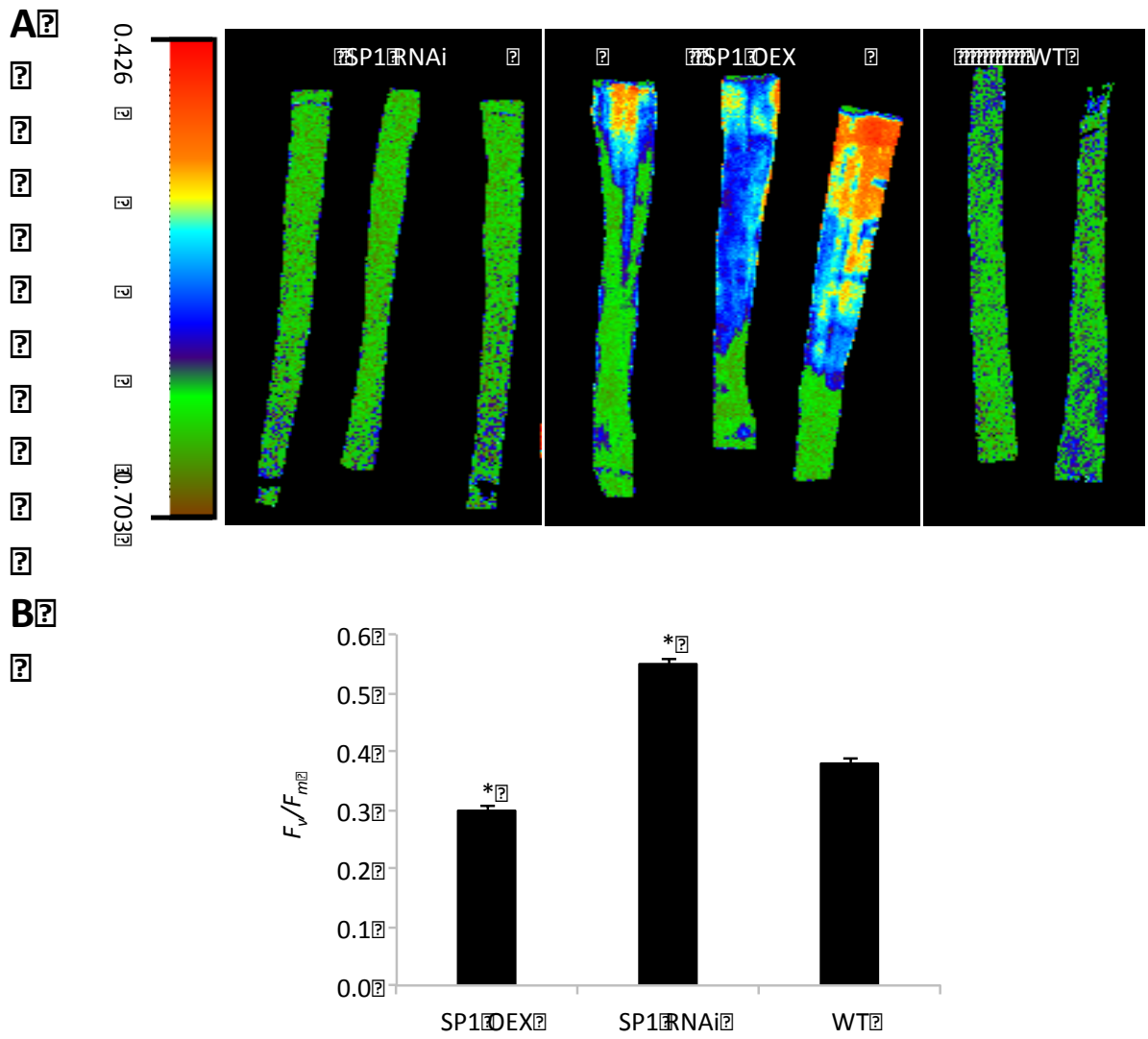

Figure 4.5. Evaluation of the effect of TaSP1 on photosynthetic performance during dark-induced senescence in detached wheat leaves. The plants used in the analysis were described in Figure 4.4. (A) Chlorophyll fluorescence analysis using a CF Imager revealed photosynthetic differences in senescent leaves of SP1 OEX and SP1 RNAi plants, relative to corresponding WT leaves. The leaves analysed here are from Day 7. A colour spectrum representing the range of F_v/F_m values recorded is shown to the left of the panel. (B) Average F_v/F_m values for whole leaves were calculated using the images shown in (A) and other similar images. Data are mean +SEM for at least 3 leaves per genotype. Asterisks above the columns indicate a significant difference relative to WT (Student's *t*-test, *P<0.05).

4.2.4 Evaluation of the effect of TaSP1 on wheat yield

Wheat transgenic lines with modified TaSP1 expression described in Figure 4.3 were grown under optimal growth conditions in the greenhouse until maturity. The assessment of yield-related parameters that may be related to amyloplast development was conducted by measuring seed harvest and seed weight as shown in Figure 4.6.

The apparent 'stay-green' phenotype of the TaSP1 RNAi lines (Figure 4.3C) was reflected in higher yield in average seed harvest compared to WT and TaSP1 OEX. Attenuation of senescence in TaSP1 RNAi lines may also increase yield as the average seed harvest increased by 14%, while acceleration of senescence in TaSP1 OEX reduced the seed harvest by 35%, relative to WT (Figure 4.6A). The total seed number and grain weight for each genotype is shown in Table 4.1. This observation is proportional to the reduction and increment in SP1 expression of SP1 RNAi and SP1 OEX to WT expression level, respectively (Figure 4.2).

However, the effect of SP1 on wheat yield is dependent not only on the seed harvest, but also on seed weight. Although TaSP1 RNAi the showed highest seed harvest, the lowest seed weight in TaSP1 RNAi suggests that a lack of SP1 causes inefficiencies in developmental proteome transitions, which may be linked to starch synthesis in storage organ or amyloplast development process and which might have caused inefficient remobilization of nutrient to the seeds during the grain filling phase (Figure 4.6B). In contrast, TaSP1 OEX seed weight was indistinguishable from that of WT and might be due to a modest increment (about 2.0-fold) in expression of the wheat SP1 genes (Figure 4.2). The indistinguishable difference found in TaSP1 OEX and WT seed weight might change if the level of overexpression is improved. More experiments would be necessary to determine whether other yield parameters including seed number per spike, spike numbers, as well as chloroplast or amyloplast ultrastructure were also affected by SP1 modifications.

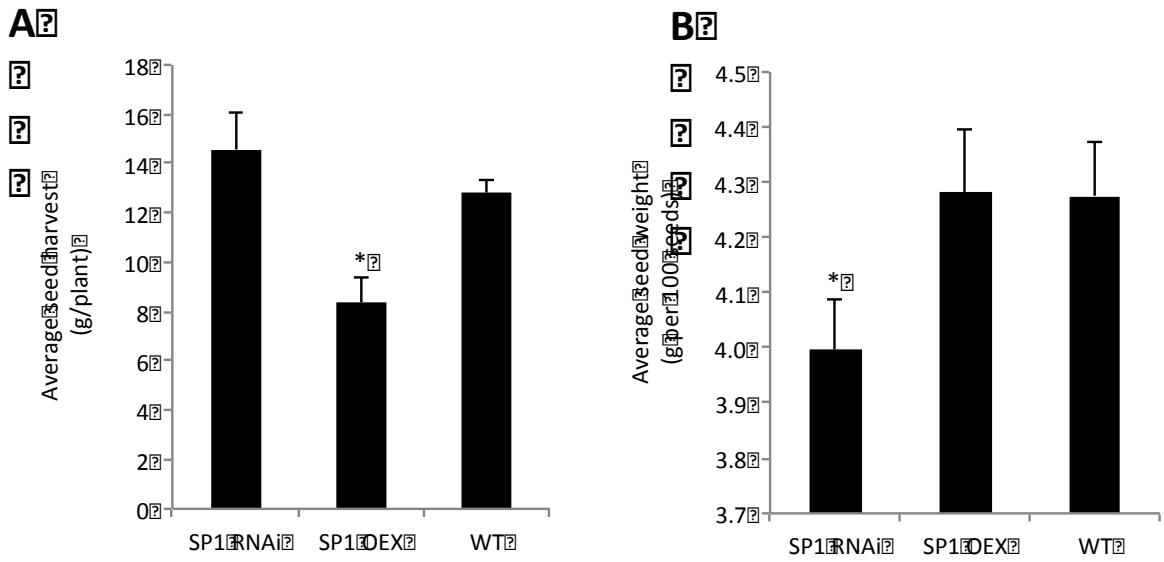

Figure 4.6. Evaluation of the effect of TaSP1 on grain yields of wheat plants. The plants described in Figures 4.3 were allowed to grow to maturity and set seed. Total number of SP1 OEX, SP1 RNAi and WT plants used for the analysis were 15, 14 and 10, respectively. The seeds were then harvested and weighed on a per plant basis. (A) The average seed harvest was calculated based on ratio of total seed weight per plant while (B) the average seed weight was calculated based on the weight per 100 seeds. Asterisks indicate a significant difference relative to WT (Student's *t*-test, **P*<0.05). Student's *t*-test also revealed no significant differences in average seed harvest of SP1 RNAi and average seed weight of SP1 OEX, relative to WT.

Table 4.1. The total seed number and grain weight for each genotype to evaluate the effect of TaSP1 on wheat yield

Total	Grain Weight (g)	Total Grains (Seed Number)
SP1 RNAi	204.03	5105
SP1 OEX	125.50	2931
WT	128.14	2997

4.3 Conclusion

This set of results shows that despite only a modest level of increment and reduction in *TaSP1* gene expression of transgenic plants compared to WT, it is sufficient to influence the leaf senescence process and grain yields in wheat. The overexpression of TaSP1 was seen to cause enhanced leaf senescence, both under natural aging and detached leaves under dark-induced conditions, whereas the reduction of TaSP1 expression attenuated these processes.

Additionally it became clear that the yield depended not only on the seed harvest, but also on seed weight. The apparent 'stay-green' phenotype of the TaSP1 RNAi showed highest seed harvest but lowest seed weight which suggest SP1 involvement in developmental proteome transitions, not only during leaf senescence, but also during starch synthesis in storage organ or amyloplast development process. However, more experiments would be necessary to determine whether other yield parameters were also affected by SP1 modifications. These parameters can be measured not only under optimal growth conditions but also following post-anthesis under stress conditions, as it is known that 'stay-green' varieties can offer performance advantages under such circumstances (Tian et al., 2012).

In addition, a strategy to introduce stable mutant lines would be more amenable and could become agriculturally advantageous to modify SP1 gene through CRISPR/Cas9 genome editing (Belhaj et al., 2015; Bortesi and Fischer, 2015), so that any advantageous or disadvantageous aspects of SP1 loss can be critically examined.

Chapter 5: Analysis of Tomato and Wheat Transgenic Lines with Altered SP1 Expression under Abiotic Stress Conditions

5.1 Introduction

Abiotic stress is one of the major challenges facing agriculture. When plants experience stress conditions, their growth and productivity may be affected. Various physiological studies comparing plants under stress and normal conditions have been conducted, providing a better understanding of the responses of plants to adverse conditions (Hirayama and Shinozaki, 2010).

Reactive oxygen species (ROS) play a key role in the regulation of many plant developmental processes (Muñoz and Munné-Bosch, 2018), and in plant responses to biotic (Torres, 2010; Baxter et al., 2013) and abiotic (Gill and Tuteja, 2010; Suzuki et al., 2012) stresses. ROS generation in plants has been reported to be stimulated in association with morphological and biochemical changes connected to plastids, such as during the transition of chloroplasts into chromoplasts (Pech et al., 2014) and in root plastids (Mittova et al., 2002). Particularly under stress conditions, ROS can be overproduced as a result of imbalances in the photosynthetic electron transport systems. Photosynthesis and the related metabolism are among the processes most strongly affected by abiotic stresses due to ROS overproduction (Saibo et al., 2009; Taylor et al., 2009). As ROS have the potential to cause serious cellular damage, plants also need adaptive mechanisms to minimize and manage the damaging effects of ROS. For example, plants activate antioxidative systems that balance the production of ROS and their detoxification during leaf, flower and fruit development (Muñoz and Munné-Bosch, 2018).

The activity of photosystem II (PSII) can be restricted by photoinhibition under strong light and environmental stresses. Photoinhibition occurs when the rate of photodamage to PSII exceeds

the rate at which PSII can be repaired. ROS inhibits the repair of PSII and suppresses the synthesis of the proteins needed for the assembly of the active PSII complex, further limiting the repair process (Murata et al., 2007). But the damaging effects of stress are not restricted to PSII. For example, immunoblotting analysis of *Chlamydomonas reinhardtii* algal cells grown under high salt conditions revealed that levels of PSI reaction centre proteins, which include PsaD, were reduced due to the stress (Subramanyam et al., 2010). Such reduction in PsaD protein abundance has also been reported to be the cause of impaired photosynthetic performance (Romani et al., 2012; Tiller and Bock, 2014).

Recent studies by Ling and Jarvis (2015) showed that, in Arabidopsis, the chloroplast E3 ligase SP1 has an important role in managing the stress-linked overproduction of ROS. The action of SP1 aids the survival of stressed plants by reducing photosynthetic activity to minimize ROS production. This ROS-avoidance strategy relies on SP1's ability to selectively control the level of the TOC protein transport machinery, and thereby limit photosystem assembly (Ling and Jarvis, 2015). To date, the role of SP1 in stress has largely been studied under salinity and osmotic stress conditions, which are related to oxidative stress, and this is now well understood. As other types of abiotic stress, such as drought and extreme temperature, have interrelated effects and responses (Shanker and Venkateswarlu, 2011), there is a possibility that the role of SP1 extends to a variety of other environmental conditions, either singly or in combination. For example, SP1 may conceivably act at extreme temperatures and light intensities (Murata et al., 2007), in biotic stress (Basnayake et al., 2011), and/or in antioxidant defence networks (Vickers et al., 2009; Caverzan et al., 2016), although at present the evidence in this regard is limited (Ling and Jarvis, 2015).

The ability of plants to tolerate environmental stresses is determined by the age of the plants and the time of exposure to stress conditions. In tomato, the damaging effects of high salt concentration were most pronounced when plants were exposed to saline conditions during the early vegetative growth stage (Dumbroff and Cooper, 1974). A delay in the onset of flowering could be an indicator of sensitivity to stress conditions (Katerji et al., 2003). Altering

the onset of flowering due to stress will not only affect the yield of fruit but also their quality. Studies by Mitchell et al. (1991) found that tomato fruits have a higher starch concentration during early fruit development and are more acidic as a result of water deficiency and high salinity growth conditions. In wheat, analysis of yield-related parameters in a 'stay-green' mutant (such mutants retain green leaves for longer, owing to attenuated senescence), following the post-anthesis application of drought stress, have indicated performance advantages under such circumstances (Tian et al., 2012).

Based on the previous report showing SP1 involvement in stress tolerance in Arabidopsis (Ling and Jarvis, 2015), I hypothesized that the SP1's role in plant physiological responses to abiotic stresses and its link to ROS levels are conserved across plants, including crop species such as tomato and wheat. I further hypothesized that SP1 in crops operates via regulatory mechanisms of chloroplast protein import under stress (as shown in Arabidopsis), by depleting the TOC machinery to reduce plastid import of photosynthesis proteins to aid plant survival. To address these hypotheses, I conducted detailed analyses of tomato and wheat plants with altered SP1 expression, characterising the transgenic plants at different developmental stages, before and after flowering, upon exposure to salinity stress and/or osmotic stress. Elucidating the potential adaptive stress-response regulation of SP1 in crops could facilitate strategies to minimize the effects of stress in crop species, reducing agricultural yield losses irrespective of the time that exposure to stress begins. As plastids and SP1 proteins are ubiquitous in plants, manipulating SP1 in transgenic plants not only provides a possible means of improving stress tolerance in crops, but it also potentially gives a means by which our understanding of the physiological processes and mechanisms underlying stress tolerance in plants can be improved.

5.2 Results and discussion

5.2.1 Expression of *SlSP1* and *TaSP1* under salt stress conditions in tomato and wheat

The expression pattern of *SlSP1* and *TaSP1* under salinity stress was studied using semiquantitative RT-PCR. WT tomato seeds were germinated on soil, and then equally developed 1-week-old plants were treated with salt solution. Young leaves were harvested for total RNA extraction and gene expression analysis, both before the treatment (0 hour) and after 24 hours of exposure to the salt treatment. The resulting data showed that *SP1* transcript levels in both tomato (Figure 5.1, A and B) and wheat (Figure 5.1, A and C) were elevated under salt stress conditions. These results are consistent with the publicly available expression data held at Genevestigator, where *SP1* transcript levels in Arabidopsis are elevated under various abiotic stresses including high salinity (Hruz et al., 2008), and further suggest the potential involvement of the crop plant *SP1* genes in abiotic stress tolerance.

In addition, the elevated transcript level of other plant RING E3 Finger ligases induced by various abiotic stresses was observed in previous studies. The expression level of *Salt- and Drought-Induced RING Finger1* (*SDIR1)* in Arabidopsis was induced by salt and drought stress treatment, suggesting its involvement in stress response (Zhang et al., 2007). Another type of RING E3 Ligase called *SpRing*, a stress-inducible gene that involved in salt stress signaling in wild tomato species *Solanum pimpinellifolium* also exerted strong effects on the induction of transcripts level under salt, drought, mannitol and ABA treatment (Qi et al., 2016). However, *SpRing* transcripts were repressed under cold, jasmonic acid and ethylene treatment. As it has previously been established in Arabidopsis that SP1 is involved in the tolerance of some (e.g. salinity and osmotic stresses), but not all, abiotic stresses (e.g. temperature and high-light stresses), it is reasonable to compare involvement of *SP1* genes under salinity and osmotic stresses in tomato and wheat with findings in Arabidopsis (Ling and Jarvis, 2015).

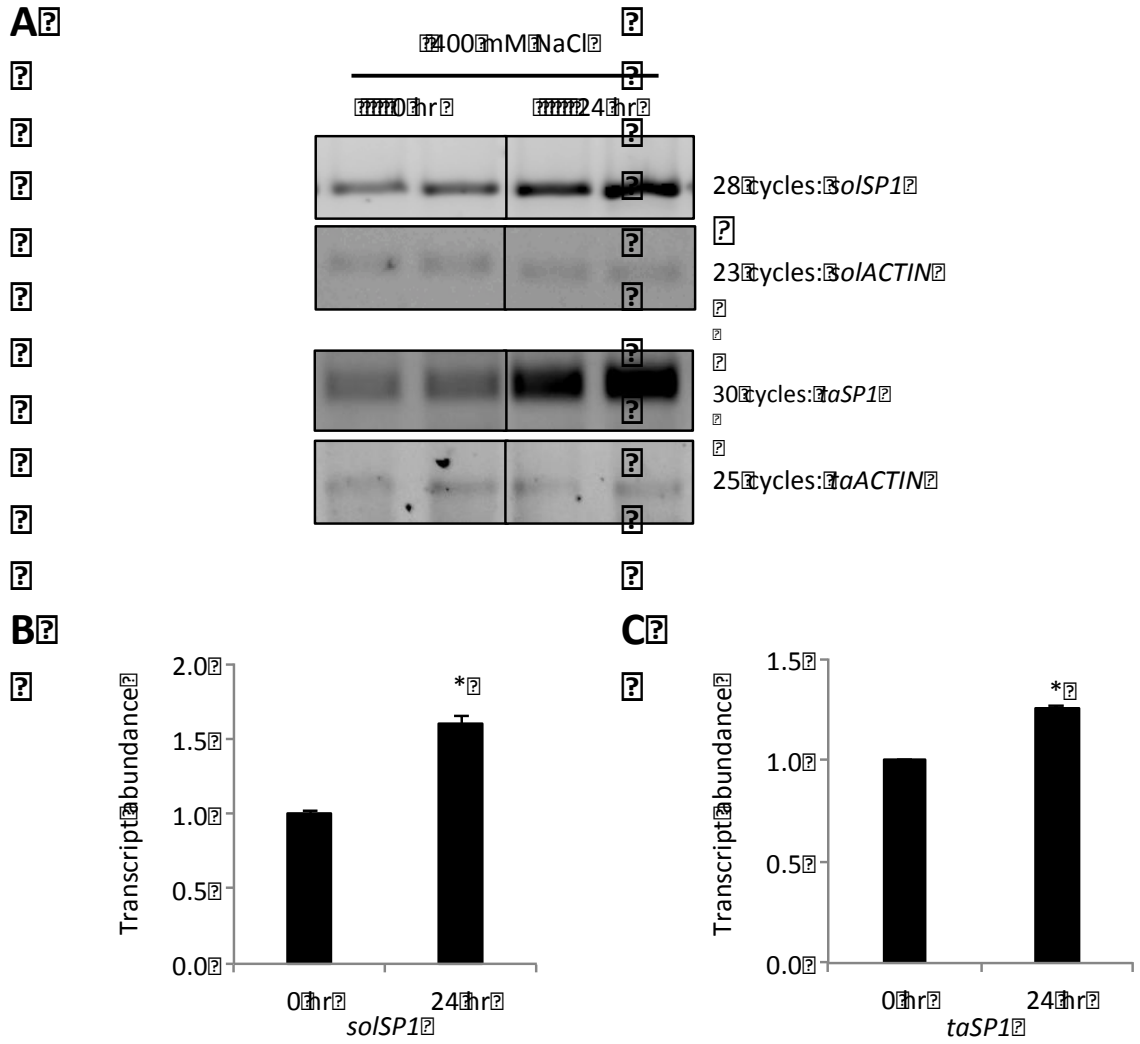

Figure 5.1. Expression analysis of *SlSP1* in tomato and *TaSP1* in wheat under salinity stress conditions. Equally developed 1-week-old plants of each species were exposed to salt stress by applying 50 mL of 400 mM NaCl into individual 0.25 L pots. Total RNA was extracted from duplicate leaves of each sample, both before (0 hr) and after (24 hr) initiation of the NaCl treatment, and subjected to semiquantitative RT-PCR analysis using *SP1* and *ACTIN* primers. Following resolution of the bands by electrophoresis and staining (A), bands corresponding to *SP1* and *ACTIN* were quantified (B). The *SP1* data were normalized using the corresponding *ACTIN* values. All values were expressed relative to the corresponding 0 hr value, which was set to 1. The data represent the mean +SEM for 2 biological replicates at each time point and for each species. Asterisks above the bars indicate significant difference relative to 0 hr (Student's *t*-test, **P*<0.05).

5.2.2 Expression analysis of stress-related genes under abiotic stress conditions in tomato and wheat

To verify that the salt stress conditions applied above were suitable, and to investigate the possibility of expression pattern similarities between *SP1* and other stress-related genes, I analysed the expression of genes known to be responsive to abiotic stresses using semiquantitative RT-PCR. As before, equally developed 1-week-old WT plants were treated with 400 mM NaCl, and the leaves were used for gene expression analysis, both before treatment (0 hour) and after 24 hours of exposure to the stress conditions. In this experiment, an additional osmotic stress treatment, involving the application of 400 mM mannitol in a similar way, was also applied. Plant response to stress is highly dependent on the dose and the type of stress, as well as a range of different response mechanisms (Claeys et al., 2014). In this experiment, very high concentrations of stress-inducing agents (400mM NaCl and 400mM mannitol) were used to focus on severe and acute stress response by measuring the level of stress-related gene transcripts before and after treatment.

The known stress-responsive genes used in this analysis were tomato *NCED3* and wheat *Di19a*. In Arabidopsis, *AtNCED3* is involved in ABA biosynthesis in response to osmotic stresses (Hirayama and Shinozaki, 2010), while in tomato the expression of *SlNCED3* increased under abiotic stress conditions (Qi et al., 2016). In wheat, *Di19a* is constitutively expressed in roots and leaves of seedlings grown under non-stressed conditions, and is up-regulated by both abiotic stress and stress-related hormones (Li et al., 2010). My results showed that the transcript levels of *SlNCED3* in tomato are elevated after 24 hours of exposure to both high salinity and osmotic stress conditions (Figure 5.2, A and B). Similarly, I observed increased expression of *TaDi19a* in wheat after stress treatment (Figure 5.2, A and C). Overall, these results were consistent with expectations based on the literature, and so confirmed that my stress treatment conditions were suitable. The substantially similar expression patterns of the stress-related genes (Figure 5.2) and the *SP1* gene (Figure 5.1)

were supportive of a potential involvement of *SP1* in abiotic stress responses in tomato and wheat.

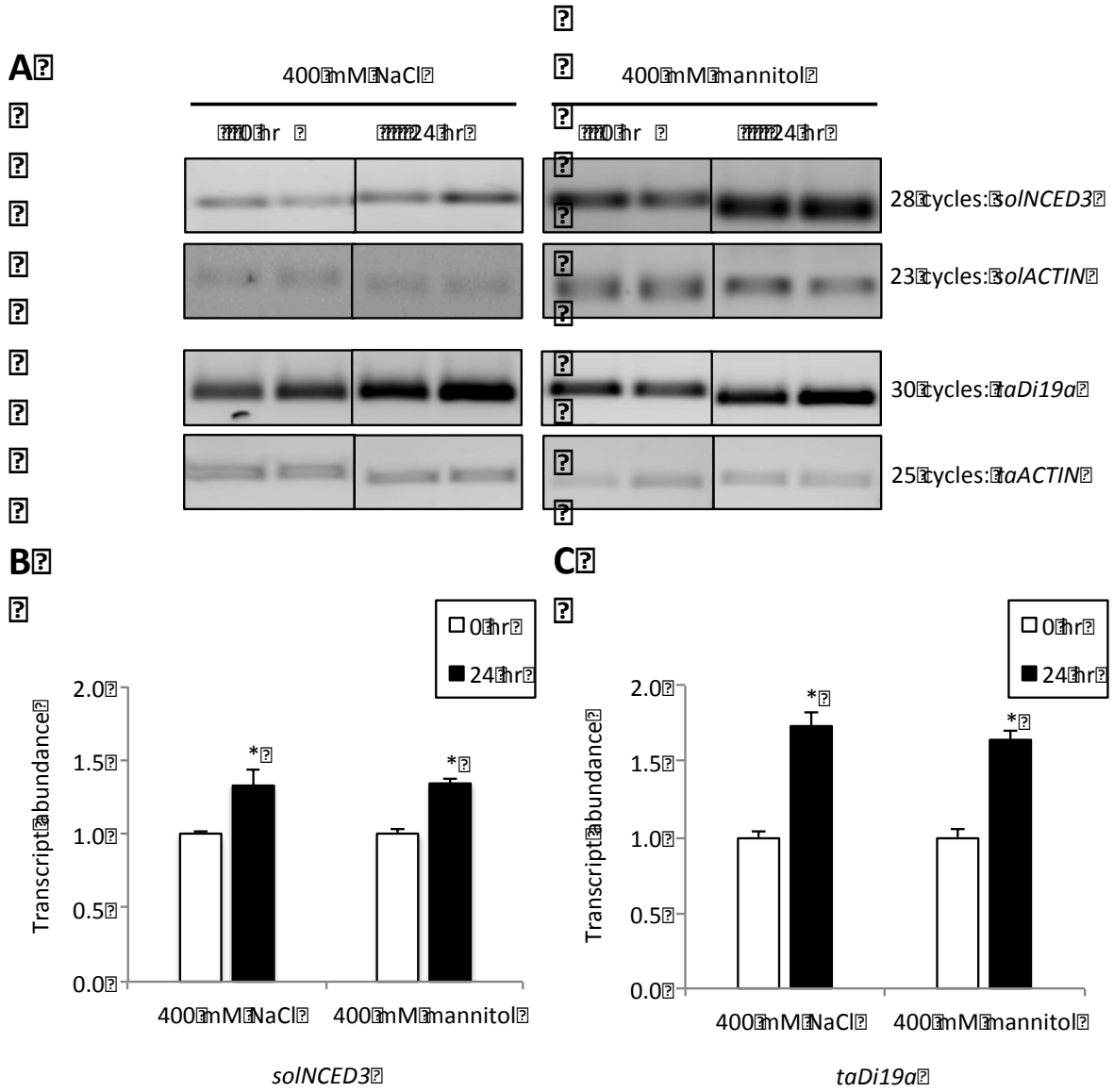

Figure 5.2. Expression analysis of *SlNCED3* in tomato and *TaDi19a* in wheat under abiotic stress conditions. Equally developed 1-week-old plants of each species were exposed to stresses by applying 50 mL of 400 mM NaCl and 400 mM mannitol into individual 0.25 L pots. Total RNA was extracted from duplicates of each sample, both before (0 hr) and after (24 hr) initiation of the NaCl and mannitol treatment, and subjected to semiquantitative RT-PCR analysis using *NCED3*, *Di19a* and *ACTIN* primers. Following resolution of the bands by electrophoresis and staining (A), bands corresponding to *NCED3*, *Di19a* and *ACTIN* were

quantified (B, C). The *SP1* data were normalized using the corresponding *ACTIN* values. All values were expressed relative to the corresponding 0 hr value, which was set to 1. The data represent the mean +SEM for 2 biological replicates at each time point and for each species. Asterisks above the bars indicate significant difference relative to 0 hr (Student's *t*-test, **P*<0.05).

5.2.3 Plant physiological analysis following stress conditions on SP1 transgenic plant lines

The previous report by Ling and Jarvis (2015) showed that SP1 plays an important role in salinity stress tolerance in Arabidopsis seedlings. To further investigate the function of SP1 in stress responses in other plants and at different developmental stages, I conducted analyses of both pre- and post-flowering stage crop plants with altered SP1 expression, following their exposure to salinity stress at various concentrations, characterising the changes in the transgenic plants relative to WT. The reason for analysing plants at two different developmental stages is that evidence in the literature indicates that plants respond differently to stresses depending on whether or not they have flowered (Cuartero and Fernandez-Munoz, 1999).

In tomato, the pre-flowering stage or vegetative growth stage was typically analysed at around 14-15 days after germination, whereas the post-flowering stage was defined as being after the appearance of the first flower, which typically occurred when the plants reached 1 month after germination. In wheat, I defined the pre-flowering stage as when the plants had completed the tillering stage, which was approximately 28-30 days after germination. I have not included any data on wheat stress responses at the post-flowering stage in this thesis; however, I would define it as after the completion of head emergence, which is typically around 58-60 days after germination.

5.2.3.1 Effect of salinity stress in SlSP1 transgenic tomato plants: pre-flowering stage

To study the effects of salt stress on pre-flowering tomato plants with altered SP1 expression, WT, SP1 OEX and SP1 RNAi tomato seeds were first germinated on soil. Then, equally

developed 2-week-old plants were selected and transferred to MS solution containing 100 mM NaCl, and allowed to continue to grow for 3 days. Leaf chlorophyll levels were then measured in the same plants on Day 0 (before the start of stress) and Day 3 after the initiation of the salinity treatment. The SP1 OEX plants showed the highest chlorophyll levels at the end of the treatment and so were considered more stress tolerant than WT, while SP1 RNAi plants had chlorophyll contents that were not significantly different from those in WT (Figure 5.3A). The percentage of chlorophyll loss was calculated using these data (as the difference in chlorophyll levels between Day 0 and Day 3 of the treatment), and this was significantly smaller for SP1 OEX than for WT (Figure 5.3B). However, the percentage of chlorophyll loss in SP1 RNAi was also indistinguishable from that in WT under these conditions (Figure 5.3B).

More obvious differences between the genotypes were observed when 2-week-old plants were grown in saline-treated soil at higher salt concentrations for 2 weeks (200 mM NaCl) or 3 weeks (400 mM NaCl). In parallel, equivalent sets of plants were allowed to grow under normal growth conditions for equivalent durations, and these acted as controls for the experiments. In this work, stress tolerance was assessed by measuring the leaf chlorophyll contents, the latter being used to calculate percentage chlorophyll loss values (Figure 5.4, A and B), and photochemical efficiency of photosystem II (F_v/F_m) (Figure 5.4, C and D). Under these higher salinity conditions, SP1 RNAi plants were considerably more sensitive to salinity stress than WT, having the highest chlorophyll loss values (Figure 5.4, A and B) and lowest F_v/F_m values (Figure 5.4, C and D). In contrast, SP1 OEX plants were significantly more stress-tolerant than WT, having the lowest chlorophyll loss values (Figure 5.4, A and B) and the highest the F_v/F_m values (Figure 5.4, C and D). Although some of these differences between the transgenic lines and WT did not prove to be statistically significant, many of the differences clearly were. When this is considered in conjunction with the consistency of the trends in the data, a convincing picture emerges of the important role that SlSP1 plays in abiotic stress tolerance in pre-flowering tomato plants.

Subsequently, the plants treated with 400 mM NaCl were allowed to continue growing on the saline-treated soil in order to observe the effects of salinity on later plant development. The plants were photographed on Day 45 and Day 60 after the initiation of the salinity treatment, and scored for the onset of flowering as a measure of stress tolerance (Figure 5.5). Delayed flowering is one of the deleterious effects of stress on tomato plants exposed to saline conditions at the early seedling stage (Dumbroff and Cooper, 1974). In the absence of stress, the first flower is expected to appear at around 20-30 days after germination (Jones, 2007). Although I did not include unstressed control plants in this particular analysis, my results suggested that the onset of flowering was delayed by the stress in all genotypes, as expected. In my experiment, the first flowers appeared earliest in the SP1 OEX and WT plants (within 45 days); in other words, the SP1 RNAi plants exhibit the largest delay in the onset of flowering and fruiting. This further suggested greater sensitivity to salinity conditions in the SP1 RNAi plants (Figure 5.5A). Scoring for the onset of flowering on Day 60 according to the tomato plant developmental stages described by Jones (2007) gave the following results: 50% of SP1 OEX plants had reached the flowering to fruit setting stage, with none left at the vegetative stage; 75% of WT plants had reached the vegetative to flowering stage, with none having yet reached the flowering to fruit setting stage; and 75% of SP1 RNAi plants were retained at the vegetative stage with only 25% having reached the vegetative to flowering stage (Figure 5.5B).

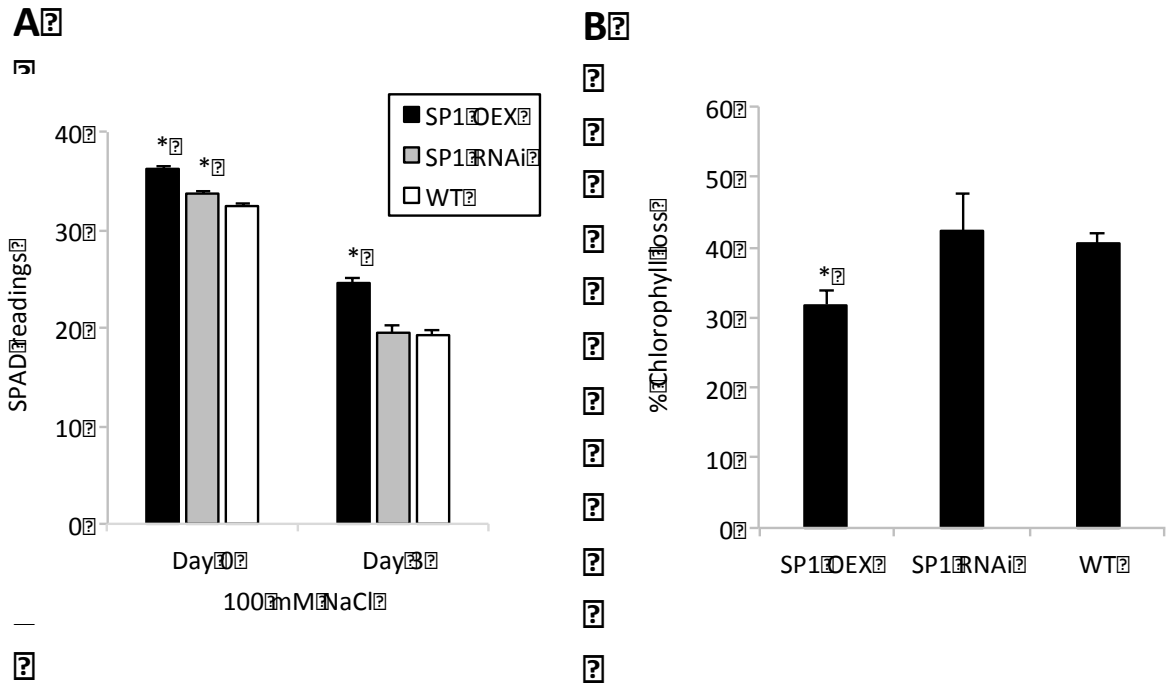

Figure 5.3. Determination of the effect of SlSP1 on leaf chlorophyll concentration in pre-flowering tomato plants under low salt concentration. (A) Tomato seeds were first germinated on soil. Then, the developmentally equivalent 2-week-old plants were transferred to MS solution containing 100 mM NaCl, and allowed to grow for 3 days. Leaf chlorophyll measurements using a SPAD-502 meter were made on the same leaf on Day 0 (before the start of stress) and Day 3 after the initiation of the salinity treatment. (B) The percentage of chlorophyll loss was calculated as the difference in chlorophyll amount between Day 0 and Day 3 of the treatment. Data are mean +SEM for 4 measurements per leaf from 6 plants per genotype at each time-point. Asterisks above the columns indicate a significant difference relative to WT (Student's *t*-test, **P*<0.05). Student's *t*-test also revealed no significant differences in SP1 RNAi on Day 3 in (A) and percentage of chlorophyll loss of SP1 RNAi in (B), relative to WT.

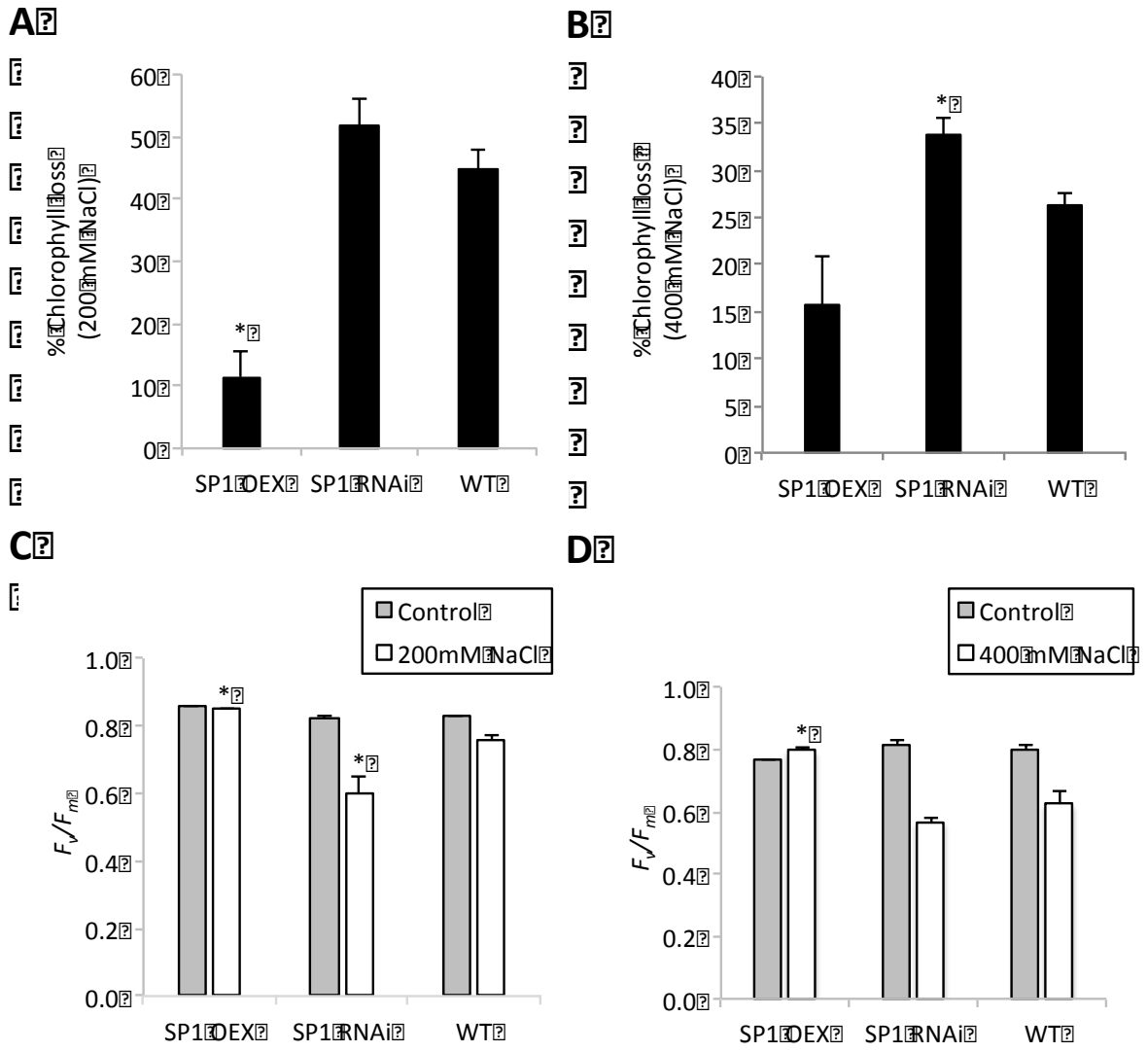

Figure 5.4. Determination of the effect of SlSP1 on photosynthetic performance and leaf chlorophyll concentration in pre-flowering tomato plants under high salt concentrations. Developmentally equivalent 2-week-old plants grown on soil in individual 0.25 L pots with sufficient watering were placed in a tray (6 pots per tray). The trays were allowed to dry before the plants were subjected to stronger salinity stress treatments by applying 1 L of 200 mM or 400 mM NaCl solution to the tray once. The plants were then watered with 1 L of water per tray each week post-treatment and allowed to grow on for a further 2-3 weeks. Control plants were grown similarly but without salinity treatment. (A, B) Percentage of chlorophyll loss, calculated here as the difference in leaf chlorophyll concentration between control and stressed plants at the end of the treatments normalized relative to chlorophyll concentration

at the start of the stress treatment, was determined using a SPAD-502 meter, and (C, D) photochemical efficiency of photosystem II (F_v/F_m) was determined using a CF Imager. Data are mean +SEM for at least 4 measurements per leaf from 3 plants per genotype per condition. Asterisks above the columns indicate a significant difference relative to WT (Student's *t*-test, *P<0.05). Student's *t*-test also revealed no significant differences in percentage of chlorophyll loss in SP1 RNAi in (A) and SP1 OEX in (B), relative to WT, and F_v/F_m values of SP1 RNAi in (D), relative to WT.

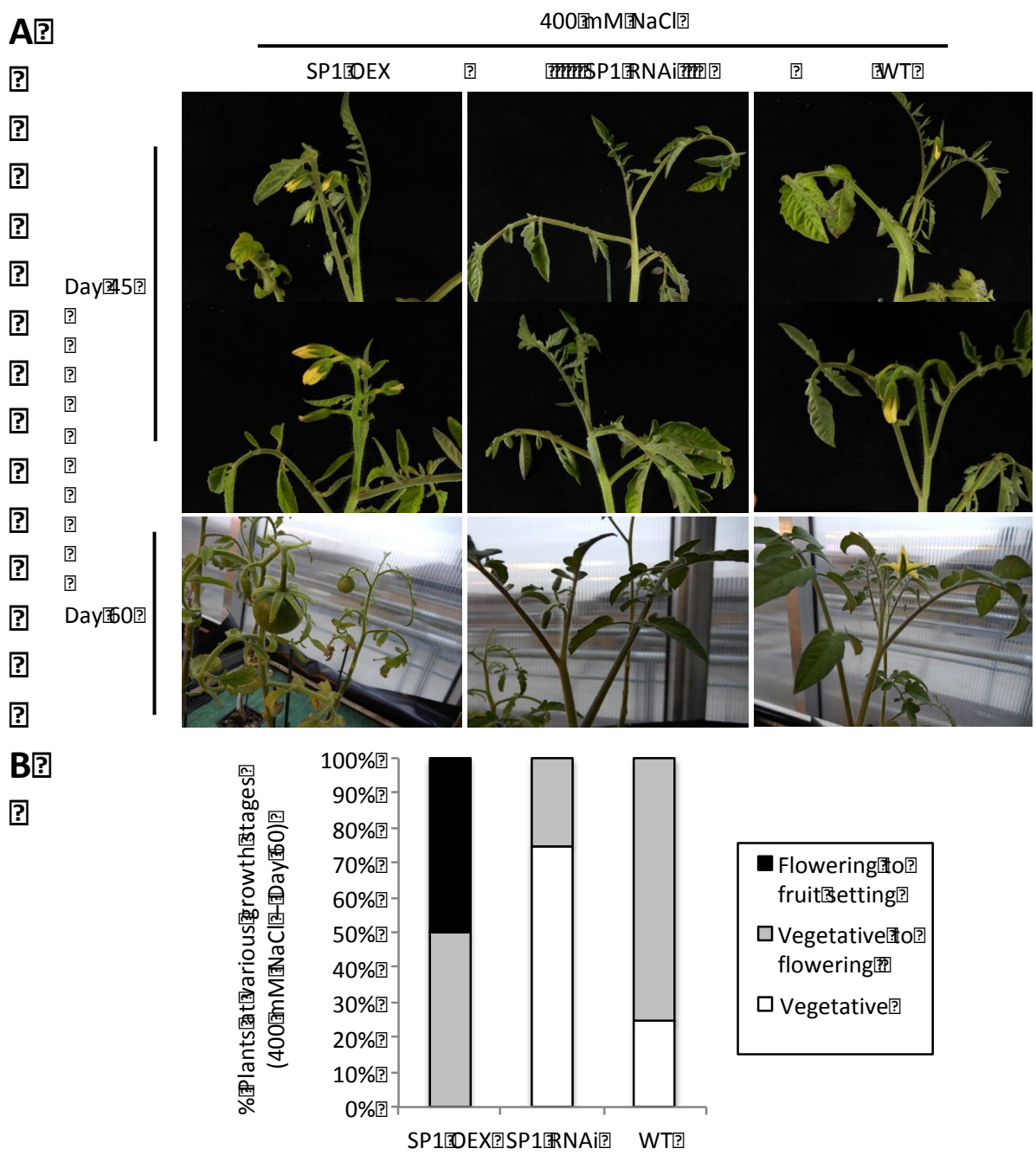

Figure 5.5. Determination of the effect of SlSP1 on flowering onset and development of saline-treated plants. The plants treated with 400 mM NaCl in Figure 5.4 (4 plants per genotype) were allowed to continue growing on the saline-treated soil until Days 45 and 60 after the initiation of the treatment, and were then photographed. (A) Representative images of images of the plants are shown at each time-point. (B) At Day 60, the plants were also scored according to the developmental stages described by Jones (2007). The percentage of plants at each of three developmental stages is shown.

5.2.3.2 Effect of salinity stress in SlSP1 transgenic tomato plants: post-flowering stage

The effects of salinity on tomato plant growth and fruit production depend largely on which plant developmental stage during which the stress exposure begins (Cuartero and Fernandez-Munoz, 1999). To investigate SP1's role in salt tolerance in plants at post-flowering stages, 1-month-old WT, SP1 OEX and SP1 RNAi plants were treated with 200 mM NaCl applied directly to the soil. In parallel, an equivalent set of plants was allowed to grow under normal growth conditions for the same duration, as a control for the experiments, and indirectly can be used to compare with results on natural senescence process as shown in Figure 3.11. To assess stress tolerance, chlorophyll levels were measured on Day 0 (before the start of stress) and Day 12 relative to the initiation of stress, while the photochemical efficiency of photosystem II (F_v/F_m) was measured using a CF Imager at the end of treatment (Day 12). The percentage of chlorophyll loss was calculated as the difference in chlorophyll concentration between Day 0 and Day 12, in both salt-treated and control plants. The results indicated that the effect of SP1 on tolerance to salinity stress applied after flowering was opposite to its earlier described effect on tolerance to stress applied before flowering (Figures 5.3 and 5.4). Under both salinity stress and control conditions, chlorophyll concentration at the end of the experiment were highest in SP1 RNAi plants and lowest in SP1 OEX plants (Figure 5.6, A and B); accordingly, chlorophyll loss values were generally lowest in SP1 RNAi plants and highest in SP1 OEX plants (Figure 5.6, C and D). Consistent trends were seen in the F_v/F_m data, where I generally recorded the highest values in SP1 RNAi plants and the lowest values in SP1 OEX plants (Figure 5.6, E and F).

Although the differences between transgenic genotypes and WT described above were not statistically significant in every case, the overall trends were clear and similar under both salinity stress and control conditions: the senescence process was delayed in SP1 RNAi plants, and accelerated in SP1 OEX plants. The results for control conditions presented here are consistent with those shown in Figure 3.11. These observations not only confirmed that SlSP1 has a function in leaf senescence similar to that reported for Arabidopsis SP1 by Ling

et al. (2012), but also indicated that SP1 RNAi plants have an improved ability to tolerate post-flowering stress conditions owing to the generation of a ‘stay-green’ trait. Such traits have been found to promote stress tolerance in other crop plants (Thomas and Smart, 1993; Tian et al., 2012).

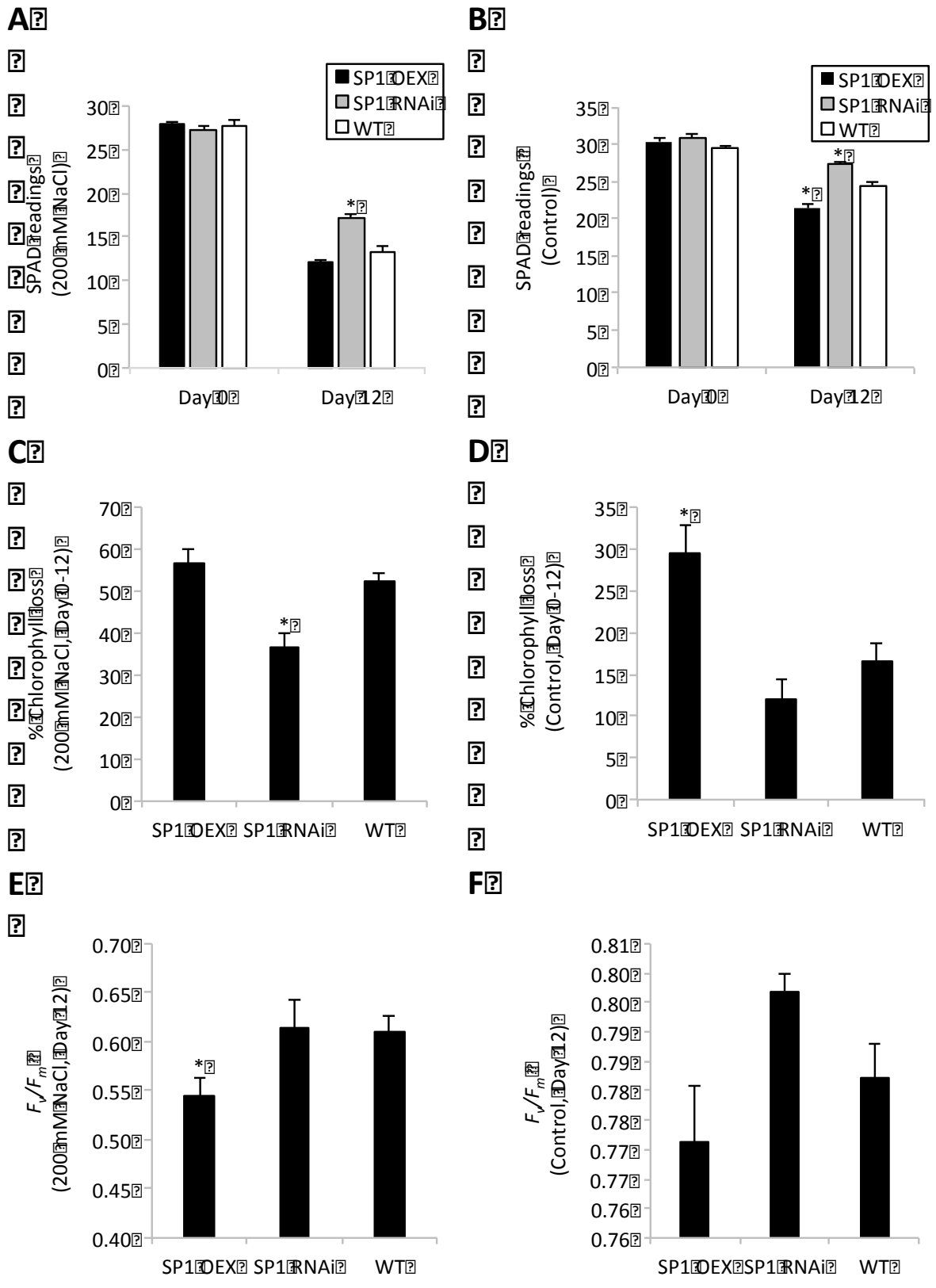

Figure 5.6. Determination of the effect of SlSP1 on leaf chlorophyll content and photosynthetic performance in post-flowering tomato plants under salinity stress conditions. Developmentally

equivalent 1-month-old plants grown in 0.25 L pots were subjected to salinity stress treatment by applying 100 mL of 200 mM NaCl solution to the soil and allowing the plants to grow on for a further 12 days (A, C, E). Control plants were grown similarly but without salinity treatment (B, D, and F). (A, B) Leaf chlorophyll measurements were made using a SPAD-502 meter on Day 0 (before the start of stress) and Day 12 relative to the initiation of the treatment. (C, D) The percentage of chlorophyll loss was calculated as the difference in chlorophyll content between Day 0 and Day 12. (E, F) The photochemical efficiency of photosystem II (F_v/F_m) was measured on Day 12 only. Data are mean +SEM derived from measurements of at least 3 plants per genotype per condition. Asterisks above the columns indicate a significant difference relative to WT (Student's *t*-test, **P*<0.05). Student's *t*-test also revealed no significant differences in SPAD readings in SP1 OEX in (A), percentage of chlorophyll loss in SP1 OEX in (C) and SP1 RNAi in (D), and F_v/F_m values of SP1 RNAi in (E) and SP1 OEX and SP1 RNAi in (F), relative to WT, respectively.

5.2.3.3 Effect of salinity and osmotic stresses in TaSP1 transgenic wheat plants: pre-flowering stage

To study the effects of salt stress on pre-flowering wheat plants with altered SP1 expression, WT, SP1 OEX and SP1 RNAi wheat seeds were first germinated on soil. When the plants were 1 month old, they were subjected to salinity stress by applying 400 mM NaCl directly to the soil on Day 0 (before the start of stress) and allowed to grow for another 24 days (Day 24). In parallel, a comparable set of plants was allowed to grow under normal growth conditions for a similar length of time as a control for the experiments. As a measure of stress tolerance, chlorophyll levels were again measured on Days 14, 21 and 24 (Figure 5.7); an additional time-point (on Day 30) was included for the control plants to assess further changes between the genotypes. To ensure that the SPAD-502 measurements were recorded at an equivalent position on equally developed leaves, the second leaf to emerge from the main shoot after seed germination was labelled and marked at approximately 10 cm from the leaf tip, enabling subsequent measurements to be made at the same place (as described in Figure 4.3A). In

addition, the percentage of chlorophyll loss was calculated as the difference in chlorophyll content between Day 14 and Day 24 (for salt-treated plants), and Day 14 and Day 30 (for control) (Figure 5.8). Based on the recorded SPAD readings, Day 14 is considered to be the point where the leaves are fully developed and containing the highest level of chlorophyll. Therefore, I used it as the starting point for calculating percentage of chlorophyll loss in Figure 5.8.

At around 2 weeks after the initiation of the salt treatment, I observed that the SP1 OEX plants experienced a developmental delay, giving rise to chlorophyll values that were lower than those in WT and SP1 RNAi plants (Figure 5.7A). However, as the stress conditions persisted, SP1 OEX plants later showed improvements in chlorophyll levels, relative to WT, and were considerably more stress tolerant; in contrast, SP1 RNAi plants were more sensitive to salinity than WT plants, with lower chlorophyll values (Figure 5.7A). These observations are consistent with those shown by Ling and Jarvis (2015), where SP1 overexpression was seen to attenuate photosynthetic activity and initially retard growth, but eventually enabled improved stress tolerance. The salt-tolerant phenotype of SP1 OEX wheat plants, as indicated by lowest percentage of chlorophyll loss at the end of the treatment (Figure 5.8A), was similar to that observed for SP1 OEX tomato plants following exposure to high salinity conditions at the pre-flowering stage (Figures 5.3 and 5.4). Similarly, the salt-sensitive phenotype of SP1 RNAi wheat plants, as indicated by the highest percentage of chlorophyll loss (Figure 5.8A), paralleled the observations made using pre-flowering tomato plants (Figures 5.3 and 5.4). These similarities between wheat and tomato suggest a conserved role of SP1 in promoting stress tolerance across different plant species.

The control plants grown under normal conditions showed a different pattern of chlorophyll accumulation and loss (Figure 5.7B), which was indicative of a function for TaSP1 in leaf senescence similar to that reported for Arabidopsis SP1 by Ling et al. (2012), and as reported earlier in Figure 4.3. Additional SPAD-502 meter readings on Day 30, where plants have potentially reached the final stages of leaf development, were conducted to further assess the

extent of leaf senescence. At this final stage, the chlorophyll content in SP1 OEX leaves was significantly lower than in WT, while that in SP1 RNAi leaves was higher than in WT; this indicated accelerated and attenuated senescence, respectively, relative to WT (Figure 5.7B). The different patterns of chlorophyll accumulation and loss throughout leaf development in the control (Figure 5.7B) and salt-treated (Figure 5.7A) plants points towards an important role for SP1 in balancing chloroplast development, photosynthetic activity, and stress tolerance.

Subsequently, the same plants were allowed to grow until maturity, at which point they were analysed again for total grain yield as a further measure of stress tolerance. The salt stress treatment caused a developmental delay in the plants (data not shown), interrupting their growth and grain maturation, especially in plants with low SP1 levels. As a result, the grain yield of SP1 RNAi plants grown under salt stress condition was reduced compared to WT, whereas that of the SP1 OEX plants was possibly slightly improved (Figure 5.9). Although these differences, with the current data, were not found to be statistically significant, indicating that further analysis will be required to provide corroboration, the trends are in line with those arising from other indicators of stress tolerance presented earlier in this chapter. Thus, the data add support to the notion of an important role for SP1 in plant responses to abiotic stress, and suggest that SP1 could be usefully applied to improve crop performance and mitigate agricultural yield losses.

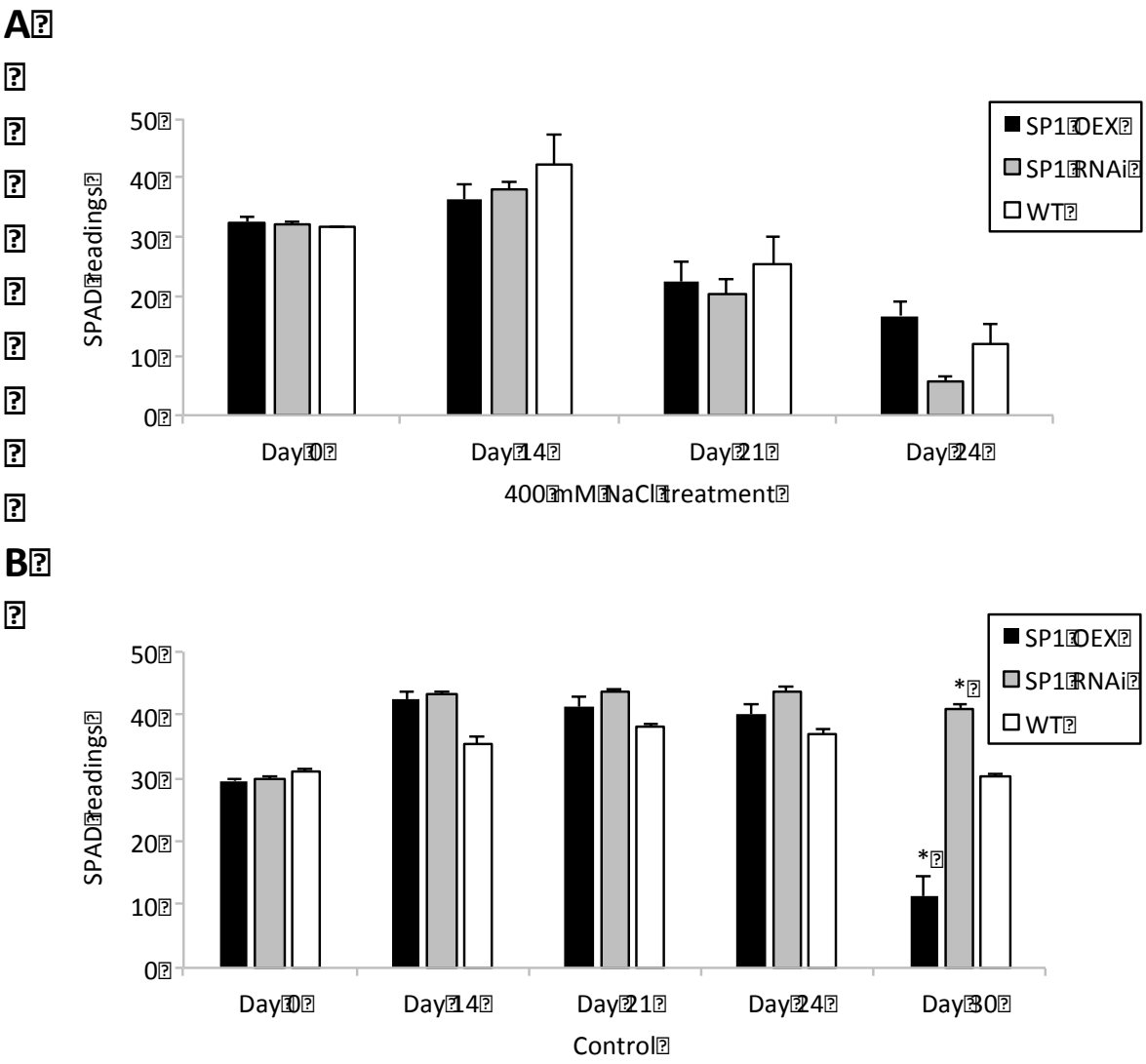

Figure 5.7. Determination of the effect of TaSP1 on leaf chlorophyll concentration in pre-flowering wheat plants under salinity stress condition. Developmentally equivalent 1-month-old plants grown on soil in individual 1 L pots with sufficient watering were placed in a tray (6 pots per tray). The trays were allowed to dry before the plants were subjected to salinity stress treatment by applying 1 L of 400 mM NaCl solution to the tray once. The plants were then watered with 1 L of water per tray each week post-treatment and allowing the plants to grow on for a further 24 days (A). Control plants were grown similarly for up to 30 days but without salinity treatment (B). Leaf chlorophyll measurements were made using a SPAD-502 meter on the same leaf on Days 0, 14, 21 and 24 relative to the initiation of the treatment; control plants received an additional measurement on Day 30. Data are mean +SEM for at least 4

measurements per leaf from each of 3 plants per genotype at each time-point. Asterisks above the columns indicate a significant difference relative to WT (Student's *t*-test, **P*<0.05). Student's *t*-test also revealed no significant differences in SPAD readings in SP1 OEX and SP1 RNAi in (A), relative to WT.

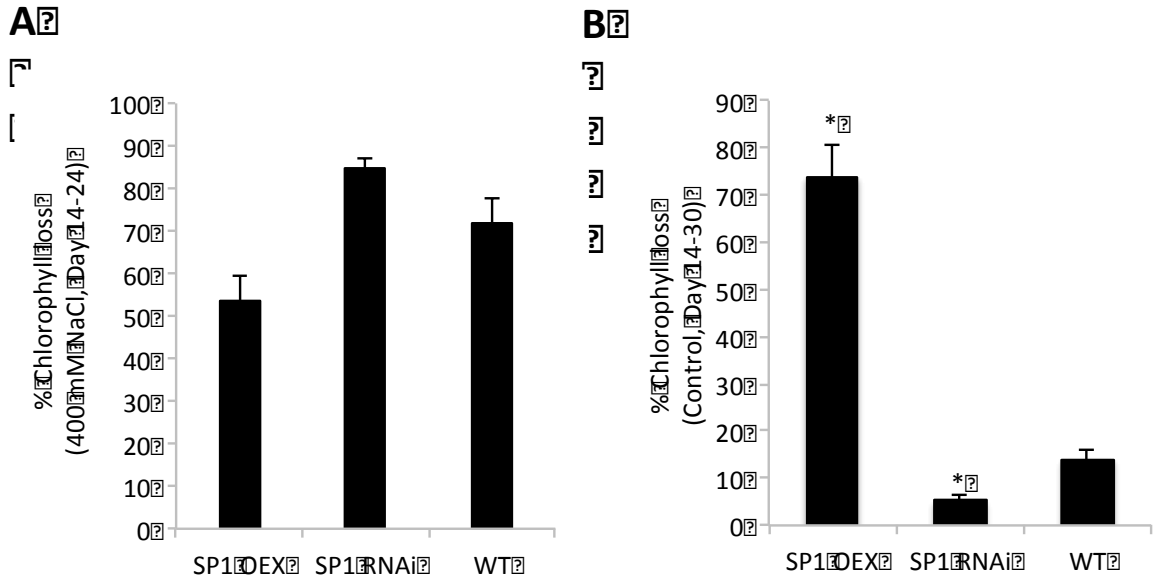

Figure 5.8. Determination of the effect of TaSP1 on pre-flowering salinity treatment on leaf chlorophyll loss. Using the chlorophyll measurements performed on plants subjected to 400 mM NaCl treatment shown in Figure 5.7, the percentage of chlorophyll loss was calculated as the difference in chlorophyll level between Day 14 and Day 24 after initiation of the treatment (A) and Day 14 and Day 30 in plants used as control (B). Data are mean +SEM for 4 measurements per leaf from each of 3 plants per genotype at each time-point. Asterisks above the columns indicate a significant difference relative to WT (Student's *t*-test, **P*<0.05). Student's *t*-test revealed no significant differences in percentage of chlorophyll loss in SP1 OEX and SP1 RNAi, relative to WT in (A).

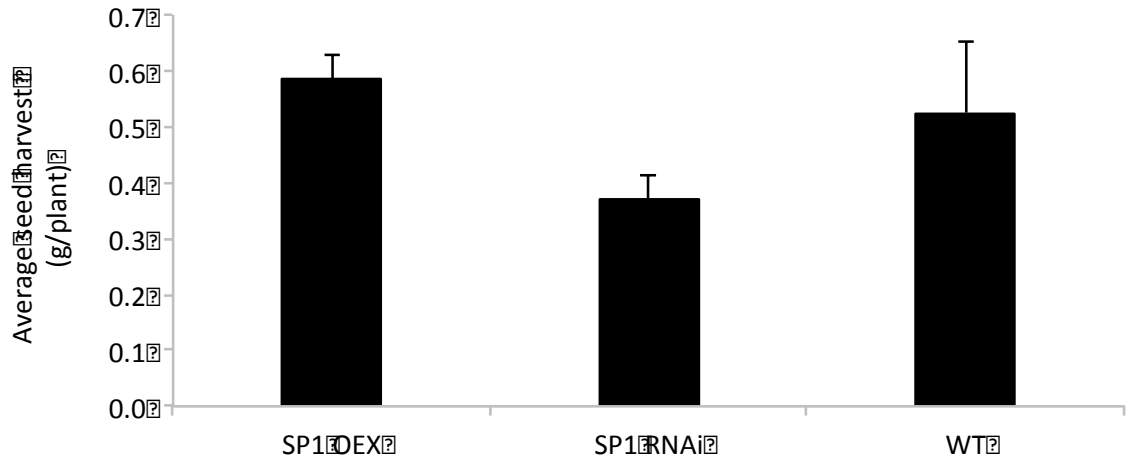

Figure 5.9. Determination of the effect of TaSP1 on pre-flowering salinity treatment on grain yields. The plants subjected to 400 mM NaCl treatment described in Figures 5.7 and 5.8 were allowed to grow to maturity and set seed. The seeds were then harvested and weighed on a per plant basis. Data are mean +SEM for 3 plants per genotype. Student's *t*-test revealed no significant differences in average seed harvest in SP1 OEX and SP1 RNAi, relative to WT.

Next, the effects of osmotic stress on pre-flowering wheat plants were assessed. Seeds of WT, SP1 OEX and SP1 RNAi were first germinated on soil. When the plants were 1 month old, they were subjected to osmotic stress by applying 400 mM mannitol directly to the soil on Day 0 (before the start of stress). As these high osmotic stress conditions caused severe effects, especially to the stress-sensitive SP1 RNAi plants, it was not possible to conduct this experiment for an extended duration over various time-points. Measuring leaf chlorophyll concentrations on Day 0 and Day 8 assessed the degree of tolerance to the osmotic stress relative to the initiation of the stress treatment. To ensure that the chlorophyll measurements were recorded at an equivalent position on equally developed leaves, the second leaf to emerge from the main shoot after seed germination was labelled and marked at approximately 10 cm from the leaf tip, enabling subsequent measurements to be made at the same place as described in Figure 4.3. The percentage of chlorophyll loss was calculated as the difference in chlorophyll content between Day 0 and Day 8 (Figure 5.10A). The results revealed that the SP1 RNAi plants were more sensitive to the osmotic stress than WT, and that SP1 OEX plants were more tolerant of the stress, paralleling the salt stress results presented earlier: the highest percentage chlorophyll loss occurred in SP1 RNAi plants, whereas the lowest percentage chlorophyll loss occurred in SP1 OEX plants (Figure 5.10A), and this is reflected in the greener appearance of their leaves (see marked areas in Figure 5.10B),

Subsequently, the same mannitol-treated wheat plants were allowed to grow on further, prior to photography at Day 14 and Day 30 relative to the initiation of the treatment (Figure 5.11). Most notably, I found that the SP1 RNAi plants were unable to survive such prolonged osmotic stress treatment. At Day 14, the SP1 RNAi plants displayed more extended areas of leaf senescence than either of the other two genotypes. The severely affected SP1 RNAi plants were unable to continue growing much longer, and by Day 30 these plants were dead and so failed to reach maturity. In contrast, the SP1 OEX and WT plants were better able to survive these conditions, and this is reflected in the greener appearance of the plants (Figure 5.11, Day 14), and in the emergence of new tiller stems (see white arrows in Figure 5.11, Day 30).

Overall, these results are supportive of a conserved function of wheat SP1 in plant responses to abiotic stress, including both salt stress and osmotic stress. The results parallel those described earlier for tomato in relation to salt stress, and those reported previously for Arabidopsis, where SP1 was shown to promote tolerance of both salt stress and osmotic stress, respectively delivered by treatment with NaCl and mannitol (Ling and Jarvis, 2015).

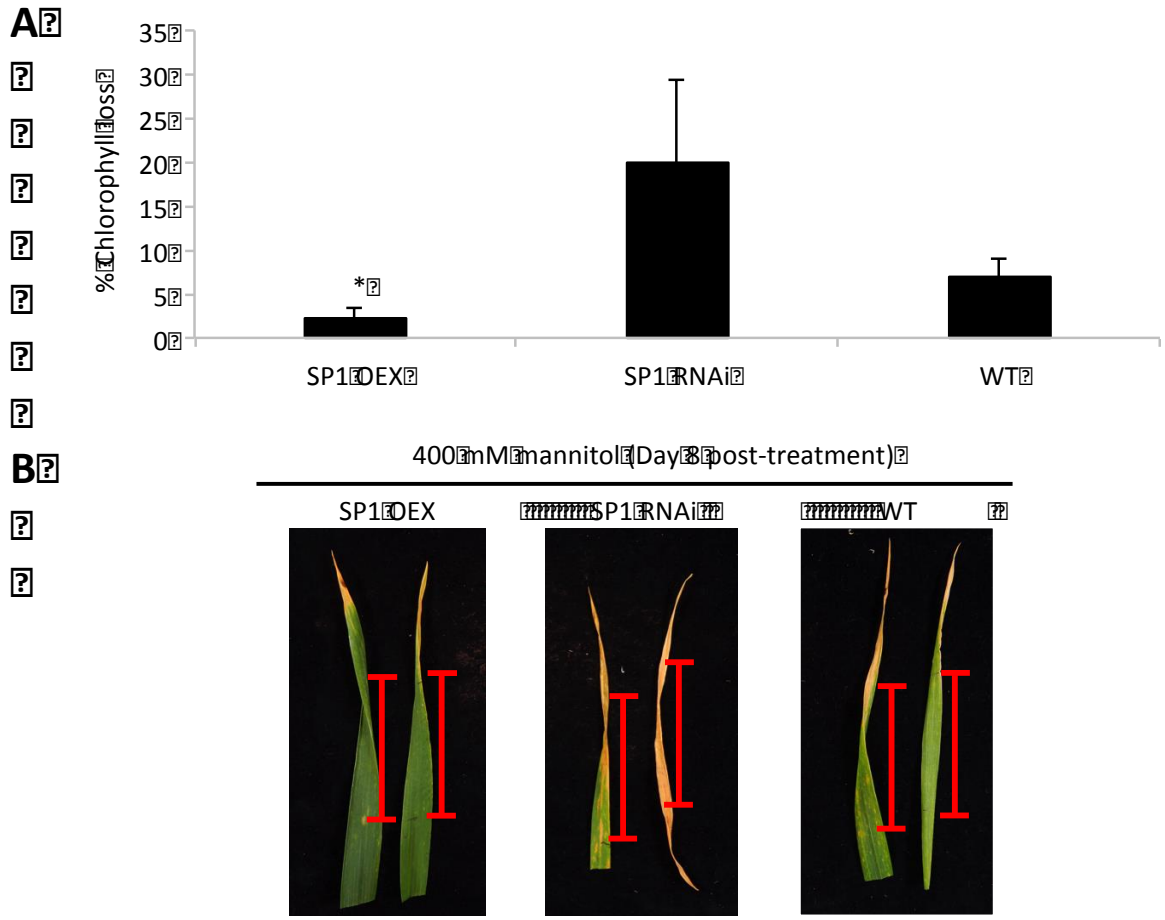

Figure 5.10. Determination of the effect of TaSP1 on leaf chlorophyll loss in pre-flowering wheat plants under osmotic stress condition. Developmentally equivalent 1-month-old plants grown on soil in individual 1 L pots with sufficient watering were placed in a tray (6 pots per tray). The trays were allowed to dry before the plants were subjected to osmotic stress by applying 1 L of 400 mM mannitol solution to the tray once and allowing the plants to grow on for a further 8 days. Leaf chlorophyll measurements were made using a SPAD-502 meter on Day 0 (before the start of stress) and Day 8 relative to the initiation of the treatment. (A) The percentage of chlorophyll loss was calculated as the difference in chlorophyll content between Day 0 and Day 8. (B) Representative images of each genotype on Day 8 post-treatment are shown. The red bars indicate the 10 cm marked areas on the leaves where the SPAD-502 meter measurements were done. Data are mean +SEM for 4 measurements per leaf from 3 plants per genotype. Asterisks above the columns indicate a significant difference relative to

WT (Student's *t*-test, **P*<0.05). Student's *t*-test also revealed no significant differences in percentage of chlorophyll loss in SP1 RNAi, relative to WT.

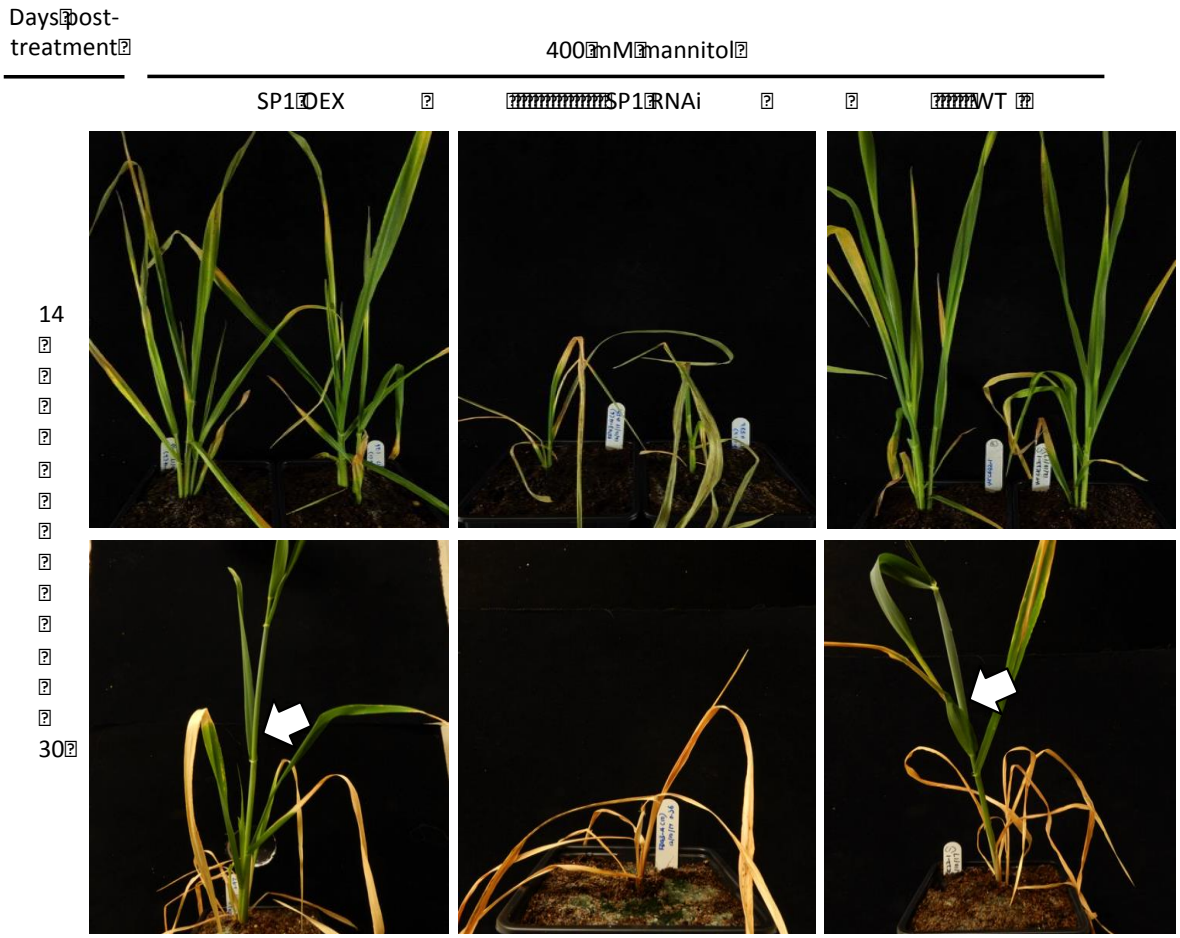

Figure 5.11. Determination of the effect of prolonged osmotic stress on the growth of TaSP1 transgenic plants. The plants subjected to 400 mM mannitol treatment described in Figure 5.10 were allowed to grow on for up to approximately 3 weeks prior to photography. Each week post-treatment the plants were watered with 1 L of water per tray. Representative images of each genotype on Day 14 and Day 30 relative to the initiation of the stress treatment are shown. White arrows indicate the emergence of new tillers.

5.2.4 Analysis of ROS levels in SP1 transgenic plants during abiotic stress responses

Abiotic stress conditions are well known to trigger excessive ROS production. The accumulation of the stress-related pigment, anthocyanin, is a sign of ROS overproduction (Nagata et al., 2003). It has previously been established in Arabidopsis that the role of SP1 under stress is to control ROS levels, and that manipulating SP1 expression causes changes in both ROS levels and anthocyanin accumulation (Ling and Jarvis, 2015). An initial indication that SP1 may be similarly involved in controlling ROS levels under stress conditions in crops came with the observation that 2-week-old tomato plants treated with 400 mM NaCl solution display genotype-dependent differences in the accumulation of anthocyanin: the pigment was apparent on the abaxial side of WT and SP1 RNAi leaves after three days of stress, but not in SP1 OEX leaves (Figure 5.12).

To more directly investigate the level of ROS overproduction in stressed crops, pre-flowering tomato and wheat plants were subjected to salt stress by applying 400 mM NaCl directly to the soil. After 1 week, the leaves of both tomato and wheat plants were stained with 3, 3'-diaminobenzidine (DAB) to detect hydrogen peroxide accumulation (which is indicated in this assay by brown staining). As noted above, this was done in young plants prior to the onset of flowering, when SP1 OEX promotes stress tolerance and SP1 RNAi increases stress sensitivity. Representative images of stained tomato and wheat leaves are shown in Figure 5.13A and Figure 5.14A, respectively. Brown DAB staining was most apparent in the SP1 RNAi leaves, whereas reduced staining was seen in SP1 OEX leaves in comparison to WT. To provide a more quantitative assessment, the percentage of leaf area showing significant DAB staining area was calculated, and the results robustly supported the aforementioned trends, for both species (Figures 5.13B and 5.14B). These results are supportive of the notion that SP1 function promotes stress tolerance in tomato and wheat by inhibiting ROS accumulation, and are consistent with the findings in Arabidopsis reported by Ling and Jarvis (2015). The data provide further support for the functional conservation of SP1 in different crop species.

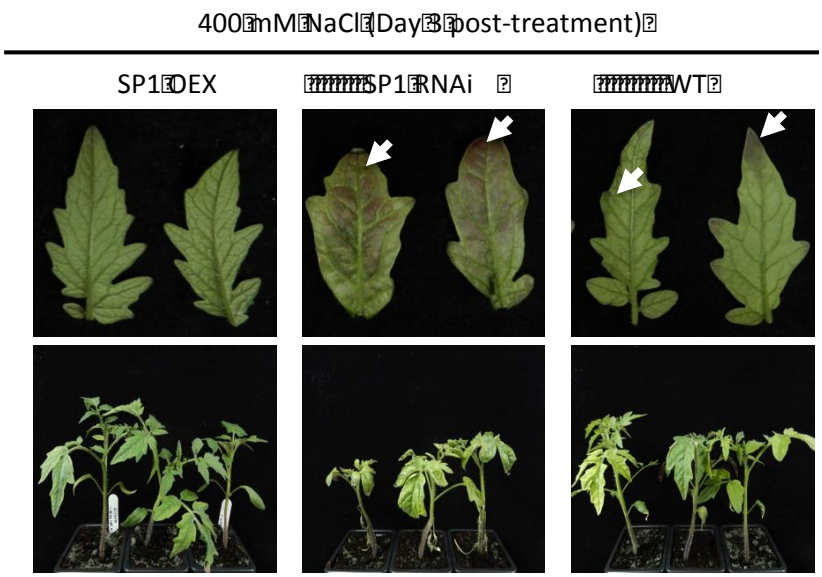

Figure 5.12. Accumulation of anthocyanin in leaves of salt-stressed SlSP1 transgenic tomato plants. Developmentally equivalent 2-week-old plants grown in 0.25 L pots were subjected to salinity stress by applying 50 mL of 400 mM NaCl solution directly to the soil. The plants were photographed on Day 3 relative to the initiation of the stress treatment, and representative images of leaves and the corresponding plants are shown. The white arrows indicate prominent anthocyanin pigment accumulation on the abaxial side of the leaves on Day 3.

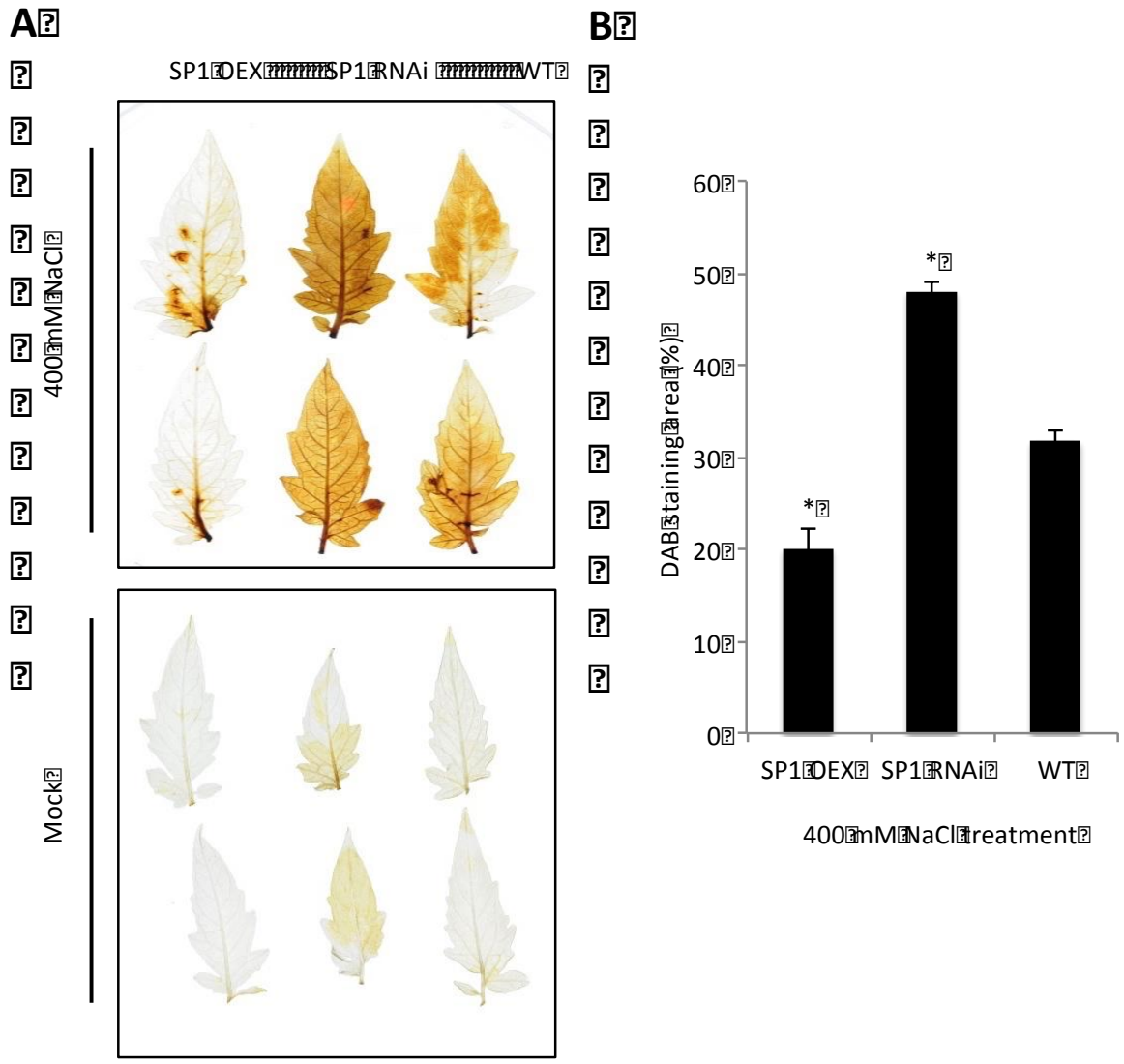

Figure 5.13. Accumulation of ROS in pre-flowering SlSP1 transgenic tomato plants exposed to salt stress. Developmentally equivalent 2-week-old tomato plants grown in 0.25 L pots were subjected to salinity stress by applying 50 mL of 400 mM NaCl directly to the soil. After a further 1 week of growth, developmentally equivalent leaves were harvested and subjected to DAB staining. (A) Brown staining indicates the accumulation of hydrogen peroxide (H_2O_2), which is an important and stable ROS. Representative images of each genotype are shown. Mock images show leaves without DAB staining as technical controls. (B) The percentage of the total leaf surface area showing significant DAB staining was determined for each genotype. Values are mean +SEM for 2 leaves per plant for 3 plants per genotype. Asterisks above the columns indicate a significant difference relative to WT (Student's *t*-test, **P*<0.05).

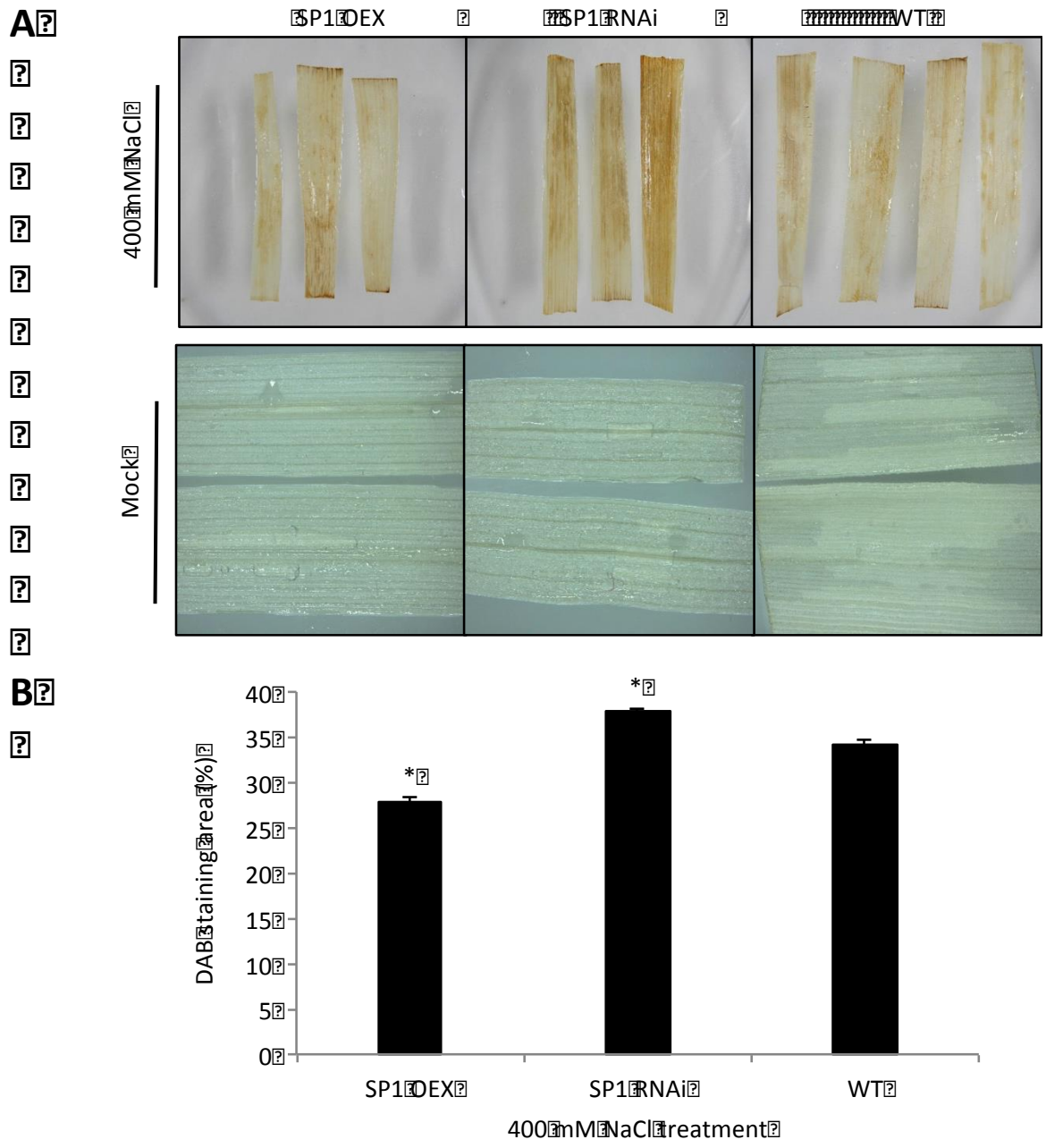

Figure 5.14. Accumulation of ROS in pre-flowering TaSP1 transgenic wheat plants exposed to salt stress. Developmentally equivalent 1-month-old wheat plants grown in 0.25 L pots were subjected to salinity stress by applying 50 mL of 400 mM NaCl directly to the soil. After a further 1 week of growth, developmentally equivalent leaves were harvested and subjected to DAB staining. (A) Brown staining indicates the accumulation of hydrogen peroxide (H_2O_2), which is an important and stable ROS. Representative images of each genotype are shown. Mock images show leaves without DAB staining, as technical controls. (B) The percentage of

the total leaf surface area showing significant DAB staining was determined for each genotype. Values are mean +SEM for 2 leaves per plant for 3 plants per genotype. Asterisks above the columns indicate a significant difference relative to WT (Student's *t*-test, **P*<0.05).

5.3 Conclusion

This work described in this chapter provided information on the role of the SP1 E3 ligase in regulating plant responses to environmental stress signals in two major crops, tomato and wheat, and enabled important comparisons with the reported regulatory mechanisms operating in Arabidopsis (Ling and Jarvis, 2015). When the data presented here are considered in conjunction with previous results showing the importance of SP1 for plastid proteome changes during plant development and stress tolerance, it is clear that there are significant potential applications of SP1 in crop improvement. Genetic engineering of SP1 overexpression in plants substantially reduces ROS accumulation and significantly promotes stress tolerance (as measured by improved in photosynthetic activity and chlorophyll levels) in plants experiencing stress exposure at a young seedling stage. Alternatively, downregulation of SP1 can be used to enhance a plant's ability to tolerate post-flowering stress conditions, by generating a 'stay-green' phenotype. The data presented here may help to design a suitable strategy for improving abiotic stress tolerance in crops regardless of the time of exposure to stress. Such a strategy might involve the upregulated expression of SP1 in seedlings using a strong promoter known to be active only during early development, possibly in a genetic background that is null for the native *SP1* gene, which could be engineered through CRISPR/Cas9 genome editing (Belhaj et al., 2015; Bortesi and Fischer, 2015).

Chapter 6: Analysis of SPL2 in Tomato

6.1 Introduction

SP1 is an E3 ligase, a component of the ubiquitin-proteasome system, which is a system of targeting proteins for degradation via their post-translational modification with ubiquitin. SP1 was found to localize to the chloroplast outer envelope membrane and to interact with TOC proteins *in vitro* and *in vivo*, with the intermembrane space domain of SP1 mediating these interactions (Ling et al., 2012). The biological relevance of this regulation has been demonstrated in Arabidopsis; it facilitates plastid type transitions, and helps to maintain plastidic and photosynthetic homeostasis during abiotic stress (Ling et al., 2012; Ling and Jarvis, 2015).

As discussed in Chapter 3, studies in Arabidopsis have revealed that SP1 is important for regulation of developmental transitions that require reorganization of the plastid proteome, such as de-etiolation and leaf senescence. This work suggested potential agricultural applications of SP1 in crop species. With this in mind, an analysis of the tomato SP1 homologue, SlSP1, was conducted, and this was discussed in Chapter 3. As part of that study, an expression analysis was conducted, which revealed that *SlSPL2* (*SP1-Like Locus2*) is expressed across various tissues and fruit developmental stages with a similar pattern to *SlSP1*, albeit at a much lower level than *SlSP1* (Figure 3.3A). Thus, I was interested to extend my analysis of tomato development to include studies on the other tomato SP1 homologue, SlSPL2, to investigate if SlSPL2 also governs plastid protein import.

The association of SPL2 with chloroplasts was first reported by Ling et al. (2012), who presented a subcellular localization analysis showing that Arabidopsis SPL2 is localized around the chloroplast envelope. This localization analysis is in line with the chloroplast localization of Arabidopsis SPL2 described by Pan et al. (2016). Additionally, Pan et al. (2016)

reported that SPL2 may show very weak or partial peroxisomal localization; however, it is possible that these results were artefacts of the experimental system used (Ling et al., 2017).

In another Arabidopsis study by Li et al. (2008b), it was reported that the *NFYA5* is an important drought-stress inducible transcription factor gene not only at transcriptional level but also at the post-transcriptional level by down-regulation of a small RNA, called miR169a that targets *NFYA5* transcripts for cleavage. Further studies by Gao et al. (2015) have identified a natural *cis*-antisense transcript (NAT) gene of *NFYA5*, called the *NFYA5 Enhancing RING FINGER* (*NERF*) which encodes a RING E3 ligase, that enhances the expression of its antisense gene *NFYA5* and was reported as important for drought resistance. The antisense strand of *NERF* in the 3' untranslated region (UTR) region overlaps with the gene coding for the NFYA5 transcription factor at their overlapping region (OR), to form a *cis*-NAT gene pair, which can produce an endogenous short interfering RNA (siRNA) and affect *NFYA5* transcripts by functioning together with miR169. The analysis of NERF transgenic lines with modified NERF expression showed similar functions between NERF and NFYA5 in controlling stomatal aperture and drought resistance. As both NERF and SPL2 belong to an E3 Ubiquitin ligase family protein and share the same gene ID (At1g54150), the regulatory model of NERF might indicate indirect involvement of Arabidopsis SPL2 in drought stress tolerance. However, the regulation of NERF might not be applicable to SPL2 function in plastid biogenesis.

The aim of the work described in this chapter was to elucidate the roles of SPL2 in organelle biogenesis, which prior to the onset of this study had not been properly analysed. Unfortunately, because of the unavailability of SlSPL2 OEX plants for analysis, only characterization of SlSPL2 RNAi plants (conducted in comparison with SlSP1 OEX, SlSP1 RNAi and WT tomato plants) is discussed in this chapter.

6.2 Results and discussion

6.2.1 Sequence analysis of SlSPL2

Because the annotation for the *SlSPL2* from the Phytozome 12 database was incorrect during the time of initial generation of SlSPL2 transgenic lines, the verified coding region of *SlSPL2* (Solyc12g049330) from *Solanum lycopersicum* (cv. Ailsa Craig) was sequenced to determine the structure of the gene. *SlSPL2* encodes a protein of 391 amino acids with two transmembrane domains (TMD) and a conserved C3HC4-type RING finger (RNF) domain (Figure 6.1A). The SlSPL2 transmembrane domain was predicted using TMPred program (Hofmann, 1993). Alignment of SlSPL2 and its paralogue SlSP1 (Solyc06g084360) with homologues from other species, namely AtSP1 (At1g63900) and AtSPL2 (At1g54150) from *Arabidopsis thaliana* and mitochondrial protein MULAN (NM_024544) from humans, indicated a highly conserved RING motif (Figure 6.1B). As described in Section 3.2.1, SlSPL2 shares 47.1% and 62.3% amino acid sequence identity with AtSPL2 over the full-length sequence and RNF domain, respectively. By contrast, SlSPL2 shares only 18.5% and 39.6% identity with SlSP1 over the full-length sequence and RNF domain, respectively.

Data on a translational fusion to yellow fluorescent protein (YFP) in Figure 6.1C have shown that the SlSPL2 protein is localized to the chloroplast envelope (unpublished). This localization is in-line with the reported subcellular localization of AtSPL2 (Ling et al., 2012; Pan et al., 2016), and is likely to be dependent on the two predicted transmembrane spans shown in Figure 6.1A. Localization of SlSPL2 to chloroplasts points towards a conserved function of SPL2 in different species, and the possibility that its role is related to that of SP1.

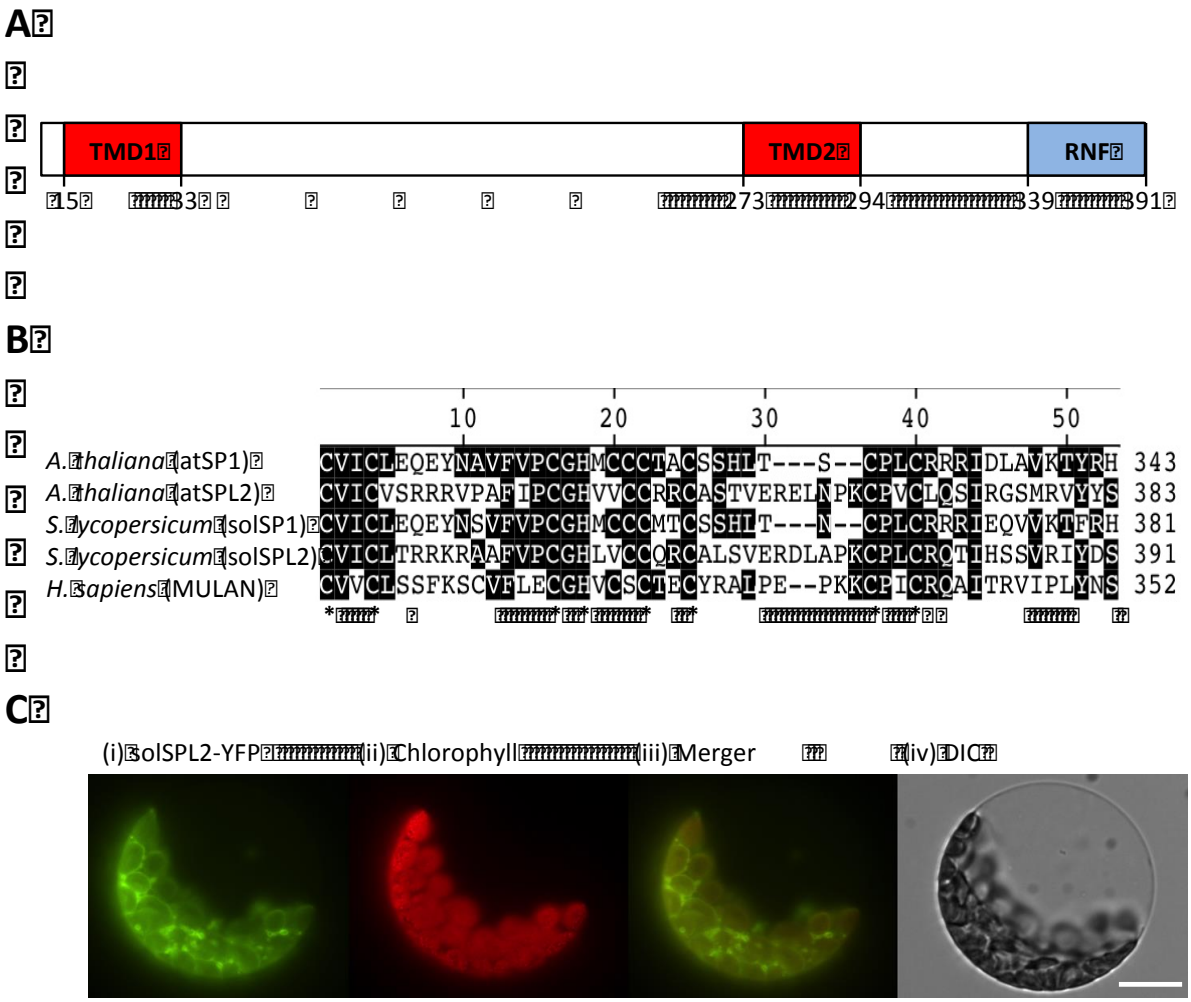

Figure 6.1. Sequence analysis of SlSPL2. (A) Schematic drawing of the structure of SlSPL2 protein showing two transmembrane domains (TMD) and a RING finger domain (RNF). (B) Amino acid sequence alignment of the C3HC4-type RNF domains of AtSP1 and AtSPL2 (from *Arabidopsis thaliana*), SlSP1 and SlSPL2 (from *Solanum lycopersicum*), and MULAN (from *Homo sapiens*), performed using MegAlign by the Clustal W method (DNASTAR Lasergene). Identical residues to MULAN are marked in black. The critical conserved Cys and His residues are indicated with asterisks. (C) Confocal images of protoplasts transiently expressing SlSPL2-YFP (i), chlorophyll signal (ii), superimposition of CFP and chlorophyll florescent signal (iii) and image of differential interference contrast (DIC) microscopy (iv). Images were obtained from Yunliu Zeng. Scale bar = 10 μm.

6.2.2 Gene expression analysis of SlSPL2 transgenic lines

To investigate the function of SlSPL2 in tomato, transgenic tomato lines with reduced *SlSPL2* expression were generated. These SlSPL2 RNAi lines were generated in the lab by Yunliu Zeng following the protocol by Sun et al. (2006). The initial SlSPL2 OEX lines were generated using an incorrect gene sequence owing to an annotation error in the Phytozome 12 database. While replacement of the SPL2 OEX lines using the correct gene sequence have been generated, the plants were not ready for analysis at the time of writing.

The silencing of *SlSPL2* in the T2 generation of the homozygous transgenic plants was confirmed by qPCR, relative to the expression in the WT plants, normalized to *SlACTIN* (Figure 6.2). To ensure continued stable silencing of the transgene, further gene expression analysis was done prior to all of the analyses involving T2 homozygous SlSPL2 RNAi transgenic tomato plants.

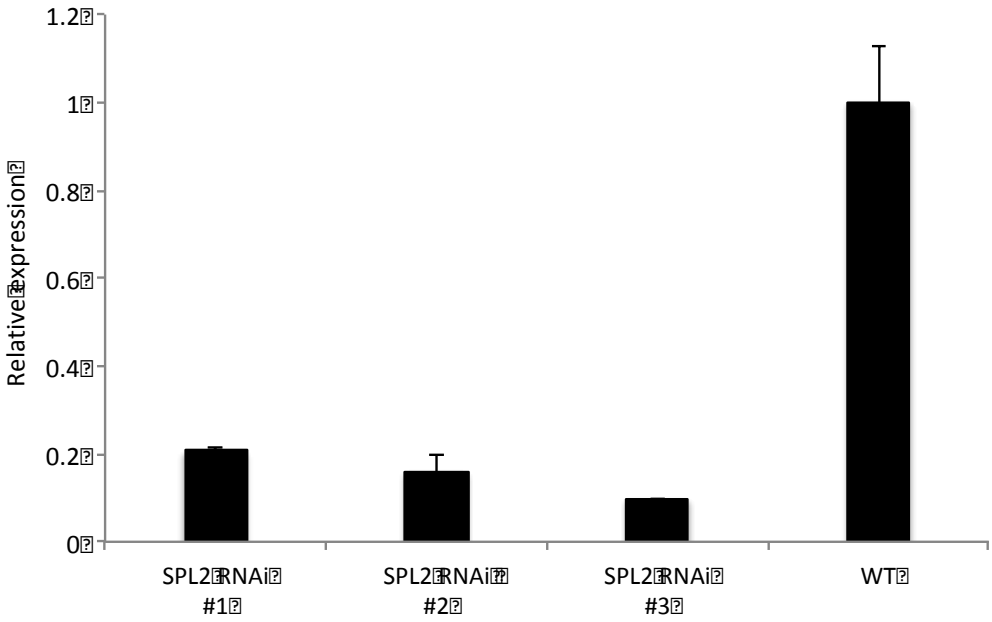

Figure 6.2. Expression analysis of *SlSPL2* in transgenic tomato plants. The analysis was done using qPCR using the leaves of 2-week-old tomato plants. The values shown are relative to the expression in the WT plants, and normalized to *SlACTIN*. The numbers preceded by the # symbol identify independent transgenic lines. SlSPL2 RNAi represent transgenic tomato

plants with expression less than a 0.2-fold relative to WT. The data represent the mean +SEM for 3 biological replicates.

6.2.3 Fruit ripening analysis of SlSPL2 transgenic plants

The analysis of fruit ripening with the SlSPL2 RNAi plants was done following the same methods as used in the analysis of the SlSP1 transgenic, using detached tomato fruits. The transgenic fruits were harvested at the onset of breaker stage and incubated at 25°C in the dark. Chroma meter readings (*a**/*b** values) were used as a parameter to determine tomato ripeness based on changes in fruit skin colour, and were recorded on a daily basis all the way through to the mature red stage. The *a**/*b** ratio values were used in relation to the USDA tomato colour stages, as described by Batu (2004). The fruits for analysis were randomly chosen, but as the SlSPL2 transgenic plants were of the same generation as the SlSP1 transgenics, and because the growth conditions used here were at the same time as those used in Chapter 3 for the fruit related analysis (ripening, size and firmness), the data derived here can be meaningfully compared with the corresponding data on SlSP1 from Chapter 3. Figure 6.3 shows that the SlSPL2 RNAi lines display a delay in ripening that is broadly similar to the ripening delay seen in SlSP1 RNAi plants, relative to WT. In contrast, and as noted earlier in Chapter 3, the fruit ripening process in SlSP1 OEX lines is more rapid than that in WT. The similar ripening phenotypes of the SlSPL2 RNAi and SlSP1 RNAi lines are further reinforced by the images in Figure 6.4, which show typical fruit on Day 1 at breaker stage and Day 8 post breaker stage. At Day 1, all of the fruits looked similarly green, whereas at Day 8 clear difference between the genotypes were apparent. The significant delay in the change of colour from green to yellow and red, in both SlSPL2 RNAi and SlSP1 RNAi fruits, relative to WT, was observed consistently across the whole fruit populations used in the analysis.

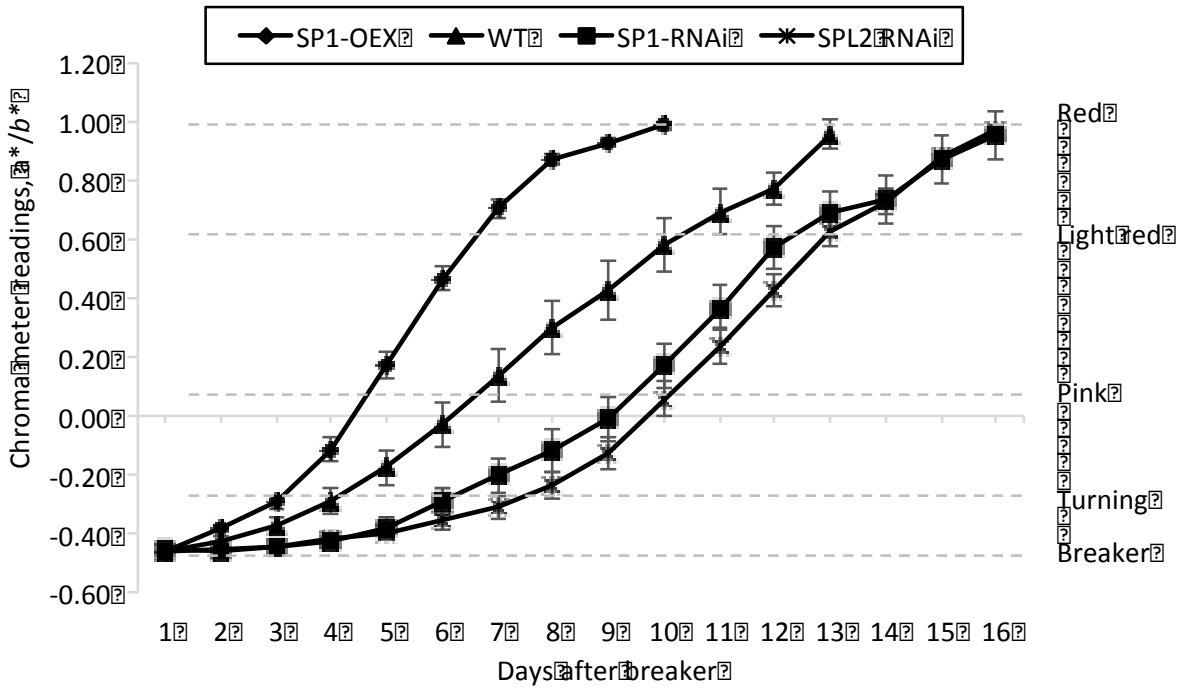

Figure 6.3. Ripening analysis of detached SlSPL2 tomato fruits. The fruit stages indicated to the right are defined following USDA standards (Anon, 1975). The analysis was carried out by determining chroma meter readings (*a** and *b** values) for the blossom-end of the fruits from T2 generation plants on a daily basis, all the way through to the mature red stage. The colour (a*/b*) values of tomatoes at USDA colour stages were described by Batu (2004). Fruits were collected at breaker stage (as determined by comparing the *a**/*b** ratios to the USDA standards), and then stored under dark incubation at 25°C. The fruit populations used in the ripening analysis were collected from two individual T2 generation tomato plants of each of two independent SPL2 RNAi transformants. WT fruits were collected from non-transformed plants. The SlSP1 data are the same data as presented in Figure 3.5 of Chapter 3, as the experiments were done at the same time. Data are mean +SEM for at least 30 fruits per genotype.

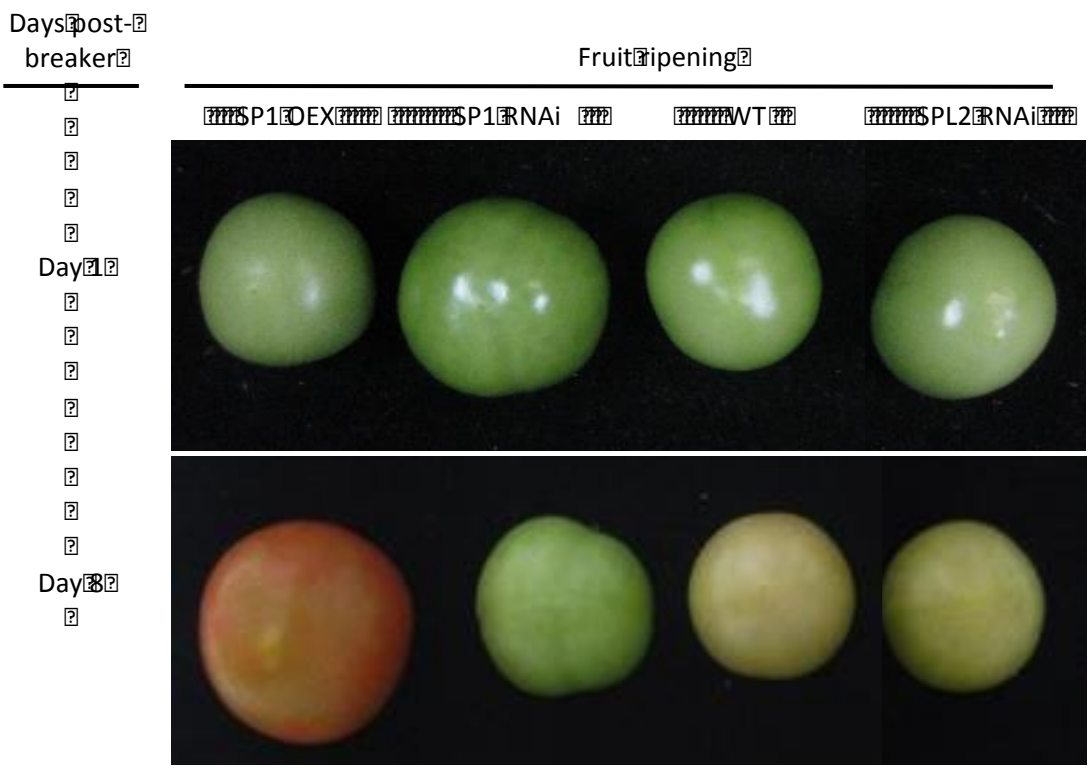

Figure 6.4. Evaluation of the effect of SlSPL2 on fruit ripening. Representative images of tomato fruits of each genotype on the day after breaker stage is reached (Day 1) and Day 8 post breaker stage. The fruit populations used in the ripening analysis were collected from two individual T2 generation tomato plants of each of two independent transformants for SlSP1 OEX, SlSP1 RNAi and SlSPL2 RNAi. WT fruits were collected from non-transformed plants.

6.2.4 Analysis of fruit quality in SlSPL2 transgenic plants: fruit firmness and fruit size

Tomato fruit ripening has been described to involve various structural modifications (Rosso, 1968; Spurr and Harris, 1968; Harris and Spurr, 1969), tightly controlled by hormone homeostasis (Pandolfini, 2009) and regulated by various ripening-related genes (Gray et al., 1994). Thus, it was important to further assess the changes in fruit ripening seen in the SlSPL2 RNAi lines by measuring fruit firmness, as another parameter linked to ripening. As in Chapter 3, the firmness of the fruits was measured using a durometer. Although SlSPL2 RNAi and SlSP1 RNAi were both observed to display a significant (and similar) delay in ripening in detached tomato fruits (Figure 6.3), no obvious differences in fruit firmness were observed between the genotypes at the breaker and mature red stages (Figure 6.5). Thus, in spite of the changes in the rate of the ripening process seen in the transgenic lines, the modifications apparently caused no changes in the extent of softening of the fruits at defined stages.

As with the analysis described in Section 3.2.5, to avoid mistakenly including immature fruit in the ripening analysis here, which could adversely influence the results due to their incomplete growth (Chevalier, 2007), fruit size was measured using a calliper at breaker stage, when the fruits were detached from the plants at the beginning of the analysis. Figure 6.6 shows that the fruit of the SlSP1 OEX, SlSP1 RNAi and SlSPL2 RNAi transgenic lines were not significantly different in size from those of the WT, at breaker stage. This indicated that the fruit used in the ripening analysis were not harvested too young, before reaching their full size.

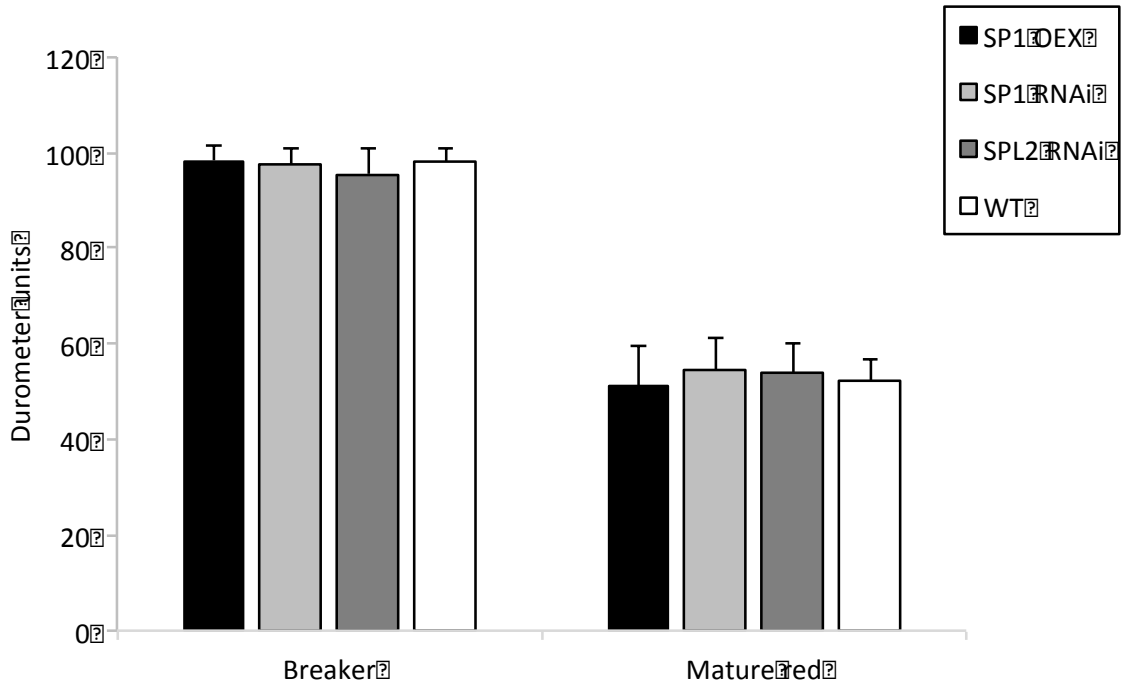

Figure 6.5. Determination of firmness of detached SlSPL2 tomato fruits using a durometer at breaker and mature red stages. The fruit used in this analysis were randomly chosen from the fruit populations from T2 generation plants used in the ripening analysis in Figure 6.3. The SlSP1 data are the same data as was presented in Figure 3.7 of Chapter 3. Data are mean +SEM for at least 5 fruits per genotype. Student's *t*-test revealed no significant differences in firmness of breaker and mature red fruits between genotypes, relative to WT.

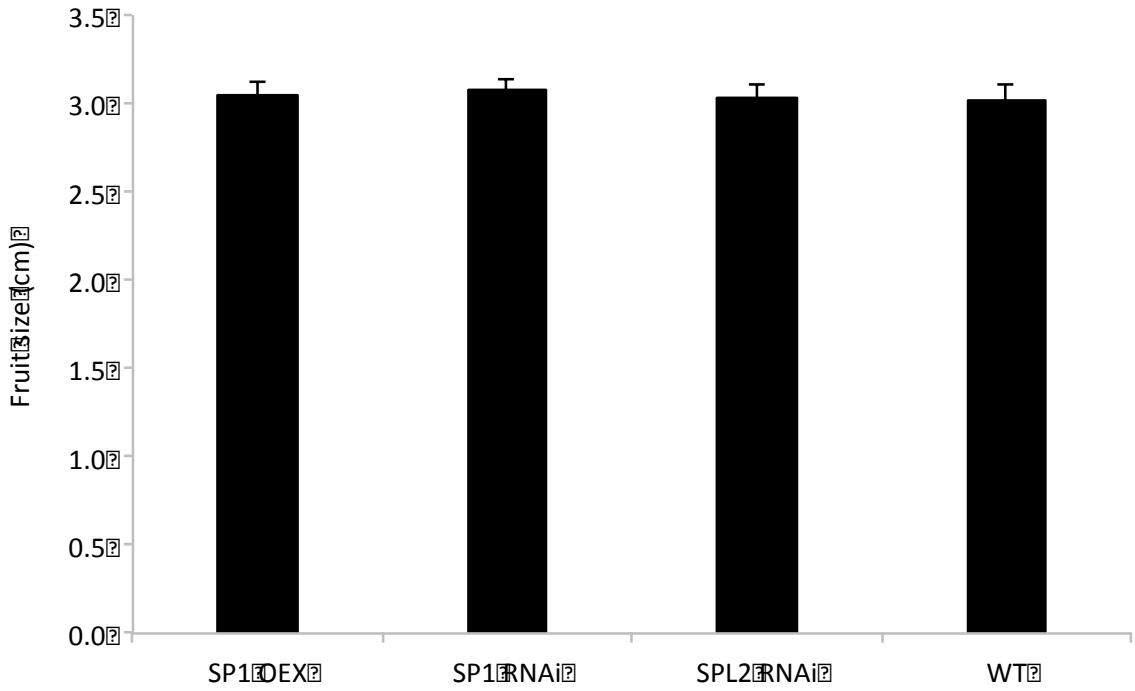

Figure 6.6. Measuring sizes of the SlSPL2 fruits used in the ripening analysis. The measurement of the average equatorial diameter of tomato from T2 generation plants was done using a calliper at breaker stage. The fruits were then detached from the plants and incubated at 25°C in the dark for the ripening analysis in Figure 6.3. The SlSP1 data are the same data as was presented in Figure 3.8 of Chapter 3. Data are mean +SEM for at least 20 fruits per genotype. Student's *t*-test revealed no significant differences between genotypes relative to WT.

6.2.5 Analysis of the role of SlSPL2 in leaf senescence

To analyse the functions of SlSPL2 in the tomato leaf senescence process, I compared the SlSPL2 RNAi lines to the SlSP1 OEX and SlSP1 RNAi lines and WT, in dark-induced leaf senescence experiments (Schelbert et al., 2009) similar to those conducted in Arabidopsis (Ling et al., 2012). The extent of senescence in leaves induced by dark treatment was determined by measuring declining chlorophyll levels and photochemical efficiency of photosystem II (F_v/F_m).

For senescence induction, at least three individual tomato leaves, 6-7 cm in length, from 2-month-old plants were covered with aluminium foil. Chlorophyll levels were measured using a SPAD-502 meter in the same leaf on Day 1 (before covering with foil) and on Day 16 after the initiation of the dark treatment. On this occasion, the plants were grown in a growth cabinet, under normal conditions, and the shortened period of analysis here (16 days compared to the 30 days used Section 3.2.6) was due to the size limitation placed on the plants by the cabinet.

On Day 16, the leaves were first inspected visually. The SlSP1 OEX and WT leaves showed visible leaf yellowing, with the former showing a stronger response, providing an indication of accelerated leaf senescence as expected (Figure 6.7). In contrast, both the SlSP1 RNAi leaves and the SlSPL2 RNAi leaves appeared greener and healthier than WT leaves, and did not show visible signs of senescence (Figure 6.7). Although the differences in leaf colour were not as clear as those shown in Figure 3.10 (owing to the shorter period of dark treatment), the aforementioned trends were clearly supported by the chlorophyll concentration measurements, which showed significant differences between the genotypes at the end of the treatment (Figure 6.8A). The extent of chlorophyll loss was greatest in SP1 OEX leaves, and least in the SPL2 RNAi leaves (Figure 6.8B).

Average whole-leaf F_v/F_m values were calculated based on images recorded using a CF Imager at Day 16. In line with the chlorophyll measurements, the lowest F_v/F_m values were recorded in the SlSP1 OEX leaves, indicating accelerated senescence in this genotype

(Figure 6.9A). In contrast, both SlSP1 RNAi and SlSPL2 RNAi leaves showed higher F_v/F_m values than WT, indicating attenuated senescence, with the highest values being recorded in SPL2 RNAi leaves (Figure 6.9A). The results for SlSP1 presented here are consistent with those shown in Figure 3.11B. The images presented in Figure 6.9B reveal that F_v/F_m was lowest at the leaf edges, at the tip and towards the lower part of the leaf, and that this loss of photosynthetic efficiency was most noticeable in SlSP1 OEX leaves and least obvious in the SlSP1 RNAi and SlSPL2 RNAi leaves.

Overall, this evaluation of leaf senescence induced by dark treatment confirmed the results presented in Chapter 3 (which demonstrated the importance of SlSP1 in the senescence process), and revealed an important new role for SlSPL2 in the process. The fact that SlSPL2 silencing had an even stronger effect on senescence than SlSP1 silencing is remarkable, especially given that the transcript abundance for *SlSPL2* is low compared to that of *SlSP1* (Figure 3.3A). These results also reveal a conserved function of SP1 homologues in plastid biogenesis.

Figure 6.7. Evaluation of the effect of SlSPL2 on dark-induced senescence in tomato leaves. Leaves of 2-month-old plants of equal length (6-7 cm) were covered with aluminium foil for 16 days. At the end of the treatment, a representative leaf from each genotype was photographed and is shown. Enhanced yellowing was observed in SP1 OEX leaves, whereas SP1 and SPL2 RNAi leaves appeared greener than WT leaves.

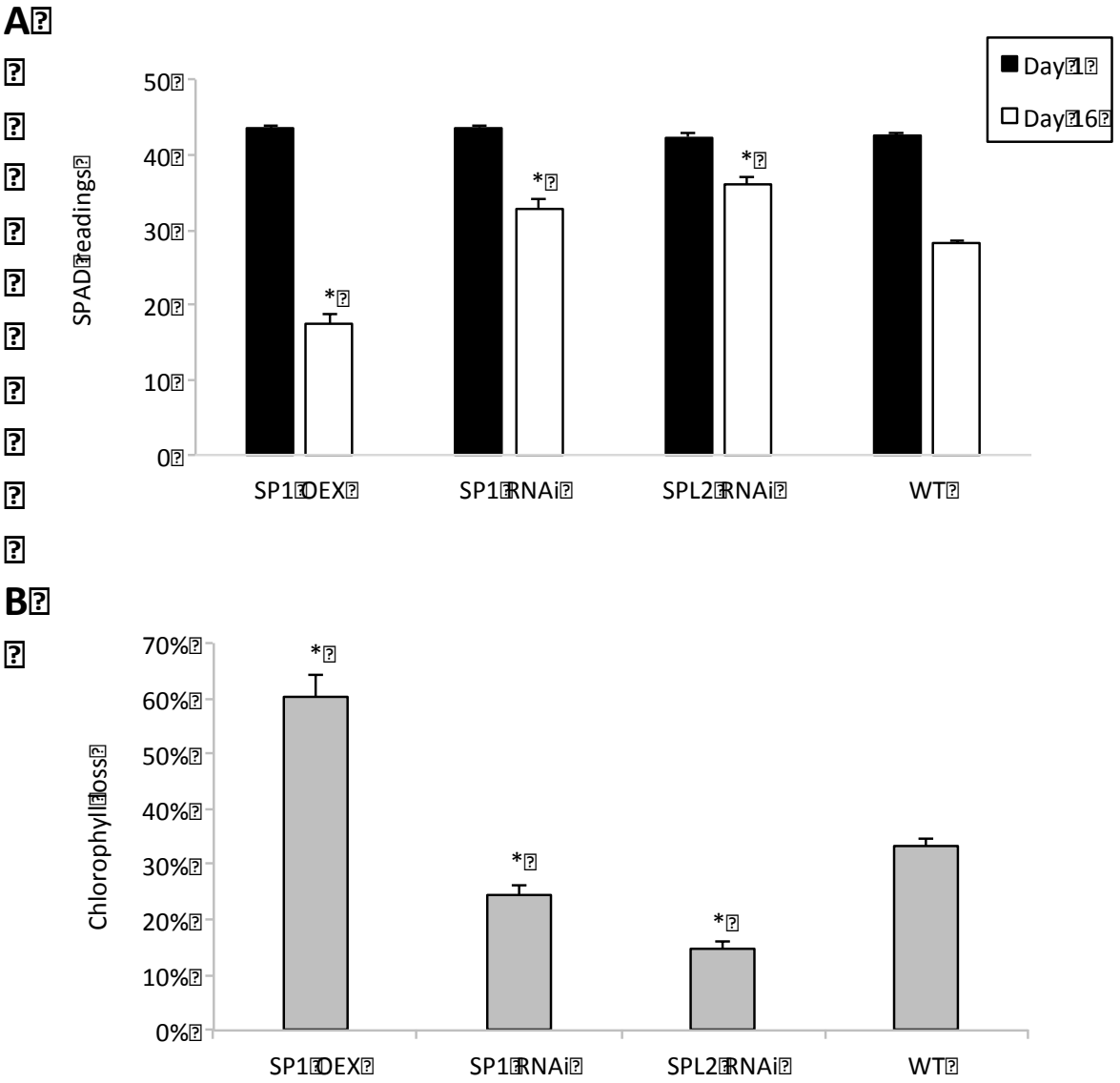

Figure 6.8. Measuring the effect of SlSPL2 on the extent of senescence induced by dark treatment in tomato leaves. (A) Chlorophyll measurements were made using a SPAD-502 meter in the same leaf on Day 1 (before covering with foil) and on Day 16 after the initiation of the dark treatment. (B) The percentage of chlorophyll loss was calculated as the difference in chlorophyll concentration between Day 1 and Day 16. Data are mean +SEM for at least 3 leaves per genotype. Asterisks above the bars indicate a significant difference relative to WT (Student's *t*-test, **P*<0.05).

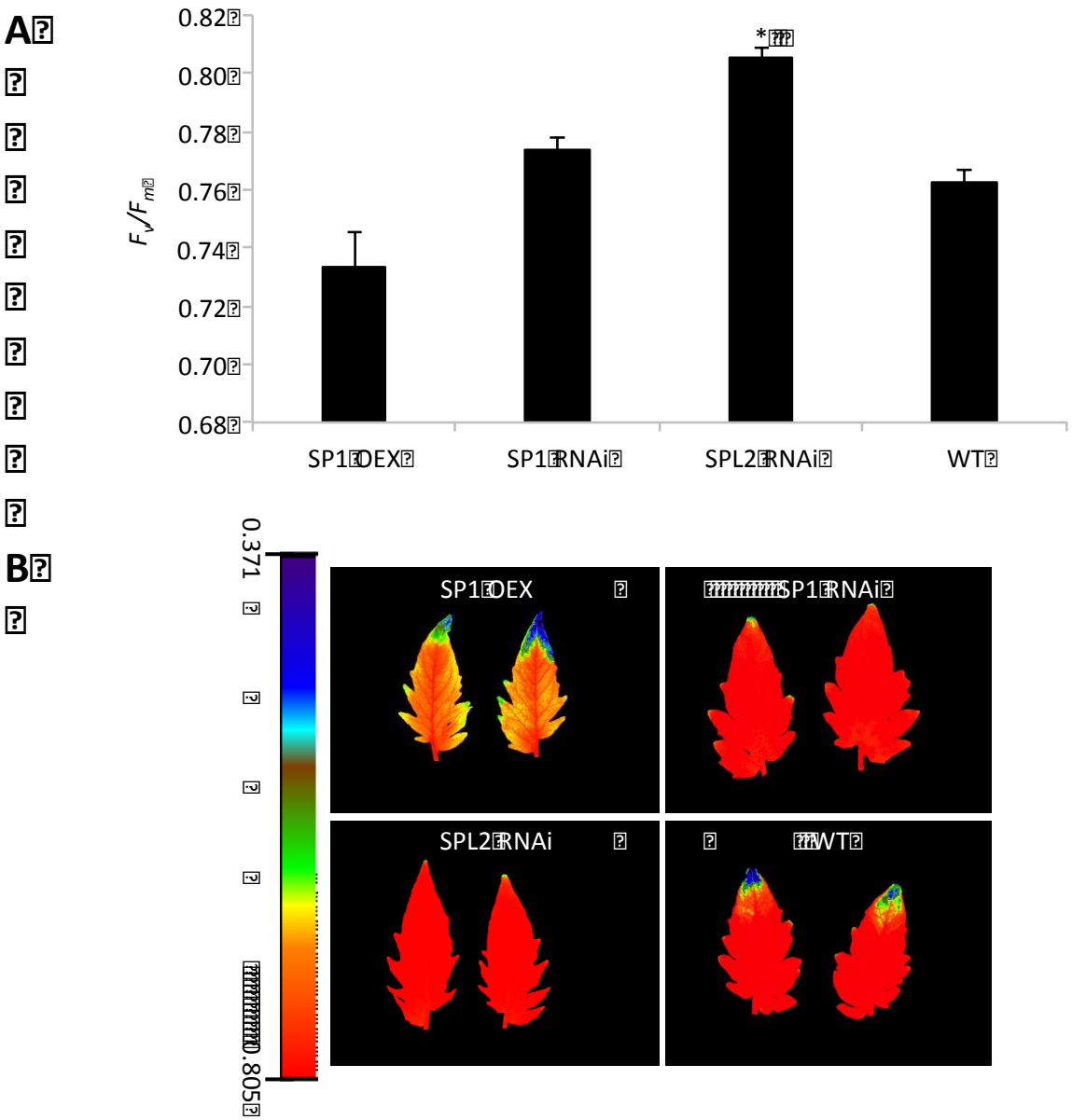

Figure 6.9. Determination of the effect of SlSPL2 on photosynthetic efficiency in tomato leaves induced to senesce by dark treatment. (A) Chlorophyll fluorescence parameters were recorded using a CF Imager on Day 16, after the completion of the dark treatment described in Figures 6.7 and 6.8, and used to calculate F_v/F_m values for whole leaves. (B) Images representative of those used to calculate the F_v/F_m values are shown. The colour spectrum to the left defines the range of F_v/F_m values shown. Data are mean +SEM for at least 3 leaves per genotype. Asterisks above the columns indicate a significant difference relative to WT (Student's *t*-test, *P<0.05). Student's *t*-test also revealed no significant differences in F_v/F_m values of SP1 OEX and SP1 RNAi relative to WT in (A).

6.2.6 Analysis of the role of SlSPL2 in plant responses to salinity stress

To study the effects of salt stress on SlSPL2 RNAi pre-flowering tomato plants in comparison to WT, SlSP1 OEX and SlSP1 RNAi plants, tomato seeds were first germinated on soil. Then, equally developed 2-week-old plants of each genotype were selected and exposed to stress by applying salt solution (400 mM NaCl). In parallel, an equivalent set of plants was allowed to grow under normal growth conditions, as controls for the experiment. After 15 days of treatment, plant response to the stress treatment was assessed by measuring chlorophyll content and the photochemical efficiency of photosystem II (F_v/F_m).

The SlSP1 OEX plants had the highest chlorophyll levels at the end of the treatment, and so were considered more stress tolerant than WT, while the SlSP1 RNAi and SlSPL2 RNAi leaves had the lowest at values the end of the treatment (Figure 6.10A). Although all the plants were of identical age, and equally developed leaves were chosen for analysis (the first leaf next to an inflorescence), the chlorophyll values on Day 1 were unequal between genotypes (Figure 6.10A and 6.10C). Thus, the percentage of chlorophyll loss (i.e., the difference in chlorophyll content between Day 1 and Day 15) in the same leaves over the course of the experiment was considered to be a more reliable indicator of stress tolerance in this case. Percentage of chlorophyll loss was calculated and was found to be smaller than WT for SlSP1 OEX, and larger than WT for SlSP1 RNAi and SlSPL2 RNAi (Figure 6.10B). The trends observed here for the SP1-modified plants were in line with those shown in Figure 5.4 for tomato, and Figure 5.8 for wheat, where overexpression of SP1 delivered improved stress tolerance and SP1 deficiency caused greater stress sensitivity, relative to WT.

Interestingly, the chlorophyll content (Figure 6.10C) and percentage chlorophyll loss (Figure 6.10D) data for the control, unstressed plants showed a comparable trend to corresponding data from the leaf senescence experiment in Figure 6.8, where SlSP1 OEX displayed the lowest chlorophyll content and the highest percentage of chlorophyll loss, and SlSP1 RNAi and SlSPL2 RNAi displayed the highest chlorophyll contents and the lowest percentages of

chlorophyll loss. Notably, the trend of chlorophyll loss differences between the genotypes in these control plants (Figure 6.10D) is the diametric opposite of the trend seen in the stressed plants (Figure 6.10B); this suggests that the differences observed between the genotypes under stress conditions are meaningful, in spite of the lack of statistical significance.

Overall, these results support the notion of conserved functions of multiple SP1 homologues in tomato under abiotic stress conditions.

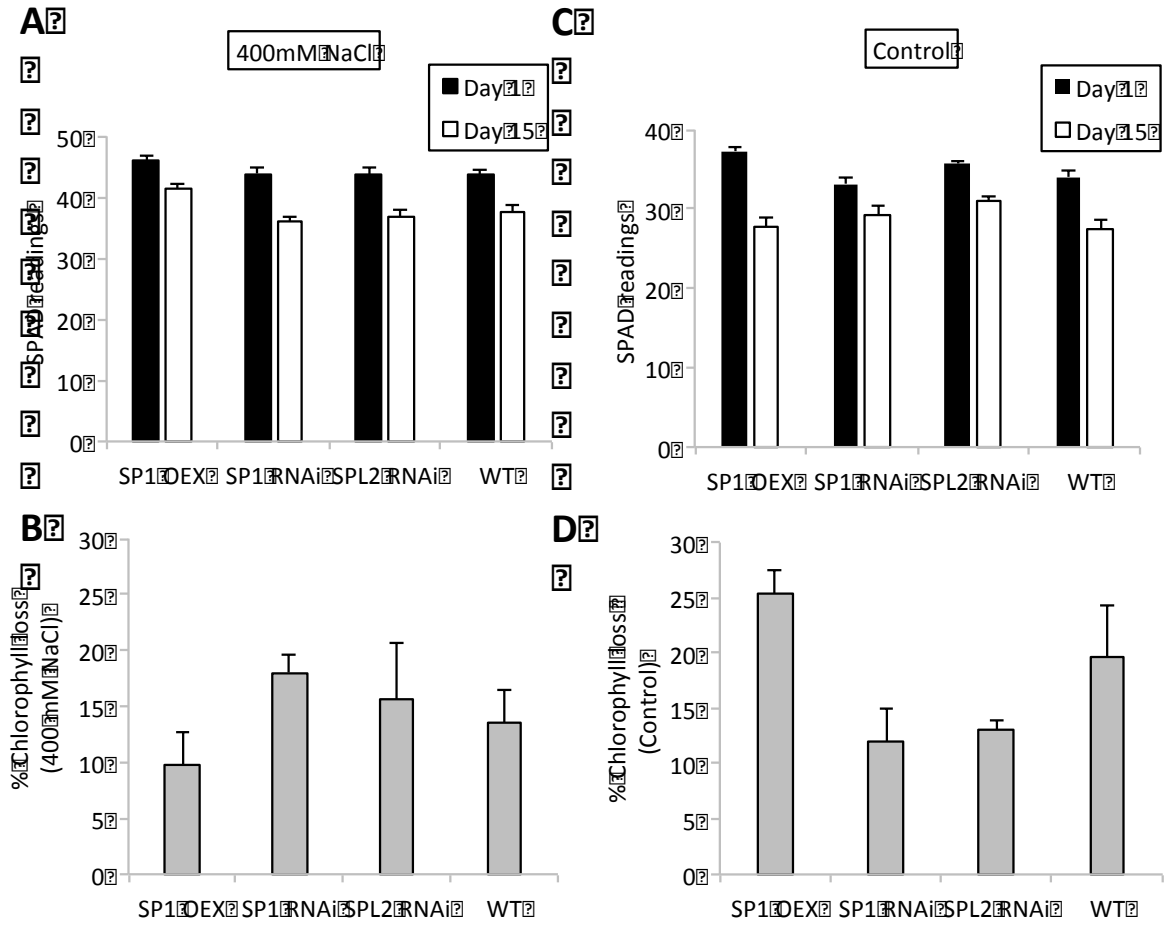

Figure 6.10. Determination of the effect of SlSPL2 on salinity tolerance in pre-flowering tomato plants. Developmentally equivalent 2-week-old plants grown on soil in individual 0.25 L pots with sufficient watering were placed in a tray (6 pots per tray). The trays were allowed to dry before the plants were subjected to salinity stress treatments by applying 1 L of 400 mM NaCl solution to the tray once. The plants were then watered with 1 L of water per tray each week post-treatment and allowed to grow on for a further 15 days. Control plants were grown similarly, but without salinity treatment. (A, C) Chlorophyll measurements were made using a SPAD-502 meter on developmentally equivalent leaves of the salt-treated (A) and control plants (C), using the same leaf on Day 1 and on Day 15 after the initiation of the treatment. (B, D) The percentage of chlorophyll loss was calculated as the difference in chlorophyll level between Day 1 and Day 15, for both salt-treated plants (B) and control plants (D). Data are mean +SEM for 3 leaves per genotype per condition. Student's *t*-test revealed no significant differences in percentage of chlorophyll loss in all genotypes, relative to WT in (B) and (D).

6.3 Conclusion

In this chapter, the experiments were conducted to investigate whether a tomato SP1 homolog, SlSPL2, also governs plastid biogenesis. Although the *SlSPL2* gene expression analysis of various plant tissues revealed a similar pattern to *SlSP1*, the transcript abundance of *SlSPL2* was much less than that of *SlSP1* (Figure 3.3A). In spite of this, the results indicated that the *SlSPL2* gene is able to influence fruit ripening, leaf senescence, and abiotic stress responses in tomato.

In the fruit ripening analysis, SPL2 RNAi plants displayed a delay in ripening duration that was indistinguishable from that seen in SP1 RNAi plants. In spite of this, the SPL2 RNAi tomato fruits were indistinguishable from the WT (and from the SP1 transgenics) in relation fruit firmness and size at defined developmental stages, ruling these out as contributing factors concerning the modification of ripening duration. The analysis of leaf senescence induced by dark treatment (as measured by declining chlorophyll levels and F_v/F_m values) revealed an even greater delay in the senescence process in SPL2 RNAi plants than in SP1 RNAi plants. While a separate natural senescence experiment (which was primarily set up as a control for salt stress experiment in Figure 6.10) did not reveal similar differences in senescence between SPL2 RNAi and SP1 RNAi, it seems likely that the duration of this experiment was not optimal (i.e., too short) in this regard.

Analysis of the plants under salinity stress conditions revealed that the percentage of chlorophyll loss in SPL2 RNAi leaves was higher than that in WT leaves, suggesting that this genotype (like SP1 RNAi) is more sensitive to high salt concentrations (400 mM NaCl) than WT. An indirect involvement of Arabidopsis *SPL2* in drought stress tolerance (wherein the UTR of the *SPL2* gene was reported to regulate the expression of a transcription factor gene with an important role in stress responses) was reported previously by Gao et al. (2015), although that study did not suggest direct involvement of the SPL2 protein in stress responses. Further analysis including various other abiotic stress conditions, of varying severity, will help

to provide a clearer view of the role of SPL2 in stress, and might reveal more clear functional differences between the SP1 homologues.

Overall, the results in this chapter shed significant new light on the role of the SP1 homologue, SPL2, in plant development, using tomato as a model system. Broadly speaking, the results presented here are in line with those on the SP1-mediated effects described in Chapters 3, 4 and 5, where plants with modified SP1 expression experienced a delay or acceleration in plant developmental processes linked to plastid type changes and/or plastid proteome reorganization, or altered sensitivity to abiotic stress conditions. An even better understanding of SPL2's role in plastid biogenesis would be possible if this study were expanded to include tomato SPL2 OEX and SP1/SPL2 double RNAi knockdown lines, both of which might help to reveal additional roles of SlSPL2 that potentially were masked in the current study owing to redundancy with SlSP1.

Chapter 7: General Discussion

7.1 The context of this work

The *suppressor of ppi1 locus 1* was characterized by Ling et al. (2012), and this work revealed that SP1 is part of a molecular mechanism that targets the components of the TOC complex for degradation by the cytosolic 26S proteasome.

Interestingly, homologues of SP1 are widely distributed in plants suggesting that its important functions may be well conserved and are likely to have relevance in other important species. Although the role of SP1 during plastid development, particularly during de-etiolation and senescence, and under abiotic stress conditions such as salinity, osmotic and oxidative stresses, has been extensively studied in the model plant Arabidopsis (Ling et al., 2012; Ling and Jarvis, 2015), its role in other species was unknown at the outset of this work.

This lack of knowledge, in particular on SP1 functions during other types of plastid transition, is what motivated the initiation of this project. In particular, it spurred the development of tomato transgenics to shed light on the importance of SP1 regulation during chloroplast-to-chromoplast conversions during fruit ripening, and to possibly enable alteration of the ripening process. Employment of another important crop species, wheat, not only enabled assessment of SP1 function in a monocotyledonous species for the first time, and in particular a direct comparison with the analysis of leaf senescence in Arabidopsis by Ling et al. (2012), but also suggested ways to improve yield-related parameters in a major field crop.

In addition, the project was extended to include analysis of a tomato SP1 homologue, SPL2, in respect of its functions during plastid biogenesis and interconversions, and during stress conditions.

7.2 Summary of key findings

This work was carried out to assess SP1's role in two different crop species, tomato and wheat. As already noted, the work in tomato was extended to include analysis of another tomato SP1 homologue, SPL2. Overall, this project revealed that SP1 in crops has similar functions to those described for SP1 in Arabidopsis, with regard to both plastid interconversions and abiotic stress responses. The data on tomato SPL2 are rather more preliminary in nature, and while they require additional evidence to provide a comprehensive picture of SPL2 function, it appears that it too is functionally similar to the SP1 paradigm, as defined in Arabidopsis (Ling et al., 2012; Ling and Jarvis, 2015).

In both tomato and wheat, it was found that the leaf senescence process, when chloroplasts are degraded to gerontoplasts, is accelerated when SP1 is overexpressed, and delayed when SP1 is deficient. These results were identical under both natural and dark-induced senescence conditions. The data strongly supported an important role for SP1 in promoting leaf senescence in both species, and directly reflected the observations made in Arabidopsis. Interestingly, in wheat, it was found that the SP1-mediated alteration of the senescence process is linked to a modification of yield. The delay in senescence in SP1-deficient wheat plants gave rise to an obvious 'stay-green' phenotype, and promoted better average seed harvest per plant. In contrast, the average weight of the harvested grain was slightly reduced, which suggested that SP1 deficiency might cause inefficiencies in grain filling possibly linked to amyloplast development effects.

With regard to tomato fruit ripening, it was found that SP1's role influences the duration of ripening, presumably linked to effects on chromoplast biogenesis. The ripening of detached transgenic tomato fruits was accelerated when SP1 is overexpressed, and delayed when SP1 is less abundant. These observations revealed a function of SP1 in promoting a developmental process linked to plastid transitions that had not previously been studied, but were broadly consistent with the previously characterized and published functions of SP1 in

promoting other transitions in Arabidopsis (Ling et al., 2012). However, the observations concerning the total duration of ripening for fruits on the vine did not reveal a similar dependence on the level of SP1 expression, and the significance of this is presently unclear. In the future, more specific assays related to the metabolic changes that underlie fruit ripening and fruit quality will be informative, and could help to better define SP1's function in fruit development and the prospects for using SP1 as a biotechnological tool.

With regard to abiotic stress tolerance, it was found that the effect of SP1 is related to the developmental stage of the plants (i.e., before or after flowering) during which exposure to the stress (either salinity stress or osmotic stress) occurs. When exposure to stress conditions occurred at a pre-flowering stage, it was found that SP1 promotes stress tolerance and aids plant survival, in accordance with the previously characterized role for SP1 in Arabidopsis seedlings experiencing stress (Ling and Jarvis, 2015). In contrast, when plants experienced stress conditions at a post-flowering stage, SP1 was found to suppress the plants' ability to survive, such that SP1 overexpressors were more sensitive to stress. In tomato, the adaptation to stress conditions via SP1 function was found to have an impact on flowering onset and development, while in wheat, it was found to have impact on the yield.

In addition, there is another plant RING E3 ligase, SpRing, which is also involved in adaptation to abiotic stresses. The expression level of *SpRing*, which localized on the endoplasmic reticulum membrane was induced by various abiotic stresses, suggesting its involvement in stress response (Qi et al., 2016). In vitro ubiquitination assay revealed that both SP1 and SpRing are indeed the E3 ubiquitin ligases and the RING finger conserved region is required for their activity (Ling et al., 2012; Qi et al., 2016). Furthermore, *sp1* mutant and *SpRing*-silenced plants both showed a higher level of hydrogen peroxide (H_2O_2), while overexpression of these genes in Arabidopsis resulted in enhanced salt tolerance during seed germination and early seedling development under stress conditions (Ling and Jarvis, 2015; Qi et al., 2016).

Although there are similarities in the functional and physiological behaviour between SP1 and SpRing proteins, there are differences in their regulatory mechanism for stress tolerance. Under stress, SP1 depletes the TOC machinery of chloroplast protein import to reduce import of photosynthesis proteins, as SP1 overexpression was seen to attenuate photosynthetic activity and initially retard growth, but eventually enabled improved stress tolerance (Ling and Jarvis, 2015). In contrast, SpRing involvement in stress regulation does not directly related to chloroplast protein import mechanism, but its functions as a positive regulator of salt tolerance involved both ABA-dependent and ABA-independent signalling pathways (Qi et al., 2016).

Although the analysis of *SlSPL2* gene expression in various plant tissues revealed a similar pattern to *SlSP1* expression, the transcript abundance of *SlSPL2* was much lower than that of *SlSP1*. In spite of this, the results indicated that the *SlSPL2* gene is able to influence fruit ripening, leaf senescence, and abiotic stress responses in tomato. While my analyses of SP1 in crops were essentially an extension of those previously conducted in Arabidopsis (Ling et al., 2012; Ling and Jarvis, 2015), my analysis of SlSPL2 was unique in the sense that the role of Arabidopsis SPL2 in plastid biogenesis and function has not been described. A major limitation of my study of SPL2 was the use of only SPL2 RNAi transgenic tomato plants as a model system. It might help to shed light on the roles of SlSPL2 if the analyses were expanded in the future to include SPL2 OEX and SP1/SPL2 double RNAi knockdown tomato lines; this might reveal functions that were masked in the current study owing to redundancy with SlSP1.

7.3 Assessment of the ability of SP1 and its homologue to contribute for crop improvements

Previous work showed that the SP1 ubiquitin E3 ligase regulates the TOC machinery to facilitate reconfiguration of the plastid proteome, which is essential during developmental transitions that involve the interconversion of different plastid types (Ling et al., 2012). This study revealed a clear role for SP1 in tomato fruit ripening, when chloroplasts transform into chromoplasts. In tomato plants with SP1 deficiency, the fruit display a much delayed ripening.

This trait may be highly beneficial agriculturally. Fruits that are picked whilst still green or at breaker stage, but which nonetheless have reached full size, will continue to develop and reach the mature red stage. A delay in the ripening of detached fruits has the potential to extend shelf life during postharvest storage and transportation, giving farmers and the supply chain greater flexibility in marketing their goods and ensuring freshness for consumers (Arah et al., 2016). Thus, manipulating the ripening duration of fruits could, in conjunction with recent improvements in postharvest storage and transportation, help to increase tomato production and profits by reducing fruit loss after harvest.

This study also revealed a conserved function of SP1 during leaf senescence, when chloroplasts transform into gerontoplasts, in both tomato and wheat. Wheat SP1-deficient plants showed attenuation of the decline in photosynthetic efficiency normally associated with senescence, producing a 'stay-green' phenotype that was linked to improvements in the average seed harvest per plant. As many studies in maize and wheat have shown, a 'stay-green' phenotype increases yield by extending photosynthetic production (Spano et al., 2003; Tian et al., 2012; Thomas and Ougham, 2014). Thus, it is possible that SP1 manipulation may provide a novel means of improving yields in field crops by keeping leaves green at the last stages of grain development. Although the SP1 RNAi plants experienced delay in the leaf aging process, causing an increment in average seed harvest per plant, the average seed weight of SP1 RNAi was reduced, which may be related to effects on amyloplast development. If SP1 does indeed modulate amyloplast biogenesis, then SP1 modification could be used to influence seed quality in cereal crops in relation to starch synthesis, which affects eating and cooking qualities, nutritional goodness, and the suitability of the resulting flour for a variety of food preparation processes (Hurkman et al., 2008).

The conserved role of SP1 in abiotic stress responses, wherein it promotes plant stress tolerance by setting in motion a chain of events that limits the possibility for overaccumulation of harmful ROS, provides a further avenue for biotechnological exploitation. It is known that 'stay-green' wheat varieties can offer performance advantages under stress conditions (Tian

et al., 2012), and so implementation of SP1 as a tool in this regard may enable crops to grow in places which are not currently suitable for plant growth (Katerji et al., 2003; Gregersen et al., 2013).

7.4 Future perspectives

My work has shown that SP1 function is conserved in two of the world's most important crop species, and it is evident that SP1 homologues are present throughout the plant kingdom and in the most important crop species (Figure 7.1). The phylogenetic analysis reflected the evolution in plant lineage as SP1 is present throughout bryophytes and angiosperms. The homologues identified in other crop species shown in Figure 7.1 are likely to be true orthologues of SP1, as they were identified using Arabidopsis SP1 as a query in BLAST searches, and they reciprocally returned SP1 from Arabidopsis in subsequent BLAST searches.

Moreover, it is likely that these putative SP1 orthologues are functional proteins employing a mechanism similar to Arabidopsis SP1, as alignment of their amino-acid sequences with that of SP1 revealed a conserved C3HC4-type RING Finger (RNF) domain, which is a characteristic feature of many ubiquitin E3 ligases (Figure 7.2). Additional characteristics of these putative orthologues, which further suggest that they are likely to be functionally similar to SP1, include the size similarity and topology to AtSP1 as described in Table 7.1.

Overall, my studies of SP1 function in tomato and wheat not only provide new information on the functions of SP1, but also demonstrated clearly the translational potential of fundamental knowledge gained previously from studies on SP1 in the model plant, Arabidopsis. As plastids and SP1-type proteins are ubiquitous in plants (Figure 7.1), the knowledge gained through this work may ultimately be transferred to, and applied in, a variety of different crop species. Doing so may contribute to improved food security, not only by increasing yields or grain quality, but also by enabling crop species to deal with adverse environmental conditions (such as drought, high salinity, high temperature, or nutrient deficiency) that may occur more

frequently in the future as a result of climate change (Lobell and Gourdji, 2012; Gregersen et al., 2013).

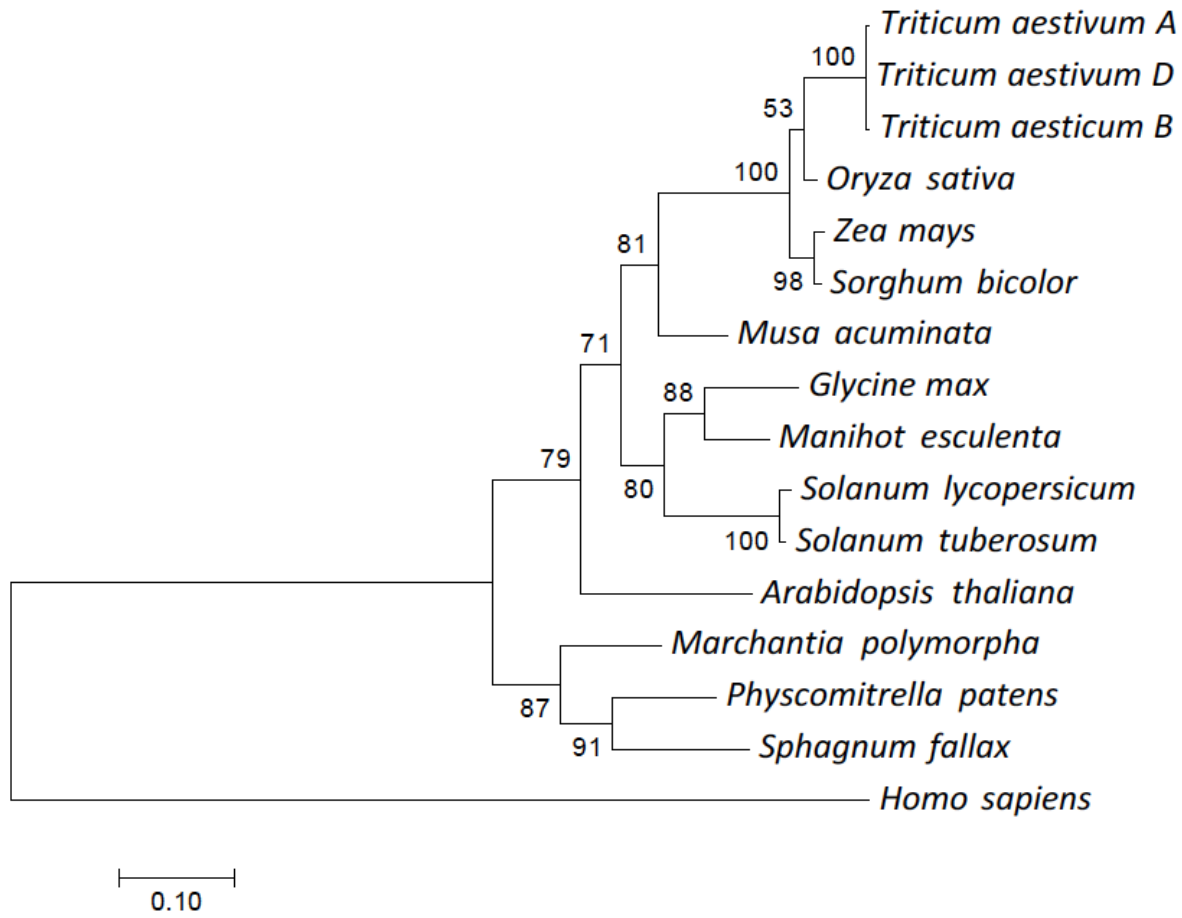

Figure 7.1. Phylogenetic analysis of SP1 homologues from selected species. Predicted protein sequences homologous to Arabidopsis SP1 from a variety of plants were retrieved from the National Center for Biotechnology Information (NCBI), Ensembl Plants and Phytozome 12 database and BLASTP analysis using Arabidopsis SP1 as the query (Johnson et al., 2008; Goodstein et al., 2012; Bolser et al., 2014); results of reciprocal BLASTP searches using the same databases was used to inform selection of suitable orthologues for analysis. The species used in the analysis were *T. aestivum* (wheat), *B. distachyon* (grass), *S. bicolor* (sorghum), *Z. mays* (maize), *O. sativa* (rice), *M. acuminata* (banana), *G. max* (soybean), *M. esculenta* (cassava), *S. lycopersicum* (tomato), *S. tuberosum* (potato), *A. thaliana* (thale cress), *M. polymorpha* (liverwort), *P. patens* (moss), *S. fallax* (peat moss) and *H. sapiens* (human). The

retrieved sequences were used to perform a boot-strapped maximum-likelihood phylogenetic analysis. The closest human relative to SP1 is included as the outgroup. Sequences were aligned with MEGA (M7: Alignment Explorer). Phylogenetic and molecular evolutionary analyses were conducted using MEGA version 7 (Kumar et al., 2016), and boot-strapped 1000 times. The percentage of trees in which the associated taxa clustered together is shown next to the branches. Scale bar represents 0.1 changes per site.

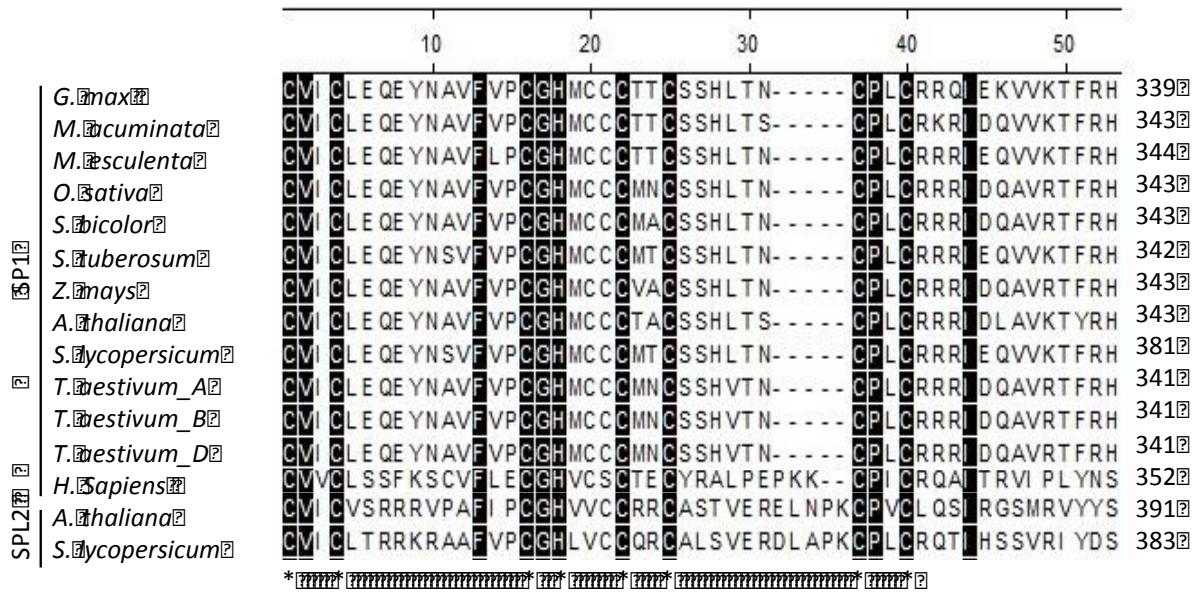

Figure 7.2. Amino acid sequence alignment of the C3HC4-type RNF domains of SP1 homologues from important crop species. The sequences used in the analysis were from *G. max* (soybean), *M. acuminata* (banana), *M. esculenta* (cassava), *O. sativa* (rice), *Z. mays* (maize), *A. thaliana* (thale cress), *S. lycopersicum* (tomato), *T. aestivum* (wheat) and *H. sapiens* (human). Alignment of SP1 homologues, SlSPL2 from *S. lycopersicum* and AtSPL2 from *A. thaliana* was included in this sequence alignment. Sequences were identified as described in Figure 7.1, and aligned using MegAlign by the Clustal W method (DNASTAR Lasergene). Black marking shows residues that are identical in all species. The critical conserved Cys and His residues of the RNF domains are indicated with asterisks.

Table 7.1. The topology and size of SP1 putative orthologues. The topologies were predicted using TMPred program (Hofmann, 1993). Studies in Arabidopsis by Ling et al. (2012) showed AtSP1 as an integral component of the plastid outer membrane, and was predicted to have two TMDs (TMD1 and TMD2), a C-terminal, cytosol-facing RING domain and an intermembrane space domain. The similarity in the number of amino acid and topology between these orthologues further suggest that they are likely to be functionally similar to AtSP1.

Species	**Sequence accession no.**	**Total number of amino acid**	**Number of predicted TMDs**	**Position of TMD1**	**Position of TMD2**
Glycine max	XP_003518933 / Glyma.02G149800.1	339	2	1-20	225-242
Musa acuminata	XP_009410049 / GSMUA_Achr7T18450_001	343	2	1-20	226-248
Manihot esculenta	XP_021614013 / Manes.05G072700.1	344	2	1-20	227-244
Oryza sativa	XP_015644605 / Os07g45350.1	343	2	2-20	224-245
Sorghum bicolor	XP_002463293 / Sobic.002G399100.1	343	2	2-20	227-245
Solanum tuberosum	XP_006352786 / PGSC0003DMT400051847	342	2	1-20	226-244
Zea mays	XP_008670617 / GRMZM2G020574_T08	343	2	2-20	227-244
Arabidopsis thaliana	NP_176574 / At1g63900	343	2	1-19	221-241
Solanum lycopersicum	XP_010323033 / Solyc06g084360.2.1	381	2	41-60	266-284
Triticum aestivum A	TRIAE_CS42_2AS_TGACv1_114976_AA0370300	341	2	2-20	224-245
Triticum aestivum B	TRIAE_CS42_2BS_TGACv1_146843_AA0473840	341	2	2-20	224-245
Triticum aestivum D	TRIAE_CS42_2DS_TGACv1_178131_AA0591470	341	2	2-20	224-245

Bibliography

Amoah, B., Wu, H., Sparks, C., and Jones, H. (2001). Factors influencing *Agrobacterium*-mediated transient expression of *uidA* in wheat inflorescence tissue. J. Exp. Bot. **52,** 1135-1142.

Amunts, A., Drory, O., and Nelson, N. (2008). A glimpse into the atomic structure of plant photosystem I. In Photosynthetic Protein Complexes, P. Fromm, ed (Wiley-VCH Verlag GmbH & Co. KGaA), pp. 65-81.

Anon. (1975). Color classification requirements in United States standards for grades of fresh tomatoes. USDA Visual Aid TM-L-1 (Lansing, Michigan, USA: The John Henry Co.).

ap Rees, T., and Entwistle, G. (1989). Entry into the amyloplast of carbon for starch synthesis. In Physiology, Biochemistry, and Genetics of Nongreen Plastids, C.D. Boyer, J.C. Shannon, and R.C. Hardison, eds (Rockville, MD: American Society of Plant Physiologists), pp. 49-62.

Apel, K., and Hirt, H. (2004). Reactive oxygen species: metabolism, oxidative stress, and signal transduction. Annu. Rev. Plant Biol. **55,** 373-399.

Arah, I.K., Ahorbo, G.K., Anku, E.K., Kumah, E.K., and Amaglo, H. (2016). Postharvest handling practices and treatment methods for tomato handlers in developing countries: A mini review. J. Adv. Agric. **2016,** 8.

Arazuri, S., Jaren, C., Arana, J.I., and de Ciriza, J.P. (2007). Influence of mechanical harvest on the physical properties of processing tomato (*Lycopersicon esculentum* Mill.). J. Food Eng. **80,** 190-198.

Arias, R., Lee, T.C., Specca, D., and Janes, H. (2000). Quality comparison of hydroponic tomatoes (*Lycopersicon esculentum*) ripened on and off vine. J. Food Sci. **65,** 545-548.

Aronsson, H., Boij, P., Patel, R., Wardle, A., Töpel, M., and Jarvis, P. (2007). Toc64/OEP64 is not essential for the efficient import of proteins into chloroplasts in *Arabidopsis thaliana*. Plant J. **52,** 53-68.

Asada, K. (2006). Production and scavenging of reactive oxygen species in chloroplasts and their functions. Plant Physiol. **141,** 391-396.

Austin, R.B., Flavell, R.B., Henson, I., and Lowe, H. (1986). Molecular biology and crop improvement: a case study of wheat, oilseed rape and faba beans. (UK: Cambridge University Press).

Bahaji, A., Li, J., Sanchez-Lopez, A.M., Baroja-Fernandez, E., Munoz, F.J., Ovecka, M., Almagro, G., Montero, M., Ezquer, I., Etxeberria, E., and Pozueta-Romero, J. (2014). Starch biosynthesis, its regulation and biotechnological approaches to improve crop yields. Biotechnol. Adv. **32,** 87-106.

Balmer, Y., Vensel, W.H., DuPont, F.M., Buchanan, B.B., and Hurkman, W.J. (2006). Proteome of amyloplasts isolated from developing wheat endosperm presents evidence of broad metabolic capability. J. Exp. Bot. **57,** 1591-1602.

Balsera, M., Soll, J., and Buchanan, B.B. (2010). Redox extends its regulatory reach to chloroplast protein import. Trends Plant Sci. **15,** 515-521.

Barsan, C., Sanchez-Bel, P., Rombaldi, C., Egea, I., Rossignol, M., Kuntz, M., Zouine, M., Latche, A., Bouzayen, M., and Pech, J.C. (2010). Characteristics of the tomato chromoplast revealed by proteomic analysis. J. Exp. Bot. **61,** 2413-2431.

Barsan, C., Zouine, M., Maza, E., Bian, W., Egea, I., Rossignol, M., Bouyssie, D., Pichereaux, C., Purgatto, E., Bouzayen, M., Latche, A., and Pech, J.C. (2012). Proteomic analysis of chloroplast-to-chromoplast transition in tomato reveals metabolic shifts coupled with disrupted thylakoid biogenesis machinery and elevated energy-production components. Plant Physiol. **160,** 708-725.

Bartels, D., and Sunkar, R. (2005). Drought and salt tolerance in plants. CRC Crit. Rev. Plant Sci. **24,** 23-58.

Basnayake, B.M., Li, D., Zhang, H., Li, G., Virk, N., and Song, F. (2011). *Arabidopsis* DAL1 and DAL2, two RING finger proteins homologous to *Drosophila* DIAP1, are involved in regulation of programmed cell death. Plant Cell Rep. **30,** 37-48.

Bathgate, B., Purton, M.E., Grierson, D., and Goodenough, P.W. (1985). Plastid changes during the conversion of chloroplasts to chromoplasts in ripening tomatoes. Planta **165,** 197-204.

Batu, A. (2004). Determination of acceptable firmness and colour values of tomatoes. J. Food Eng. **61,** 471-475.

Bauer, J., Chen, K., Hiltbunner, A., Wehrli, E., Eugster, M., Schnell, D., and Kessler, F. (2000). The major protein import receptor of plastids is essential for chloroplast biogenesis. Nature **403,** 203-207.

Baxter, A., Mittler, R., and Suzuki, N. (2013). ROS as key players in plant stress signalling. J. Exp. Bot. **65,** 1229-1240.

Bédard, J., and Jarvis, P. (2005). Recognition and envelope translocation of chloroplast preproteins. J. Exp. Bot. **56,** 2287-2320.

Belhaj, K., Chaparro-Garcia, A., Kamoun, S., Patron, N.J., and Nekrasov, V. (2015). Editing plant genomes with CRISPR/Cas9. Curr. Opin. Biotechnol. **32,** 76-84.

Bemer, M., Karlova, R., Ballester, A.R., Tikunov, Y.M., Bovy, A.G., Wolters-Arts, M., Rossetto Pde, B., Angenent, G.C., and de Maagd, R.A. (2012). The tomato FRUITFULL homologs TDR4/FUL1 and MBP7/FUL2 regulate ethylene-independent aspects of fruit ripening. Plant Cell **24,** 4437-4451.

Bin, W.S., Wei, L.K., Ping, D.W., Li, Z., Wei, G., Bing, L.J., Gui, P.B., Jian, W.H., and Feng, C.J. (2012). Evaluation of appropriate reference genes for gene expression studies in pepper by quantitative real-time PCR. Mol. Breed. **30,** 1393-1400.

Bobik, K., and Burch-Smith, T.M. (2015). Chloroplast signaling within, between and beyond cells. Front. Plant Sci. **6,** 1-26.

Bolser, D.M., Kerhornou, A., Walts, B., and Kersey, P. (2014). Triticeae resources in Ensembl plants. Plant Cell Physiol. **56,** 1-11.

Bortesi, L., and Fischer, R. (2015). The CRISPR/Cas9 system for plant genome editing and beyond. Biotechnol. Adv. **33,** 41-52.

Bruce, B.D. (2000). Chloroplast transit peptides: structure, function and evolution. Trends Cell Biol. **10,** 440-447.

Bushuk, W., and Rasper, V.F. (1994). Wheat: production, properties and quality. (UK: Springer Science & Business Media).

Camara, B., Hugueney, P., Bouvier, F., Kuntz, M., and Moneger, R. (1995). Biochemistry and molecular biology of chromoplast development. Int. Rev. Cytol. **163,** 175-247.

Carretero-Paulet, L., Ahumada, I., Cunillera, N., Rodriguez-Concepcion, M., Ferrer, A., Boronat, A., and Campos, N. (2002). Expression and molecular analysis of the *Arabidopsis* DXR gene encoding 1-deoxy-D-xylulose 5-phosphate reductoisomerase, the first committed enzyme of the 2-C-methyl-D-erythritol 4-phosphate pathway. Plant Physiol. **129,** 1581-1591.

Cartelat, A., Cerovic, Z.G., Goulas, Y., Meyer, S., Lelarge, C., Prioul, J.L., Barbottin, A., Jeuffroy, M.H., Gate, P., Agati, G., and Moya, I. (2005). Optically assessed contents of leaf polyphenolics and chlorophyll as indicators of nitrogen deficiency in wheat (*Triticum aestivum* L.). Field Crops Res. **91,** 35-49.

Caverzan, A., Casassola, A., and Brammer, S.P. (2016). Antioxidant responses of wheat plants under stress. Genet. Mol. Biol. **39,** 1-6.

Chattopadhyay, S., Ang, L.-H., Puente, P., Deng, X.-W., and Wei, N. (1998). *Arabidopsis* bZIP protein HY5 directly interacts with light-responsive promoters in mediating light control of gene expression. Plant Cell **10,** 673-683.

Chetty, V., Ceballos, N., Garcia, D., Narváez-Vásquez, J., Lopez, W., and Orozco-Cárdenas, M. (2013). Evaluation of four *Agrobacterium tumefaciens* strains for the genetic transformation of tomato (*Solanum lycopersicum* L.) cultivar Micro-Tom. Plant Cell Rep. **32,** 239-247.

Chevalier, C. (2007). Cell cycle control and fruit development. In Annual Plant Reviews Volume 32: Cell Cycle Control and Plant Development, I. Dirk, ed (UK: Blackwell Publishing Ltd), pp. 269-293.

Chi, W., Sun, X.W., and Zhang, L.X. (2013). Intracellular signaling from plastid to nucleus. Annu. Rev. Plant Biol. **64,** 559-582.

Ciais, P., Reichstein, M., Viovy, N., Granier, A., Ogée, J., Allard, V., Aubinet, M., Buchmann, N., Bernhofer, C., and Carrara, A. (2005). Europe-wide reduction in primary productivity caused by the heat and drought in 2003. Nature **437,** 529-533.

Ciechanover, A. (1998). The ubiquitin–proteasome pathway: on protein death and cell life. EMBO J. **17,** 7151-7160.

Claeys, H., Van Landeghem, S., Dubois, M., Maleux, K., and Inzé, D. (2014). What is stress? Dose-response effects in commonly used in vitro stress assays. Plant Physiol. **165,** 519-527.

Consortium, T.G. (2012). The tomato genome sequence provides insights into fleshy fruit evolution. Nature **485,** 635-641.

Cruz de Carvalho, M.H. (2008). Drought stress and reactive oxygen species: production, scavenging and signaling. Plant Signal. Behav. **3,** 156-165.

Cuartero, J., and Fernandez-Munoz, R. (1999). Tomato and salinity. Sci. Hortic. **78,** 83-125.

Dalal, M., Chinnusamy, V., and Bansal, K.C. (2010). Isolation and functional characterization of *Lycopene β-cyclase* (*CYC-B*) promoter from *Solanum habrochaites*. BMC Plant Biol. **10,** 1-15.

Dall'Osto, L., Cazzaniga, S., North, H., Marion-Poll, A., and Bassi, R. (2007). The *Arabidopsis aba4-1* mutant reveals a specific function for neoxanthin in protection against photooxidative stress. Plant Cell **19,** 1048-1064.

De Bie, P., and Ciechanover, A. (2011). Ubiquitination of E3 ligases: self-regulation of the ubiquitin system via proteolytic and non-proteolytic mechanisms. Cell Death Differ. **18,** 1393–1402.

Demidchik, V. (2015). Mechanisms of oxidative stress in plants: from classical chemistry to cell biology. Environ. Exp. Bot. **109,** 212-228.

Dietz, K.-J., Turkan, I., and Krieger-Liszkay, A. (2016). Redox-and reactive oxygen species-dependent signaling into and out of the photosynthesizing chloroplast. Plant Physiol. **171,** 1541-1550.

Dumbroff, E.B., and Cooper, A.W. (1974). Effects of salt stress applied in balanced nutrient solutions at several stages during growth of tomato. Bot. Gaz. **135,** 219-224.

Egea, I., Barsan, C., Bian, W., Purgatto, E., Latche, A., Chervin, C., Bouzayen, M., and Pech, J.C. (2010). Chromoplast differentiation: current status and perspectives. Plant Cell Physiol. **51,** 1601-1611.

Endo, T., Uebayashi, N., Ishida, S., Ikeuchi, M., and Sato, F. (2014). Light energy allocation at PSII under field light conditions: How much energy is lost in NPQ-associated dissipation? Plant Physiol. Biochem. **81,** 115-120.

Ettinger, W.F., and Theg, S.M. (1991). Physiologically active chloroplasts contain pools of unassembled extrinsic proteins of the photosynthetic oxygen-evolving enzyme complex in the thylakoid lumen. J. Cell Biol. **115,** 321-328.

Faurobert, M., Pelpoir, E., and Chaïb, J. (2007). Phenol extraction of proteins for proteomic studies of recalcitrant plant tissues. In Plant Proteomics: Methods and Protocols, H. Thiellement, M. Zivy, C. Damerval, and V. Méchin, eds (Totowa, NJ: Humana Press), pp. 9-14.

Fernandez, A.I., Viron, N., Alhagdow, M., Karimi, M., Jones, M., Amsellem, Z., Sicard, A., Czerednik, A., Angenent, G., and Grierson, D. (2009). Flexible tools for gene expression and silencing in tomato. Plant Physiol. **151,** 1729-1740.

Flores-Pérez, Ú., and Jarvis, P. (2013). Molecular chaperone involvement in chloroplast protein import. Biochim. Biophys. Acta **1833,** 332-340.

Foolad, M.R. (2007). Genome mapping and molecular breeding of tomato. Int. J. Plant Genomics **2007,** 1-52.

Foyer, C., Descourvieres, P., and Kunert, K. (1994). Protection against oxygen radicals: an important defence mechanism studied in transgenic plants. Plant Cell Environ. **17,** 507-523.

Fu, D., Uauy, C., Blechl, A., and Dubcovsky, J. (2007). RNA interference for wheat functional gene analysis. Transgenic Res. **16,** 689-701.

Gao, W., Liu, W., Zhao, M., and Li, W.-X. (2015). *NERF* encodes a RING E3 ligase important for drought resistance and enhances the expression of its antisense gene *NFYA5* in *Arabidopsis*. Nucleic Acids Res. **43,** 607-617.

Garcia, D., Narvaez-Vasquez, J., and Orozco-Cardenas, M.L. (2015). Tomato (*Solanum lycopersicum*). Methods Mol Biol **1223,** 349-361.

Geigenberger, P. (2011). Regulation of starch biosynthesis in response to a fluctuating environment. Plant Physiol. **155,** 1566-1577.

Genty, B., Briantais, J.M., and Baker, N.R. (1989). The relationship between the quantum yield of photosynthetic electron-transport and quenching of chlorophyll fluorescence. Biochim. Biophys. Acta **990,** 87-92.

Gill, S.S., and Tuteja, N. (2010). Reactive oxygen species and antioxidant machinery in abiotic stress tolerance in crop plants. Plant Physiol. Biochem. **48,** 909-930.

Giovanelli, G., Lavelli, V., Peri, C., and Nobili, S. (1999). Variation in antioxidant components of tomato during vine and post-harvest ripening. J Sci Food Agr **79,** 1583-1588.

Goldschmidt-Clermont, M. (1997). Coordination of nuclear and chloroplast gene expression in plant cells. Int. Rev. Cytol. **177,** 115-180.

González-Aguilera, K.L., Saad, C.F., Chávez Montes, R.A., Alves-Ferreira, M., and de Folter, S. (2016). Selection of reference genes for Quantitative Real-Time RT-PCR studies in tomato fruit of the Genotype MT-*Rg1*. Front. Plant Sci. **7,** 1386-1386.

Goodstein, D.M., Shu, S.Q., Howson, R., Neupane, R., Hayes, R.D., Fazo, J., Mitros, T., Dirks, W., Hellsten, U., Putnam, N., and Rokhsar, D.S. (2012). Phytozome: a

comparative platform for green plant genomics. Nucleic Acids Res. **40,** D1178-D1186.

Granato, D., and Masson, M.L. (2010). Instrumental color and sensory acceptance of soy-based emulsions: a response surface approach. Food Sci. Technol. **30,** 1090-1096.

Grandillo, S., Ku, H.M., and Tanksley, S.D. (1999). Identifying the loci responsible for natural variation in fruit size and shape in tomato. Theor. Appl. Genet. **99,** 978-987.

Gray, J.C. (2005). Regulation of nuclear gene expression by plastid signals. Plastids. Oxford: Blackwell Publishing**,** 237-267.

Gray, J.E., Picton, S., Giovannoni, J.J., and Grierson, D. (1994). The use of transgenic and naturally-occurring mutants to understand and manipulate tomato fruit ripening. Plant Cell Environ. **17,** 557-571.

Gregersen, P.L., Culetic, A., Boschian, L., and Krupinska, K. (2013). Plant senescence and crop productivity. Plant Mol.Biol. **82,** 603-622.

Grierson, D., and Kader, A.A. (1986). Fruit ripening and quality. In The Tomato Crop: A scientific basis for improvement, J.G. Atherton and J. Rudich, eds (Dordrecht: Springer Netherlands), pp. 241-280.

Gutensohn, M., Schulz, B., Nicolay, P., and Flügge, U.I. (2000). Functional analysis of the two *Arabidopsis* homologues of Toc34, a component of the chloroplast protein import apparatus. Plant J. **23,** 771-783.

Hannah, L.C., and James, M. (2008). The complexities of starch biosynthesis in cereal endosperms. Curr. Opin. Biotechnol. **19,** 160-165.

Harris, W.M., and Spurr, A.R. (1969). Chromoplasts of tomato fruits. I. Ultrastructure of low-pigment and high-beta mutants. Carotene analyses. Am. J. Bot. **56,** 369-379.

Hauenstein, M., Christ, B., Das, A., Aubry, S., and Hörtensteiner, S. (2016). A role for TIC55 as a hydroxylase of phyllobilins, the products of chlorophyll breakdown during plant senescence. Plant Cell **28,** 2510-2527.

Havaux, M., and Niyogi, K.K. (1999). The violaxanthin cycle protects plants from photooxidative damage by more than one mechanism. Proc. Natl. Acad. Sci. U. S. A. **96,** 8762-8767.

Havaux, M., Eymery, F., Porfirova, S., Rey, P., and Dörmann, P. (2005). Vitamin E protects against photoinhibition and photooxidative stress in *Arabidopsis thaliana*. Plant Cell **17,** 3451-3469.

Heldt, H.W., Flügge, U.-I., and Borchert, S. (1991). Diversity of specificity and function of phosphate translocators in various plastids. Plant Physiol. **95,** 341-343.

Hellmann, H., and Estelle, M. (2002). Plant development: regulation by protein degradation. Science **297,** 793-797.

Hiei, Y., Ishida, Y., Kasaoka, K., and Komari, T. (2006). Improved frequency of transformation in rice and maize by treatment of immature embryos with centrifugation and heat prior to infection with *Agrobacterium tumefaciens*. Plant Cell Tissue Organ Cult. **87,** 233-243.

Hirayama, T., and Shinozaki, K. (2010). Research on plant abiotic stress responses in the post-genome era: past, present and future. Plant J. **61,** 1041-1052.

Hirsch, S., Muckel, E., Heemeyer, F., von Heijne, G., and Soll, J. (1994). A receptor component of the chloroplast protein translocation machinery. Science **266,** 1989-1992.

Ho, L.C., and Hewitt, J.D. (1986). Fruit development. In The tomato crop: A scientific basis for improvement, J.G. Atherton and J. Rudich, eds (Dordrecht: Springer Netherlands), pp. 201-239.

Hobson, G.E., Adams, P., and Dixon, T.J. (1983). Assessing the color of tomato fruit during ripening. J Sci Food Agr **34,** 286-292.

Hofmann, K., Stoffel, W.,. (1993). TMbase: A database of membrane spanning protein segments. Biol. Chem. **374,** p. 166.

Hofmann, N.R., and Theg, S.M. (2005). Toc64 is not required for import of proteins into chloroplasts in the moss *Physcomitrella patens*. Plant J. **43,** 675-687.

Hørtensteiner, S., and Krautler, B. (2011). Chlorophyll breakdown in higher plants. Biochim. Biophys. Acta **1807,** 977-988.

Hruz, T., Laule, O., Szabo, G., Wessendorp, F., Bleuler, S., Oertle, L., Widmayer, P., Gruissem, W., and Zimmermann, P. (2008). Genevestigator V3: A reference expression database for the meta-analysis of transcriptomes. Adv. Bioinformatics **2008,** 1-5.

Huang, W., Ling, Q., Bédard, J., Lilley, K., and Jarvis, P. (2011). In vivo analyses of the roles of essential Omp85-related proteins in the chloroplast outer envelope membrane. Plant Physiol. **157,** 147-159.

Hurkman, W.J., Vensel, W.H., Dupont, F.M., Altenbach, S.B., and Buchanan, B.B. (2008). Endosperm and amyloplast proteomes of wheat grain. In Plant Proteomics, K.A. Ganesh and R. Randeep, eds (John Wiley & Sons, Inc.), pp. 207-222.

Initiative, A.G. (2000). Analysis of the genome sequence of the flowering plant *Arabidopsis thaliana*. Nature **408,** 796–815.

Ivanova, Y., Smith, M.D., Chen, K., and Schnell, D.J. (2004). Members of the Toc159 import receptor family represent distinct pathways for protein targeting to plastids. Mol. Biol. Cell **15,** 3379-3392.

James, M.G., Denyer, K., and Myers, A.M. (2003). Starch synthesis in the cereal endosperm. Curr. Opin. Plant Biol. **6,** 215-222.

Jarvis, P. (2008). Targeting of nucleus-encoded proteins to chloroplasts in plants. New Phytol. **179,** 257-285.

Jarvis, P., and López-Juez, E. (2013). Biogenesis and homeostasis of chloroplasts and other plastids. Nat. Rev. Mol. Cell Biol. **14,** 787-802.

Jarvis, P., Chen, L.-J., Li, H.-m., Peto, C.A., Fankhauser, C., and Chory, J. (1998). An *Arabidopsis* mutant defective in the plastid general protein import apparatus. Science **282,** 100-103.

Johnson, M., Zaretskaya, I., Raytselis, Y., Merezhuk, Y., McGinnis, S., and Madden, T.L. (2008). NCBI BLAST: A better web interface. Nucleic Acids Res. **36,** W5-W9.

Jones, J.B., Jr. Boca Raton, FL. (2007). Tomato plant culture: in the field, greenhouse, and home garden. (CRC Press).

Karimi, M., Inze, D., and Depicker, A. (2002). GATEWAY((TM)) vectors for *Agrobacterium*-mediated plant transformation. Trends Plant Sci. **7,** 193-195.

Kasuga, M., Miura, S., Shinozaki, K., and Yamaguchi-Shinozaki, K. (2004). A combination of the *Arabidopsis* DREB1A gene and stress-inducible *rd29A* promoter improved drought-and low-temperature stress tolerance in tobacco by gene transfer. Plant Cell Physiol. **45,** 346-350.

Katerji, N., van Hoorn, J.W., Hamdy, A., and Mastrorilli, M. (2003). Salinity effect on crop development and yield, analysis of salt tolerance according to several classification methods. Agric. Water Manag. **62,** 37-66.

Kessler, F. (2012). Chloroplast Delivery by UPS. Science **338,** 622-623.

Kessler, F., and Schnell, D.J. (2002). A GTPase gate for protein import into chloroplasts. Nat. Struct. Mol. Biol. **9,** 81.

Kessler, F., and Schnell, D. (2009). Chloroplast biogenesis: diversity and regulation of the protein import apparatus. Curr. Opin. Cell Biol. **21,** 494-500.

Kessler, F., Blobel, G., Patel, H.A., and Schnell, D.J. (1994). Identification of two GTP-binding proteins in the chloroplast protein import machinery. Science **266,** 1035-1039.

Khraiwesh, B., Zhu, J.-K., and Zhu, J. (2012). Role of miRNAs and siRNAs in biotic and abiotic stress responses of plants. Biochim. Biophys. Acta **1819,** 137-148.

Kikuchi, S., Bedard, J., Hirano, M., Hirabayashi, Y., Oishi, M., Imai, M., Takase, M., Ide, T., and Nakai, M. (2013). Uncovering the protein translocon at the chloroplast inner envelope membrane. Science **339,** 571-574.

Klee, H.J., and Giovannoni, J.J. (2011). Genetics and control of tomato fruit ripening and quality attributes. Annu. Rev. Genet. **45,** 41-59.

Koornneef, M., Van Diepen, J., Hanhart, C., Kieboom-de Waart, A., Martinelli, L., Schoenmakers, H., and Wijbrandi, J. (1989). Chromosomal instability in cell-and tissue cultures of tomato haploids and diploids. Euphytica **43,** 179-186.

Kouranov, A., and Schnell, D.J. (1997). Analysis of the interactions of preproteins with the import machinery over the course of protein import into chloroplasts. J. Cell Biol. **139,** 1677-1685.

Kouranov, A., Chen, X., Fuks, B., and Schnell, D.J. (1998). Tic20 and Tic22 are new components of the protein import apparatus at the chloroplast inner envelope membrane. J. Cell Biol. **143,** 991-1002.

Kovacheva, S., Bédard, J., Patel, R., Dudley, P., Twell, D., Ríos, G., Koncz, C., and Jarvis, P. (2005). In vivo studies on the roles of Tic110, Tic40 and Hsp93 during chloroplast protein import. Plant J. **41,** 412-428.

Kubis, S., Baldwin, A., Patel, R., Razzaq, A., Dupree, P., Lilley, K., Kurth, J., Leister, D., and Jarvis, P. (2003). The Arabidopsis *ppi1* mutant is specifically defective in the expression, chloroplast import, and accumulation of photosynthetic proteins. Plant Cell **15,** 1859-1871.

Kumar, S., Stecher, G., and Tamura, K. (2016). MEGA7: molecular evolutionary genetics analysis version 7.0 for bigger datasets. Mol. Biol. Evol. **33,** 1870-1874.

Kwok, E.Y., and Hanson, M.R. (2004). GFP-labelled Rubisco and aspartate aminotransferase are present in plastid stromules and traffic between plastids. J. Exp. Bot. **55,** 595-604.

Laemmli, U.K. (1970). Cleavage of structural proteins during the assembly of the head of bacteriophage T4. Nature **227,** 680–685.

Lee, J., Kim, D.H., and Hwang, I. (2014). Specific targeting of proteins to outer envelope membranes of endosymbiotic organelles, chloroplasts, and mitochondria. Front. Plant Sci. **5,** 1-5.

Leister, D., and Pesaresi, P. (2018). The genomic era of chloroplast research. Annu. Rev. Plant Biol.**,** 1-29.

Li, H.-m., and Chiu, C.-C. (2010). Protein transport into chloroplasts. Annu. Rev. Plant Biol. **61,** 157-180.

Li, L., and Yuan, H. (2013). Chromoplast biogenesis and carotenoid accumulation. Arch. Biochem. Biophys. **539,** 102-109.

Li, S., Xu, C., Yang, Y., and Xia, G. (2010). Functional analysis of *TaDi19A*, a salt-responsive gene in wheat. Plant Cell Environ. **33,** 117-129.

Li, W., Bengtson, M.H., Ulbrich, A., Matsuda, A., Reddy, V.A., Orth, A., Chanda, S.K., Batalov, S., and Joazeiro, C.A.P. (2008a). Genome-wide and functional annotation of human E3 ubiquitin ligases identifies MULAN, a mitochondrial E3 that regulates the organelle's dynamics and signaling. PLoS One **3,** 1-14.

Li, W.X., Oono, Y., Zhu, J.H., He, X.J., Wu, J.M., Iida, K., Lu, X.Y., Cui, X.P., Jin, H.L., and Zhu, J.K. (2008b). The *Arabidopsis* NFYA5 transcription factor is regulated transcriptionally and posttranscriptionally to promote drought resistance. Plant Cell **20,** 2238-2251.

Lim, P.O., Kim, H.J., and Nam, H.G. (2007). Leaf senescence. Annu. Rev. Plant Biol. **58,** 115-136.

Ling, Q., and Jarvis, P. (2013). Dynamic regulation of endosymbiotic organelles by ubiquitination. Trends Cell Biol. **23,** 399-408.

Ling, Q.H., and Jarvis, P. (2015). Regulation of chloroplast protein import by the ubiquitin E3 ligase SP1 is important for stress tolerance in plants. Curr. Biol. **25,** 2527-2534.

Ling, Q.H., Li, N., and Jarvis, P. (2017). Chloroplast ubiquitin E3 ligase SP1: does it really function in peroxisomes? Plant Physiol. **175,** 586-588.

Ling, Q.H., Huang, W.H., Baldwin, A., and Jarvis, P. (2012). Chloroplast biogenesis is regulated by direct action of the ubiquitin-proteasome system. Science **338,** 655-659.

Livak, K.J., and Schmittgen, T.D. (2001). Analysis of relative gene expression data using real-time quantitative PCR and the $2^{-\Delta\Delta C_T}$ method. Methods **25,** 402-408.

Lobell, D.B., and Gourdji, S.M. (2012). The influence of climate change on global crop productivity. Plant Physiol. **160,** 1686-1697.

López Camelo, A.F., and Gómez, P.A. (2004). Comparison of color indexes for tomato ripening. Hortic. Bras. **22,** 534-537.

Lopez-Juez, E., and Pyke, K.A. (2005). Plastids unleashed: their development and their integration in plant development. Int. J. Dev. Biol. **49,** 557-577.

Lübeck, J., Soll, J., Akita, M., Nielsen, E., and Keegstra, K. (1996). Topology of IEP110, a component of the chloroplastic protein import machinery present in the inner envelope membrane. EMBO J. **15,** 4230-4238.

Martin, C., and Smith, A.M. (1995). Starch biosynthesis. Plant Cell **7,** 971-985.

Martin, W., and Herrmann, R.G. (1998). Gene transfer from organelles to the nucleus: how much, what happens, and why? Plant Physiol. **118,** 9-17.

Martin, W., Stoebe, B., Goremykin, V., Hansmann, S., Hasegawa, M., and Kowallik, K.V. (1998). Gene transfer to the nucleus and the evolution of chloroplasts. Nature **393,** 162-165.

Martin, W., Rujan, T., Richly, E., Hansen, A., Cornelsen, S., Lins, T., Leister, D., Stoebe, B., Hasegawa, M., and Penny, D. (2002). Evolutionary analysis of Arabidopsis, cyanobacterial, and chloroplast genomes reveals plastid phylogeny and thousands of cyanobacterial genes in the nucleus. Proc. Natl. Acad. Sci. U. S. A. **99,** 12246-12251.

Matile, P. (2000). Biochemistry of Indian summer: physiology of autumnal leaf coloration. Exp. Gerontol. **35,** 145-158.

Mcelroy, D., Zhang, W.G., Cao, J., and Wu, R. (1990). Isolation of an efficient actin promoter for use in rice transformation. Plant Cell **2,** 163-171.

Mitchell, J.P., Shennan, C., Grattan, S.R., and May, D.M. (1991). Tomato fruit yields and quality under water deficit and salinity. J. Am. Soc. Hortic. Sci. **116,** 215-221.

Mittova, V., Guy, M., Tal, M., and Volokita, M. (2002). Response of the cultivated tomato and its wild salt-tolerant relative Lycopersicon pennellii to salt-dependent oxidative

stress: Increased activities of antioxidant enzymes in root plastids. Free Radical Res **36,** 195-202.

Mujeeb-Kazi, A. (2006). Utilization of genetic resources for bread wheat improvement. CRC Crit. Rev. Plant Sci.**,** 61-97.

Muñoz, P., and Munné-Bosch, S. (2018). Photo-oxidative stress during leaf, flower and fruit development. Plant Physiol. **176,** 1004-1014.

Murata, N., Takahashi, S., Nishiyama, Y., and Allakhverdiev, S.I. (2007). Photoinhibition of photosystem II under environmental stress. Biochim. Biophys. Acta **1767,** 414-421.

Nagata, T., Todoriki, S., Masumizu, T., Suda, I., Furuta, S., Du, Z., and Kikuchi, S. (2003). Levels of active oxygen species are controlled by ascorbic acid and anthocyanin in *Arabidopsis*. J. Agric. Food Chem. **51,** 2992-2999.

Nakai, M. (2015). The TIC complex uncovered: the alternative view on the molecular mechanism of protein translocation across the inner envelope membrane of chloroplasts. Biochim. Biophys. Acta **1847,** 957-967.

Neuhaus, H.E., and Emes, M.J. (2000). Nonphotosynthetic metabolism in plastids. Annu. Rev. Plant Physiol. Plant Mol. Biol. **51,** 111-140.

Nott, A., Jung, H.-S., Koussevitzky, S., and Chory, J. (2006). Plastid-to-nucleus retrograde signaling. Annu. Rev. Plant Biol. **57,** 739-759.

Oh, Y.J., and Hwang, I. (2015). Targeting and biogenesis of transporters and channels in chloroplast envelope membranes: unsolved questions. Cell Calcium **58,** 122-130.

Ohdan, T., Francisco Jr, P.B., Sawada, T., Hirose, T., Terao, T., Satoh, H., and Nakamura, Y. (2005). Expression profiling of genes involved in starch synthesis in sink and source organs of rice. J. Exp. Bot. **56,** 3229-3244.

Okita, T.W. (1992). Is there an alternative pathway for starch synthesis? Plant Physiol. **100,** 560-564.

Okita, T.W., Nakata, P.A., Ball, K., Smith-White, B.J., and Preiss, J. (1993). Enhancement of plant productivity by manipulation of ADPglucose

pyrophosphorylase. In Gene Conservation and Exploitation, Gustafson J.P., Appels R., and R. P., eds (Boston, MA: Springer,), pp. 161-191.

Okuley, J., Lightner, J., Feldmann, K., Yadav, N., Lark, E., and Browse, J. (1994). Arabidopsis *FAD2* gene encodes the enzyme that is essential for polyunsaturated lipid synthesis. Plant Cell **6,** 147-158.

Ossowski, S., Schwab, R., and Weigel, D. (2008). Gene silencing in plants using artificial microRNAs and other small RNAs. Plant J. **53,** 674-690.

Osterlund, M.T., Hardtke, C.S., Wei, N., and Deng, X.W. (2000). Targeted destabilization of HY5 during light-regulated development of Arabidopsis. Nature **405,** 462-466.

Oyama, T., Shimura, Y., and Okada, K. (1997). The Arabidopsis *HY5* gene encodes a bZIP protein that regulates stimulus-induced development of root and hypocotyl. Genes Dev. **11,** 2983-2995.

Paila, Y.D., Richardson, L.G., and Schnell, D.J. (2015). New insights into the mechanism of chloroplast protein import and its integration with protein quality control, organelle biogenesis and development. J. Mol. Biol. **427,** 1038-1060.

Pan, R., Satkovich, J., and Hu, J. (2016). E3 ubiquitin ligase SP1 regulates peroxisome biogenesis in *Arabidopsis*. Proc. Natl. Acad. Sci. U.S.A. **113,** E7307-E7316.

Pandolfini, T. (2009). Seedless fruit production by hormonal regulation of fruit set. Nutrients **1,** 168-177.

Parry, C., Blonquist, J.M., and Bugbee, B. (2014). In situ measurement of leaf chlorophyll concentration: analysis of the optical/absolute relationship. Plant Cell Environ. **37,** 2508-2520.

Pathare, P.B., Opara, U.L., and Al-Said, F.A. (2013). Colour measurement and analysis in fresh and processed foods: A review. Food Bioproc. Tech. **6,** 36-60.

Pavan, S., van Heusden, A.W., and Bai, Y. (2009). *Solanum lycopersicum* (Tomato). In Encyclopedia of Life Sciences (ELS) (John Wiley & Sons, Ltd), pp. 1-4.

Pech, J.C., Bouzayen, M., and Latché, A. (2014). Cellular, metabolic and molecular aspects of chromoplast differentiation in ripening fruit. In Fruit ripening: Physiology,

signaling and genomics, P. Nath and M. Bouzayen, eds (UK: CAB International), pp. 28-47.

Peng, C.-L., Lin, Z.-F., Su, Y.-Z., Lin, G.-Z., Dou, H.-Y., and Zhao, C.-X. (2006). The antioxidative function of lutein: electron spin resonance studies and chemical detection. Funct. Plant Biol. **33,** 839-846.

Pesaresi, P., Mizzotti, C., Colombo, M., and Masiero, S. (2014). Genetic regulation and structural changes during tomato fruit development and ripening. Front. Plant Sci. **5,** 1-14.

Pogson, B.J., Woo, N.S., Förster, B., and Small, I.D. (2008). Plastid signalling to the nucleus and beyond. Trends Plant Sci. **13,** 602-609.

Preiss, J. (1982). Regulation of the biosynthesis and degradation of starch. Annu. Rev. Plant Physiol. **33,** 431-454.

Preiss, J. (1991). Biology and molecular biology of starch synthesis and its regulation. In Oxford surveys of plant molecular and cell biology, B.J. Miflin, ed (Oxford: Oxford University Press), pp. 59-114.

Qi, S.L., Lin, Q.F., Zhu, H.S., Gao, F.H., Zhang, W.H., and Hua, X.J. (2016). The RING finger E3 ligase SpRing is a positive regulator of salt stress signaling in salt-tolerant wild tomato species. Plant Cell Physiol. **57,** 528-539.

Race, H.L., Herrmann, R.G., and Martin, W. (1999). Why have organelles retained genomes? Trends Genet. **15,** 364-370.

Ren, Z.-H., Gao, J.-P., Li, L.-G., Cai, X.-L., Huang, W., Chao, D.-Y., Zhu, M.-Z., Wang, Z.-Y., Luan, S., and Lin, H.-X. (2005). A rice quantitative trait locus for salt tolerance encodes a sodium transporter. Nat. Genet. **37,** 1141-1146.

Rick, C.M., and Yoder, J.I. (1988). Classical and molecular genetics of tomato: highlights and perspectives. Annu. Rev. Genet. **22,** 281-300.

Risacher, T., Craze, M., Bowden, S., Paul*, W., and Barsby, T. (2009). Highly efficient *Agrobacterium*-mediated transformation of wheat via *in planta* inoculation. In

Transgenic Wheat, Barley and Oats: Production and Characterization Protocols, H.D. Jones and P.R. Shewry, eds (Totowa, NJ: Humana Press), pp. 115-124.

Rodriguez-Concepcion, M., Ahumada, I., Diez-Juez, E., Sauret-Gueto, S., Lois, L.M., Gallego, F., Carretero-Paulet, L., Campos, N., and Boronat, A. (2001). 1-Deoxy-D-xylulose 5-phosphate reductoisomerase and plastid isoprenoid biosynthesis during tomato fruit ripening. Plant J. **27,** 213-222.

Romani, I., Tadini, L., Rossi, F., Masiero, S., Pribil, M., Jahns, P., Kater, M., Leister, D., and Pesaresi, P. (2012). Versatile roles of *Arabidopsis* plastid ribosomal proteins in plant growth and development. Plant J. **72,** 922-934.

Rosso, S.W. (1968). The ultrastructure of chromoplast development in red tomatoes. J. Ultrastruct. Res. **25,** 307-322.

Saibo, N.J.M., Lourenco, T., and Oliveira, M.M. (2009). Transcription factors and regulation of photosynthetic and related metabolism under environmental stresses. Ann. Bot. **103,** 609-623.

Sakamoto, W., Miyagishima, S.-y., and Jarvis, P. (2008). Chloroplast biogenesis: control of plastid development, protein import, division and inheritance. The Arabidopsis Book **6,** 1-30.

Sato, S., Nakamura, Y., Kaneko, T., Asamizu, E., and Tabata, S. (1999). Complete structure of the chloroplast genome of *Arabidopsis thaliana*. DNA Res. **6,** 283-290.

Schelbert, S., Aubry, S., Burla, B., Agne, B., Kessler, F., Krupinska, K., and Hortensteiner, S. (2009). Pheophytin pheophorbide hydrolase (Pheophytinase) is involved in chlorophyll breakdown during leaf senescence in *Arabidopsis*. Plant Cell **21,** 767-785.

Schmittgen, T.D., and Livak, K.J. (2008). Analyzing real-time PCR data by the comparative C_T method. Nat. Protoc. **3,** 1101-1108.

Schnell, D.J., Kessler, F., and Blobel, G. (1994). Isolation of components of the chloroplast protein import machinery. Science **266,** 1007-1012.

Schunmann, P.H.D., Surin, B., and Waterhouse, P.M. (2003). A suite of novel promoters and terminators for plant biotechnology. II. The pPLEX series for use in monocots. Funct. Plant Biol. **30,** 453-460.

Schwab, R., Ossowski, S., Riester, M., Warthmann, N., and Weigel, D. (2006). Highly specific gene silencing by artificial microRNAs in Arabidopsis. Plant Cell **18,** 1121-1133.

Seedorf, M., Waegemann, K., and Soll, J. (1995). A constituent of the chloroplast import complex represents a new type of GTP-binding protein. Plant J. **7,** 401-411.

Shanker, A.K., and Venkateswarlu, B. (2011). Abiotic Stress Response in Plants - Physiological, Biochemical and Genetic Perspectives (Croatia: In Tech).

Shannon, J.C., Garwood, D.L., and Boyer, C.D. (2009). Genetics and physiology of starch development. In Starch (Third Edition), B. James and W. Roy, eds (USA: Academic Press), pp. 23-82.

Shapiguzov, A., Vainonen, J., Wrzaczek, M., and Kangasjärvi, J. (2012). ROS-talk–how the apoplast, the chloroplast, and the nucleus get the message through. Front. Plant Sci. **3,** 1-9.

Shewry, P.R., and Hey, S.J. (2015). The contribution of wheat to human diet and health. Food Energy Secur. **4,** 178-202.

Shiferaw, B., Smale, M., Braun, H.-J., Duveiller, E., Reynolds, M., and Muricho, G. (2013). Crops that feed the world 10. Past successes and future challenges to the role played by wheat in global food security. Food Sec. **5,** 291-317.

Shipman-Roston, R.L., Ruppel, N.J., Damoc, C., Phinney, B.S., and Inoue, K. (2010). The significance of protein maturation by plastidic type I signal peptidase 1 for thylakoid development in *Arabidopsis* chloroplasts. Plant Physiol. **152,** 1297-1308.

Simkin, A.J., Gaffé, J., Alcaraz, J.-P., Carde, J.-P., Bramley, P.M., Fraser, P.D., and Kuntz, M. (2007). Fibrillin influence on plastid ultrastructure and pigment content in tomato fruit. Phytochemistry **68,** 1545-1556.

Smith, M.D., Hiltbrunner, A., Kessler, F., and Schnell, D.J. (2002). The targeting of the atToc159 preprotein receptor to the chloroplast outer membrane is mediated by its GTPase domain and is regulated by GTP. J. Cell Bio. **159,** 833-843.

Smith, M.D., Rounds, C.M., Wang, F., Chen, K., Afitlhile, M., and Schnell, D.J. (2004). atToc159 is a selective transit peptide receptor for the import of nucleus-encoded chloroplast proteins. J. Cell Bio. **165,** 323-334.

Sohrt, K., and Soll, J. (2000). Toc64, a new component of the protein translocon of chloroplasts. J. Cell Biol. **148,** 1213-1222.

Sowden, R.G., Watson, S.J., and Jarvis, P. (2018). The role of chloroplasts in plant pathology. Essays Biochem. **62,** 21-39.

Spano, G., Di Fonzo, N., Perrotta, C., Platani, C., Ronga, G., Lawlor, D.W., Napier, J.A., and Shewry, P.R. (2003). Physiological characterization of 'stay green' mutants in durum wheat. J. Exp. Bot. **54,** 1415-1420.

Sperling, U., Franck, F., van Cleve, B., Frick, G., Apel, K., and Armstrong, G.A. (1998). Etioplast differentiation in *Arabidopsis*: both PORA and PORB restore the prolamellar body and photoactive protochlorophyllide–F655 to the *cop1* photomorphogenic mutant. Plant Cell **10,** 283-296.

Spurr, A.R., and Harris, W.M. (1968). Ultrastructure of chloroplasts and chromoplasts in *Capsicum annuum*. I. Thylakoid membrane changes during fruit ripening. Am. J. Bot. **55,** 1210-1224.

Stitt, M., Lunn, J., and Usadel, B. (2010). *Arabidopsis* and primary photosynthetic metabolism–more than the icing on the cake. Plant J. **61,** 1067-1091.

Subramanyam, R., Jolley, C., Thangaraj, B., Nellaepalli, S., Webber, A.N., and Fromme, P. (2010). Structural and functional changes of PSI-LHCI supercomplexes of *Chlamydomonas reinhardtii* cells grown under high salt conditions. Planta **231,** 913-922.

Sun, H.-J., Uchii, S., Watanabe, S., and Ezura, H. (2006). A highly efficient transformation protocol for Micro-Tom, a model cultivar for tomato functional genomics. Plant Cell Physiol. **47,** 426-431.

Sun, Y.-J., Forouhar, F., Li, H.-m., Tu, S.-L., Yeh, Y.-H., Kao, S., Shr, H.-L., Chou, C.-C., Chen, C., and Hsiao, C.-D. (2002). Crystal structure of pea Toc34, a novel GTPase of the chloroplast protein translocon. Nat. Struct. Mol. Biol. **9,** 95-100.

Sunkar, R., Chinnusamy, V., Zhu, J., and Zhu, J.-K. (2007). Small RNAs as big players in plant abiotic stress responses and nutrient deprivation. Trends Plant Sci. **12,** 301-309.

Suzuki, M., Takahashi, S., Kondo, T., Dohra, H., Ito, Y., Kiriiwa, Y., Hayashi, M., Kamiya, S., Kato, M., and Fujiwara, M. (2015). Plastid proteomic analysis in tomato fruit development. PLoS One **10,** 1-25.

Suzuki, N., Koussevitzky, S., Mittler, R., and Miller, G. (2012). ROS and redox signalling in the response of plants to abiotic stress. Plant Cell Environ. **35,** 259-270.

Taylor, N.L., Tan, Y.-F., Jacoby, R.P., and Millar, A.H. (2009). Abiotic environmental stress induced changes in the *Arabidopsis thaliana* chloroplast, mitochondria and peroxisome proteomes. J. Proteomics **72,** 367-378.

Theg, S.M., Bauerle, C., Olsen, L., Selman, B., and Keegstra, K. (1989). Internal ATP is the only energy requirement for the translocation of precursor proteins across chloroplastic membranes. J. Biol. Chem. **264,** 6730-6736.

Thomas, H., and Smart, C.M. (1993). Crops that stay green. Ann. Appl. Biol. **123,** 193-219.

Thomas, H., and Ougham, H. (2014). The stay-green trait. J. Exp. Bot. **65,** 3889-3900.

Thordal-Christensen, H., Zhang, Z.G., Wei, Y.D., and Collinge, D.B. (1997). Subcellular localization of H_2O_2 in plants. H_2O_2 accumulation in papillae and hypersensitive response during the barley-powdery mildew interaction. Plant J. **11,** 1187-1194.

Tian, F.X., Gong, J.F., Wang, G.P., Wang, G.K., Fan, Z.Y., and Wang, W. (2012). Improved drought resistance in a wheat stay-green mutant *tasg1* under field conditions. Biol. Plant. **56,** 509-515.

Tiller, N., and Bock, R. (2014). The translational apparatus of plastids and its role in plant development. Mol. Plant. **7,** 1105-1120.

Tomato Genome, C. (2012). The tomato genome sequence provides insights into fleshy fruit evolution. Nature **485,** 635-641.

Torres, M.A. (2010). ROS in biotic interactions. Physiol. Plant. **138,** 414-429.

Tranel, P., Froehlich, J., Goyal, A., and Keegstra, K. (1995). A component of the chloroplastic protein import apparatus is targeted to the outer envelope membrane via a novel pathway. EMBO J. **14,** 2436-2446.

Travella, S., Klimm, T.E., and Keller, B. (2006). RNA interference-based gene silencing as an efficient tool for functional genomics in hexaploid bread wheat. Plant Physiol. **142,** 6-20.

Tu, S.-L., Chen, L.-J., Smith, M.D., Su, Y.-s., Schnell, D.J., and Li, H.-m. (2004). Import pathways of chloroplast interior proteins and the outer-membrane protein OEP14 converge atToc75. Plant Cell **16,** 2078-2088.

Umezawa, T., Fujita, M., Fujita, Y., Yamaguchi-Shinozaki, K., and Shinozaki, K. (2006). Engineering drought tolerance in plants: discovering and tailoring genes to unlock the future. Curr. Opin. Biotechnol. **17,** 113-122.

Valenciano, J.D.P., and Battistuzzi, M.Á.G. (2012). Analytical model for the global consumption of tomatoes-The Spanish case. African Journal of Agricultural Research **7,** 2328-2335.

Vickers, C.E., Gershenzon, J., Lerdau, M.T., and Loreto, F. (2009). A unified mechanism of action for volatile isoprenoids in plant abiotic stress. Nat. Chem. Biol. **5,** 283-291.

Vierstra, R.D. (2009). The ubiquitin-26S proteasome system at the nexus of plant biology. Nat. Rev. Mol. Cell Biol. **10,** 385-397.

Wallas, T.R., Smith, M.D., Sanchez-Nieto, S., and Schnell, D.J. (2003). The roles of toc34 and toc75 in targeting the toc159 preprotein receptor to chloroplasts. J. Biol. Chem. **278,** 44289-44297.

Wang, Y.Q., Yang, Y., Fei, Z., Yuan, H., Fish, T., Thannhauser, T.W., Mazourek, M., Kochian, L.V., Wang, X., and Li, L. (2013). Proteomic analysis of chromoplasts from six crop species reveals insights into chromoplast function and development. J. Exp. Bot. **64,** 949-961.

Wise, R.R. (2007). The diversity of plastid form and function. In The structure and function of plastids. Advances in photosynthesis and respiration, Wise R.R. and H. J.K., eds (Springer, Dordrecht), pp. 3-26.

Woodson, J.D., Joens, M.S., Sinson, A.B., Gilkerson, J., Salomé, P.A., Weigel, D., Fitzpatrick, J.A., and Chory, J. (2015). Ubiquitin facilitates a quality-control pathway that removes damaged chloroplasts. Science **350,** 450-454.

Wrzaczek, M., Brosché, M., and Kangasjärvi, J. (2013). ROS signaling loops—production, perception, regulation. Curr. Opin. Plant Biol. **16,** 575-582.

Wu, C., Seibert, F.S., and Ko, K. (1994). Identification of chloroplast envelope proteins in close physical proximity to a partially translocated chimeric precursor protein. J. Biol. Chem. **269,** 32264-32271.

Yan, J., Campbell, J.H., Glick, B.R., Smith, M.D., and Liang, Y. (2014). Molecular characterization and expression analysis of chloroplast protein import components in tomato (*Solanum lycopersicum*). PLoS ONE **9,** e95088 (95081-95011).

Yoon, H.S., Hackett, J.D., Ciniglia, C., Pinto, G., and Bhattacharya, D. (2004). A molecular timeline for the origin of photosynthetic eukaryotes. Mol. Biol. Evol. **21,** 809-818.

Zelman, A. (2015). Tomato seedlings in aseptic culture for experiments in liquid media (unpublished work).

Zhang, X., Zou, Z., Gong, P., Zhang, J., Ziaf, K., Li, H., Xiao, F., and Ye, Z. (2011). Over-expression of microRNA169 confers enhanced drought tolerance to tomato. Biotechnol. Lett. **33,** 403-409.

Zhang, Y.Y., Yang, C.W., Li, Y., Zheng, N.Y., Chen, H., Zhao, Q.Z., Gao, T., Guo, H.S., and Xie, Q. (2007). SDIR1 is a RING finger E3 ligase that positively regulates stress-responsive abscisic acid signaling in *Arabidopsis*. Plant Cell **19,** 1912-1929.

Zhao, B., Liang, R., Ge, L., Li, W., Xiao, H., Lin, H., Ruan, K., and Jin, Y. (2007). Identification of drought-induced microRNAs in rice. Biochem. Biophys. Res. Commun. **354,** 585-590.

Zimorski, V., Ku, C., Martin, W.F., and Gould, S.B. (2014). Endosymbiotic theory for organelle origins. Curr. Opin. Microbiol. **22,** 38-48.

Appendix

Appendix 1: Full amino acid sequences of SP1 putative orthologues used for phylogenetic tree.

No.	Species	Amino acid sequences
1	*Arabidopsis thaliana*	MIPWGGVTCCLSAAALYLLGRSSGRDAEVLETVTRVNQLKELAQLLELDSKILPFIVAVSGRVGSETPIKC EHSGIRGVIVEETAEQHFLKHNETGSWVQDSALMLSMSKEVPWFLDDGTSRVHVMGARGATGFALTVG SEVFEESGRSLVRGTLDYLQGLKMLGVKRIERVLPTGIPLTIVGEAVKDDIGEFRIQKPDRGPFYVSSKSL DQLISNLGKWSRLYKYASMGFTVLGVFLITKHVIDSVLERRRRRQLQKRVLDAAAKRAELESEGSNGTRE SISDSTKKEDAVPDLCVICLEQEYNAVFVPCGHMCCCTACSSHLTSCPLCRRRIDLAVKTYRH
2	*Glycine max*	MIPWGGLSCCLSAAALYLLGRSSGRDAEILKSVTRVNQLKELAQLLDAEILPLIVTISGRVSSETPINCEFS GLRGVIVEETAEQHFLKHNDAGSWIQDSALMLSMSKEVPWYLDDGTDRVHVVGARGAAGFALPVGSEA FEESGRSLVRGTLDYLQGLKMLGVKRIERVLPVGTSLTVVGEAAKDDVGAFRIQRPHKGPFYVSPKTIDQ LIANLGKWARWYKYASMGLTVFGAYLIAKHAIRYILERRRRSELQRRVLAAAAKKSGQNNDVEKADGLSD GVKKDRLMPDLCVICLEQEYNAVFVPCGHMCCCTTCSSHLTNCPLCRRQIEKVVKTFRH
3	*Solanum tuberosum*	MVPWGGLSCCLSAAALYLLGRSSGRDAEVLKSVTRVNQLKDLAQLLDTASKVLPLVVTISGRVGSDTPIN CEYSGLRGVIVEETAEQHFLKHNDAGSWIQDSALMLSMCKEVPWYLDDDTGRTFVVGGRGATGLVLTV GSEIFEEAGRSFVRGTLDYLQGLKMLGVKRIERVLPVGTPLTVVGEAVKDDIGTVRIQRPHKGPFYISHKTI DQLIANLGRWARWYKYASMGFTAVGVYLLVKHTFHYMMERKRHWELRRRVLAAAAKRAGHEDEGSNA TAENGVDNKKDLLMPNLCVICLEQEYNSVFVPCGHMCCCMTCSSHLTNCPLCRRRIEQVVKTFRH
4	*Solanum lycopersicum*	MATKKKKKKNEEEEEEEVDGWIIELLKERFRFYYPFELPEMVPWAGLSCCLSAAALYLLGRSSGRDAEVL KSVTRVNQLKDLAQLLDTASKVLPLVVTISGRVGSDTPINCEYSGLRGVIVEETAEQHFLKHNDAGSWIQD SALMLSMCKEVPWYLDDGTGRTFIVGGRGATGLVLTVGSEAFEEAGRSFVRGTLDYLQGLKMLGVKRIE RVLPVGTPLTVVGEAVKDDIGTVRIQRPHKGPFYISHKTIDQLIANLGRWARWYKYASMGFTAVGVYLLV KHTFHYMMERKRHWELRRRVLAAAAKRAGDEDEGSDATAENGVDNKDLLMPDLCVICLEQEYNSVFVP CGHMCCCMTCSSHLTNCPLCRRRIEQVVKTFRH
5	*Manihot esculenta*	MLPWGGISCCLSAAALYLLGRSSGRDAEVLKSVTRVNQLKELAKLLDIESNISPSVVSISGRVGSETPINC EYSGLRGVIVEETAEQHFLKHNDAGSWIQDSALMLSMSKEVPWYLDDGTDRVYVVGARGASGFVLTVG SEVFEESGRSLVRGTLDYLQGLKMLGVKRIERVLPTGTSLTVVGEAVKDDIGTVRVQRPHKGPFYVSPRT IDELIGNLGKWARWYRYASVSLTVFGAFLIAKHAIQYIMERRRRWELQSRVLAAAAAKRQGQDSEGSNG KAENGSDNSKRERPVPDLCVICLEQEYNAVFLPCGHMCCCTTCSSHLTNCPLCRRRIEQVVKTFRH

6	*Musa acuminata*	MIPWGGLGCCASAAALYLLGRNSGRDANVLRSVTRVNQLKDLAVLLDTACKVLPLVVTVTGRVGSETPIN CEQSGLRGVIVEETAEQHFLKHNDAGSWIQDSALMLSMSKEVPWYLDDGSGRVYVVGARGATGLVLTV ASEVFEDSGRSLVRGTLDYLQGLKMLGVKRTERILPTGTALTIVGEAVKDDVGKIRIQRPHKGPFYVSPKN IDQLIVNLGKWARWYQFASMGFTVFGVFLLAKHALQYILERRRRRELQKRVLSAAAARQARDAEGSNQE SEKLSDNMKKDHLMLDICVICLEQEYNAVFVPCGHMCCCTTCSSHLTSCPLCRKRIDQVVKTFRH
7	*Oryza sativa*	MLIPWGGVGCCLSAAALYLLGRSSGRDAEVLRSVARAGSTKDLAAILDTASKVLPLVVAVSGRVGSDTPL ICQQSGMRGVIVEETAEQHFLKHNDAGSWIQDSAVMLSVSKEVPWYLDDGTGRVFVVGARGAAGLVLT VASEVFEESGRTLVRGTLDYLQGLKMLGVKRTERVLPTGTSLTVVGEAIKDDVGTIRIQRPHKGPFYVSP KSIDQLIMNLGKWAKLYQLASMGFAAFGVFLLAKRALQHFLERKRRHELQKRVHAAAAQRQAREAEGGN GTSDVDSNNKKDQLVLDICVICLEQEYNAVFVPCGHMCCCMNCSSHLTNCPLCRRRIDQAVRTFRH
8	*Zea mays*	MMIPWGGVGCCLSAAALYLLGRSSGRDAEVLRSVARAGSMKDLAAILDTASKVLPLVVAVSGRVGSDTP LICQQSGMRGVIVEETAEQHFLKHNDAGSWIQDSAVMLSVSKEVPWYLDDGTGRVYMVGARSAAGLILT VASEVFEESGRTLVRGTLDYLQGLKMLGVKRTERVLPTGISLTVVGEAIKDDVGTIRIQRPHKGPFYVSPK SIDQLIMNLGKWAKLYRLASMGFATFGAFLLAKRAIQHFLERKRRHELQKRVLNAAAQRQAREAEGSIGS SDTEPNSKKDQLVLDICVICLEQEYNAVFVPCGHMCCCMACSSHLTNCPLCRRRIDQAVRTFRH
9	*Sorghum bicolor*	MMIPWGGVGCCLSAAALYLLGRSSGRDAEVLRSVARAGSMKDLAAILDTASKVLPLVVAVSGRVSSDTP LICQQSGMRGVIVEETAEQHFLKHNDAGSWIQDSAVMLSVSKEVPWYLDDGTGRVYVVGARSAAGLILT VASEVFEESGRTLVRGTLDYLQGLKMLGVKRTERVLPTGTSLTVVGEAIRDDVGTIRIQRPHKGPFYVSP KSIDQLIMNLGKWAKLYRLASMGFATFGVFLLAKRAIQHFLERKRRHELQKRVLNAAAQRQAREAEGSN GSSDTEPNSKKDQLVLDICVICLEQEYNAVFVPCGHMCCCMACSSHLTNCPLCRRRIDQAVRTFRH
10	*Triticum aestivum A*	MLVPWGGVGCCLSAAALYLLGRSSGRDAEVLRSVARTGSLKDLAAILDTASKVLPLVVAVSGRVSSDTPL ICQQSGMRGVIVEETAEQHFLKHNDAGSWIQDSAVMLSVSKEVPWYLDDGTGRVYIVGARSAAGLILTV ASEVFEESGRTLVRGTLDYLQGLKMLGVKRTERVLPTGTSLTVVGEAIKDDVGTIRIQRPHKGPFYASPK SIDQLILNLGKWAKLYQLASMGFAAFGVFLLAKRALDHFLQRKRQREFHKKARAAAAQRQARDAEGGNG TSDGEPKKDQLVLEICVICLEQEYNAVFVPCGHMCCCMNCSSHVTNCPLCRRRIDQAVRTFRH
	Triticum aestivum B	MLVPWGGFGCCLSAAALYLLGRSSGRDAEVLRSVARTGSLKDLAAILDTASKVLPLVVAVSGRVSSDTPL ICQQSGMRGVIVEETAEQHFLKHNDAGSWIQDSAVMLSVSKEVPWYLDDGTGRVYVVGARSAAGLILTV ASEVFEESGRTLVRGTLDYLQGLKMLGVKRTERVLPTGTSLTVVGEAIKDDVGTIRIQRPHKGPFYASPK SIDQLILNLGKWAKLYQLASMGFAAFGVFLLAKRALDHFLQRKRQREFHKKARAAAAQRQARDAEGGNG TSDGEPKKDQLVLEICVICLEQEYNAVFVPCGHMCCCMNCSSHVTNCPLCRRRIDQAVRTFRH
	Triticum aestivum D	MLVPWGGVGCCLSAAALYLLGRSSGRDAEVLRSVARTGSLKDLAAILDTASKVLPLVVAVSGRVSSDTPL ICQQSGMRGVIVEETAEQHFLKHNDAGSWIQDSAVMLSVSKEVPWYLDDGTGRVYVVGARSAAGLILTV ASEVFEESGRTLVRGTLDYLQGLKMLGVKRTERVLPTGTSLTVVGEAIKDDVGTIRIQRPHKGPFYASPK SIDQLILNLGKWAKLYQLASMGFAAFGVFLLAKRALDHFLQRKRQREFHKKARAAAAQRQARDAEGGNG TSDGEPKKDQLVLEICVICLEQEYNAVFVPCGHMCCCMNCSSHVTNCPLCRRRIDQAVRTFRH

11	*Marchantia polymorpha*	MLSWGGLTLCLSGAALYCLSSNSGRDAATLRNVKRVNQLRDLAILLESACKALPVVVTVAGRVGSETPIS CEHSSLRGVILEETAEQHFLKHNDTGSWIQDSALMLSISKEVPWYLEDGSGRVYVVGARGATGMELTVA SEVFEESGRSLVRGTLDYLQGLKMLGVKRVERVLPTGTALTVVGEAVQDDRGILRIQRPHKGPFYVSPK SIDQLIANLGKWSRWYKYLSLGFTAFGIYLLTSHAVKHFLEKRRRAALQRRVMEAAAQRLERRTDMEDN REGTTDKCDIDTTVKKDGTLPDLCVICFEHEYNAVFVPCGHMCCCTSCSSQLVYCPLCRSRINQVVKAYR H
12	*Sphagnum fallax*	MLSWSGITLCLSGAALYCLSRNTGRDALTLKSVQRVNQLQDLALLLQSACKVLPVIVTVAGRVGSDTPITC EHSSLRGVILEETAEQHFLKHNDTGSWIQDSALMLSVSKEVPWYLEDGTGRIYVVGARNATGMELTVAS EVFEESGRSLVRGTLDYLQGLKMLGVKRVERVLPTGTALTVVGEAVQDDRGLIRIQKPHKGPFYVTPKS MEQLIMNLGKWSRWYKYLSIGVTLFGLCLIASRAAKYVMEKRRRAALHRRVMEAAAQRLCRTGSDGERP EALNEQDNKDAISIKEGHAPNLCVICLEQDYNAVFVPCGHMCCCISCSAQLTTCPLCRHHIDQLVRTYRH
13	*Physcomitrella patens*	MLSWGGITLCLSGAALYCLSRNTGRDALNLRSIERVNQLKDLAILLESACKVVPLVVTVAGRVGSETPIAC EHSSLRGVILEETAEQHFLKHNDTGSWIQDSALMLSISKEVPWYLEDGTGRVYIVGARNAAGMELTVASE VFEESGRSLVRGTLDYLQGLKMLGVKRVERVLPTGTNLTVVGEAVQDDRGLIRIQKPNKGPFYVTPKSLD QLVANLGRWSRWYKYMSLGFTIVGIYFITSHAIKHFMERRRREALHRRVMEAAALRQASQREGGDGDM GDVTSHPLDDSVDTSQKKDRGTPDLCVICLEQDYNAVFLPCGHMCCCTSCSAQLTSCPLCRRHIDKFVK TYRH
14	*Homo sapiens*	MESGGRPSLCQFILLGTTSVVTAALYSVYRQKARVSQELKGAKKVHLGEDLKSILSEAPGKCVPYAVIEG AVRSVKETLNSQFVENCKGVIQRLTLQEHKMVWNRTTHLWNDCSKIIHQRTNTVPFDLVPHEDGVDVAV RVLKPLDSVDLGLETVYEKFHPSIQSFTDVIGHYISGERPKGIQETEEMLKVGATLTGVGELVLDNNSVRL QPPKQGMQYYLSSQDFDSLLQRQESSVRLWKVLALVFGFATCATLFFILRKQYLQRQERLRLKQMQEEF QEHEAQLLSRAKPEDRESLKSACVVCLSSFKSCVFLECGHVCSCTECYRALPEPKKCPICRQAITRVIPLY NS

Appendix 2: Full amino acid sequences of SPL2.

No.	Species	Amino acid sequences
1	*Arabidopsis thaliana*	MSSPERALLNLLTDIALSFDGAILGLTLAVSAVGSALKYASTNAALKKIKDAPEVSISDLRSLLPASEDKSET NDNRKSNDQRIVVVRGVVKPKISGDEGYKNNNVLISPETGDKALIIQRTQTYVYSGWKRLFQSTGHRFML ERSLRKHGADFTRTVPFVIVGKDQQSNSSFVAVNMDGSRQPLPLTTVYNRLQPINSSFLQAFLYPDYPV GLLDIEKILPPGKDITAVGIYSFNNGVPEIKSCQDLPYFLSEMTKDKMIEDLMEQTNFIFLGSVILGIVSVGIL SYAAVRTWNKWKQWNHQRELPQRPNDSVVDDEPEDADEIPDGELCVICVSRRRVPAFIPCGHVVCCRR CASTVERELNPKCPVCLQSIRGSMRVYYS
2	*Solanum lycopersicum*	MSIYDQAAAAVLSQIATAADGALIGLALAYVAVRSIVKFKANSSALHKINDAPSLNVSDLRSLLSSSDNSDS SNHSDDGKLVIVRGTVEAKSAVEGNWKSLRANILSAHNSAEKGVILQHTQTCIYNEWRGFFSWAGDLYSI FPRVRKDQQSSSLRTVPFVLIETGRWPQPKYVNVNMDGSTHSLPLVTVYHHLQPLHATPLTFIQALFGHH YPVGVLDEEKILPLGKDITAIGVCSSKDGILEIKSCEDLPYFLSDMTKDQMLVELAFKTKILMWSGVLFGSV AVGVLGYAVVRNWNRWKLWRHQRQAQQQRDAASNDDDVQVSADEESGDVPDGQLCVICLTRRKRAA FVPCGHLVCCQRCALSVERDLAPKCPLCRQTIHSSVRIYDS

Appendix 3: The coding sequences of solSP1, solSPL2, and taSP1.

No.	Species	Gene	Coding sequences (5’ to 3’)
1	*Solanum lycopersicum*	*solSP1*	ATGGCTACAAAAAAAAAAAAAAAAAAAACGAAGAAGAAGAAGAAGAAGAAGTGGATGGAT GGATTATAGAGTTGTTGAAGGAGAGGTTTAGGTTCTATTATCCCTTCGAGCTACCGGAAATG GTTCCATGGGCCGGACTCTCTTGCTGTTTGAGTGCAGCTGCTCTTTACCTTCTCGGTAGGA GCAGTGGAAGAGATGCTGAAGTTCTTAAATCCGTTACAAGGGTTAATCAATTGAAGGATCTT GCACAACTACTAGATACTGCATCCAAGGTGTTGCCTCTGGTGGTTACTATATCTGGAAGGG TTGGATCAGATACACCAATTAACTGTGAGTACAGTGGTCTACGAGGCGTGATTGTGGAAGA AACTGCCGAACAACATTTTCTGAAACACAATGATGCAGGTTCTTGGATACAGGATTCTGCCT TGATGCTCTCAATGTGTAAAGAAGTTCCGTGGTACCTGGATGATGGCACAGGTCGCACTTT TATTGTTGGTGGCCGTGGTGCCACGGGTTTGGTACTGACAGTTGGAAGTGAAGCCTTCGAG GAAGCAGGGAGATCATTTGTGCGAGGGACATTGGATTATCTTCAAGGTCTTAAGATGCTTG GAGTAAAGAGGATTGAACGTGTGCTGCCAGTTGGTACTCCTTTGACTGTTGTTGGCGAGGC TGTCAAAGATGACATTGGGACAGTTCGGATCCAGCGACCACACAAAGGCCCATTTTATATCT CTCATAAAACTATTGACCAGCTCATTGCAAATCTTGGGAGATGGGCAAGGTGGTACAAGTAT GCTTCAATGGGTTTTACTGCTGTCGGTGTATATCTACTTGTGAAGCATACTTTTCATTATATG ATGGAAAGAAAGCGTCACTGGGAATTGCGCAGGAGAGTTCTTGCTGCTGCTGCTAAAAGAG CAGGAGATGAGGATGAAGGTTCTGATGCTACAGCTGAGAATGGAGTGGATAATAAGGACCT CTTAATGCCAGATCTATGTGTTATATGTCTGGAGCAGGAATACAACTCAGTTTTTGTCCCGT GTGGTCATATGTGCTGTTGCATGACGTGCTCTTCACACTTGACAAACTGCCCACTATGTAGG AGACGGATCGAGCAGGTTGTGAAAACTTTTCGCCATTGA
2	*Solanum lycopersicum*	*solSPL2*	ATGTCAATATACGATCAAGCGGCAGCTGCCGTGCTATCGCAAATAGCTACGGCGGCGGAT GGCGCACTTATTGGCTTAGCCCTAGCTTACGTTGCCGTACGGAGTATTGTCAAGTTCAAAG CCAATTCTTCCGCCCTTCACAAAATCAACGATGCGCCGTCGCTTAATGTCTCCGATCTCCGT TCATTACTTTCTTCTTCCGACAACTCTGATAGTTCAAATCATTCCGATGACGGTAAGCTTGTG ATTGTTCGCGGTACTGTGGAGGCGAAATCGGCGGTTGAGGGTAACTGGAAAAGCTTGAGA GCTAATATTCTCTCAGCTCATAATTCTGCTGAAAAAGGCGTTATATTGCAACATACTCAAACA TGTATCTATAATGAGTGGAGAGGCTTCTTTTCGTGGGCTGGTGATCTGTATTCAATATTTCC AAGAGTCCGGAAGGATCAACAATCGTCCTCTTTGAGAACGGTTCCCTTTGTTCTTATTGAAA CTGGGAGGTGGCCGCAACCAAAATATGTTAATGTCAATATGGATGGTTCTACGCATTCCCTA CCTCTTGTGACAGTTTATCATCACTTGCAACCTTTACATGCTACGCCTCTCACTTTTATCCAG

			GCTCTCTTTGGTCATCACTATCCTGTTGGAGTATTGGATGAAGAAAAAATTCTACCACTTGG TAAAGATATAACCGCTATTGGTGTTTGCAGCTCAAAAGATGGGATTTTGGAGATCAAATCAT GTGAAGACCTACCCTATTTCTTGTCTGATATGACCAAGGATCAAATGCTGGTAGAGCTTGCC TTCAAAACAAAAATTCTGATGTGGAGTGGAGTTTTATTTGGTTCAGTTGCAGTTGGTGTCCTT GGATATGCTGTTGTGAGGAACTGGAATCGATGGAAGCTGTGGAGACACCAGAGGCAGGCT CAGCAACAAAGGGATGCTGCAAGCAATGACGATGATGTGCAGGTTAGTGCTGATGAGGAAT CTGGAGATGTTCCCGATGGTCAGTTGTGTGTGATATGCCTTACGAGGAGGAAGCGCGCAG CATTTGTTCCGTGTGGACACCTGGTATGTTGCCAGCGCTGTGCCTTGTCAGTTGAACGTGA TTTAGCACCCAAGTGTCCTTTATGTAGGCAGACAATTCATAGTTCTGTAAGGATATATGATTC TTGA
3	*Triticum aestivum A*	*taSP1 A*	ATGTTGGTCCCGTGGGGAGGGGTCGGGTGCTGCCTCAGCGCCGCGGCGCTGTATCTCCT CGGGAGGAGCAGCGTCAGGGACGCGGAGGTGCTGCGATCGGTGGCGAGGACCGGCAGC CTGAAGGATTCAGCTGCTATCTTGGACACTGCAAGTAAAGTCCTGCCACTTGTAGTGGCGG TTTCTGGGCGAGTTAGTTCAGATACACCACTTATATGCCAACAAAGTGGTATGAGAGGTGTA ATGTCGAGGAAACGGCAGAGCAACACTTCCTGAAGCACAATGATGCTGGATCCTGGATTCA AGATTCTGCTGTGATGCTTTCTGTTAGCAAAGAGGTTCCATGGTACCTGGATGATGGCACT GGGCGTGTCTATATTGTTGGCGCTCGTTCTGCGGCAGGGTTAATTTTAACTGTTGCCAGTG AGGTTTTTGAGGAGTCAGGGCGGACTCTTGTACGTGGAACTCTGGATTATTTACAAGGACT GAAGATGCTCGGAGTAAAGCGAACTGAAAGGGTTCTTCCAACTGGAACTTCATTGACTGTT GTTGGTGAGGCCATTAAAGATGATGTTGGAACTATTCGGATTCAGCGGCCACACAAAGGAC CATTTTATGCATCTCCAAAAAGCATCGATCAACTTATCTTGAATCTCGGGAAATGGGCCAGG TTATACCAACTTGCTTCCATGGGCTTTGCAGCTTTTGGTGTATTTCTTCTTGCTAAGCGTGCA CTTGATCATTTTCTACAAAGAAAGCGCCAGCGTGAATTTCACAAGAAGGCTCGTGCTGCTG CAGCACAAAGGCAGGCTAGGGACGCTGAAGGAGGCAATGGCACATCAGACGGAGAGCCT AAGAAGGATCAATTGGTATTAGAAATATGTGTCATATGCCTTGAACAGGAGTATAATGCAGT TTTTGTGCCGTGTGGCCACATGTGTTGCTGTATGAACTGCTCTTCTCACGTAACAAACTGTC CACTCTGCCGACGAAGAATAGACCAAGCTGTCAGAACATTCCGTCACTGA
	Triticum aestivum B	*taSP1 B*	ATGTTGGTCCCGTGGGGCGGGTTCGGGTGCTGCCTCAGCGCCGCGGCGCTCTATCTCCTC GGGAGGAGCAGCGTCAGGGACGCGGAGGTGCTGCGATCAGTGGCGAGGACAGGCAGCC TGAAGGATTCAGCTGCTATCTTGGACACTGCAAGTAAAGTCCTGCCACTTGTAGTGGCAGT TTCTGGGCGAGTTAGTTCAGATACACCACTTATATGCCAGCAAAGTGGTATGAGAGGTGTA ATAGTCGAGGAAACGGCAGAGCAACACTTCCTGAAGCACAATGATGCTGGATCCTGGATTC AAGATTCTGCTGTGATGCTTTCTGTTAGCAAAGAGGTTCCATGGTACCTGGATGATGGCACT GGGCGTGTCTATGTTGTTGGCGCTCGTTCTGCGGCAGGGTTAATTTTAACTGTTGCCAGTG AGGTTTTTGAGGAGTCAGGGCGAACCCTTGTACGTGGAACTCTAGATTATTTACAAGGACT

			GAAGATGCTCGGAGTAAAGCGAACTGAAAGGGTTCTTCCAACTGGAACTTCATTGACTGTT GTTGGTGAGGCCATTAAAGATGATGTTGGAACTATTCGGATTCAGCGGCCACACAAAGGAC CATTTTATGCATCTCCAAAAAGCATCGATCAACTTATCTTGAATCTCGGGAAATGGGCCAGG TTATACCAACTTGCTTCCATGGGCTTTGCAGCTTTTGGTGTATTTCTTCTTGCGAAGCGTGC ACTTGATCATTTTCTACAAAGAAAGCGCCAGCGTGAATTTCACAAGAAGGCTCGTGCTGCTG CAGCACAAAGGCAGGCTAGGGACGCTGAAGGGGGCAATGGCACATCAGACGGAGAGCCT AAGAAGGATCAATTGGTATTAGAAATATGTGTCATATGCCTTGAACAGGAGTATAATGCAGT TTTTGTGCCGTGTGGCCACATGTGCTGCTGTATGAACTGCTCTTCTCACGTAACAAACTGTC CACTCTGCCGACGAAGAATTGACCAAGCTGTCAGAACATTCCGTCACTGA
	Triticum aestivum D	*taSP1 D*	ATGTTGGTCCCGTGGGGCGGGGTCGGGTGCTGCCTCAGCGCCGCGGCGCTCTATCTCCT CGGGAGGAGCAGCGTCAGGGATGCGGAGGTGCTGCGATCGGTGGCGAGGACGGGCAGC CTGAAGGATTCAGCTGCTATCTTGGACACTGCAAGTAAAGTCCTGCCACTTGTAGTGGCAG TTTCTGGGCGAGTTAGTTCAGATACACCACTTATATGCCAGCAAAGTGGTATGAGAGGTGTA ATAGTCGAGGAAACGGCAGAGCAACACTTCCTGAAGCACAATGATGCTGGATCCTGGATTC AAGATTCTGCTGTGATGCTTTCTGTTAGCAAAGAGGTTCCATGGTACCTGGATGATGGCACT GGGCGTGTCTATGTTGTTGGCGCTCGTTCTGCGGCAGGGTTAATTTTAACTGTTGCCAGTG AGGTTTTTGAGGAGTCAGGGCGAACCCTTGTACGTGGAACTCTAGATTATTTACAAGGACT GAAGATGCTCGGAGTAAAGCGAACTGAAAGGGTTCTTCCAACTGGAACTTCATTGACTGTT GTTGGTGAGGCCATTAAAGATGATGTTGGAACTATTCGGATTCAGCGGCCACACAAAGGAC CATTTTATGCATCTCCAAAAAGCATCGATCAACTTATCTTGAATCTCGGGAAATGGGCCAGG TTATACCAACTTGCTTCCATGGGCTTTGCAGCTTTTGGTGTATTTCTTCTTGCTAAGCGTGCA CTTGATCATTTTCTACAAAGAAAGCGCCAGCGTGAATTTCACAAGAAGGCTCGTGCTGCTG CAGCACAAAGGCAGGCTAGGGACGCTGAAGGGGGCAATGGAACATCAGACGGAGAGCCT AAGAAGGATCAATTGGTATTAGAAATATGTGTCATATGCCTTGAACAGGAGTATAATGCAGT TTTTGTGCCGTGTGGCCACATGTGTTGCTGTATGAACTGCTCTTCTCACGTAACAAACTGTC CACTCTGCCGACGAAGAATTGACCAAGCTGTCAGAACATTCCGTCACTGA